

PhD Thesis

**PERFORMANCE IMPROVEMENT OF RADIO OVER
FIBER COMMUNICATION SYSTEM WITH DISPERSION
AND NONLINEARITY COMPENSATION**

Submitted to

COCHIN UNIVERSITY OF SCIENCE AND TECHNOLOGY

for the award of the degree of

DOCTOR OF PHILOSOPHY

by

ASHA R.S

Under the guidance of

Dr. Jayasree V.K

Research Guide

DEPARTMENT OF ELECTRONICS ENGINEERING

MODEL ENGINEERING COLLEGE

COCHIN - 682 021, INDIA

November 2017

*PERFORMANCE IMPROVEMENT OF RADIO OVER FIBER COMMUNICATION
SYSTEM WITH DISPERSION AND NONLINEARITY COMPENSATION*

Ph.D. Thesis in the field of Radio over Fiber Communication

Author

*Asha R.S
Research Scholar
Department of Electronics
Model Engineering College
Cochin-682 021, India
e-mail: asharspillai@gmail.com*

Research Advisor

*Dr. Jayasree V.K
Research Guide
Department of Electronics
Model Engineering College
Cochin-682 021, India
e-mail: jaya@mec.ac.in*

November, 2017

Dedicated to.....

My Parents, Husband & Son

Certificate

This is to certify that this thesis entitled **Performance Improvement of Radio over Fiber Communication System with Dispersion and Nonlinearity Compensation**, is a bonafide record of the research work carried out by Smt. Asha R.S. under my supervision of the Department of Electronics Engineering, Model Engineering College, Kochi. The results presented in this thesis or part of it has not been presented for the award of any other degree(s).

I further certify that the corrections and modifications suggested by the audience during pre-synopsis seminar recommended by the Doctoral Committee of Mrs. Asha R.S. have been incorporated in this thesis.

Cochin-682 021
06-11-2017

Dr. Jayasree V.K
(Supervising Guide)

DECLARATION

I hereby declare that the work presented in the thesis entitled **“Performance Improvement of Radio over Fiber Communication System with Dispersion and Nonlinearity compensation”** is a bonafide record of the research work done by me under supervision of Dr. Jayasree V.K, Professor, in the Department of Electronics Engineering, College of Engineering, Adoor and Research Guide, Model Engineering College, Thrikkakara, Kochi. The result presented in this thesis or parts of it have not been presented for other degree(s).

Cochin-21
06-11-2017

Asha R.S

Acknowledgement

First and foremost, I would like to thank **GOD Almighty** for giving me the strength, knowledge, ability and opportunity to undertake this research and to persist and complete it satisfactorily. Without his blessings, this achievement would not have been possible.

I take pride in acknowledging the insightful guidance of **Prof.(Dr). Jayasree V.K.**, and Principal, College of Engineering, Adoor, for her excellent guidance and support. With her constant help and suggestions, she has been a great source of inspiration for me.

I sincerely thank **Prof. (Dr.) V. P. Devassia**, Principal, Model Engineering College, Thrikkakara, for extending the facilities in the college for the research work and for his valuable suggestions and credible ideas throughout the research.

I am sincerely acknowledging my gratitude to **Prof. (Dr.) Xavier Fernando**, Ryerson University, Canada, for his valuable suggestions and encouragement.

I am sincerely acknowledging my gratitude to **Prof. (Dr.) Mhatli Sofien**, for his valuable suggestions and encouragement.

I am sincerely acknowledging my gratitude to **Prof. (Dr.) N. Unnikrishnan**, Former Vice Chancellor of Cochin University of Science and Technology, for his valuable suggestions and encouragement.

Let me express my sincere gratitude to **Prof. (Dr.) Mini M.G.**, Principal, Govt. Engineering College, Cherthala, for her valuable suggestions and comments. I would also like to express my gratitude to **Dr. Vinu Thomas**,

Dr. Jobymol Jacob, Dr. Jessy John and Dr. Laila D., Associate Professors, Model Engineering College, for their valuable suggestions.

I have great pleasure in acknowledging my gratitude to my fellow research scholars of the department, especially **Dr. Simi Zerine Sleeba, Dr. Neethu M. Sasi, Dr. Rekha Lakshmanan** and **Dr. Arya Devi P.S.** for their friendly and supportive attitude.

My sincere thanks to all the faculty members, particularly, **Mrs. Vineetha George, Mrs. Jiby John, Mrs. Shiji T. P., and Mr. Rajesh Mohan R.**, Associate Professors, Model Engineering College, for their support.

I also thank to **Mr. Jagadeesh kumar, Mrs. Aparna Devi P.S, Mr. Joseph George K.N, Mr. Bineesh T., Mr. Rashid, Mrs. Shaija Johnson,** Assistant Professors, Model Engineering College, for their support and help.

I thank the non-teaching, library and administrative staff of the Model Engineering College for their cooperation and support.

It is beyond words to express my gratitude to my husband **Dr. Anoop T.R**, my son **Gautham Krishna A.**, my parents **Mr. M.K.S.Pillai** and **Mrs. Radhamani Amma P.**, sister **Mrs. Shermila**, brother, and family members for their sacrifice and help. Without their cooperation, I am sure I could not have accomplished this task. I also thank to my in-laws for their support and understanding.

Asha R.S.

Abstract

This thesis proposes a solution to reduce the nonlinearities and to improve the dynamic range of the RoF communication system. In the RoF architecture, data signals are generated at a Central Station, modulated by an optical carrier, transported over an optical fiber to many BSs and is transmitted to the receiver. This hybrid RoF system has separated the conventional radio spectrum into a number of channels for transmission. The used RF bands are higher than a 2.4 GHz RF band of the current 3G systems. Therefore, a major problem of RoF networks is nonlinearity issues of the various devices in the link.

For a directly modulated multi channel RF signal, the dynamic nonlinearity due to the square-law characteristic of the photodiode produces harmonic distortion in the detected signal. This significantly reduces the effectiveness of RoF communication. The performance of the communication system is also affected by the nonlinearities in the channel.

Transmission of microwave and millimeter wave signals through optical fiber has low-cost antenna terminals and large active frequencies. For simple far off antenna stations, the microwave carrier passing through the radio channel has directly modulated in the optical wavelength. However, it produces severe harmonic distortion caused by optical fiber chromatic dispersion and its degrading effect on the received signal increases to the square of the amplitude of the radio carrier. The performance of communication system is reduced by the nonlinearities at the receiver.

The thesis covers the reduction of nonlinearities at the fiber, photodetector, wireless channel and receiver. One method has proposed to reduce the nonlinear distortion at the photodetector. Its performance is

analyzed in single sideband and double sideband carrier suppressed modulation techniques. A novel method of Weiner filter is used to reduce the nonlinear distortion in the wireless channel. The performance is analyzed in OFDM and DPSK modulation schemes. Four different methods are used to reduce the nonlinearities in the fiber. Three methods are used to reduce the chromatic dispersion. One method is used to reduce the group velocity and third order distortion in the optical fiber. In addition, a multiband millimeter wave is transmitted in three frequencies with good performance. A 200 GHz millimeter wave is transmitted for peer-to-peer communication. In each method, we have compared the results with the existing methods. Finally, the existing RoF communication system is modified by integrating different nonlinearity reduction methods. Two performance improvement methods and two cost reduction methods are integrated. The SNR performance of the proposed system is compared with the existing system. Result shows that the proposed system has given the best performance.

Key words: *millimeter wave, SNR, Central Station, Nonlinearities, OFDM, DPSK, peer to peer communication*

Abbreviations

ASE -	Amplified Spontaneous Emission
AWG -	Arrayed Waveguide Grating
AWGN -	Additive White Gaussian Noise
BER –	Bit Error Rate
BPSK -	Binary Phase Shift Keying
CDMA-	Code Division Multiple Access
CIR-	Channel Impulse Response
CNR –	Carrier to Noise Ratio
CPM -	Cross Phase Modulation
CSNR –	Carrier to Signal Noise Ratio
CW –	Continuous Wave
DAS –	Digital Antenna System
DCF-	Dispersion Compensation Fiber
DEMZM –	Dual Electrode Mach Zehnder Modulator
DPSK -	Differential Phase Shift Keying
DSB –	Double Sideband Modulation
DWDM -	Digital Wavelength Division Multiplexing
EAM -	Electro Absorption Modulator
EE -	Electrical Equalizer
EDFA –	Erbium Dopped Fiber Amplifier
EOPM -	Electro Optical Phase Modulator
ESNR -	Electrical Signal to Noise Ratio
FEC –	Forward Error Correction
FTTH –	Fiber To The Home
FWM -	Four Wave Mixing
Gbps –	Giga bits per second

GVD –	Group Velocity Dispersion
HFR –	Hybrid Fiber Radio
HD –	Harmonic Dispersion
IM –	Intensity Modulation
IMD –	Intensity Modulation Dispersion
ISI –	Inter Symbol Interference
LAN –	Local Area Network
LAWN-	Local Area Wireless Network
LD –	Laser Diode
LOS-	Line of Sight
MATLAB –	Matrix Lab
MAC –	Medium Access Control
MSSI-	Mid Span Spectral Inversion
MZM -	Mach Zehnder Modulator
OCS -	Optical Carrier Suppression
OPC-	Optical Phase Conjugation
OSSB -	Optical Single Sideband Modulation
PMD –	Polarization Mode Dispersion
PN -	Pseudo Noise
Q factor -	Quality Factor
RAU -	Remote Access Unit
RIN –	Relative Intensity noise
SFDR-	Spurious Free Dynamic Range
SOA –	Semiconductor Optical Amplifier
SPM –	Self Phase Modulation
SMF –	Single Mode Fiber
SPICE -	Simulation Program with Integrated Circuit Emphasis

SQRT – Squareroot
TOD- Third Order Dispersion
UMTS - Universal mobile Telecommunication
UT – User Terminal
VCT – Vector Control Theory
VCSEL- Vertical Cavity Surface Emitting Laser
VANET - Vehicular Adhoc Network
WIMAX - Worldwide Interoperability for Microwave Access

Contents

<i>Acknowledgement</i>	<i>i</i>
<i>Abstract</i>	<i>iii</i>
<i>Abbreviations</i>	<i>v</i>
<i>Contents</i>	<i>ix</i>
<i>List of Tables</i>	<i>xv</i>
<i>List of Figures</i>	<i>xvii</i>

Chapter1	Introduction	1
1.1	Radio over Fiber Technology	1
1.2	RoF Architecture	2
1.3	Method of Generation of RoF Signals	4
1.3.1	Intensity Modulation using Direct Detection	5
1.3.2	Remote Heterodyne Detection Technique	7
1.4	Key Issues and Challenges of RoF Technology	8
1.4.1	Attenuation of the Optical Fiber	8
1.4.2	Dispersion of the Optical Fiber	9
1.4.3	Nonlinearities in the Optical Fiber	10
1.4.4	Photodetection in the Optical Receiver	11
1.4.5	Noises Added by the RoF Link	11
1.4.6	Wireless Channel	12
1.5	RoF Signal Characteristics	14
1.5.1	Optical Intensity Modulation	14
1.5.2	Optical Single Sideband Intensity Modulation	16
1.5.3	Optical Carrier Suppression Modulation	18
1.6	Motivation	19
1.7	Objectives of Research	20
1.8	Methodology	21
1.8.1	Matlab	21

1.8.2 Optisystem -----	21
1.9 Impact on the Society-----	23
1.10 Organization of the thesis-----	23
Chapter2 Literature Review -----	25
2.1 Challenges and Mitigation Methods in RoF Technology -----	25
2.2 Impact of Chromatic Dispersion and Mitigation -----	27
2.3 Nonlinear Distortion and Mitigation -----	29
2.4 Performance Evaluation Parameters-----	32
2.4.1 Quality Factor -----	32
2.4.2 Bit Error Rate (BER)-----	33
2.4.3 Signal to Noise Ratio (SNR)-----	35
2.4.4 Eye Diagram-----	37
2.5 Performance Evaluation Criteria -----	38
Chapter3 Reduction of Nonlinear Distortion in the Photodetector of RoF Communication System-----	39
3.1 Introduction -----	39
3.1.1 Different Carrier Suppression Techniques -----	42
3.2 Case I OSSB on RoF communication using SQRT nonlinear equalizer-----	42
3.2.1 Theoretical analysis of SSB modulated THz Signal using balanced MZM -----	42
3.2.2 Simulation Setup-----	45
3.2.3 Results and Discussion -----	47
3.2.4 Conclusion -----	50

3.3	Case II – ODSB-CS with Reduced Photodetector Nonlinearity -----	51
3.3.1	Principle of Optical Double Side Band Suppressed Carrier (ODSB-CS) Modulation -----	51
3.3.2	Simulation Setup -----	54
3.3.3	Results and Discussion -----	56
3.3.4	Conclusion -----	62
3.3.5	Validation -----	63

Chapter4 Performance Evaluation of RoF Systems in Different Channels and Reduction of Channel Distortion ----- 63

4.1	Introduction -----	63
4.2	RoF for Fiber Aided Wireless (Fi-Wi) Systems -----	64
4.3	System Modeling -----	68
4.4	Modulation schemes -----	71
4.4.1	OFDM modulated RoF System -----	71
4.4.2	DPSK Modulated RoF System -----	71
4.5	Channel Model -----	72
4.5.1	AWGN Noise Channel -----	72
4.5.2	Rayleigh Fading Channel -----	72
4.5.3	Rician Fading Channel -----	73
4.6	Wiener Filter for Additive Noise Reduction -----	73
4.7	Signal to Noise Ratio (SNR) -----	73
4.8	Simulation Setup of Radio over Fiber System Using OFDM -----	75
4.9	Results and Discussion -----	79
4.10	Conclusion -----	83
4.11	Validation -----	84

Chapter5 Nonlinear Distortion Reduction in the Fiber ----- 85

5.1	Introduction -----	85
5.2	Case 1: Chromatic Dispersion Compensation Using Optical Phase Conjugation in Semiconductor Optical Amplifier -----	87
5.2.1	Overview -----	87
5.2.2	Simulation Setup -----	89
5.2.3	Results and Discussion -----	94
5.2.4	Conclusion -----	95
5.3	Case 2: Group Velocity Dispersion and Third Order Dispersion in External and Direct Intensity Modulated RoF Link -----	95
5.3.1	Overview -----	95
5.3.2	The Optical Link Challenges -----	96
5.3.3	Theoretical Analysis -----	97
5.3.4	Simulation Setup and Results -----	100
5.3.5	Results and Discussion -----	107
5.3.6	Conclusion -----	107
5.4	Case 3: Fiber Dispersion Compensation in Single Side Band optical Communication system using Ideal Fiber Bragg Grating and Chirped Fiber Bragg Grating without DCF -----	108
5.4.1	Overview -----	108
5.4.2	Theoretical analysis -----	110
5.4.2.1	Single Sideband Theory -----	110
5.4.2.2	Fiber Bragg Grating(FBG) -----	111
5.4.3	Experimental Setup -----	112

5.4.4	Results and Discussion -----	114
5.4.5	Conclusion -----	117
5.5	Case 4: Mitigation of Chromatic Dispersion using Symmetrical Compensation -----	117
5.5.1	Dispersion Compensation Using DCF Technology -----	117
5.5.2	System Description and Simulation Details-----	118
5.5.3	Results and Discussions -----	121
5.5.4	Conclusion -----	124
5.5.5	Validation -----	125
Chapter 6	Multiband Access RoF Link Optical Millimeter Wave Dispersion Tolerant Transmission-----	127
6.1	Introduction -----	127
6.2	Theoretical Analysis-----	130
6.3	Simulation Setup and Results-----	134
6.4	Conclusion -----	141
6.5	Validation -----	142
Chapter 7	Peer-to-Peer 200 GHz Millimeter Wave Long Haul RoF Networks Through AWGN Wireless channel -----	143
7.1	Introduction -----	143
7.2	Generation of Optical Millimeter Wave -----	144
7.3	Characteristics of Millimeter Wave Signals -----	146
7.4	Principle -----	147
7.5	Experimental setup -----	151
7.6	Results and Discussion-----	156

7.7	Conclusion	-----	156
7.8	Validation	-----	157
Chapter8	Performance Improvement of RoF Communication System	-----	159
8.1	Introduction	-----	159
8.2	Performance Improvement and Cost Reduction Methods in RoF Communication	-----	163
8.3	Design Issues	-----	164
8.4	RoF communication System with Nonlinearities Reduction Methods	-----	165
8.5	Results and Discussion	-----	167
8.6	Conclusion	-----	167
Chapter9	Conclusion and Future Work	-----	169
9.1	Conclusion	-----	165
9.2	Future Work	-----	167
	References	-----	169
	Publications	-----	219
	Resume		

List of Tables

<i>Table No</i>	<i>Title</i>	<i>Page No</i>
3.1	Simulation Parameters-----	46
3.2	Simulation parameters-----	54
3.3	Result comparison of existing and proposed methods-----	62
3.4	Validation o results-----	63
4.1	Comparison of Results (OFDM Modulation)-----	76
4.2	Comparison of Results (DPSK modulation)-----	82
4.3	Comparison of Results (OFDM modulation using weiner filter)---	82
4.4	Comparison of Results (DPSK modulation using wiener filter)---	83
4.5	Result analysis of the existing and proposed methods-----	83
4.6	Result analysis of the existing and proposed methods-----	84
4.7	Validation-----	84
5.1	Typical Values of Parameters-----	101
5.2	Typical Values of Parameters-----	102
5.3	Simulation Parameters-----	113
5.4	Simulation parameters-----	119
5.5	Result analysis of various existing and proposed methods-----	125
5.6	Validation of results-----	126
6.6	Validation of results-----	142
7.1	Simulation Parameters-----	152

List of Figures

1.1	General block diagram of RoF communication system -----	3
1.2	External intensity modulation -----	6
1.3	Optical heterodyning -----	8
1.4	RoF communication basic processes with noises present in the path -----	8
1.5	Optical Double Side Band Intensity Modulation -----	15
1.6	Optical modulation formats(a) Optical Double Sideband modulation (b) Optical Single Sideband modulation (c) Optical Carrier Suppressed modulation -----	16
1.7	Optical SSB generation using Fiber Bragg Grating (FBG) -----	17
1.8	External modulation using (a) Single drive MZM (b) Dual Drive MZM -----	18
2.1	Losses, Gain and Noises in a RoF communication system -----	36
3.1	Single-tone OSSB–RoF transmission system -----	43
3.2	Block diagram of SSB communication System -----	47
3.3	(a) RF input (modulating signal) at a frequency of 60 GHz -----	48
3.3	(b) Laser input (optical carrier) at a center frequency of 193.1 THz -----	48
3.4	(a) SSB (MZM) output at quadrature operating point -----	48
3.4	(b) Photodetector output -----	48
3.5	(a) SQRT nonlinear equalizer output, -----	49
3.5	(b) RC BPF output (detected message signal) at 60 GHz -----	48
3.6	SNR (at 4 GHz and 5 GHz) of photodetector -----	49
3.7	SNR (at 4 GHz and 5 GHz) of photodetector with- SQRT nonlinear equalizer -----	50
3.8	Direct laser modulation process -----	52
3.9	Sub carrier multiplication and modulation through MZM modulator -----	53

3.10	Schematic diagram of the optical mm-wave generation using balanced MZM biased in OCS Modulation-----	53
3.11	Block diagram of ODSB- CS-RoF communication system -----	56
3.12	BER & Eye height of 5Gbps, 50 GHz ODSB-CS receiver -----	57
3.13	BER & Eye height of 10 Gbps, 60 GHz ODSB-CS receiver-----	57
3.14	Q- factor of back-to-back propagation in ODSB-CS Receiver-----	58
3.15	Eye height of back-to-back propagation in the ODSB-CS Receiver -----	58
3.16	BER and Eye height of back-to-back propagation for different laser powers -----	59
3.17	Q and log(BER) of the ODSB-CS receiver (back-back) transmission -----	59
3.18	SNR of the ODSB-CS communication with and without SQRT non linear equalizer -----	60
4.1	Radio over Fiber System -----	65
4.2	Losses, amplifications, and added noise to the radio signal -----	66
4.3	System model -----	69
4.4	Block Diagram of RoF transmitter unit -----	77
4.5	Block diagram of remote access point-----	78
4.6	Block diagram of receiver unit -----	78
4.7	Time domain plot of RoF -in AWGN channel -----	79
4.8	Time domain plot of RoF in Rayleigh Channel-----	79
4.9	Time domain plot of RoF in Rician channel -----	80
4.10	Power spectrum of RoF in AWGN channel -----	80
4.11	Power spectrum of RoF in Rayleigh channel -----	81
4.12	Power spectrum of RoF in Rician channel -----	81
5.1	FWM method of SOA -----	88
5.2	Block diagram of optical phase conjugation using travelling wave SOA -----	90
5.3	Optical phase conjugated output spectrum of SOA -----	91

5.4	Filtered optical phase conjugated signal of SOA -----	92
5.5	Optical output power of the existing method (pd) and proposed method(eg)-----	92
5.6	OSNR of the converted signal using proposed method (pd) and existing method (eg) -----	93
5.7	Electrical power output of proposed (pd) and existing method (eg) -----	93
5.8	FWM conversion efficiency of the SOA for proposed (pd) and existing method (eg) -----	94
5.9	External modulation using dual electrode MZM -----	102
5.10	Q factor and RF signal output of MZM in the presence of TOD -----	103
5.11	Q factor and RF signal output of MZM in the presence of GVD ----	103
5.12	Eye diagram of the electrical signal at the receiver(a) L=20 km, (b) L=90 km-----	104
5.13	(a)Relationship between Q-factor and BER(b) Relationship between Q-factor and eye amplitude(c) Relationship between eye amplitude and time -----	104
5.14	Direct modulations using VCSEL -----	105
5.15	Spectrum of (a) Direct laser (b) VCSEL (c) Saturated VCSEL -----	106
5.16	(a) Measured V-I curve (b) Measured L-I curve of VCSEL -----	106
5.17	Generation of optical SSB signal -----	110
5.18	Block diagram of dispersion compensation in SSB -optical communication using FGB and chirped FBG -----	113
5.19	Performance of ER, Q factor, and RF output power for chirped FBG 5.20Performance of ER, Q factor and RF output power for FBG-----	114
5.20	Performance of ER, Q-factor and RF output power for FBG -----	115
5.21	Performance of Q factor, BER and electrical signal power for FBG of fiber length 20 km [input power = 0 dBm to 8dBm] -----	116
5.22	Performance of Q factor, BER and electrical signal power forchirped FBG of fiber length 20 km [input power = 0 dBm to 8 dBm] -----	116
5.23	Post compensation using DCF -----	120

5.24	Pre-compensation using DCF -----	120
5.25	Symmetric/mix compensation using DCF -----	121
5.26	Eye diagram obtained (a) without compensation(b) with pre compensation using DCF -----	122
5.27	Eye diagram obtained (a) with post compensation using DCF(b) with symmetric compensation using DCF-----	122
5.28	Comparison of DCF compensation techniques -----	123
5.29	Signal power of the symmetric compensated and uncompensated system -----	124
6.1	Block diagram of multiband transmitter -----	136
6.2	(a)Optical SSB spectrum of the upper MZM-----	137
6.2	(b)RF-OCS optical spectrum of the lower MZM-----	137
6.3	Generated optical spectrum of the main MZM -----	137
6.4	Output optical power and OSNR of the generated optical millimeter wave for different length of fiber (km) -----	138
6.5	Block diagram of multiband base station -----	138
6.6	Output optical signal power of millimeter wave at data rates of 80 Gbps and 10 Gbps-----	139
6.7	Received electrical spectra of millimeter waves at (a) 40 GHz (b) 80 GHz (c) 120 GHz-----	139
6.8	Q-factor and eye diagram performance of the received mm waves for frequencies 40 GHz, 80 GHz and 120 GHz -----	140
6.9	BER performances of 40 GHz, 80 GHz and 120 GHz millimeter wave signals at B-T-B, 10 km, 20 km and 30 km of fiber length -----	140
7.1	Basic diagram of the proposed P2P interconnected system -----	148
7.2	Schematic diagram of AWGN channel-----	151
7.3	Block diagram of 200 GHz peer to peer millimeter wave RoF transmission -----	153
7.4	200 GHz millimeter wave generated spectrum -----	154
7.5	6 GHz millimeter wave received spectrum -----	154
7.6	10 GHz millimeter wave received spectrum -----	154

7.7	Q factor and BER for different input powers	-----	155
7.8	Q factor and BER for 10 GHz Peer to Peer Transmission	-----	155
7.9	Q factor and BER for different transmission distances (6 GHz)	----	155
7.10	Q factor and BER for different transmission distances (10 GHz)	-----	155
8.1	RoF Challenges	-----	161
8.2	Design constraints of RoF communication	-----	165
8.3	Integrated RoF communication system with VCSEL source	-----	166
8.4	Performance comparison of VCSEL and MZM modulated integrated methods	-----	166

1.1 Radio over Fiber Technology
1.2 RoF Architecture
1.3 Method of Generation of RoF Signals
1.4 Key Issues and Challenges of RoF Technology
1.5 RoF Signal Characteristics
1.6 Motivation
1.7 Objectives
1.8 Methodology
1.9 Impact on the Society
1.10 Organization of Thesis

Abstract

This chapter briefs about generation and characteristics of the RoF signals. It also deals with the architecture and challenges in the RoF communication. Chapter ends up with objectives, motivation, social relevance and organization of the thesis.

1.1 Radio over Fiber Technology

Radio over Fiber (RoF) Technology is an emerging technology with the advantages of wireless and optical networks. RoF has different advantages like low attenuation, mobility of wireless access, large bandwidth of fiber and low electrical interference. Optic fibers can satisfy the high speed requirement of next generation networks. RoF is more popular with its multi access ability, higher information capacity and transmission distance [1].

In a RoF communication System, wireless signals are transmitted in optical form between a Central Station (CS) and a set of Base Stations (BS) before being radiated into the air medium. RoF technology also integrates different networks like 3G, 4G, WiMAX and other protocols [2], [3].

RoF architecture has different advantages like simple BS and dynamic allocation of radio carriers. As RoF is integrated with wireless technology, it could supply higher data rates. Wireless LAN offers up to a data rate of 54 Mbps and carrier frequencies from 2.4 GHz to 5 GHz, 3G mobile networks, recommends up to 2Mbps in 2GHz, and 4G offers up to 40 Mbps and carrier frequencies from 2 GHz to 8 GHz. The wireless standard IEEE 802.16 Mobile and Fixed WiMAX renders carrier frequencies from 2 GHz to 66 GHz [3]-[5].RoF can be used in different applications where normal wireless communication cannot be used. It can be used in tunnels, hazardous areas etc.

1.2 RoF Architecture

In the RoF communication system, the Radio Frequency (RF) signal is modulated by the optical carrier and it is transmitted through an optical fiber to the receiver. At the receiver, RF signal is detected and has radiated to the wireless end user. RoF communication can integrate all RF signal processes in one shared CS and can transmit through the optical fiber. It offers low attenuation (0.2 dB/km for 1550 nm wavelength, and 0.5 dB/km for 1310 nm wavelength) to transmit the RF signals to the Remote Antenna Units (RAU). RoF communication deployed an optical fiber to disperse radio frequency signals from a CS to different physically separate RAUs [6]. It is the integration of the wireless communication and optical communication technology. RAUs have performed optoelectronic (O/E & E/O) conversion and amplification as shown in Fig.1.1.

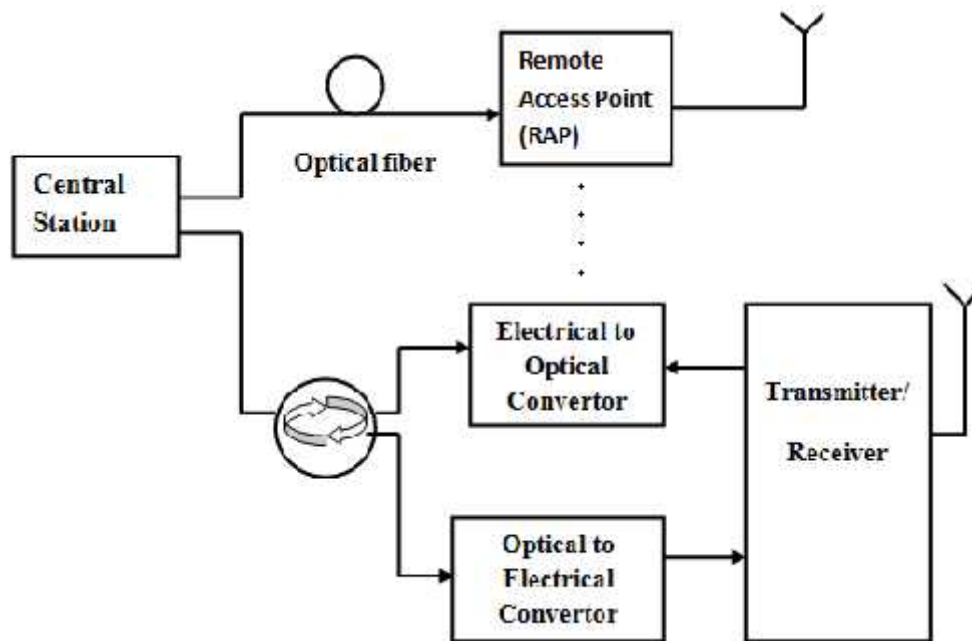


Fig.1.1 General block diagram of RoF communication system

As the entire signal processing functions are held at CS, it is provided equipment distribution, dynamic allocation of resources and easier system performance and preservation [7]. Due to reduced cell size, a large number of low cost base stations are included to provide sufficient radio coverage. As the radio cell size is small, a certain area is covered by many antennas. Such an area may include the rooms in a flat, a hospital, an airport terminal, a conference site, an office building, stadium etc. It becomes economically unattractive to generate and modulate the microwave signal at every antenna, but optical fibers with their inherent low losses and wide bandwidth can transport the signal to the antennas. The antennas only need to do the simple optical-to-electrical conversion and to emit and receive the wireless signal from the CS [8].

1.3 Method of Generation of RoF Signals

Various methods had used for the production of RF optical signals in optical wireless systems. The optical heterodyne method [9], self-heterodyne method [10] and pulsed lasers [11], [12] were few methods. However, the basic method of the RF signal generation is an Intensity Modulation (IM) technique with direct or external modulation of a laser.

Two important methods of RoF signal generation and reception are Intensity Modulation using Direct Detection and Remote Heterodyne Detection Technique. Intensity modulation is again classified into direct intensity modulation and external intensity modulation. Direct intensity modulation can be used for modulating frequencies less than laser cutoff frequencies. They are explained in detail as section 1.3.1.

Another scheme makes use of a single Opto-Electronic device, Electro-Absorption Modulator (EAM), works as a photodiode for the downlink process and as a modulator for the uplink process. It was later replaced the laser, photodiode, circulator [13]–[16] and so it is called as Electro-Absorption Transceiver. In another proposed method, the aim was to produce a double-sideband optical mm signal (RoF) with time shift of the sidebands on its transmission performance and fading effect [17]. A 2.5 Gbps data was effectively transmitted over 20 km single mode fiber with a low power penalty by using Four Wave Mixing (FWM) in Semiconductor Optical Amplifier (SOA) [18] and with multiple frequency Brillouin fiber-ring laser [19]. To increase the capacity and mobility of existing communication

technique and to support both fixed and mobile users, a new scheme of Binary Phase Shift Keying (BPSK) signals for RoF system has been proposed [20]. This duplex RoF technique has produced both 20 GHz and 40 GHz mm wave signals with a data rate of 1.25 Gbps, with one Electro-Optical Phase Modulator (EOPM) and one Mach–Zehnder Modulator (MZM) at the CS and with one MZM at the BS. The Optical Single Side Band (OSSB) signal, generated by the conventional modulation schemes suffered severe distortion at the BS for large RF modulation index. The performance of the transmission link was enhanced in single channel and Dense Wavelength-Division Multiplexing (DWDM) with the reduction of unwanted higher order harmonics based on a novel MZM technique[21] with an optical phase modulator waveguide.

An optical mm wave (60 GHz RoF signal) was generated and transmitted for 1.25 Gbps downstream data with a gain switched laser [22]. A 64 GHz optical mm wave generated using a LiNbO₃MZM with an 8 GHz local oscillator [23], one dual-parallel MZM through optical carrier suppression [18], without carrier suppression [24] and frequency 12-Tupling [25].

1.3.1 Intensity Modulation using Direct Detection

This is the basic method of RoF signal generation [26], [27]. The intensity of the optical signal is varied in respect of the intensity of the RF signal. Intensity modulation has been performed by using direct modulation or external modulation. In the direct intensity modulation, the RF signal is used to drive the input optical source as in Fig.1.2. The RF signal is superposed with the DC bias so that the intensity of the output optical signal is directly proportional to the

intensity of the RF signal. This is the most cost effective and simplest method. But this method is not suitable for high frequency RoF communication.

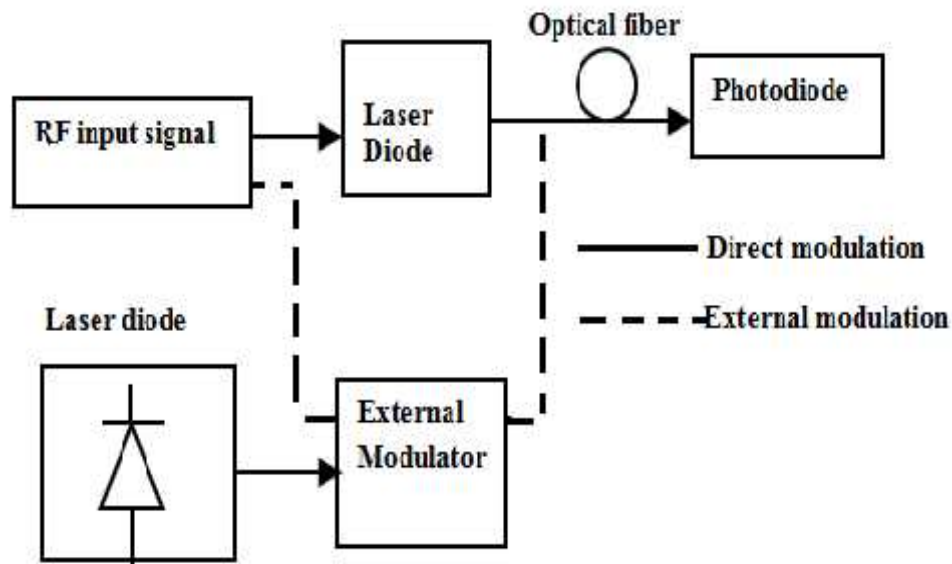


Fig.1.2 External intensity modulation

It cannot be used in millimeter wave band frequencies due to bandwidth of the modulating signal is reduced by the bandwidth of the optical sources. To generate high frequencies, modulating frequencies should be high which cannot be made possible due to the nonlinearity of the optical sources.

In the external modulation, the intensity of the optical carrier is varied by the modulator. Commonly, modulation is performed by a MZM [28]. In the external modulation, the dispersion introduced in the fiber can be reduced by using SSB modulation [29]. The intensity modulated Direct Detection can be used in Single Side Band (SSB) or Double Side Band (DSB) modulation schemes. The RF signal can be recovered by using a photodiode at the receiver section.

1.3.2 Remote Heterodyne Detection Technique

The RoF signal is produced by the coherent mixing of two optical carriers in a photodetector and will produce a high frequency current at the photodetector. The principle of optical heterodyning is shown in Fig.1.3 [30]. The RF signal is directly modulated by the laser diode and it is externally modulated by the optical modulator. The modulated optical signal is mixed with the unmodulated optical signal (Reference input). The modulated signal is transmitted through an optical fiber and reached at the receiver. A photodetector is used as the receiver to convert optical signal to the electrical signal. The unmodulated optical signal is injection locked with harmonics and their difference will produce millimeter (mm) wave frequency. The unmodulated carrier has higher power consumption and lowers the optical bandwidth. But the converted RF signal has good quality due to lesser laser noise [30]. The combined signal passes through the optical fiber and reaches at the photodetector.

The coherent mixing will produce RF signal both at the sum and difference of their frequencies including multiple harmonics at the photodetector [30]. An electronic band pass filter is used to extract the RF signal. The frequency of the modulated signal is obtained from the frequency difference of the two input carriers.

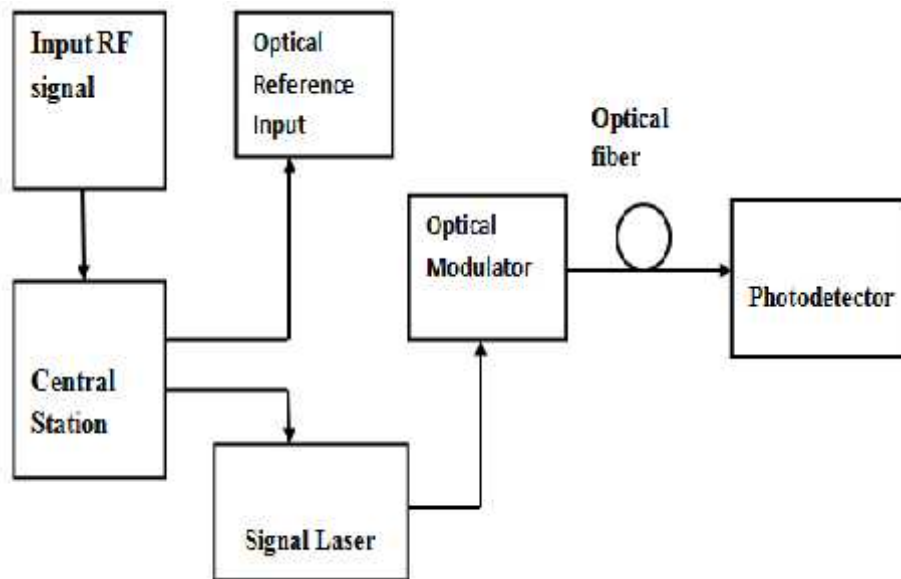


Fig.1.3 Optical heterodyning

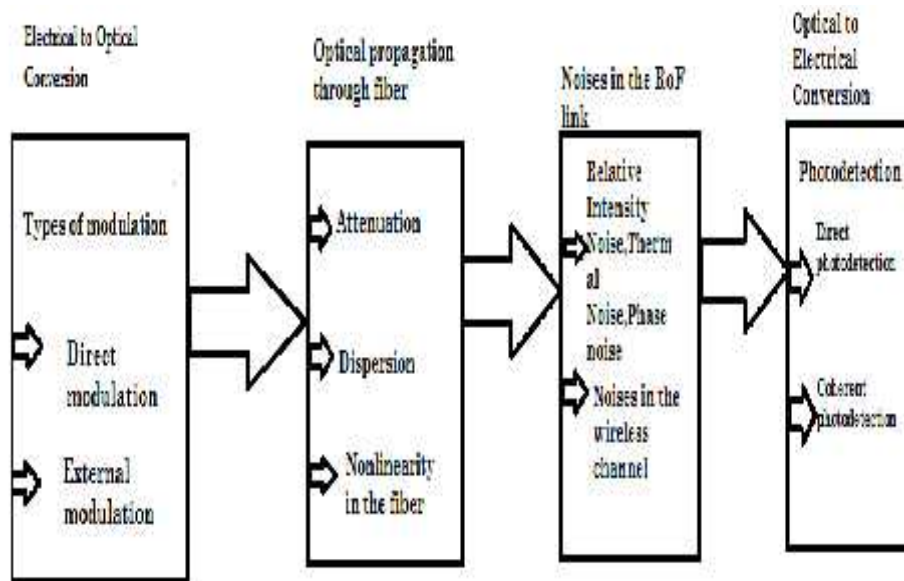


Fig.1.4RoF communication basic processes with noises present in the path

1.4 Key Issues and Challenges of RoF Technology

The propagation of optical signal is affected by the attenuation, dispersion and nonlinearities of optical fiber, nonlinearities in the wireless

channel and nonlinearities in the photodetector as shown in Fig.1.4. They are discussed in the following sections.

1.4.1 Attenuation of the Optical Fiber

When an optical signal is propagated through an optical fiber [31], signal power is reduced due to material absorption and the Rayleigh scattering. If $P_{\text{transmitted}}$ is the optical power of the applied optical signal and the signal has transmitted through the fiber of length Z km, the received power, P_{received} is expressed as

$$P_{\text{received}} = P_{\text{transmitted}} \cdot e^{-\alpha Z} \quad (1.1)$$

where α is the fiber attenuation constant in Np/km and has a typical value of 0.023 Np/km [31].

1.4.2 Dispersion of the Optical Fiber

The wavelength of the transmitting optical wave is changed with the changes in fiber's refractive index $n(\lambda)$ [31]. If V_p is the phase velocity of the propagating optical wave, then

$$V_p = \frac{c}{n} \quad (1.2)$$

Where c is the speed of light. As the propagation velocity is varied with the optical frequency, dispersion will be generated.

If ω and λ are the angular frequency and wavelength of the optical carrier, then the dispersion parameter D is represented as [31]:

$$D = \frac{-2}{\lambda^3} \frac{c \beta_2}{c^2} \quad (1.3)$$

Where $\beta_2 = \frac{1}{c} \left[2 \frac{d}{d\omega} + \omega \left(\frac{d}{d\omega} \right)^2 \right] / \omega = \omega_c$. This fiber dispersion is also known as second order dispersion or Group Velocity Dispersion (GVD) [31].

1.4.3 Nonlinearities in the Optical Fiber

When a fiber is polarized by an electric field E , is referred to as a dielectric medium. The total polarization P responds non-linearity of the electric field E , and results in nonlinear effects. The total polarization P corresponds to the nonlinearity is represented as [32],

$$P = P_1 + P_2 + P_3 + \dots \quad (1.4)$$

In Equation (1.4), the term P_1 is the linear component. The second-order nonlinear effects like Second Harmonic Generation (SHG) may be present in non-Centro-symmetric crystals only [32]. Glass-based optical fiber does not have second-order nonlinear effects like SiO_2 and has a symmetric structure [32]. The third order nonlinearities like Self Phase Modulation (SPM)/ Cross-Phase Modulation (XPM) and FWM are generated from nonlinear polarization component P_3 [32]. These effects appear in both Centro-symmetric crystals and non-Centro-symmetric crystals [32]. As the total signal power, $P(t)$ affects the value of the fiber's refractive index, a non-linear refractive index effect will be produced. This variation of the refractive index causes a variation in the phase of the optical signal. These phase modulations have produced both SPM and XPM [31]. SPM is produced by the instantaneous power variation of the transmitted signal versus time. But the XPM is generated due to the propagation of multiple optical signals through the fiber. The optical power of each signal and the co-propagating signals suffer due to the nonlinear distortion introduced by XPM [31]. As the different optical signals are transmitted through a nonlinear medium like Single Mode

optical Fiber (SMF), the beating of these optical signals generate FWM. For example, when three optical signals at frequencies f_1 , f_2 , and f_3 are transmitting through an optical fiber, FWM is generated at,

$$f_{FW} = f_1 \pm f_2 \pm f_3 \quad (1.5)$$

The most relevant FWM frequencies are at

$$f_{Fj} = 2f_i - f_j \quad (1.6)$$

where $i, \text{ and } j \in 1, 2, 3$.

Stimulated Brillouin Scattering (SBS) and Stimulated Raman Scattering (SRS) [31] are nonlinear effects that may be generated. When the optical power is transferred from a higher frequency optical signal to a lower frequency signal, the photons of the incident field get eradicated.

1.4.4 Photodetection in the Optical Receiver

Photodetection is the process of conversion of an optical signal to an electrical signal using a photodiode. The generated current is proportional to the power of the incident optical signal. In this square-law photo-detection, the responsivity, R of the photodiode, is defined as the ratio of the output photocurrent to the incident optical power. "Two types of photodetection are Coherent photodetection and Direct photodetection [33]". For the Direct photodetection method, the photocurrent, $I(t)$ of an optical field [33], $E_s(t)$ is,

$$I(t) = R |E_s(t)|^2 \quad (1.7)$$

where R is the responsivity of the photodetector.

1.4.5 Noises Added by the RoF Link

The major noises presented in a RoF link are Relative Intensity Noise (RIN), Amplified Spontaneous Emission (ASE) noise, shot noise and receiver thermal noise. When a constant drive current is applied, the spontaneous emission of photons in an optical source causes certain variations in the output phase, frequency and the intensity [31], which results in RIN. The non-zero spectral line width is formed due to phase/frequency noise, but the SNR is degraded by the intensity noise [31]. For an average photo-current of I_{dc} , the RIN noise power is expressed as [31],

$$\frac{z}{R} = K_R I_{dc} \Delta f \quad (1.8)$$

Here K_R is a device-dependent constant that is commonly represented in dB/Hz and Δf is the bandwidth of the receiver. A usual value of K_R is -150 dB/Hz. The ASE noise is produced due to the spontaneous emission within an optical amplifier and it is amplified by the gain of the amplifier [31]. The Shot noise is produced by the quantum noise effect in the photo-detected signal [31]. If e is the charge of an electron, then the shot noise power can be expressed as [31],

$$\frac{z}{S} = 2eI_{dc} \Delta f \quad (1.9)$$

When the electrons move randomly with respect to temperature, the thermal noise is added by the load resistor and the electrical amplifiers in the optical receiver [34]. The performance of coherent optical links is also degraded by laser's phase noise because a carrier recovery circuit may have problems in tracking rapid phase variations. The phase noise effects are characterized by the total linewidth to bit rate ratio [31]. Here the total linewidth is the sum of the linewidths of the transmitter laser and the local oscillator laser. For

practical lasers, they have a finite spectral width around the operating frequency ω , is referred to as the laser's linewidth.

1.4.6 Wireless Channel

The wireless transmission is represented as [35],

$$y = Hx + n, \quad (1.10)$$

where x is the symbol vector of the transmitted signal, n is the Gaussian noise vector, H is the channel matrix and y is the symbol vector of the received signal. H is a unitary matrix for a Gaussian wireless channel. But for a fading channel, H consists of Rayleigh or Rician distributed channel coefficients [35]. In the case of mm wave transmission, the higher wireless path loss was overcome by beam forming using an array of antenna elements. These antenna outputs are constructively interfered in a desired direction, but destructively interfered in other directions [36].

The radio communication issues are related to the integration of a wireless network with a RoF backhaul. This includes power budgeting and the presence of the accumulating noise [37]. These issues are explicated in the design of a RoF and transmitted through a Gaussian wireless channel. The RF signal $x_R^B(t)$ has a power of P_R^B . This power is attenuated by a factor of L_{\square} in the RoF link to produce a photo-detected signal $x_R^R(t)$ that has a power of P_R^R , where L_{\square} accounts for the electrical to optical conversion loss, fiber propagation loss, insertion losses of the optical components as well as the optical to electrical conversion loss. The wireless noise power is k times greater than that of the optical noise power; the following can be stated as [38],

$$\text{SNR}_{\text{t}} = \text{SNR}_{\text{R}} \frac{1}{\left(1 + K \frac{1}{\frac{1}{\text{SNR}_{\text{R}}}}\right)} \quad (1.11)$$

$$= \text{SNR}_{\text{R}} \frac{1}{\left(1 + \frac{1}{\text{SNR}_{\text{R}}}\right)} \quad \text{for } K = 1 \quad (1.12)$$

Here SNR_{R} is the SNR of the RoF link and SNR_{t} is the SNR of the total link (optical and wireless links).

1.5 RoF Signal Characteristics

Fig. 1.5 shows the type of optical modulation as well as the type of optical multiplexing format used in the RoF communication. Optical angle modulation and optical intensity modulation are the different modulation methods used in RoF communication. Subcarrier multiplexing and wavelength division multiplexing are the different multiplexing methods as in fig. 1.5. As seen in Fig. 1.5, for a RF modulating signal, both the intensity and the angle of the optical carrier can be modulated in a RoF link.

1.5.1 Optical Intensity Modulation

The intensity of the optical carrier is varied by modulating a RF signal and this type of modulation is called as the Intensity Modulation (IM). It is classified into Optical Double Side Band (ODSB), Optical Single Side Band (OSSB) and Optical Carrier Suppression (OCS).

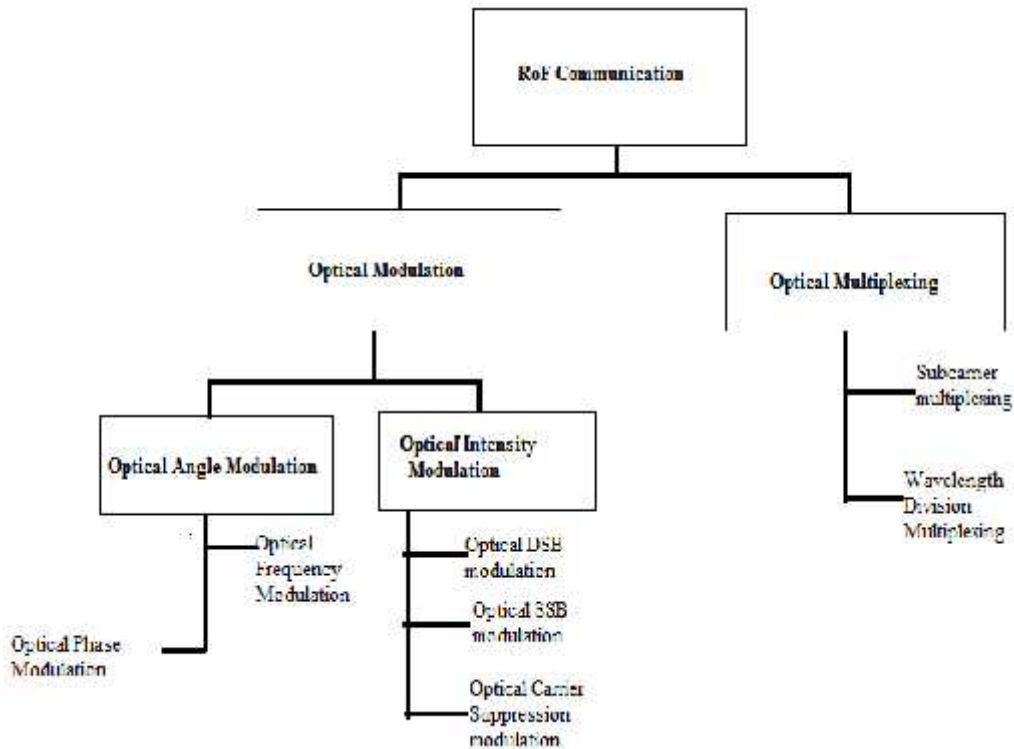


Fig.1.5 Optical Double Sideband Intensity Modulation

The ODSB signal consists of the lower and upper optical sidebands appearing at equal sides of the central optical carrier at $f_c = \frac{\omega_c}{2\pi}$ Hz, shown in Fig. 1.6(a) [39]. The carrier and sidebands are separated by a frequency of f_R [39] and the modulating RF signal has a center frequency of $f_R = \frac{\omega_c}{2\pi}$ Hz. An ODSB signal is generated by both the direct modulation of lasers and external modulation using an EAM [40].

A ODSB signal is generated by the single and dual-drive MZMs. We have $V_b = \frac{V}{2} + m 2V$, or $V_b = -\frac{V}{2} + m 2V$, where m is an integer [41] and $V(t)$ is the transmitted RF signal.

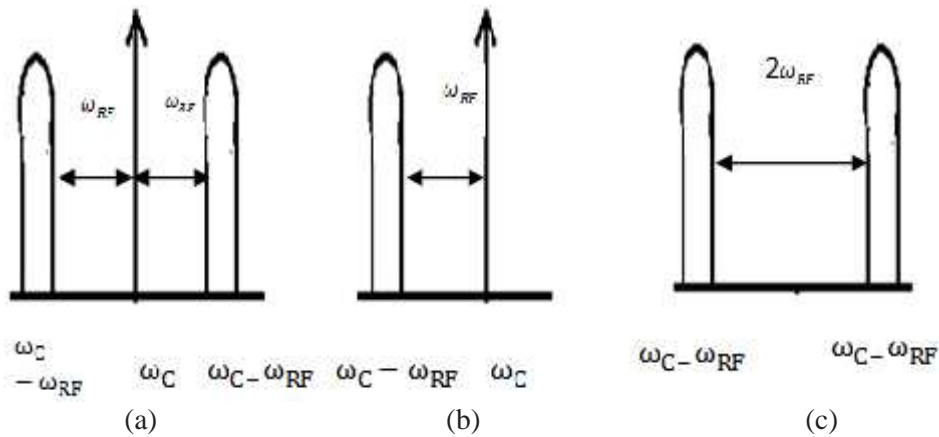


Fig. 1.6 Optical modulation formats (a) Optical Double Sideband modulation (b) Optical Single Sideband modulation (c) Optical Carrier Suppressed modulation

The bias conditions are used for generating different modulation outputs. For ODSB signals, the MZM is biased at maximum transmission point. For SSB signals, the MZM is biased at quadrature operating point. For ODSB-SC signals, the MZM is biased at minimum transmission point. When a dual-drive MZM is used for modulation, a phase difference of π is maintained between the two RF signals $V_1(t)$ and $V_2(t)$ for a chirp free output [42].

1.5.2 Optical Single Sideband Intensity Modulation

An OSSB signal contains only one of the two possible sidebands at $f_s = \frac{\omega_s}{2\pi}$ Hz and the optical carrier at $f_c = \frac{\omega_c}{2\pi}$ Hz, as seen in Fig. 1.6 (b), where the frequency of the modulating RF signal is f_R . The carrier and sideband are separated by a frequency of f_R .

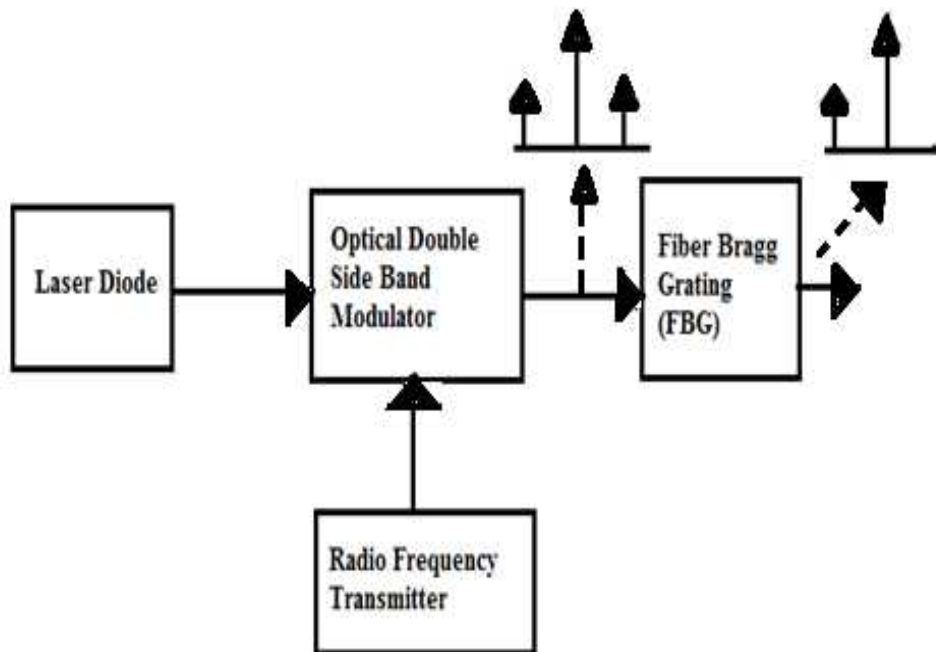


Fig. 1.7 Optical SSB generation using Fiber Bragg Grating (FBG)

The two important methods of generating OSSB signals are using Fiber Bragg Gratings (FBG) as shown in Fig.1.7 and the dual-drive MZM as shown in Fig.1.8 [45]. One of the sidebands of the ODSB signal is excluded by a FBG filter [43] as in Fig.1.6.A FBG reflects certain wavelengths and passes other wavelengths [44]. The reflected wavelengths, will have a frequency of f_r ,

$$f_r = \frac{v}{\lambda} \text{ Hz} \quad (1.13)$$

It depends on the periodicity of the perturbation and the effective refractive index of the fiber core. High-selectivity optical filters are used for low frequency modulating signal.

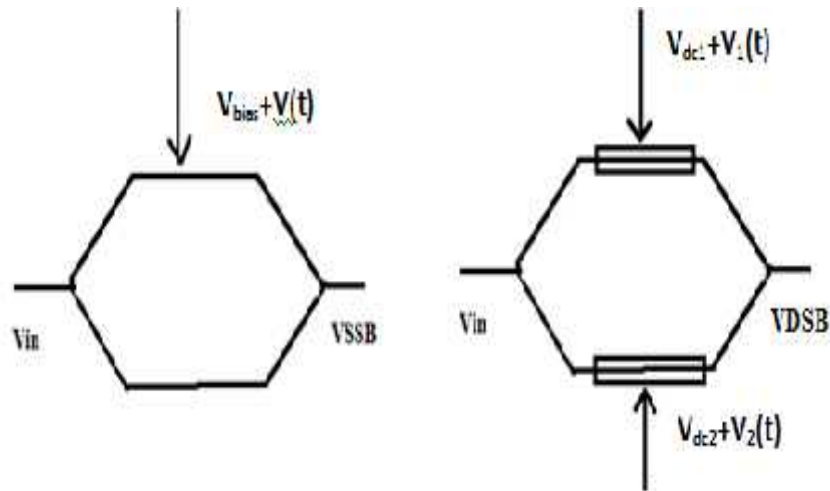


Fig.1.8 External modulation using (a) Single drive MZM (b) Dual Drive MZM

As the refractive index varies with the temperature, the reflected wavelength has a temperature dependent value [45]. An OSSB is generated by quadrature biased, dual drive MZM having a phase shift of $\frac{\pi}{2}$ between arms.

1.5.3 Optical Carrier Suppression Modulation

An OCS signal [46], consists of two sidebands at $f_c \pm f_R$ Hz, as shown in Fig. 1.6 (c), where the f_R Hz is the frequency of the modulating RF signal and f_c is the optical center frequency. A MZM biased at $V_{bias} = V_p + 2mV$, is an integer, generates an OCS signal, whose optical sidebands beat during photodetection, while generating a signal at $2f_R$ Hz [47]. As the MZM is biased at minimum transmission point, the carrier frequency is removed and two sidebands have remained.

1.6 Motivation

This research is motivated by the following factors. The beauty of optical communication overpowering the wireless communication lies with negligibly small loss of the signal. But the biggest hurdle is the successful delivering of signal with optimum strength. The factors that limit the reliable communication over a fiber-optic communication link are the noise added by the inline optical amplifiers and the nonlinear distortion due to the Kerr effect in the optical fiber. In order to reduce the impact of noise, the power of the light has reduced. As the optical power is increased, the impact of the nonlinear distortion has increased and has dominated over the noise. The signal quality is made worse by further increasing the signal launch power. The optimum launch power lies in the limit where neither noise nor nonlinear distortion can be neglected. Over the years, many methods had suggested in order to mitigate the nonlinear distortion due to the Kerr effect at high launch powers. The first method suggested is to use optical solitons in fiber-optic communication systems.

The physical effects that altered the optical field during propagation in an optical fiber are commonly divided into linear effects such as attenuation, dispersion and nonlinear effects due to the Kerr effect as well as Raman and Brillouin Scattering. At lower optical powers, the nonlinear effects are neglected. For higher optical powers, the nonlinear effects become stronger and optical signals are highly distorted.

The process of modulation methods is divided into direct and indirect modulation. Direct modulation of semiconductor lasers is used for simple and low cost systems. In a directly modulated laser, the main source of distortion is

caused by the intrinsic nonlinearities of the laser that limits the dynamic range and hence the system performance. Nonlinear distortion generated by the semiconductor laser such as intermodulation distortion is also produced interchannel interference and the quality of the received signal is reduced.

Various techniques have been proposed and established to mitigate fiber dispersion effects in RoF system including Up/Down Conversion techniques. The IF signals are transmitted over an optical fiber instead of the RF signal and having a minimum fiber dispersion induced power degradations due to low fiber dispersion effect. But unfortunately, the system cost is increased. Because additional devices are used such as high bandwidth devices like, Metal Semiconductor Metal photodetector (MSM-PD), High Electron Mobility Transistor (HEMT), and Hetero-junction Bipolar Transistor (HBT) [48]-[52].

1.7 Objectives of Research

General Objective

To study the Radio over Fiber communication and to improve the performance of Radio over Communication system by mitigating the different nonlinearities in the existing system.

Specific Objectives

- To truncate the nonlinear distortions in the photodetector
- To minimize the nonlinear distortions in the wireless channel
- To suppress the different nonlinear distortions in the optical fiber
- To reduce the nonlinearities in the multiband RoF communication system

- To subside the phase noise and frequency instability of millimeter wave RoF communication system

1.8 Methodology

1.8.1 MATLAB

MATLAB [Matlab 2011] is a high-performance language for computing. It can solve many technical computing problems, especially those with matrix and vector formulations. The name MATLAB stands for matrix laboratory. MATLAB is a standard instructional tool for introductory and advanced courses in mathematics, engineering and science. MATLAB is used as a main programming tool for high productivity research, development and analysis.

It has used for computation, visualization and programming in mathematical problems. Common applications are,

- ❖ Mathematical computation
- ❖ Algorithm development
- ❖ Modeling
- ❖ Data analysis
- ❖ Scientific and engineering graphics
- ❖ Graphical user interface building

1.8.2 OptiSystem

OptiSystem™ can minimize time requirements and cost in the design of optical systems, links and components. OptiSystem is a system level simulator with realistic modeling of fiber-optic communication systems. It is a powerful

simulation environment. OptiSystem is a pioneering, rapidly evolving, and powerful software design tool that enables users to plan, test, and simulate all optical link in the transmission layer of a broad spectrum of optical networks. It offers transmission layer design and system level design of optical communication system.

Its capabilities can be improved by the addition of components, and can be effortlessly interfaced with different tools. It's Graphical User Interface (GUI) controls the optical component design and net list, component types and graphics. It has an extensive library of active and passive components with practical, wavelength dependent parameters. Parameter sweeps helps the user to study the effect of a typical component in the system performance.

The salient features of OptiSystem are:

- ❖ **Component Library:** The OptiSystem Component Library has hundreds of components that help the user to give parameters measured from real devices. It combines test & measurement equipment from different vendors. Users can integrate new components with subsystems and can co-simulate with other softwares like MATLAB or SPICE.
- ❖ **Mixed signal representation:** OptiSystem can support mixed signal formats for optical and electrical signals in the Library. OptiSystem uses appropriate algorithms for simulation accuracy and efficiency.
- ❖ **Integration with Optiwave Software Tools:** OptiSystem has explicit Optiwave software tools for integrated optics at the component and circuit level like OptiSPICE, OptiBPM, OptiGrating and OptiFiber

- ❖ **Quality and performance algorithms:** The system performance is calculated using parameters such as BER, eye diagram, SNR and Q Factor using numerical analysis or semi-analytical methods.
- ❖ **Powerful Script language:** Helps to represent arithmetical expressions and global parameters for components and subsystems. The script language can also examine and control OptiSystem, for calculations, layout design and post-processing in the script page.
- ❖ **Multiple layouts:** The user can build many designs in the same project file that helps to create efficient designs. Each OptiSystem project file can include many designs.

1.9 Impact on the Society

1. High speed wireless data communication
2. Low electromagnetic interference
3. Can be used in crowded places without jamming
4. Can be used in tunnels and hazardous conditions where conventional communication fails

1.10 Organization of the Thesis

This thesis consolidates the whole work carried out in 9 chapters. The references relevant to each chapter are given at the end of the thesis. Chapter 1 briefs about the general introduction of RoF communication. A section of the chapter deals with the different nonlinear distortions and its method of reduction. The chapter ends up with objectives, motivation and organization of the thesis.

Chapter 2 gives the literature review of different cases related to nonlinear distortion and its reduction methods. Knowledge of the above methods is very crucial and hence develop methods for mitigation of nonlinear distortions in RoF communication. Methodology and performance evaluation parameters are also discussed.

Chapter 3 discusses the reduction of nonlinear distortion in the photodetector of the RoF communication system with a Square Root nonlinear equalizer.

Chapter 4 proposes the method of nonlinear distortion reduction in the wireless channel using MLSE equalizer. Comparison of the proposed method with the state of the art methods is also given.

Chapter 5 deals with four methods of nonlinear distortion reduction in optical fiber. These methods are compared using different performance parameters. Also, these methods are compared with the existing methods.

Chapter 6 explains an 80Gbps Multi-Band Access RoF link with SSB Optical mm Wave Dispersion Tolerant Transmission. A novel low cost RoF link is also presented with a SSB optical mm wave signal to carry the 40GHz, 80GHz and 120 GHz mm wave multiband wireless accesses.

Chapter 7 proposes a 200 GHz mm wave RoF access network using a Peer to Peer interconnection architecture. An Additive Gaussian White Noise wireless channel with long haul Single Mode Fiber of 170 Km transmission length is used against the wireless channel.

Chapter 8 provides a performance analysis of the RoF communication system with the integration of different nonlinear reduction methods. It shows that the results obtained are promising. Chapter 9 gives the conclusion and future work.

Literature Review

- 2.1 Challenges and Mitigation Methods in RoF Technology
- 2.2 Impact of Chromatic Dispersion and Mitigation
- 2.3 Nonlinear Distortion and Mitigation
- 2.4 Performance Evaluation Parameters
- 2.5 Performance Evaluation Criteria

Abstract

This chapter discusses the different nonlinearities includes the nonlinear distortion and chromatic dispersion in the optical fiber. Their reduction is explained in the literature review. The chapter concludes with the performance measures and methodology.

2.1 Challenges and Mitigation Methods in RoF Technology

Several methods have been reported for the generation of modulated RF optical carriers in fiber-wireless systems. Some methods are optical heterodyne [53] and self-heterodyne techniques [54] and method with pulsed lasers [55], [56]. An intensity modulation method with direct or external modulation of a laser is the simplest technique used for the RF signal generation and distribution. The RF signals are either externally or directly modulated onto the optical carrier. These optically modulated RF signals are transported over an analog photonic link. This approach has led to a simple BS unit design with centralized control and management of the wireless signals. So it only requires optical to electrical conversion and RF amplification. Another method employed a single optoelectronic device, Electro-Absorption Modulator (EAM), which act as a photodiode for the downlink and as a

modulator for the uplink. It could replace the laser, photodiode, circulator [57]–[60]. A new scheme was proposed to generate Double Sideband (DSB) optical millimeter (mm) wave with signal carried only by optical carrier that led to the least effect of a time shift of the sidebands and suffered by fading effect only [61]. The downlink 2.5 Gbps data was successfully transmitted over 20 km Single Mode Fiber (SMF) with less than 0.15 dB power penalty. It used the four-wave-mixing effect of semiconductor optical amplifier for mm wave generation in a mm wave RoF system [62] and multiple frequency Brillouin fiber-ring laser method [63]. A new scheme was proposed to generate a frequency diversity Binary Phase Shift Keying (BPSK) signals for RoF system. They had huge capacity, mobility and supported both fixed and mobile users [64]. This duplex system generated 20 GHz and 40 GHz mm wave signals with a data rate of 1.25 Gbps. It used one Electrical Optical Phase Modulator (EOPM) and one Mach–Zehnder Modulator (MZM) at the central station and with one additional MZM at the BS. For conventional modulation with large RF modulation index, the Optical Single Sideband (OSSB) signal experiences much distortion at the BS. The performance of the transmission link was largely improved in single channel and Dense Wavelength Division Multiplexing (DWDM) with reduction of undesired harmonics by using a novel MZM technique [65]. It had a 1×4 multimode interference MMI Coupler and four optical phase modulator waveguides to generate OSSB signals in the RoF transmission link. The other schemes involved optical mm wave generation and transmission of 1.25 Gbps downstream links with a gain switched laser [66], a 64 GHz optical mm wave generation via a nested LiNbO₃ MZM with an 8 GHz local oscillator [67], using one dual parallel MZM with optical carrier suppression [68], without carrier suppression [69] and via frequency 12-Tupling [70]. The study has

revealed that RF signals experience a number of inevitable signal impairments in RoF links such as nonlinear distortion that consist of Harmonic Distortions (HDs) and Intermodulation Distortions (IMDs). They are generated due to the nonlinear modulation characteristics of the optical modulators and reduce the dynamic range. In addition, the impact of fiber chromatic dispersion on the transported RF signals becomes more pronounced with increasing RF carrier frequency. Several different strategies have been proposed and demonstrated to measure and overcome these impairments.

2.2 Impact of Chromatic Dispersion and Mitigation

In conventional Intensity Modulation (IM), the optical carrier is modulated to generate an optical field with a carrier and two sidebands. At the optical receiver, each sideband beats with the optical carrier and two beat signals are generated. They constructively interfere to produce a single component at the RF frequency. When the signal is transmitted through an optical fiber, chromatic dispersion induces different phase shifts depending on the transmission distance, radio frequency and the dispersion parameter. These phase shifts produce a relative phase difference between the carrier and each sideband. This results in the degradation the power of the composite RF signal. These phase changes in the optical sidebands changes the resultant phase of the RF beat signals and the RF power, P_{rf} will vary [71]as,

$$P_{rf} \propto \frac{LD^2f^2}{c} \quad (2.1)$$

where D is the fiber dispersion parameter in ps/nm/km, c is the velocity of light in vacuum, L is the fiber transmission length, f is the RF carrier frequency, and λ is the carrier wavelength. From the equation (2.1), it is seen that the RF power varies in a periodic manner with complete power suppression occurring at specific modulating frequencies and at a phase difference of π . As the RF frequency

increases, the effect of dispersion becomes more pronounced and the fiber-link distance gets severely limited [71]–[73].

Various techniques were proposed and demonstrated to mitigate fiber dispersion effects in RoF system with Up/Down Conversion techniques [74]–[78]. The IF signals were transmitted over optical fiber instead of the RF signal and have minimum fiber dispersion induced power degradations due to the low fiber dispersion effect. But, unfortunately, these techniques have high cost. A simple configuration developed with high speed external modulators such as the EAM in RoF system design [79]–[83] has supported high frequency RF signals. By varying the chirp parameter of a Dual-Electrode Mach–Zehnder external modulator (DEMZM) to give large negative chirp biased at quadrature, dispersion induced power degradations were reduced in fiber-wireless systems. A data rate of 51.8 Mbps was transmitted successfully with BPSK modulation at 12 GHz frequency over standard SMF of length 80 km.

A DEMZM was used to generate an optical carrier with single sideband (SSB) modulation [79], [80] with a minimum laser spectrum width of the light source. These methods provided both simple implementation and high linearity [82]. But they suffer from RF loss, high insertion loss, frequency chirping, high drive voltage and 6 dB power penalty. The electro-optical modulator was biased at the minimum transmission point, instead of the quadrature point. It saved energy and maintained high frequency-length product in mm wave communication [83]. The optical carrier suppression techniques [83], [84] have proved to be a feasible solution for the future RoF based optical-wireless access networks. They provided a successful transmission of 2.5 Gbps data for bidirectional transmission through a fiber length of 40 km with a low power penalty. These simple methods has low cost, high spectral efficiency and good performance.

Also in addition to the above mentioned techniques, external filtering with fiber grating was also used to produce SSB optical modulation for the elimination of the fiber dispersion penalty on conventional external optical intensity modulation at mm waves [85]–[88]. A filter designed with three dynamic Bragg gratings which is controlled by an input optical DSB signal, independent of the modulated optical carrier wavelength and can generate SSB signals were used to mitigate the power degradation due to chromatic dispersion [87]. An Arrayed Waveguide Grating (AWG) device operated as a wavelength multiplexer of the different optical channels and SSB generator was used at very high frequencies (>20 GHz) to eliminate the Carrier Suppression Effects (CSE) [88]. The fiber nonlinearities such as SPM and FWM have also played a vital role to reduce the dispersion penalties [89]–[92]. A significant reduction of chromatic dispersion effects was achieved by generating a chirp distortion effect in fiber opposite to that induced by the chromatic dispersion [89], a phase-conjugated wave by means of FWM in a DSF placed at the mid span of the fiber-optic link [90] and mid-span optical-phase conjugation [93]. The Optical Heterodyne schemes [94] have offered a minimum fiber dispersion effect with high intensity of modulation depth. They provided high link gain with high Carrier-to Noise Ratio (CNR) but had a more complexed system design due to complicated light sources.

2.3 Nonlinear Distortion and Mitigation

In the RoF architecture, data signals are originated at a CS, modulated by an optical carrier, transported over an optical fiber to many BSs and then released to the medium of air for users. These hybrid RoF systems separate the conventional radio spectrum into a number of channels for transmission. The used RF bands are higher than the 2.4 GHz RF band that is used in the current 3G systems. A major problem that may be found in RoF networks will be

nonlinearity issues of the various devices in the link. When the multi-channel RF signal is directly modulated, the dynamic nonlinearity of the laser source may inflict major problems on the system performance due to Inter Modulation Distortion (IMD) effects. Many research works were done to reduce this nonlinearity issue. The external injection in the directly modulated laser from a second laser source reduce the nonlinearity of laser diodes. Using the external injection method, the relaxation frequency of the laser could be increased. Also, the modulation response at lower frequencies was more linear than that without external injection [95]–[99].

In the RoF communication links, the system performance was improved by the enhanced modulation response of the laser. But the performance of the multicarrier RoF system was degraded by the nonlinear characteristics of the laser. The linearized laser modulation response made a performance improvement of 2 dB for a multi-carrier RoF communication system working at a frequency of 6 GHz [99]. The link performance was improved by reducing the second and third-harmonic generations of single and two-tone RoF systems using external-laser modulation techniques with EDFA [100], [101]. The third-order Inter Modulation (IMD3) suppression was reduced by 38 dB even after 20 km of distance or dispersion using a Vector Control Theory (VCT) based circuit [102]. The nonlinear effects due to optoelectronic conversion were reduced by keeping the amplitude of the drive signals at low values. The RoF signals had fragile modulation due to the thin linear region of intensity modulators which causes low conversion efficiency and low carrier to side band ratio. The link performance was improved by using a high-power optical source, but this leads to increase the inter-modulation distortions at the optical receiver.

As the modulation efficiency was low at mm wave frequencies, the mm-wave radio signals were feebly modulated by the optical carrier with a large carrier to sideband ratio. The higher modulation depth helps to improve the system dynamic range and to reduce carrier to sideband ratio of the mm wave modulated signal. It must be operated above the Stimulated Brillouin Scattering (SBS) threshold voltage to reject the carrier signal and to pass the modulation sidebands with low loss [103], [104]. The efficiency was improved by using an external delay filter with MZM modulator biased at quadrature point [105] and by the carrier reduction method using a Fabry Perot filter working in the reflection mode [106]. The higher modulation depth can improve the link efficiency, but as the bias voltage is shifted to zero, the second order distortion products are increased. An alternative method of carrier filtering is done with a feedback loop to control the MZ biasing to produce a photocurrent of 1.5 mA. For carrier filtering, the MZM must be operated at the minimum transmission point. The bias shift method of carrier filtering introduces low loss and needs fewer components involvement compared with an external filter. A number of techniques have been proposed for increasing the modulation efficiency of the mm wave modulated signals, including Brillouin scattering schemes and external optical filters. But they increase the system complexity and cannot be applied to a wide range of signal formats, modulation depths and radio frequencies. Therefore, the simple and inexpensive passive techniques have been reported using narrowband fiber Bragg grating having different reflectivities. They helped in increasing the modulation depth to provide better transmission performance for RoF systems [107]–[109]. These techniques were applied to a wide range of radio frequencies and modulation depths. They are applied in a conventional downstream link and to the upstream in a wavelength-reused scheme. The

performance of the fiber-wireless links has significantly improved when the optical signal is transmitted at an optimum CSR of 0 dB [110].

The microwave carrier through the radio channel was directly modulated by the optical signal [111] at a remote antenna station. This had generated severe harmonic distortion due to optical fiber chromatic dispersion and its effect on the received signal increased as the square of the magnitude of the RF signal [112]. Many equalization methods in the electrical and optical areas have been employed with electronic equalization owing to superior adaptability and low cost. Due to the linear characteristics of the optical field, inexpensive linear equalizers were used to compensate the chromatic dispersion. But the square-law characteristic of the photodiode produced the harmonic distortion and it drastically reduced the efficiency of linear equalization [112].

2.4 Performance Evaluation Parameters

Performance measurement is a major factor required for any network. It shows the unit of the quality of the service provided by the network. These measures respond to the performance issues existing in the current communication systems. The different measures that have used to assess the performance of RoF communication are [113]:

2.4.1 Quality Factor

The Quality factor (Q factor) is an important performance parameter that shows the quality of an optical communication system. The quality of the optical signal increases with increasing Q factor. Q factor measurement is associated with the analogue signal. The Q factor gives the measure of the destruction due to optical noise, nonlinear effects and chromatic dispersion. The quality factor is defined as,

$$Q = \frac{(v_1 - v_0)}{(\sigma_1 - \sigma_0)} \quad (2.2)$$

Here, v_1 , v_0 are the average values of the signal, $v(t)$. σ_1 and σ_0 are the Root Mean Square (RMS) values of the additive white noise [113].

2.4.2 Bit Error Rate (BER)

Bit error rate BER is a parameter to give the performance indication of a data link such as radio communication or fiber communication system. As number of errors that occur in a datalink is one of the main parameters, the BER is an important parameter for performance analysis. In an optical system, the BER and Q factor are used for performance analysis. The relationship between BER and Q factor can be given as,

$$BER = \frac{1}{2} \operatorname{erfc} \left(\frac{Q}{\sqrt{2}} \right) \quad (2.3)$$

For large values of Q (typically $Q > 3$) the complementary error function may be approximated by an exponential function and the BER may be expressed as:

$$B \approx \frac{e^{-\frac{Q^2}{2}}}{Q\sqrt{2\pi}} \quad (2.4)$$

Bit Error Rate is defined as the rate at which errors occur in a transmission system. Error is basically the change of bit 1 to bit 0 and vice versa. BER gives the approximate estimation of the error probability. It can be calculated by dividing the error bits with the number of bits transmitted. It is a unitless measurement.

BER= number of erroneous bits/ total number of bits

Let the probability of receiving bit 1 when bit 0 is transmitted be denoted as $P(1/0)$ and probability of receiving bit 0 when bit 1 is transmitted be denoted as $P(0/1)$. Then BER would be given as,

$$\text{BER} = 0.5 [P(1/0)+P(0/1)] \quad (2.5)$$

Equation 2.4 shows that BER is a strong exponential function of Q .

For an optical network the value of BER should always be lesser than 10^{-9} . There are following factors that affect the BER;

Transmission Channel Noise

It is the noise which is added to the transmitted signal during its propagation through transmission channel.

Interference

The signals from the adjacent channels overlap with each other and degrade the quality of the original signal.

Bit Synchronization Problems

When the received bits are not synchronized with the transmitted bits then there is a probability of loss of data bits. This will increase the BER value of the signal.

Attenuation

When the amplitude of the received signal gets reduced in comparison to the amplitude before transmission, then attenuation is said to have taken place.

Wireless Multipath Fading

It is the fading which is caused because of the multipath propagation of the signal. For fiber optic systems, bit errors mainly result from imperfections in the components used to make the link. These include the optical driver, receiver, connectors, and the fiber.

Transmitter Power

Transmitter power has to be balanced with the factors affecting the – interference levels and the power output of the power amplifier, total power consumption etc.

Order of the Modulation

Lower order modulation schemes have lower data rate with higher robustness to noise. Also, the higher modulation schemes can support higher data rates with higher noises.

Bandwidth

The BER can be reduced by reducing the bandwidth. The noise levels can be reduced and therefore the signal to noise ratio will be higher.

2.4.3 Signal to Noise Ratio (SNR)

Even though the optical fiber provides enormous bandwidth; its power-handling performance is poor. The single-mode fiber optic cable has a small central core that permits only one mode of light to travel. Due to intricate construction of single-mode cables, their initial cost is greater than multi-mode fiber. Also, the modulation depth of RoF links should be kept small to limit nonlinear distortions of optical modulators. So only a fraction of the total power is allocated in RF sidebands. The power losses in the optical domain are found to be twice in the electrical domain due to the square-law behavior of

the photodiode. Hence the received RF power at the optical detector is typically very low depending on the fiber length . This has to be improved drastically at the Remote Access Point (RAP) before driving an antenna to overcome wireless channel path losses. In a RoF communication system, the analog RF signal suffers losses in optical and wireless channels. So the RF signal strength is weak at the optical receiver and the wireless receiver. Therefore, two SNRs such as, optical SNR (OSNR) and electrical SNR can be defined in RoF communication. An optical SNR (OSNR), is due to noise in the optical domain and an electrical SNR (ESNR) is due to noise in the electrical domain. The resulting Cumulative SNR (CSNR) is a weighted sum of two SNRs. The system performance is increased with CSNR and it is smaller than the smaller of these two SNRs.

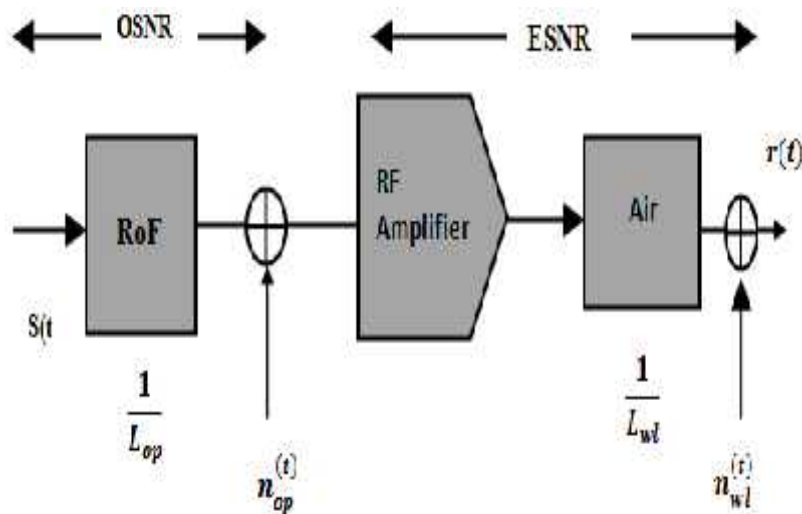


Fig.2.1 Losses, Gain and Noises in a RoF communication system

Fig. 2.1 shows the gains and losses that occur in the optical and wireless portions of the RoF communication system. The input RF signal $S(t)$ has suffered a steep loss at the RF-optical conversion stage. Then it has a linear loss as a function of fiber length due to fiber attenuation. Further, there

is a steep loss due to optical-RF conversion. All these three losses, including optical connector/splitter/splicing losses in the optical domain are cumulatively referred to as L_o . The optical link noise gets added at the optical receiver. The OSNR can be defined as the ratio between the RF signal and optical link noise powers.

Then, the optical noise plus signal is amplified by the RF amplifier at the RAP with gain G_{op} . After this stage, the RF signal (plus optical noise) is passed through a wireless channel, experiencing a loss of L_w .

SNR considering only the RoF link noises and losses is expressed as

$$OSNR = \frac{M^2 + E[I_{id(t)}^2]}{\langle I_s^2 \rangle + \langle I_R^2 \rangle + \langle I_T^2 \rangle} \quad (2.6)$$

where $M=1$, $i_{d(t)}$ = AC component of current, I_R^2 = Relative Intensity Noise power, I_s^2 = shot noise power and I_T^2 = thermal noise power.

The cumulative SNR is expressed as

$$CSNR = OSNR \left[\frac{1}{1 + \left(\frac{L_w}{G_c} \right)^2} \right] \quad (2.7)$$

where L_w is the losses in the wireless channel.

2.4.4 Eye Diagram

It is a parameter to quantify the quality of signal. It is used to measure the mutual effect of the channel noise and inter-symbol interference. Eye should be broadly opened for good transmission. The eye pattern gives different parameters and they can provide different information.

❖ **Eye height:** It quantifies the presence of additive noises.

- ❖ **Eye closure:** It is a measure of inter-symbol interference.
- ❖ **Eye overshoot / undershoot:** It shows the signal distortions due to losses in the propagation of the signal.
- ❖ **Eye width:** It shows the synchronization and jitter effects.

2.5 Performance Evaluation Criteria

The following performance parameters are used

- ❖ BER
- ❖ Q Factor
- ❖ Eye Diagram
- ❖ SNR

Reduction of Nonlinear Distortion in the Photodetector of RoF Communication System

3.1 Introduction

3.2 Case-I: OSSB on RoF Communication Using SQRT Nonlinear Equalizer

3.3 Case-II: ODSB-CS with Reduced Photodetector Nonlinearity

Abstract

This chapter describes about the reduction of nonlinear distortion in the photodetector. The proposed method is implemented in two systems. The SNR performance of the proposed method is compared with the existing methods. This chapter ends up with the conclusion that the proposed method has better performance as compared to the existing system.

3.1 Introduction

Transmission of microwave and mm wave signals through optical fiber has low cost antenna terminals and large active frequencies. For simple far-off antenna stations, the microwave carrier passing through the radio channel is directly modulated in the optical wavelength [114], but it produces severe harmonic distortion caused by optical fiber chromatic dispersion whose degrading effect on the received signal increases with the square of the amplitude of the radio carrier [115]. To compensate for this, a variety of equalization techniques, both in the optical and electrical domain have been proposed [116]–[118], with more prominence provided to electronic equalization which has high flexibility and less cost [118]. Due to the linear effect of the optical field, economical linear equalizers can entirely compensate for chromatic dispersion. The square-law characteristic of the photodiode produces harmonic distortion in the detected signal. This significantly reduces the effectiveness of linear equalization [119].

There are two methods to generate the optically modulated RF signal: direct and external modulation. The direct modulation scheme suffers a chirp effect and causes severe degradation of the system performance. However, this can be reduced by using the external-Mach Zehnder modulation scheme. Even though the external modulation scheme is used, the traditional Optical DSB (ODSB) modulation degrades the received RF signal power due to fiber chromatic dispersion. To overcome the power degradation, an OSSB signal is produced by a phase shifter and a DEMZM [120].

To meet the rapid growth for bit rate and bandwidth demands in communication systems, the convergence of wired and wireless networks is a promising solution. RoF with the combination of optical and wireless systems [121]–[125], is an effective solution for increasing the transmission capacity, flexibility, providing broad bandwidth and low attenuation characteristics. Generally, the ODSB modulation technique is employed in RoF transport systems. However, to transmit the optical carrier and both sidebands are not the most effective way of information transfer. Optical bandwidth is halved in the OSSB modulation technique since the optical signal spectrum has been reduced by a factor of two [126]. With optical SSB modulation technique, RF power degradation due to fiber dispersion is reduced and thus the performance of the system is improved. The dispersion-induced broadening of short pulses propagating in the fiber at high rate causes crosstalk between the neighboring time slots. This introduces error which eventually increases as the communication distance goes beyond the dispersion length of the fiber [127]. The introduction of Erbium-Doped Fiber Amplifiers (EDFA) working in the 1550nm region increases the link distance and reduces the fiber loss in the optical communication systems [128].

A mm wave fiber-wireless architecture consists of a CS which is connected to a large number of antennas or THz antennas [129] at the BS through RF-over-fiber, IF-over-fiber and Baseband-over-fiber [130]. Such methods use a Mach–Zehnder Intensity (MZI) modulator to generate the required optical carrier frequency to provide point to point and point to multipoint links. The RoF, such as Hybrid Fiber Radio (HFR) [131] is propagated through fiber links towards remote BSs. This architecture is an attractive method for broadband access because it permits quick and cost effective network installation. Generally in a RoF system, the CS transmits optical carriers modulated at Radio Frequency (RF) to BS. Optical fiber can be used as an excellent medium for RF signal transmission due to the very high bandwidth, low loss, small cross section and low cost. The RoF systems can be used for many wireless applications such as Fiber-to-The-Home (FTTH), Universal Mobile Telecommunications System (UMTS), Vehicular Ad-Hoc Network (VANET) [132] and microcellular system [133], [134]. The RoF THz frequency can provide these technologies to enrich the capacity and security. This makes THz communication to be one of the preferred technologies.

Square root (SQRT) transfer function [135] module (SRm) that is placed after the photodiode compensates for the square-law characteristic and thereby improve the performance of linear equalizers. The linearization capabilities of the SQRT module are analyzed using the model of the dispersive fiber and the transfer functions of the SSB modulation. The study considers the levels of second and third order harmonics generated by each scheme, for a single RF carrier signal. The spectral characteristics provide better assessment about the system linearization of linear equalizers in digital systems and are relevant to the performance measurement of broadband RoF systems [136].

The researchers are trying to reduce the penalty generated by Inter Symbol Interference (ISI) in optical communication systems. Polarization Mode

Dispersion (PMD) and Chromatic Dispersion produce ISI. As some of the distortions are linear, a linear Electronic Equalizer (EE) can be used to reduce the distortions. Although they have high flexibility and low cost, an optical communication system is inherently nonlinear because of the square-law nonlinearities that are introduced by the photodiode.

3.1.1 Different Carrier Suppression Techniques

By suppressing the optical carrier power of the mm wave, the performance of the RoF link can be improved. In long distance transmission system, the DSB-CS modulation scheme can provide the best receiver sensitivity, highest spectral efficiency and smallest power penalty [137]. A photodiode with a power penalty less than 0.3dB is used to detect the baseband (BB) and RF signal. The noise contributions such as noise figure, thermal noise and shot noise [139] can be reduced by Carrier Suppression (CS) [138]. A DSB-CS optical signal [140] can be generated by a MZM through external modulation. Different methods like, low biasing of MZM [141], optical carrier filtering [142] and Stimulated Brillouin scattering [143] can be used to suppress the undesired optical carrier.

3.2 Case I- OSSB on RoF communication using SQRT nonlinear equalizer

3.2.1 Theoretical analysis of SSB modulated THz Signal using balanced MZM

Generally, RoF systems transmit an optically modulated radio frequency signal from a CS to BS via an optical fiber. An OSSB signal is produced by a DE-MZM and a 90 degree phase shifter. The generated RF signal is optically modulated by a Laser Diode (LD) and a DEMZM [136].

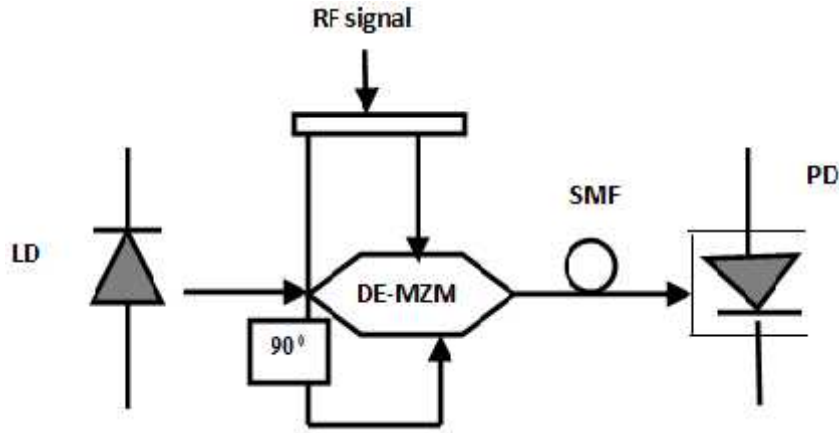


Fig. 3.1 Single-tone OSSB–RoF transmission system

RF: radio frequency signal at 20 GHz; LD: Laser Diode; DEMZM: dual-electrode Mach-Zehnder modulator; SMF: single mode fiber; PD: photodiode

The optically modulated signal is transmitted to the BS, where the received RF signal is recovered by using a photodetector and a BPF. It arrives at a User Terminal (UT) through a wireless channel as in Fig.3.1 [136]. The optical signals from the laser and the RF oscillator are represented mathematically as,

$$X_L(t) = A \exp(j(\omega_L t + \phi_L(t))) \quad (3.1)$$

$$X_R(t) = V_R \cos(\omega_R t + \phi_R(t)) \quad (3.2)$$

where A and V_R are the amplitudes of signals from the LD and the RF oscillator, respectively. The ω_L and ω_R are angular frequencies of the signals from the LD and the RF oscillator. The $\phi_L(t)$ and $\phi_R(t)$ are the phase noise processes and $\phi_L(t)$ is characterized by a Wiener process as,

$$\phi_L(t) = \int_0^t \dot{\phi}_L(t) dt \quad (3.3)$$

The time derivative $\dot{\phi}_L(t)$ is not flat at low frequencies due to $\frac{1}{f}$ noise. The white phase noise is the principal cause for line broadening and is associated with quantum fluctuations.

Thus, $\dot{\phi}_L(t)$ can be modeled as a zero-mean white Gaussian process with a PSD,

$$S_{\dot{\phi}_L}(f) = 2 \Delta\nu_L \quad (3.4)$$

where $\Delta\nu_L$ is the laser linewidth. The signal $x_R(t)$, is optically modulated by $x_L(t)$ with a DE-MZM, and the modulated signal is given by equation (3.5) as shown below,

$$E_O(t) = AL_M \left[J_0(\alpha\pi) \exp(j(\omega_L(t) + \phi_L(t) + \frac{\pi}{4})) - \sqrt{2} J_1(\alpha\pi) \exp(j(\omega_L(t) + \phi_L(t) + \omega_R(t) + \phi_R(t))) \right] \quad (3.5)$$

where $\alpha = \frac{V_R}{\sqrt{2}V}$ is the normalized ac value, V is the switching voltage of the DEMZM, L_M is the insertion loss of the DE-MZM, and ϕ is the phase shift by the phase shifter. For $V_\pi > V_R$, the high-order components of the Bessel function can be neglected. After transmitting the OSSB at the output of DEMZM through standard SSMF length, L_f is represented as,

$$E_O(L, t) = A L_M L_L 10^{-\frac{\alpha_f L_f}{2}} J_0(\alpha\pi) \exp(j(\omega_L(t) + \phi_L(t) - (\phi_{1+\tau} - \phi_{1-\tau}))) - \frac{\sqrt{2} J_1(\alpha\pi)}{J_0(\alpha\pi)} \exp(j(\omega_L(t) + \phi_L(t) + \omega_R(t) + (\phi_R(t-\tau) - \phi_R(t)))) \quad (3.6)$$

where L_L is the additional loss in the optical link, α_f is the SSMF loss, L_f is the transmission distance of the SSMF. τ and τ_+ are group

delays at a center angular frequency of $\omega_L(t)$ and an upper sideband frequency of $\omega_L(t) + \omega_R(t)$. ϕ_1 and ϕ_2 are phase-shift parameters for specific frequencies due to the chromatic dispersion. With a square-law model, the photocurrent 'i(t)' can be obtained from equation (3.6) as,

$$i(t) = R|E_{\text{opt}}(L, t)|^2 = RA_1^2 [B + 2\alpha_1 \cos(\omega_R(t) + \dots)] \quad (3.7)$$

where

$$A_1 = A \cdot L_M \cdot L_{\text{eff}} \cdot 10^{-(\alpha_f \cdot L_{\text{eff}})} / 20 \cdot J_u(\alpha)$$

$$\alpha_1 = \frac{\sqrt{2}}{J_u} J_1(\alpha\pi)$$

$$\beta = 1 + \alpha_1^2$$

where R is the Responsivity of the photodetector

3.2.2 Simulation Setup

As in fig.3.2, a simple non-linear equalizer with the square-root mathematical function, just after the photo-detector and before the conventional electronic equalizer linearizes the overall system performance of optical communication system. The optical field amplitude and generated current of a photodiode is an intrinsic square-law non-linear function. It can be reduced by a nonlinear electrical circuit with square root (SQRT) function after the photodiode. The SQRT module is designed using MATLAB programming and placed after the photodiode to reduce the square law nonlinear characteristics of the photodiode.

The important method of the optical millimeter wave generation is an intensity external modulation by using an external modulator. To reduce the power penalty problem, the SSB modulation is generated with a DD-MZM modulator. Fig.3.2 shows the simulation setup of a SSB 60 GHz RoF communication system. Continuous wave is generated from a CW laser at 193.1 THz, line width of 10 KHz and is modulated by a radio frequency of 60 GHz

analog signal through a DEMZM, which is biased at quadrature point. This RF signal is applied directly to one arm of the DEMZM modulator and the same RF signal with phase shift of 90 degree is applied to the second arm of the modulator to generate an optical single sideband RF signal as it requires less bandwidth than DSSB–RoF system and is tolerable for power degradation due to chromatic dispersion, through a standard single-mode fiber. The signal is transmitted through a SSMF of length 100 km and first order dispersion of 17 ps/nm/km. The optical signal is amplified by an EDFA. At the remote station the signal is received by a PIN photo detector. The SNR is very low due to the intrinsic square law nonlinear function of the photodetector. It is improved by using a SQRT nonlinear equalizer. The amplified signal is filtered by using a band pass filter with cutoff frequency 60 GHz and bandwidth 1GHz. The RF signal is obtained at the receiver. The simulation parameters are shown in table 3.1.

Table 3.1 Simulation Parameters

Serial No.	Quantity	UNIT
1	Laser frequency	193.1THz
2	Laser Power	10 dBm-20dBm
3	Fiber Attenuation	0.2dB/km
4	Fiber Length	100 Km
5	Fiber dispersion	16.75 ps/nm/km
6	Differential Group delay	0.2ps/km
7	Maximum phase shift	3mrad
8	Photodetector responsivity	1A/W
9	Photodetector current	10nA
10	Photodetector center frequency	193.1Thz
11	Photodetector sample rate	5Hz
12	Photodetector thermal noise	10^{-22} W/Hz

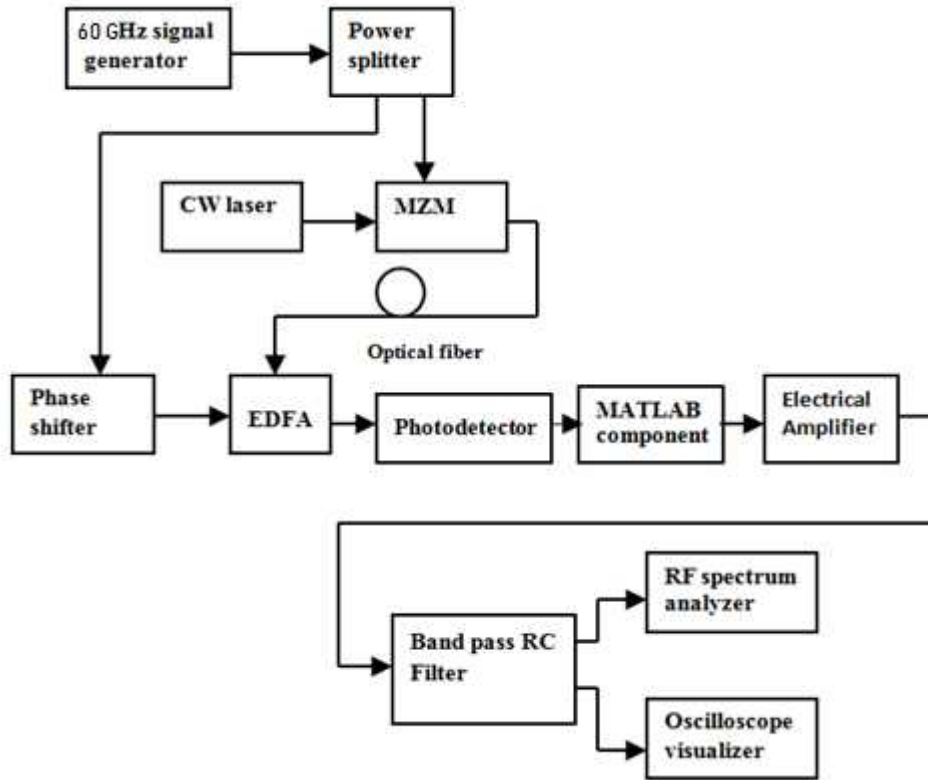


Fig. 3.2 Block diagram of SSB communication System, CW- Continuous Wave, EDFA- Erbium Doped Fiber Amplifier, PD- Photodetector

3.2.3 Results and Discussion

For intensity modulation, modulating analog signal is generated at 60GHz and optical carrier is generated at 193.1 THz as in Fig.3.3 (a) and Fig. 3.3(b). The dual electrode MZM is operating at quadrature point and the obtained SSB is shown in Fig.3.4 (a). The generated signal is transmitted through a 100 km SSMF and reached at the remote station. Fig. 3.4(b) shows the photodetector output.

A SQRT nonlinear equalizer is used to reduce the nonlinearities in the photodetector and the equalized output is shown in Fig.3.5 (a). RC band pass filter (BPF) with a cut off frequency of 60 GHz , bandwidth = 1.5 bitrate and maximum attenuation value is 100 dB is used to detect the RF signal as in

Fig.3.5 (b). The absolute results are obtained due to the ideal parameters of the RC band pass filter. An electrical carrier analyzer is used to measure the SNR for two different frequencies at 4 GHz and 5 GHz as shown in Fig.3.6. The SNR of the receiver without equalizer is measured for different carrier powers from -20dBm to +20 dBm.

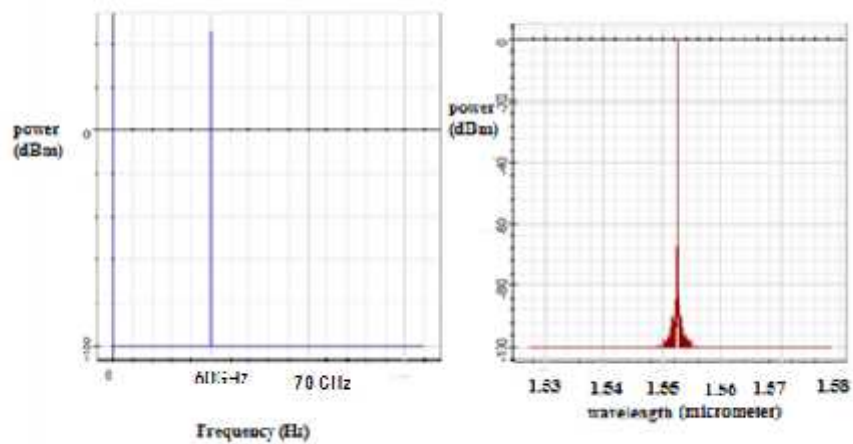


Fig. 3.3 (a) RF input (modulating signal) at a frequency of 60 GHz, (b) Laser input (optical carrier) at a center frequency of 193.1 THz

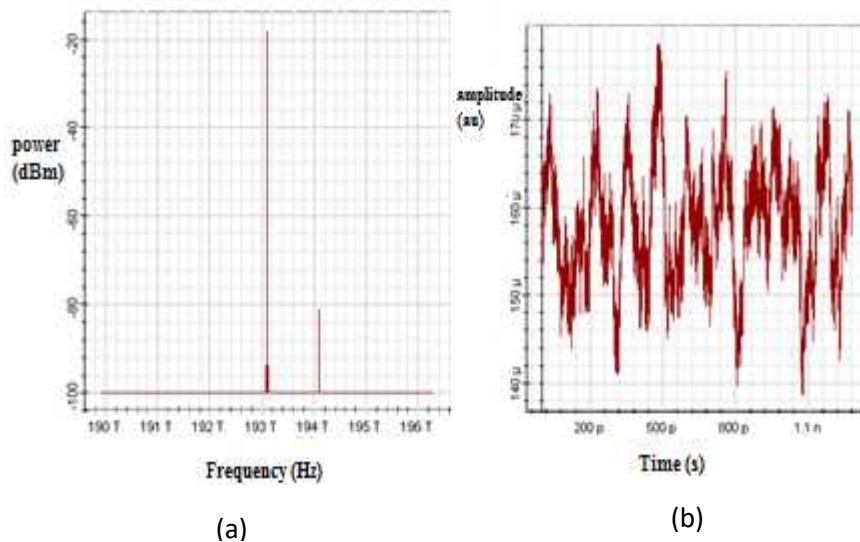


Fig. 3.4 SSB (MZM) output at quadrature operating point

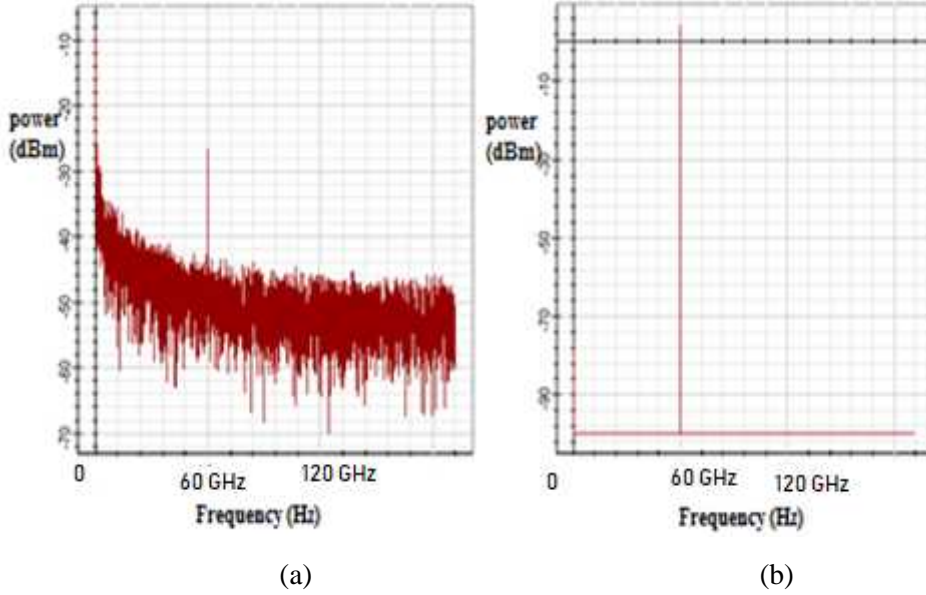


Fig. 3.5(a) SQRT nonlinear equalizer output, (b) RC BPF output (detected message signal) at 60 GHz

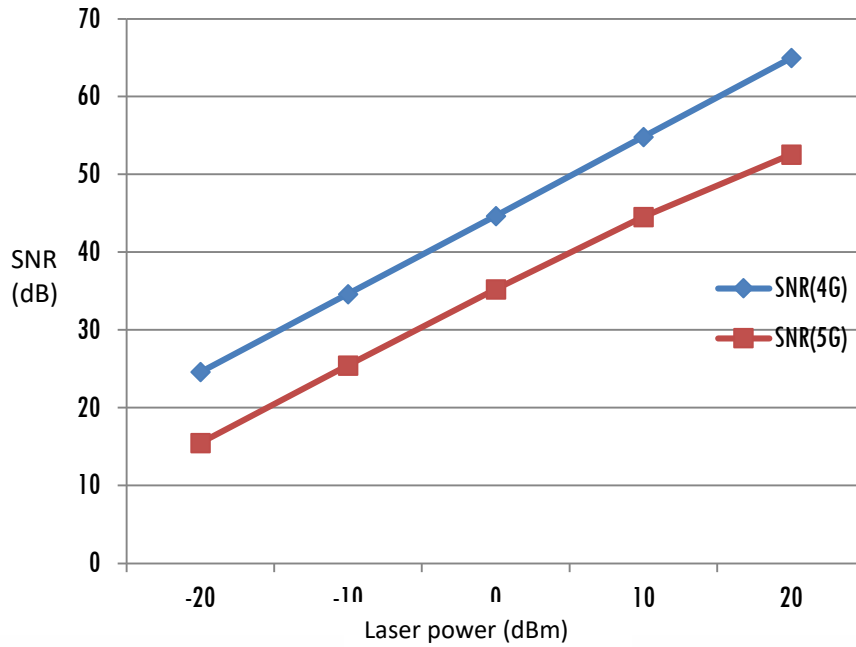


Fig. 3.6 SNR (at 4 GHz and 5 GHz) of photodetector

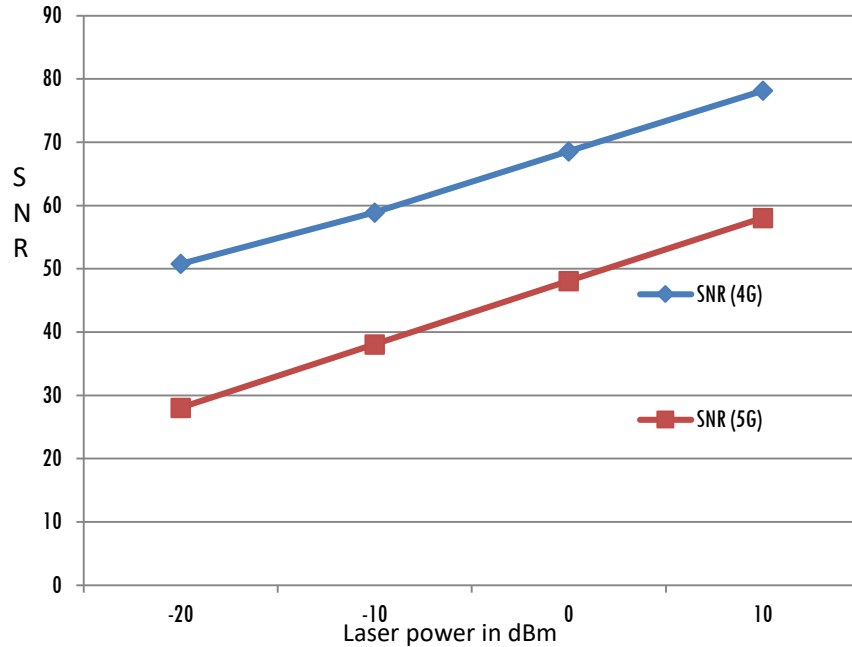


Fig. 3.7 SNR (at 4 GHz and 5 GHz) of photodetector with SQRT nonlinear equalizer

The SNR changes from 24dB to 64dB for 4 GHz and 15 dB to 52dB for 5 GHz as shown in Fig.3.7. When a SQRT equalizer is used at the receiver, the SNR is increased from 50dB to 87dB for 4 GHz and 28dB to 68dB for 5 GHz.

3.2.4 Conclusion

A SQRT nonlinear equalizer is used to reduce the nonlinearities in the photodetector. The other nonlinearities in the receiver are not considered. In practical cases there will be variation from these results due to the presence of different nonlinearities at the receiver. An electrical carrier analyzer is used to measure SNR for two different frequencies at 4 GHz and 5 GHz. The SNR of the receiver without equalizer is measured for different carrier powers from -20 dBm to +20 dBm. The SNR varies from 24 dB to 64 dB for 4 GHz and it varies from 15 dB to 52 dB for 5 GHz. When the SQRT equalizer is used at the receiver, the SNR is improved from 50 dB to 87 dB for 4 GHz and 28 dB to 68 dB for 5 GHz.

3.3 Case II – ODSB-CS with Reduced Photodetector Nonlinearity

3.3.1 Principle of Optical Double Side Band Suppressed Carrier (ODSB-CS) Modulation

There are various techniques for generation of mm wave signals that can be used in various applications. One of the simplest methods for generating and optically distributing RF signals is to directly modulate the intensity of the light source (laser) with the RF signal. The laser is driven with the desired mm wave frequency. The carrier is filtered and direct detection is used at the photodetector to recover the RF signal [144] as shown in Fig.3.8. The second option is to drive the laser in Continuous Wave (CW) mode and then utilize an external modulator such as the LiNbO₃ MZM modulators to modulate the intensity of the light. Such external modulators can sustain high frequency RF signals and can be used for generation and data up conversion through optical carrier sub multiplication as shown in Fig. 3.9[141].

Fig. 3.10 shows the principle of the optical mm-wave generation using the OCS modulation scheme. The output electrical field of the MZM is given as [141],

$$E_o(t) = E_o \cos \left[\frac{\phi(V(t))}{2} \right] \cos(\omega_c t) \quad (3.8)$$

where E_o and ω_c are the amplitude and angular frequency of the input optical carrier. $V(t)$ is the input driving voltage, and $\phi(V(t))$ is the phase difference that is generated by $V(t)$ between the two arms of the MZM.

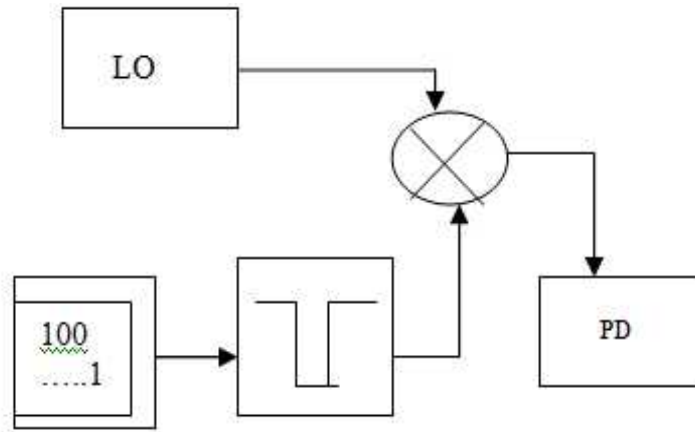


Fig.3.8 Direct laser modulation process (PD-Photodetector, LO- Local oscillator)

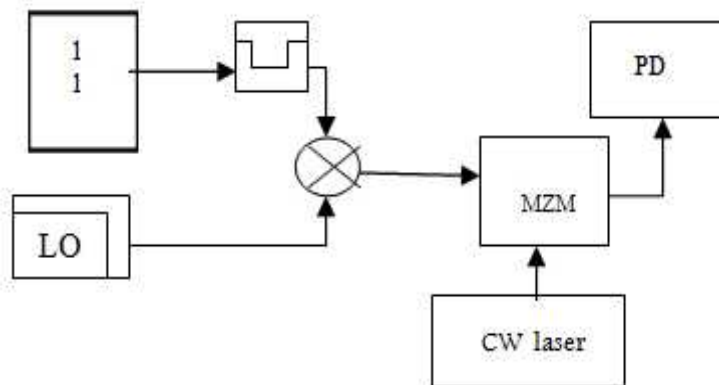


Fig.3.9 Sub carrier multiplication and modulation through MZM modulator (PD-Photodetector, LO- Local oscillator)

The loss of MZM can be neglected. $V(t)$ is the mixture of an electrical sinusoidal signal and a DC biased voltage and can be expressed as [141],

$$V(t) = V_{L-b} + V_m \cos(\omega t) \quad (3.9)$$

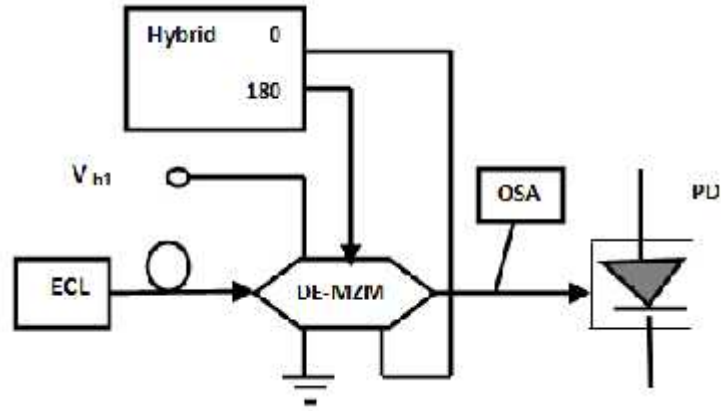


Fig.3.10 Schematic diagram of the optical mm-wave generation using balanced MZM biased in OCS Modulation [V_{b1} - V_{DC} of MZM; 'ECL' - External Cavity Laser; 'OSA' - optical spectrum analyzer; 'ESA' - Electrical Spectrum Analyzer]

Here V_{DC} is the DC bias voltage, V_m and ω_R are the amplitude and angular frequency of the electrical driving signal. The phase difference caused by $V(t)$ is given as,

$$\phi(V(t)) = \pi \left[\frac{V_{DC} - b}{V_{\pi}} + \frac{V_m \cos(\omega_R t)}{V_{\pi}} \right] \quad (3.10)$$

where ' V_{π} ' is the half-wave voltage of MZM.

The output electrical field can be written as,

$$\begin{aligned} E_o(t) &= \sqrt{L} \cos \left(\left[\frac{V_{DC}}{2V_{\pi}} \right] + m[\cos(\omega_R t)] \right) E_o(t) \\ &= \sqrt{L} \left(\begin{array}{l} \cos \left\{ \frac{V_{DC}}{2} \right\} \cos(m \cos \omega_R t) - \\ \sin \left\{ \frac{V_{DC}}{2} \right\} \sin(m \cos \omega_R t) \end{array} \right) E_o(t) \quad (3.11) \\ &= \frac{\sqrt{2L}}{2} \left((J_0(m) + \sum_{n=0}^{\infty} (-1)^n J_{2n}(m) \left(\frac{\pi V_m}{V_{\pi}} \right) \cos(2n \omega_R t) \right) E_o(t) - \\ &\quad \frac{\sqrt{2L}}{2} \left(\sum_{n=0}^{\infty} J_{2n+1}(m) \cos((2n+1) \omega_R t) \right) E_o(t) \quad (3.12) \end{aligned}$$

$$\begin{aligned}
&= \frac{P_0}{2} L \left(1 + \cos \left\{ \frac{V_{DC}}{2V} + 2m \cos \omega_{RF} t \right\} \right) \\
&= \frac{P_0}{2} L \left(1 + \cos \left\{ \pi \frac{V_D}{2} J_0 2m \right\} \right) \quad (3.13)
\end{aligned}$$

Where $E_0(t)$ is the electric field input into the MZM, L is the RoF link total loss, $V_D = V/2$ is the bias voltage of MZM and P_0 is the input optical power. The modulation index is 'm'. It is represented as,

$$m = \frac{\pi V_m}{2V_\pi}$$

Here V_{mod} is the amplitude of the input RF signal. V_π is the half wave voltage of MZM.

3.3.2 Simulation Setup

The transmission of the carrier is a waste of power since the information is carried by the sidebands. The suppression of the carrier leads to improvement of important characteristics of the fiber optic link such as dynamic range and noise figure. Fig.3.11 shows the simulation setup of an ODSB-CS RoF communication system. The MZM can be worked in three operating conditions, maximum transmission point, minimum transmission point and quadrature operating point. In the minimum transmission, the MZM has DSB-CS output. In the maximum transmission condition, the MZM has DSB output. In the quadrature operating point, the MZM has SSB output. Optical carrier is generated from a CW laser of 193.1 THz with a line width of 10 KHz and is modulated by a 50 GHz RF signal through a Dual arm MZM, which is biased at null point. The RF signal is applied directly to one arm of the DE-MZM modulator and the same RF signal is applied to the second arm of the modulator to generate an ODSB-CS RF signal. As the MZM is biased at the minimum transmission point, the output consists of two sidebands only. The optical carrier

is eliminated. It demands less bandwidth requirement than DSSB–RoF system and has high resistance to power degradation caused by chromatic dispersion. An optical attenuator of return loss 65 dB is used to reduce the optical power. The signal from the CS is amplified and transmitted through a SSMF of length 150 km and a first order dispersion of 16.75 ps/nm/km.

Table 3.2 Simulation parameters

Serial No.	Parameters	Specifications
1	Laser frequency	193.1THz
2	Laser Power	10dBm-20dBm
3	Fiber attenuation	0.2dB/km
4	Fiber Length	150 Km
5	Fiber dispersion	16.75 ps/nm/km
6	Fiber Differential group delay	0.2ps/km
7	Fiber Maximum phase shift	3mrad
8	Photodetector responsivity	1A/W
9	Photodetector current	10nA
10	Photodetector center frequency	193.1THz
11	Photodetector sample rate	5Hz
12	Photodetector thermal noise	10^{-22} W/Hz

Table 3.2 shows the global parameters used in the experiment. At the transmitter an optical source of center frequency 193.1 THz is used. Its power is varied from 10 dBm to -20 dBm. The attenuation of SSMF is 0.2 dB/km. The optical signal is amplified by an EDFA of length 5m, core radius 2.2 micrometer, and loss 0.1 dB/m.

At the remote station, the signal is received by a PIN photodetector. PIN photodetector which has a responsivity of 1 A/W.

Direct detection is used at the remote station. The amplified signal is filtered by using a low pass filter which has a sample rate of 5Hz and its center

frequency is at 193.1 THz. The BER and eyediagram performances are obtained from BER and eye diagram analyzers respectively.

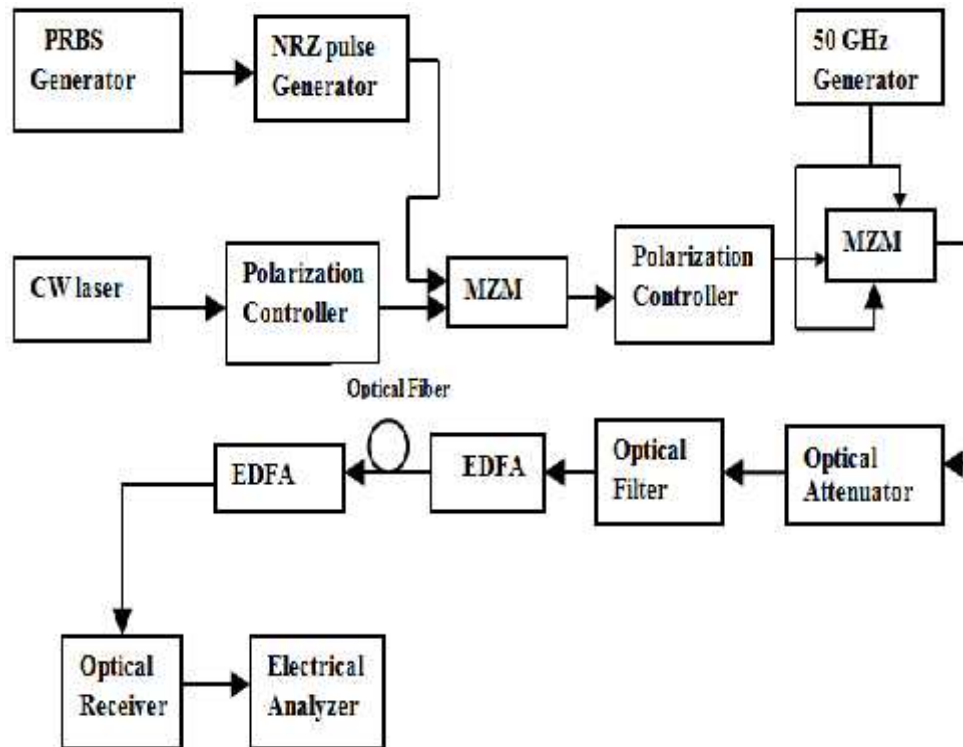


Fig. 3.11 Block diagram of ODSB- CS-RoF communication system

3.3.3 Results and Discussion

Fig. 3.12 shows the spectrum of the 5Gbps, 60 GHz ODSB-CS transmission. The spectrum consists of two sidebands and a suppressed optical carrier. The maximum sideband power and carrier power are -28 dB, -36 dB respectively. The sideband to carrier suppression ratio is 8 dB. Fig. 3.13 shows the BER of 5 Gbps and 10 Gbps, 60 GHz receiver as a function of fiber length. The maximum transmission distance is 150 km. The graph shows that BER increases with increase in fiber length. When the data rate is increased, BER

also increased as in Fig. 3.13. The BER is in the order of 10^{-2} to 10^{-3} .

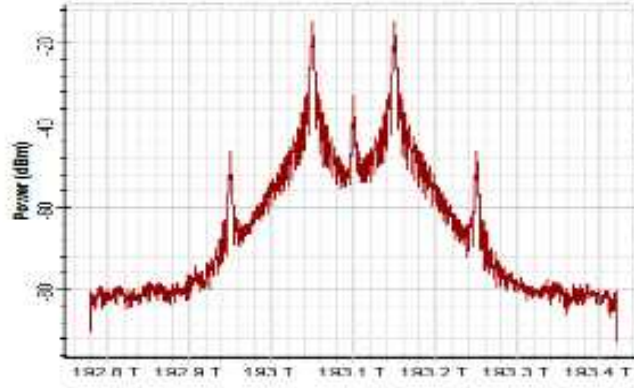


Fig.3.12 Spectrum of ODSB-CS transmission [input power-- 5 dBm]

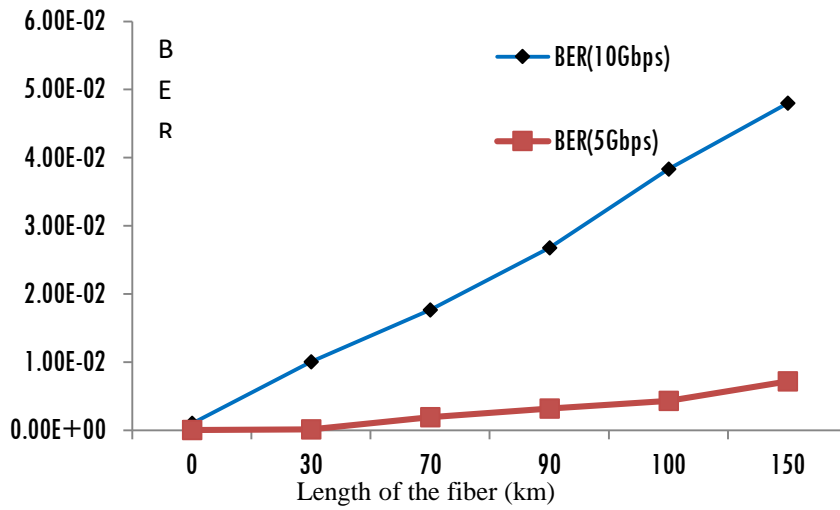


Fig. 3.13 BER of 5 Gbps and 10 Gbps, 60 GHz ODSB-CS receiver

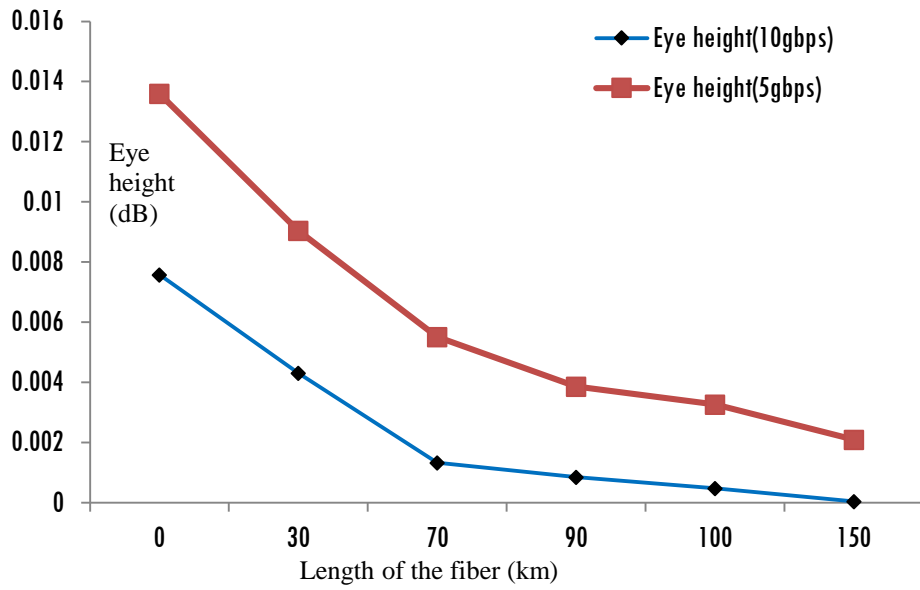


Fig. 3.14 Eye height for 5 Gbps and 10 Gbps ODSB-CS Receiver

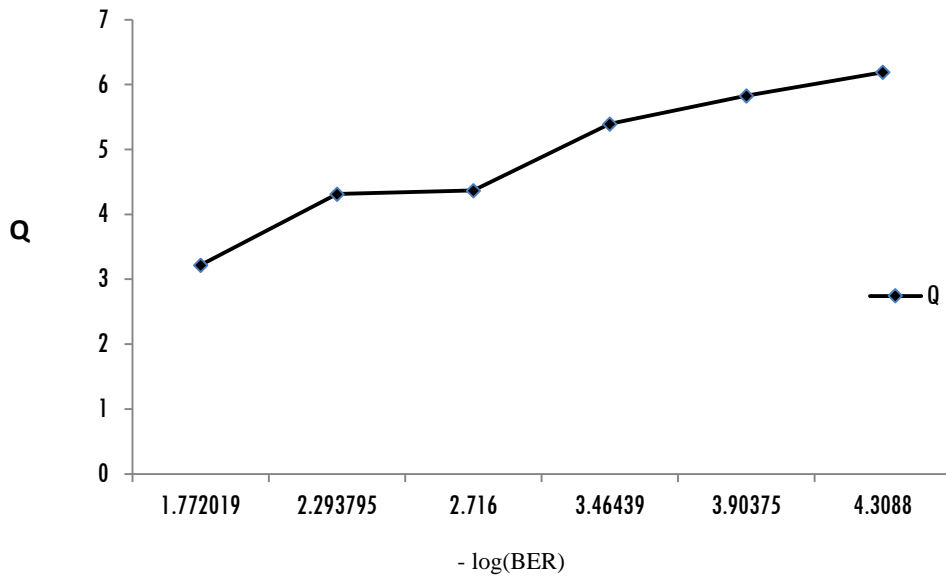


Fig. 3.15 Q- factor of back-to-back propagation in ODSB-CS Receiver

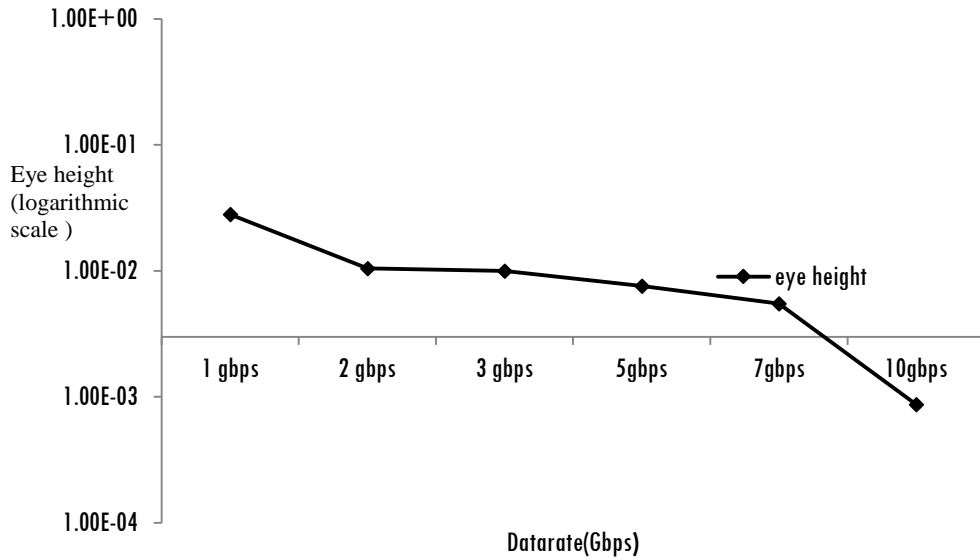


Fig. 3.16 Eye height of back-to-back propagation in the ODSB-CS Receiver

Fig. 3.14 shows the eye height of the 5 Gbps and 10 Gbps propagation in the ODSB- CS receiver. The eye-height has been decreased for long distance transmission and higher data rate propagation.

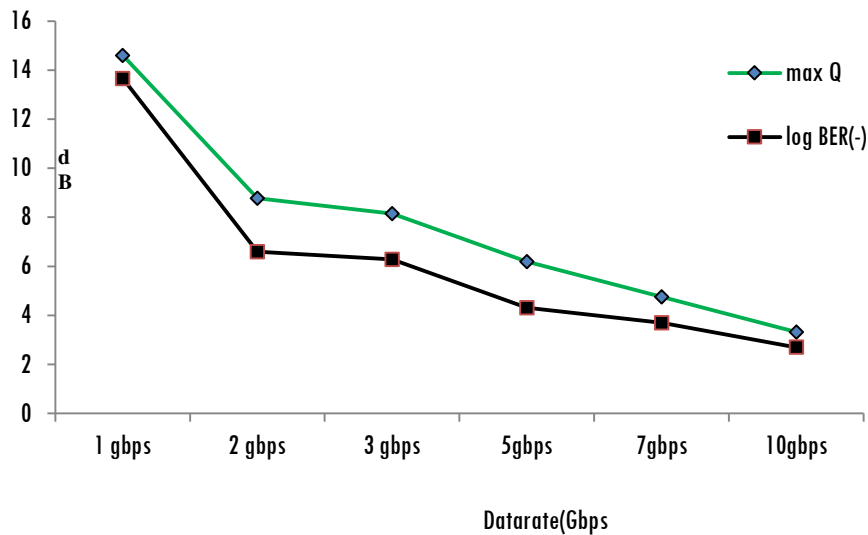


Fig. 3.17 Q and log(BER) of the ODSB-CS receiver (back-back) transmission

Fig. 3.15 shows the relation of BER with Q factor for a data rate of 10Gbps. The graph shows that BER and Q factor are inversely proportional. Fig. 3.16 shows the eye-height of back to back propagation. The maximum eye-height of 0.03dB is obtained at a minimum data rate of 1Gbps. It shows the eye-height performance variation of back to back propagation for different input optical powers. When the input power is increased, eye-height is increased. It shows that the system has better performance at higher input optical powers.

Fig. 3.17 shows the Q factor and BER performance as a function of data rates for back-to-back transmission. Maximum performances are obtained at back-to-back transmission because of minimum dispersion. Fig. 3.17 shows that Q factor and eye-height are decreased with increased data rates.

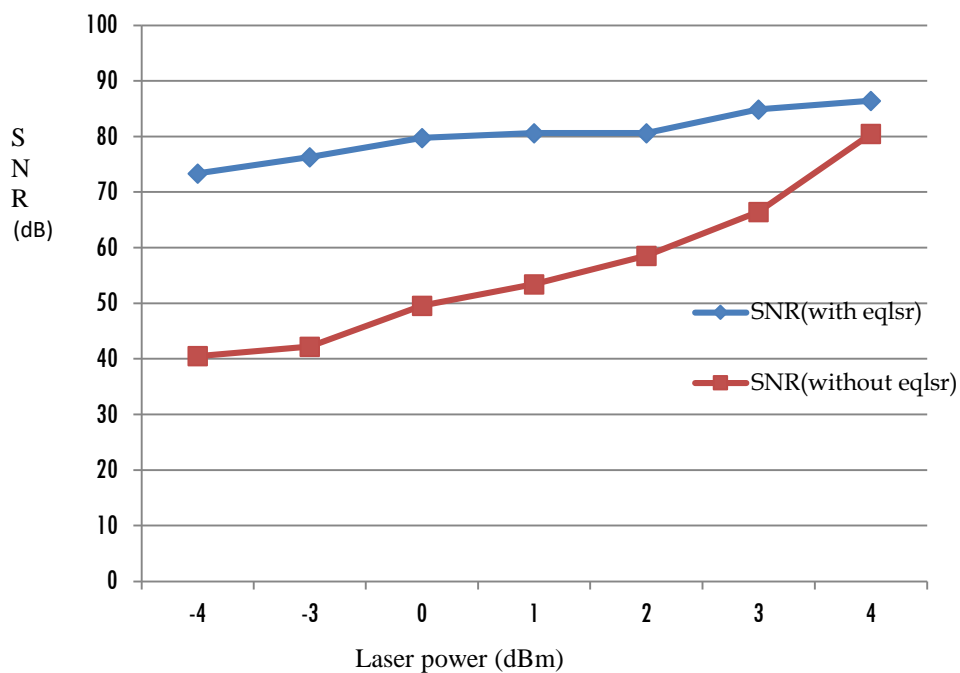


Fig. 3.18 SNR of the ODSB-CS communication with and without SQRT nonlinear equalizer

Fig. 3.18 shows the SNR of ODSB-CS communication system with and without SQRT nonlinear equalizer. For low input powers, the variation of SNR is very high and the difference reduces for higher input powers.

3.3.4 Conclusion

A bandwidth efficient optical DSB-CS transmission system using subcarrier multiplied MZM method is theoretically analyzed and its performance is investigated using Optisystem software. Results show that the performance parameters like Q-factor, Eye height (from eye diagram) are decreased as a function of increasing transmission length and data rate. Minimum BER in the order of 10^{-3} is obtained. Maximum Q factor of 15 dB is obtained at a maximum negative log (BER) of 14 dB. For higher input powers, BER is increased in the order of 10^{-2} . This BER is comparatively high (but SNR is also high). Also, the optical power is very high (up to 15 dBm), and operating frequency is 60 GHz (very high, millimeter wave transmission). Future RoF communication demands high data rates and higher bandwidth efficient modulation techniques. ODSB-CS is a highly bandwidth efficient method compared to ODSB transmission. But its performance should be supported at high data rates also. Results show that Q factor is seriously reduced to 3 dB at 10 Gbps. Using better dispersion compensation methods, the system performance can be improved.

Table 3.3 shows the performance comparison of existing and proposed methods. Performances are measured in terms of SNR and received power. It shows that the proposed methods outperform the existing methods for same transmission distances.

Table 3.3 Result comparison of existing and proposed methods

Author	Transmission distance	Received power	SNR
Joseph Prat[119]	100 km	-2 dBm	50 dB
Chunmin Prat [119]	100 km	-2 dB	50 dB
Chunmin Xia [147]	280 km	-56 dBm	22 dB
Baljeet kaur [117]	20 km	-32 dBm	46 dB
Baljeet kaur [118]	20 km	-47 dBm	44 dB
Proposed Method	20 km	-20 dBm	76.3 dB
	200 km	-36 dBm	60 dB
	280 km	-49 dBm	46.7 dB

3.3.5 Validation

Results of the proposed method [transmission distance - 20 km] are validated with the references [117] and [118]. The received power of -22 dBm is obtained with a SNR of 74 dB as the method in [117]. The received power of -24 dBm with a SNR of 72 dB is obtained for the method in [118]. The proposed method has been improved the received power about 2 dBm to 4 dBm and SNR about 2.3 dB to 4.3 dB respectively as in table 3.4.

Table 3.4 Validation of results

	Transmission distance	Received power	SNR
Proposed method	20 km	-20 dBm	76.3 dB
Baljeet kaur [117]	20 km	-22 dBm	74 dB
Baljeet kaur [118]	20 km	-24 dBm	72 dB

Performance Evaluation of RoF System In Different Channels and Reduction of Channel Nonlinear Distortion

4.1 Introduction
4.2 RoF for Fiber Aided Wireless (Fi-Wi) Systems
4.3 System Modeling
4.4 Modulation Schemes
4.5 Channel Model
4.7 Signal to Noise Ratio (SNR)
4.8 Simulation Setup of Radio over Fiber System using OFDM
4.9 Results and Discussion
4.10 Conclusion

Abstract

This chapter covers the reduction of nonlinearities in different channels. Two modulation methods with three channels are considered. The SNR performance of different channels is compared. The Q factor of the proposed method is compared with the existing method. This chapter ends up with the conclusion that the proposed system has better performance as compared to the existing system.

4.1 Introduction

Voice and low speed data services commonly use the conventional wireless communication. They have been adequately provided by the existing wireless systems having data speeds up to a few Mbps. With the advent of popular High-Definition (HD) Video and high-speed Internet, future wireless systems must offer data speeds exceeding Gbps. Because of limited frequency spectra at low frequencies, and the congestion caused by the large number of

consumer products sharing the frequency spectra, it will be necessary to use higher carrier frequencies in the future, including mm waves, for much faster wireless communication at multi-gigabit-per-second speeds [145]. Higher frequency bands are available at mm wave frequencies. Even though the mm waves provide the required bandwidth for ultra-fast wireless communication, they make wireless networking technically more challenging. Few technical challenges are higher carrier frequencies, channel nonlinearities and wider channel bandwidths. They have higher air-link loss (e.g., about 30 dB higher at 60 GHz than at the low GHz range), and low device performance. The wide channel bandwidth means higher noise power and reduced SNR. These factors make wireless networking at mm waves “Pico-cellular” for the radio cells which are smaller than 10 m. So the multi-gigabit-per-second wireless networking at mm waves needs a high-capacity feeder network to interconnect different radio access points. RoF technology can provide the required feeder network and it is best suited to the demands of small-cell wireless networks. The major advantage of a fiber-based Distributed Antenna System (DAS) is its ability to support multiple diverse wireless applications and services on the same infrastructure. But the performance requirements for RoF links employed for low frequency wireless systems differing from those required for mm wave systems [146].

4.2 RoF for Fiber Aided Wireless (Fi-Wi) Systems

The fiber-wireless architecture for cellular networks is shown in Fig.4.1 (downlink). This architecture can increase the frequency reuse and broadband access by its micro/Pico cells for cellular radio networks. The micro/Pico cells can be used with Radio Access Points (RAP) as in Fig.4.1. These low power RAPs can provide inexpensive wireless access instead of conventional base

stations because of low complexity and cost in large-scale deployment [147]. The bigger cells can be divided into smaller cells by dispersing RAPs throughout. These RAPs are connected to the central base station via the RoF links. In the RF communication system, the baseband signal is modulated to a convenient carrier frequency. The modulation scheme and the carrier frequency are predetermined. The aim of the RoF link is to provide a transparent, low distortion communication channel for the radio signal [148].

The basic fiber-based wireless system architecture is shown in Fig. 4.1. The radio signal, $S(t)$ from a CS is transmitted through an analog fiber optic link. The fiber is terminated at the RAP where the optical signal is converted to electrical signal $r(t)$, is amplified and transmitted in air (different channels). The RAP is located as an interface between the fiber and the radio links [149].

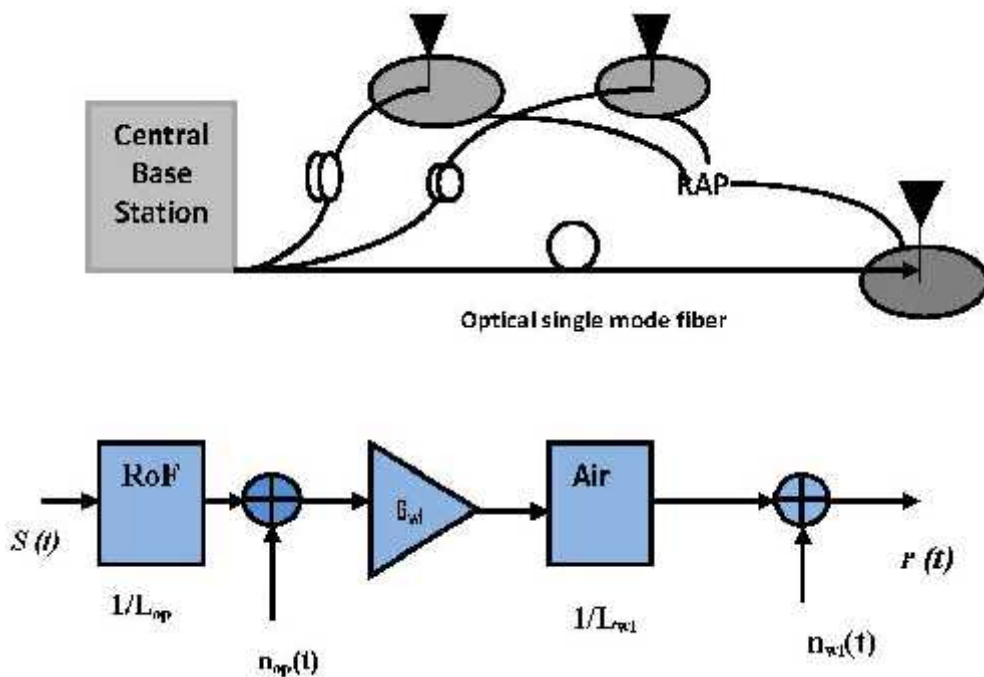


Fig. 4.1 Radio over Fiber System

Fig. 4.2 shows the gains and losses that occur in the optical and wireless regions. The input RF power has loss at the electro-optic conversion stage and has a linear loss as a function of fiber length and again a loss due to O/E conversion [147]. All these three losses (plus any optical connector/splitter/splicing loss) are referred to as L_{op} . The optical link noise n_{op} is added at the optical receiver which defines OSNR. This optical noise and signal are amplified by the optical amplifier with gain G_{op} then, goes through the wireless channel which may be Additive White Gaussian Noise (AWGN), Rayleigh or Rician channel, experiencing a loss of L_{wl} [150].

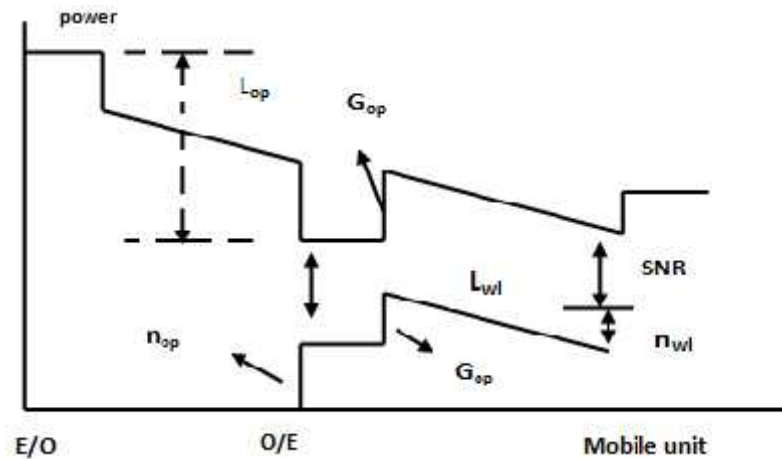


Fig. 4.2 Losses, amplifications, and added noise to the radio signal

For multipath channels, an additional margin is to be given for fading. More noise will be added at the interface of air and portable receiver front end. These different types of noises are cumulatively referred to as n_{wl} . The SNR is the ratio between the signal and appropriately weighted noise power from all the sources. Like other wireless communication networks, transmission medium contributes two important problems in Fiber aided wireless communication system. These problems are: AWGN noise & Rayleigh and Rician Fading.

In wireless communication systems, the receiver should compensate the channel effects like Rayleigh fading, Doppler frequency shift and Additive White Gaussian Noise. For this, channel equalization and Forward Error Correction (FEC) techniques are used to improve the system performance. The channel equalizer is used to detect the original signals from the received signals with multipath effect. In a communication system, the received signal $R[k]$ is expressed by,

$$R[k] = S_f[k]. H_f[k] + N[k] \quad (4.1)$$

where $S_f[k]$ is the transmitted signal, $H_f[k]$ is channel frequency response and $N[k]$ is AWGN channel.

As the wireless channel and optical link are connected in series, nonlinear distortion through E/O conversion is a major problem [151]. In a Microcell, the signal strength of the radio access point is 80 dB – 90 dB [151]. This is the requisite dynamic range for distortionless transmission. The linear range of a direct or externally modulated RoF link is low due to nonlinear distortion. Linearization problem is very important in the RoF link and high power RF amplifiers [152]. To reduce the nonlinear distortion, Nakagawa has developed a nonlinearity recovery block and Katz has developed a RF predistorter for the MZM external modulator [153], [154].

Adaptive digital predistortion methods are developed for RoF communication [155], [156]. Joint compensation is more effective and will provide better performance. An adaptive linearization method is suggested for the reduction of RoF nonlinearity in an AWGN channel [157]. The uplink compensation method is performed at the central base station. A Wiener system is used to represent the wireless fiber uplink which consists of a RoF link and wireless path. Gaussian inputs are used to estimate the Wiener

systems as in [158], [159]. The correlation properties of Pseudonoise (PN) sequences are used to identify a Wiener system [160]. The linear subsystems of Wiener–Hammerstein models are identified by cyclostationary inputs [161]. The Wiener–Hammerstein models are identified in the frequency domain [162]. For nonlinear system identification, PN sequences are used in a Code Division Multiple Access (CDMA) systems. It has been shown in [163] and [164] that the correlation properties of PN sequences are used to estimate the wireless fiber Wiener system. An algorithm is developed to estimate both RoF and wireless channels which is mathematically proved and numerically verified [163]. The transmission of one PN sequence is enough to estimate the channel in a noise free environment.

Norbert Wiener [165] separated a nonlinear system into a linear memory part and a nonlinear memory less part and it is beneficial to separate the linear and nonlinear distortion compensations. A Hammerstein type equalizer can first compensate the nonlinear distortion and then the linear distortion. The Hammerstein system has a nonlinear system and a linear system connected in the reverse order of a Wiener system. Therefore, a Hammerstein system is an inverse of a Wiener system. So the nonlinearity can be compensated independently and prior to the linear compensation. In [166] and [167], a Wiener system was precompensated by a Hammerstein system.

4.3 System Modeling

The OFDM signal $s(t)$ is transmitted through an optical link as shown in Fig. 4.3[168]. The electrical signal, i.e. OFDM signal is used to modulate the intensity of light in the fiber channel. This E/O conversion can be possible

in two ways: by directly modulating the intensity of the light source or using a constant-intensity source followed by an external modulator.

Consider a single OFDM symbol,

$$s(t) = \sum_{n=-N/2}^{N/2-1} d_n \cos((\omega_c - n\Delta) t + \phi(n)) \quad (4.2)$$

where N is the number of subcarriers separated by ω and centered at ω_c . Where d_n and $\phi(n)$ are the magnitude and phase of n subcarriers.

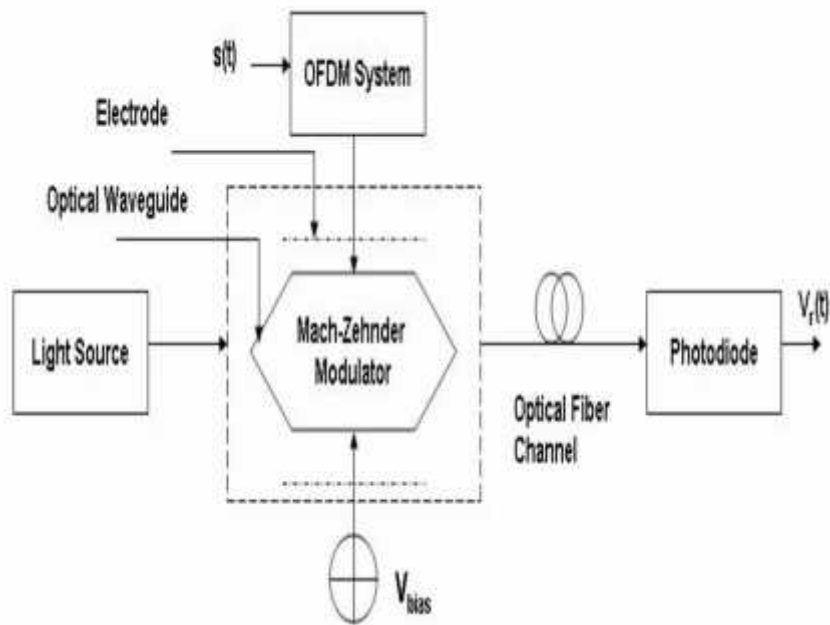


Fig. 4.3 System model

The output power after the signal has travelled through a length L_f of fiber is,

$$P_{out}(L_f) = P_{in} \{ \cos^2(DL_f \frac{2\pi f_c^2}{\lambda_0^2 c}) \} \quad (4.3)$$

where D is the dispersion parameter normally expressed in units of ps/nm/km, λ_0 is the wavelength of the optical source and c is the speed of light in free space.

Power gain G_{fiber} is only assumed for the fiber without other fiber distortions and therefore at the input of the photodetector the optical power becomes,

$$P_{0,r(t)} = G_{\text{fiber}} P_{0,t(t)} \quad (4.4)$$

Where $P_{0,t(t)}$ is the optical output of the MZM.

Neglecting all the noises in the link, the received signal of the photodetector at a load of R_L ohms is,

$$V_r(t) = R_L (R_{\text{PD}} G_{\text{fiber}} P_{0,t(t)} + N_r(t)) \quad (4.5)$$

where R_{PD} is the responsivity of the photodetector expressed in amps/watt (A/W). $N_r(t)$ is the noise in the received optical signal from the photodetector. Photodetector noise sources are thermal noise, shot (or quantum) noise, dark current and surface leakage current. The dark current is the constant response exhibited by a detector in the absence of light. Thermal noise, also known as Johnson noise is the electronic noise produced by the thermal variation of the electrons within a conductor at balance, without affecting any input voltage. Thus $s(t)$ is transmitted to the analog RoF link with a MZM and finally expanding with the Taylor series, the electrical output of the optical link is,

$$\begin{aligned} V_r^{(t)} &= k_1 \left(2S_1^{(t)} \right) \cdot \left(\left(\frac{2S_1^{(t)}}{3} \right)^3 \right) + \\ &\left(\left(\frac{2S_1^{(t)}}{5} \right)^5 \right) \dots (-1)^n \left(\left(\frac{2S_1^{(t)}}{(2n+1)} \right)^{2n+1} \right) + R_L N_r^{(t)} \\ &= K_2 S_1^{(t)} + P_N^{(t)} + R_L N_r^{(t)} \end{aligned} \quad (4.6)$$

where $K_2 = (2k_1)\Pi /$ and $P_N^{(t)}$ is the nonlinear distortion that is obtained by all of the terms in the Taylor expansion of order greater than unity.

4.4 Modulation schemes

4.4.1 OFDM modulated RoF System

RoF systems can handle wireless signals with different characteristics for achieving multi-standard system operation. Therefore, RoF systems can support single-carrier wireless signals having multilevel modulation formats and wireless signals having multicarrier modulation schemes, such as OFDM. In these systems, the sub-carriers themselves employ multilevel signal modulation. Channel uniformity is very critical for single-carrier systems [168]. The employed RoF links should be as simple as possible to reduce the cost and to provide the needed performance.

Let N denote the number of sub-carriers used for parallel information transmission and let $s_k (0 \leq k \leq N - 1)$ denote the k^{th} complex modulated symbol in a block of N information symbols. The outputs s_n of the N point Inverse Fast Fourier Transform (IFFT) of S_k are the OFDM signal samples in one symbol interval, or mathematically,

$$S_N = \frac{1}{\sqrt{N}} \sum_{k=0}^{N-1} S_k \exp\left(\frac{j2\pi nk}{N}\right) \quad (4.7)$$

4.4.2 DPSK Modulated RoF System

Differential Phase Shift Keying (DPSK) is a common form of phase modulation which conveys data by changing the phase of carrier waves. DPSK is a modulation technique that converts information by using the phase difference between two neighbouring symbols. At the transmitter, each symbol is modulated relative to the previous symbol. At the receiver, the current

symbol is demodulated using the previous symbol as a reference. The previous symbol acts as an estimate of the channel. A no change condition makes the modulated signal to remain at the same 0 or 1 state of the previous symbol. We choose 8-DPSK scheme to analyze the SNR in different fading channels [169].

4.5 Channel Model

4.5.1 AWGN Noise Channel

AWGN is a noise that affects the transmitted signal when it is passing through a channel. It has a uniform continuous frequency spectrum over a particular frequency band.

4.5.2 Rayleigh Fading Channel

When there is no Line of Sight (LOS) path between transmitter and receiver, the received signal is the sum of all the reflected and scattered waves. In wireless telecommunications, the multipath creates constructive and destructive interferences, and phase shifting of the signal. This causes Rayleigh fading. The standard statistical model of this gives a distribution known as the Rayleigh distribution [170]. Mathematically, the multipath Rayleigh fading wireless channels are modeled by the Channel Impulse Response (CIR),

$$h(t) = \sum_{l=0}^{L_p-1} \alpha_l \delta(t - \tau_l) \quad (4.8)$$

where, L_p is the number of channel paths, α_l and τ_l are the complex values and τ_l is the delay of path, respectively. The paths are assumed to be statistically independent and having normalized average power. The channel is time variant with respect to the motion of the mobile terminal, but we will assume that the CIR is constant during one OFDM symbol.

4.5.3 Rician Fading Channel

A Rician model is obtained in a system with LOS propagation and scattering effect. The model is specified by the Rician factor, denoted by k and is defined as the ratio of the line of sight and the scatter power components. The pdf of a Rician random variable x is given by

$$P(x) = 2x(1+k)e^{-k(1+k)x^2}I_0(2x\sqrt{k(k+1)}), \quad x \geq 0 \quad (4.9)$$

where $k=D^2/2\sigma^2$ and D^2 and $2\sigma^2$ are the powers of the LOS and scattered components, respectively [171].

4.6 Wiener Filter for Additive Noise Reduction

Consider a signal $x(t)$ which is mixed with a broadband additive noise $n(t)$, then the output signal, $y(t)$ is represented as,

$$y(t) = x(t) + n(t) \quad (4.10)$$

Consider that the signal and the noise are uncorrelated, and the autocorrelation matrix of the noisy signal is the sum of the autocorrelation matrix of the signal $x(t)$ and the noise $n(t)$.i.e.,

$$R_{yy} = R_{xx} + R_{nn} \quad (4.11)$$

where R_{yy} , R_{xx} and R_{nn} are the autocorrelation matrices of the noisy signal, the noise-free signal and the noise, respectively. Substituting equation (4.9) and (4.10) in the Wiener filter Equation (4.11), we get,

$$w = (R_{xx} + R_{nn})^{-1} r_{xy} \quad (4.12)$$

Equation (4.12) is the optimal linear filter for the removal of additive noise [172]. Where r_{xy} is the cross-correlation vector of the noisy signal and the noise-free signal.

The frequency response of the Wiener filter provides useful information about the operation of the Wiener filter. In the frequency domain, the noisy signal $Y(f)$ is given by,

$$Y(f) = X(f) + N(f) \quad (4.13)$$

Where $X(f)$ and $N(f)$ are the signal and noise spectra respectively. For a signal having additive random noise, the frequency-domain Wiener filter can be represented as,

$$w(f) = \frac{P_X(f)}{P_X(f) + P_N(f)} \quad (4.14)$$

and

$$w(f) = \frac{S(f)}{(S(f)+1)} \quad (4.15)$$

where $P_X(f)$ and $P_N(f)$ are the power spectra of the signal and noise. The SNR(f) is expressed in terms of the power-spectral ratio. For additive noise, the Wiener filter attenuates each frequency component in proportion to an estimate of the signal to noise ratio. The Wiener filter can be considered as one of the most fundamental noise reduction techniques.

4.7 Signal to Noise Ratio (SNR)

SNR is the ratio of the received signal power over the noise power in the frequency range of the operation. It is an important parameter of the Local Area Wireless Network (LAWN). The BER is inversely proportional to the SNR. High BER causes large amounts of packet loss, high delay and low throughput. It is tedious to find an exact relation between the SNR and the BER in the multi channel environment. The SNR is used to find out the quality of a communication link and measured in Decibels.

4.8 Simulation Setup of Radio over Fiber System Using OFDM

The simulation setup of the RoF transmission system is shown in Fig. 4.4. The signal is generated from a PRBS source and then modulated using QAM. Here 64 QAM modulator is used. The resulting signal is OFDM modulated using a MATLAB program, and then the OFDM signal is upconverted to 25 GHz. Two OFDM sidebands having center frequency of 25GHz, with a combined bandwidth of 2 GHz is formed. Both side bands transmit through the RoF system. Because the subcarriers are transmitted independently, and are demodulated independently at the receiver, the total bit-rate of the 2 GHz-wide OFDM signal is double that of the original OFDM signal generated by the MATLAB program.

The 2 GHz OFDM signal at 25 GHz is amplified and combined with a 35.5 GHz Local Oscillator signal generated by a signal generator, as shown in Fig. 4.4. The composite signal then drives a single-electrode MZM located at the Head-End Unit (HEU). The frequency of the optical transmitter is at 193.1 THz [173].

In the RF OFDM transmitter, the input data is split into multiple parallel branches. This is called as “serial-to-parallel” conversion. The number of the multiple branches equals to the number of subcarriers. Then the converted signal is mapped on to quadrature amplitude modulation (QAM). The IFFT is used to convert the mapped signal from frequency domain into time domain.

Two-dimensional complex signal is used to carry the information. A pair of electrical low-pass filters is used to remove the alias sideband signal. At the up-converter, the baseband OFDM signal is up shifted onto optical domain using an optical I/Q modulator, which is comprised by two Mach–

Zehnder modulators (MZMs) with a 90 degree optical phase shifter. The OFDM signal in optical domain is given by

$$E(t) = \exp [j\omega_{LD1}t + \phi_{LD1}] \quad (4.16)$$

Where ' $\omega_{LD1}t$ ' and ' ϕ_{LD1} ' are the frequency and phase of the transmitter laser, respectively and $S_B(t)$ is the baseband OFDM. The optical signal ' $E(t)$ ' is applied into the optical fiber link, with an impulse response of ' $h(t)$ '. The received optical signal ' $E'(t)$ ' becomes

$$E'(t) = \exp [j\omega_{LD1}t + \phi_{LD1}] S_B(t) * h(t) \quad (4.17)$$

Table 4.1 Simulation Parameters

SI. No	Parameter	Specification
1	Photodetector responsivity	1 A/w
2	Photodetector dark current	10 nA
3	Photodetector center frequency	193.1 THz
4	Fiber length	250 km
5	Photodetector sample rate	5 Hz
6	Photodetector thermal noise	10^{-23} w/Hz

The MZM modulator is biased at the point of minimum transmission in order to suppress the optical carrier. The modulated signal is amplified by an EDFA and filtered by a BPF. The modulated signal is transmitted through a

SSMF with an attenuation of 0.2 dB/km and dispersion of 16.75 ps/nm/km [Table 4.1]. The modulated optical signal is converted to an electrical signal at the Remote Access Point (RAP) is shown in Fig. 4.5. The electrical signal is amplified and transmitted in the air.

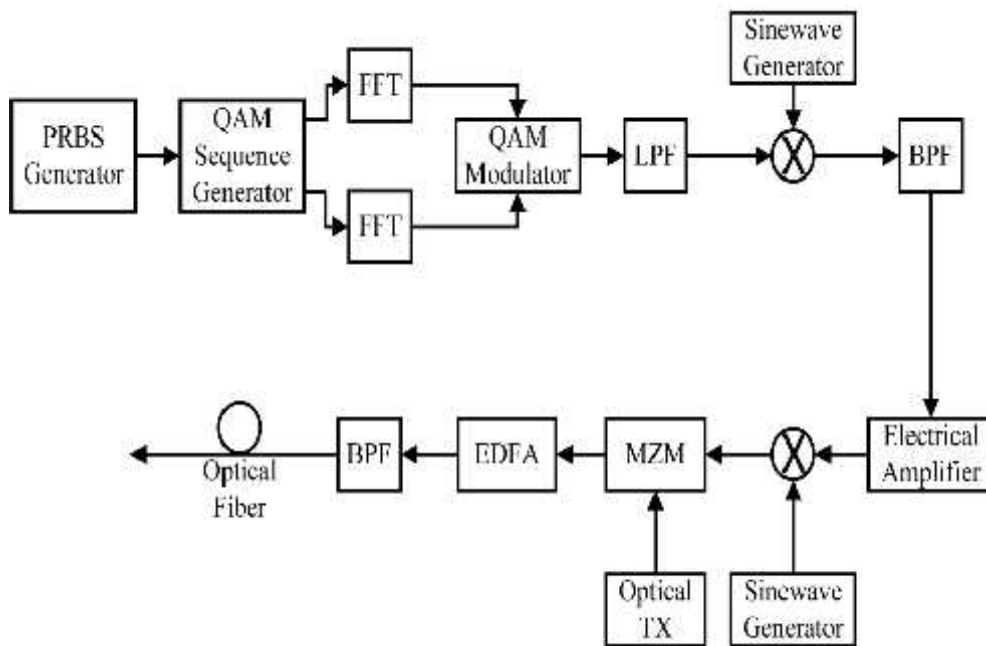


Fig. 4.4 Block Diagram of RoF transmitter unit

The wireless channel is modeled using a MATLAB software. Three different channels are considered like, AWGN channel, Rayleigh channel and Rician channel. An antenna at the receiver receives the signal which is then amplified by an electrical amplifier and up converted to a higher frequency by a local oscillator. The spectrum analyzer and oscilloscope visualizer are used to analyze the output parameters.

The signal finally reaches at the receiver as shown in Fig. 4.6. The received signal is amplified at the receiver.

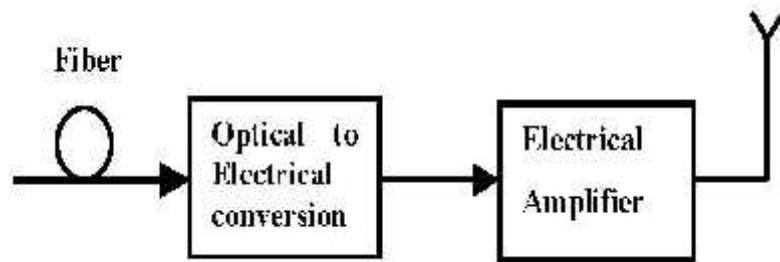


Fig. 4.5 Block diagram of remote access point

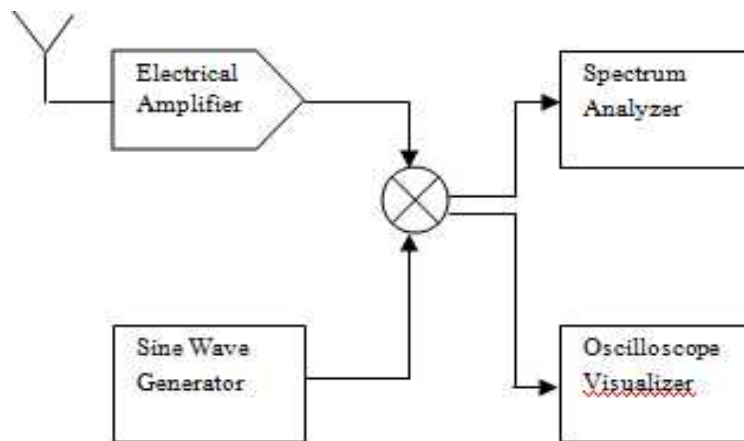


Fig. 4.6 Block diagram of receiver unit

The nonlinearities in the channels are reduced by using a Wiener filter at the receiver. The performance of Wiener filter is analyzed in AWGN channel, Rayleigh channel and Rician channel.

4.9 Results and Discussion

By using the proposed method, the RoF system was simulated for the multiuser modulation scheme (OFDM) and single user modulation scheme (DPSK) in AWGN and fading channels. The amplitude spectrum and power spectrum were simulated. Results show that the SNR is very high in Rayleigh channel as compared to Rician and AWGN channel. The amplitude spectrum of RoF transmission in AWGN channel, Rayleigh channel and Rician channel are shown in fig.4.7, fig.4.8 and fig. 4.9 respectively.

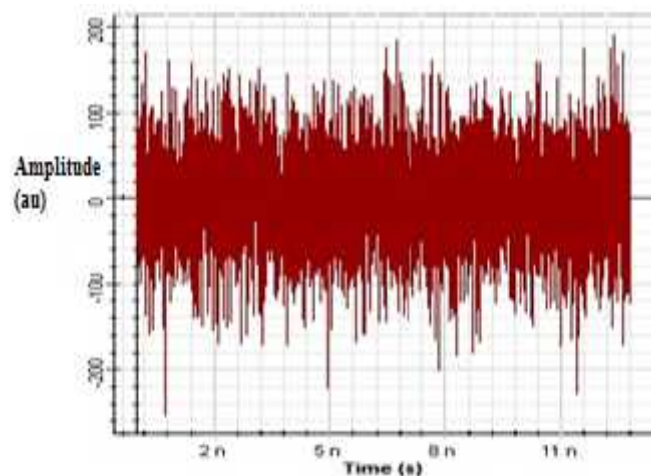


Fig. 4.7 Time domain plot of RoF in AWGN channel

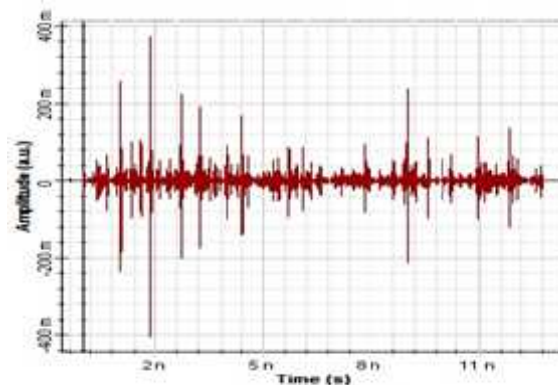


Fig. 4.8 Time domain plot of RoF in Rayleigh channel

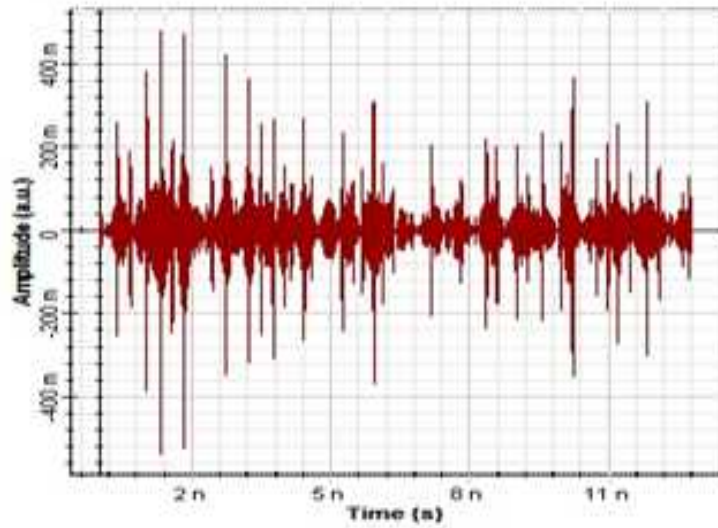


Fig. 4.9 Time domain plot of RoF in Rician channel

Fig.4.10 shows the power spectrum of RoF in AWGN channel. The power varies from 10 dBm to 40 dBm.

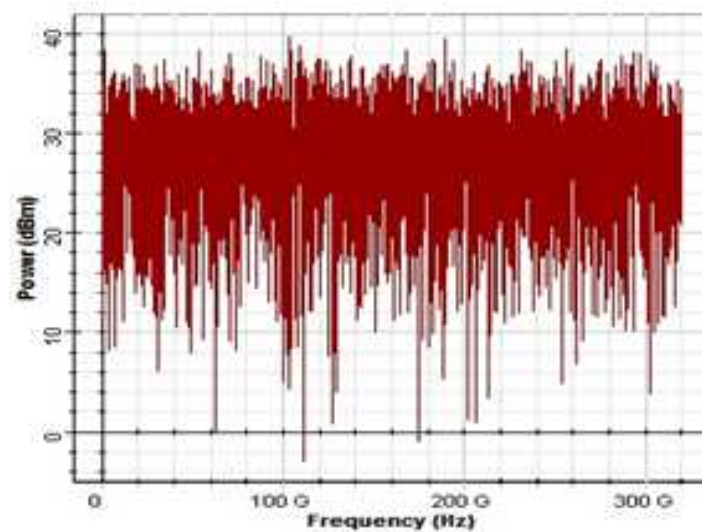


Fig. 4.10 Power spectrum of RoF in AWGN channel

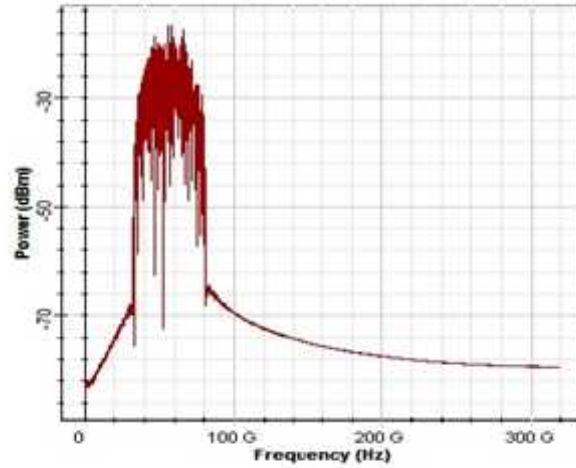


Fig. 4.11 Power spectrum of RoF in Rayleigh channel

Fig.4.11 shows the power spectrum of RoF in Rayleigh channel. The maximum output power is -18 dBm.

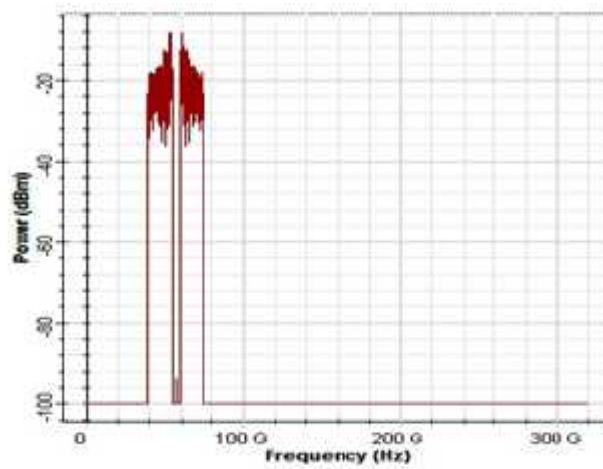


Fig. 4.12 Power spectrum of RoF in Rician channel

Fig. 4.12 shows the power spectrum of RoF in Rician channel. The maximum output power is -8 dBm. The output power is higher than Rayleigh channel.

Table 4.2 Comparison of Results (OFDM Modulation)

parameters	Channels		
	AWGN	RAYLEIGH	RICIAN
Signal Power(dBm)	69.56	66.56	65.56
Noise Power(dBm)	46.73	48.73	50.72
SNR (dB)	22.83	19.83	14.8

Table 4.3 Comparison of Results (DPSK modulation)

Parameters	Channels		
	AWGN	RAYLEIGH	RICIAN
Signal Power(dBm)	67.32	65.24	63.56
Noise Power(dBm)	48.34	50.76	52.85
SNR(dB)	18.98	14.48	10.71

For high speed DPSK optical communication systems, the nonlinear phase noise become severe. Therefore the noise power becomes high in single user DPSK modulation, as compared to multiuser OFDM modulation (Table 4.2&4.3). Tables 4.2 and 4.3 show the total power, signal power and noise power of OFDM modulation and DPSK modulation. By using Wiener filter, nonlinearities can be reduced and SNR can be improved for both DPSK and OFDM (Table 4.4&4.5) schemes.

Tables 4.3 and 4.4 show the signal power and noise power of compensated systems with OFDM and DPSK modulation. For nonlinearities, the Wiener filter attenuates each frequency component in proportion to an estimate of the SNR. The Wiener filter can improve the signal power from that of uncompensated systems. The Wiener filter is implemented in both the OFDM and DPSK modulation methods. Table 4.4 and 4.5 show that Wiener filter can improve the SNR in OFDM and DPSK modulation techniques. The SNR can be improved in Rayleigh and Rician channels rather than AWGN channel. Their effect is more pronounced in fading channels like Rayleigh and Rician channel.

Table 4.4 Comparison of Results (OFDM modulation using Wiener filter)

Parameters	Channels		
	AWGN	RAYLEIGH	RICIAN
Signal Power(dBm)	76.6	73.56	72.64
Noise Power(dBm)	43.44	45.42	46.62
SNR(dB)	33.2	28.14	26.02

Table 4.5 Comparison of Results (DPSK modulation using Wiener filter)

Parameters	Channels		
	AWGN	RAYLEIGH	RICIAN
Signal Power (dBm)	71.56	69.32	67.86
Noise Power (dBm)	44.67	46.65	48.76
SNR(dB)	26.89	22.67	19.10

4.10 Conclusion

From the simulation results, the SNR of a RoF communication system, which is an important figure of merit, is used to quantify the integrity of data transmitted through the system. The SNR of different channels were compared by using DPSK and OFDM modulation schemes. It has been found that the SNR is maximum for an AWGN channel and for Rayleigh channel it is lower than that of Rician channel. And also, if Wiener filter is used to reduce the noise, the SNR can be improved effectively in RoF communication.

Table 4.5 shows the performance comparison of existing and proposed methods. The performance is analyzed using data rate, the Q factor and transmission distance. Results show that signals in the proposed method can be transmitted to a long distance with high Q factor. The existing methods used a maximum data rate of 40 Gbps with a maximum Q factor of 10 dB. The proposed method can provide a Q factor of 14.4 dB for 1000 km transmission distance. This also provides a Q factor of 11 dB for a transmission distance of 1000 km at a data rate of 100 Gbps. Result analysis is shown in table 4.6.

Table 4.6 Result analysis of the existing and proposed methods

Author	Datarate (Gbps)	Q factor	Length of the fiber (km)
Mutsam A Jarajreh [174]	40	10	1000
Jie Pan et.al [175]	20	10	1500
Shieh W et.al [176]	20	6	200
Hwan Seok Chung [177]	20	13	1040
Proposed method	20	14.4	1000
	40	12.5	1500
	100	11	1000

4.11 Validation

The performance of the proposed method is validated with the results obtained in [174]. The Q factor obtained in the existing method [174] is 11 dB for a data rate of 40 Gbps and a transmission distance of 1500 km. The proposed method outperforms the existing method on a Q factor about 1.5 dB as shown in the table 4.7.

Table 4.7 Validation of results

	Data rate	Q factor	Length of the fiber
Proposed method	40 Gbps	12.5 dB	1500 km
Mutsam A Jarajreh [174]	40 Gbps	11 dB	1500 km

Nonlinear Distortion Reduction in the Fiber

5.1 Introduction

5.2 Case 1: Chromatic Dispersion Compensation using Optical Phase Conjugation in Semiconductor Optical Amplifier

5.3 Case 2: Group Velocity Dispersion and Third Order

Dispersion in External and Direct Intensity Modulated RoF Link

5.4 Case 3: Fiber Dispersion Compensation in Single Side Band optical Communication system using Ideal Fiber Bragg

Grating and Chirped Fiber Bragg Grating without DCF

5.5 Case 4: Chromatic Dispersion Compensation using Symmetrical Compensation Method

Abstract

This chapter considers different methods for the reduction of nonlinear distortions and chromatic dispersion in the optical fiber. Four different nonlinearity compensation methods are proposed. The performance of different method is analyzed. The OSNR and Q factor performances of the existing system and proposed system are compared. This chapter ends up with the conclusion that the proposed system has better performance as compared to the existing system.

5.1. Introduction

Chromatic dispersion in the fiber limits the transmission distance of optical systems. Dispersion Compensating Fibers (DCF) are commonly used for dispersion compensation. Chirped Fiber Grating (CFBG) with inverse dispersion has been widely used to reduce dispersion. These two dispersion-compensating techniques require accurate information about the dispersion of a span, channel wavelength, channel data rate, channel spacing and the number of channels [178]. Dispersion resistant modulation formats are used for

reducing the dispersion [179]-[180]. A Mid-Span Spectral Inversion (MSSI) technique has recently been used for the dispersion compensation in metro networks. In the MSSI technique, the dispersion compensation is performed by the use of an Optical Phase Conjugator (OPC) at the middle of a complete transmission link, which inverts the spectrum, and the phase of the optical signals distorted by the chromatic dispersion. If the phase-conjugated optical signals are passed through the same amount of dispersion throughout the link, phase distortion can be limited to a minimum value. Using the MSSI method, a 40 Gbps data transmitted through a SSMF of length 800 km [181]. The reduction of nonlinear impairments is shown in [182].

The MSSI technique avoids DCF in the optical transmission systems. So it reduces the number of amplifiers used in a link and has provided the lowest price. Cost effective transmission systems can be possible by using Semiconductor Optical Amplifiers (SOA) instead of EDFA [183]. This technique allows fractional cancellation of signal distortions due to Kerr nonlinearity and self-phase modulation [184]. In conventional FWM schemes, optical spectral inversion is associated with a net shift in the original signal frequency. The frequency shift is undesirable in both ultrahigh-bit rate Optical Time Division Multiplexing (OTDM) and ultrahigh capacity Wavelength Division Multiplexing (WDM) systems [185]. Optical spectral inversion without any shift of the central frequency is achieved by optical parametric loop mirror [186], and SOA [187]. The optical parametric loop mirror technique is not easy to apply in practical MSSI systems because a dispersive element cannot extract a generated conjugate wave from the input waves.

5.2. Case 1: Chromatic Dispersion Compensation Using Optical Phase Conjugation in Semiconductor Optical Amplifier

5.2.1. Overview

Dispersion Shifted Fiber (DSF) and SOA are the most promising methods for OPC and wavelength conversion using FWM [188], [189]. They can be effectively used in future high bit rate transmission systems for dispersion compensation using MSSSI [190], [191] and in WDM networks. However, the major issues like conversion efficiency, the low efficiency in DSF [192], and polarization independence, affect the transmission. The efficiency has been increased by using both new fibers [193] and SOAs [194]. Polarization independent FWM has been established in both SOA [195] and in DSF [196], using two orthogonally polarized pumps. With this technique, 40 Gbps 102 km MSSSI transmission has been demonstrated using SOA based conjugator [197]. But this configuration has high complexity and component count. A SOA based technique is used to generate the conjugate of an optical signal [198].

FWM supports high bit rate and conserves phase and amplitude information. FWM is the only method with transparent optical properties in the conversion process occurring within the SOA [199]. SOA based FWM wavelength conversion has high bit rate capacity up to 10 Gbps [200] or even 20 Gbps [201] have been demonstrated. FWM methods can also operate at high data rates without reducing the extinction ratio.

The SOA based phase conjugator provides higher conversion efficiency than the DSF based method for the same input powers. The ASE noise introduced by the phase conjugator must be carefully controlled to ensure the required system performance [202]. The dispersion induced carrier suppression effect is reduced in RoF communication using a phase conjugator based on a SOA [203].

The FWM method in a SOA consists of two input optical waves, each having the same state of polarization, as in Fig. 5.1[203]. The two co-propagating waves, E_{pump} and E_{probe} beat together to modulate the carrier density and generate dynamic gain and index grating. This nonlinear interference produces new waves (E_{c} and E_{s}) and they do not overlap with wavelengths. The intensity of the newly generated waves is proportional to the product of interacting wave intensities. E_{probe} is up-converted to a longer wavelength. E_{c} is at an optical frequency of $\omega_{\text{c}} = \omega_{\text{pl}} + \Delta\omega$, where $\Delta\omega$ refers to the detuning frequency. E_{c} is the phase conjugate copy of the original input signal.

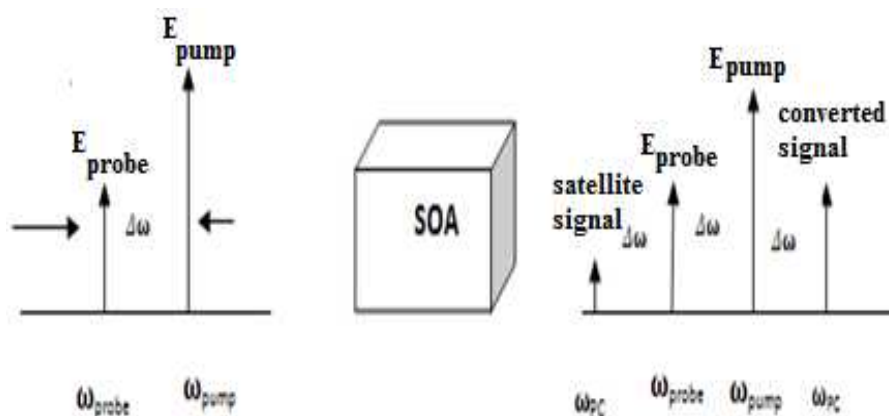


Fig. 5.1 FWM method of SOA

The conversion efficiency (dB) and the OSNR (dB) are important performance parameters that need to be considered for practical high-quality wavelength converters. The conversion efficiency (η) of any wavelength converter is defined as the ratio of the converted signal power (P_{out}) to the input pump power (P_{in}), as shown in equation (5.1) [204]. The efficiency of the wavelength converter decreases with increasing detuning of frequency. The conversion efficiency of FWM depends on various factors like pump frequency, signal frequency and the size of the active region of the SOA. The conversion efficiency of an FWM wavelength converter can be improved by increasing, the gain, saturation power, and carrier recovery rate of an SOA [205].

$$\eta = 10 \log \frac{P_{out} (\text{c})}{P_{in} (\text{p})} \quad (5.1)$$

The optical filters used in the existing method [203] are replaced by FBGs. The proposed method here uses FBGs to filter the phase conjugated signal and to reduce ASE noise. This method can increase OSNR, optical power and electrical output power of existing methods. This method can transmit an 80 Gbps data through a 400 km fiber with sufficient OSNR, which is higher than the existing methods.

5.2.2 Simulation Setup

The system performance is presented through visualizing tools, such as optical spectrum analyzer, RF spectrum analyzer, and electrical carrier visualizer. They are used to display the spectrum at the output of the circuit components. Table 5.1 shows the global parameters of the components in the setup.

Fig. 5.2 shows an 80 Gbps externally modulated RoF transmission using single Electrode MZM. A user defined random sequence with analog RF

signal as input is used to modulate the MZM. A tunable external cavity pump laser (laser 1 with 1541nm) is externally modulated by a single electrode MZM with an extinction ratio of 30dB. The result of the intensity modulation is an optical carrier with a DSB transmission. When the optical signal is transmitted through an optical fiber, the spectrum is spread over a wide range of frequencies and the quality of the signal is reduced. The optical link split into two paths. After the first half of the fiber, the signal is dispersed.

The spectral inversion is formed by using a coupler, travelling wave SOA and ideal dispersion compensation FBG. The second input of coupler is a continuous laser with 1540 nm. When the dispersed signal is fed through a spectral inverter, the signal is phase conjugated. The combined signals are passed through a travelling wave SOA of injection current 0.15A to generate the phase-converted spectrum as in Fig.5.3.

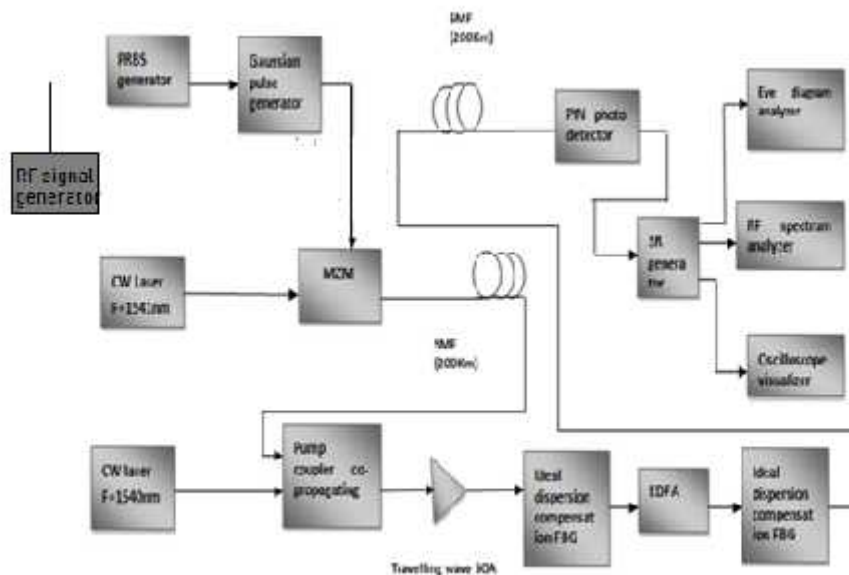


Fig. 5.2 Block diagram of optical phase conjugation using travelling wave SOA

The phase conjugated signal is filtered using an ideal dispersion compensated FBG at 1539nm and dispersion, $D = -800\text{ps/nm}$ as in Fig. 5.4. Ideal FBG means uniform FBG, it has constant period and constant peak amplitude of the refractive index variation throughout the length of the FBG. The filtered signal is amplified by an EDFA of length 5m. An EDFA is used to improve the combined signal power. A 125 GHz bandwidth ideal FBG is used with the EDFA to reduce additional ASE noise outside the signal bandwidth. Therefore, the OSNR of the converted signal is increased. This signal is passed through the second half of the fiber and the dispersion is compensated. The signal is obtained at the receiver by using a PIN photodiode with a responsivity of 1A/W and dark current 10nA .

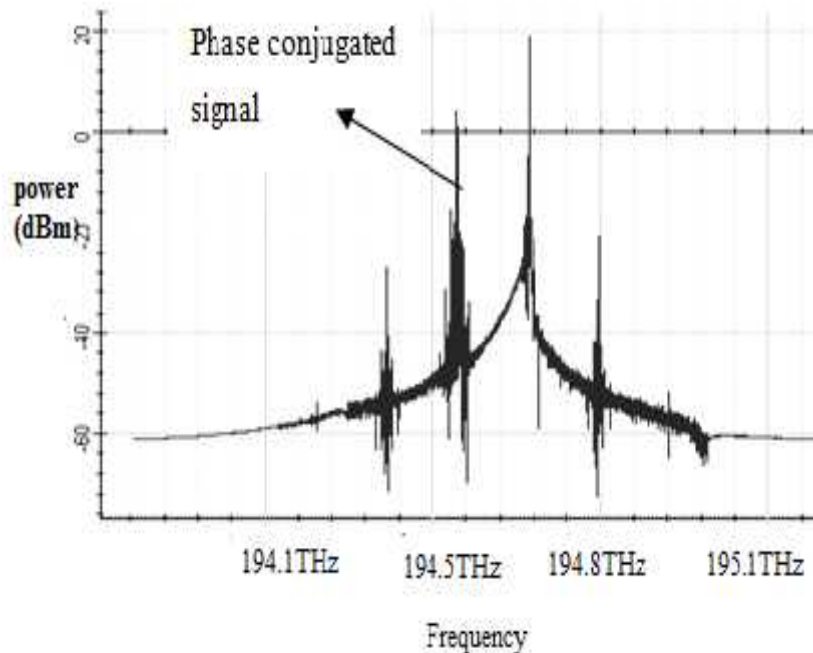


Fig. 5.3 Optical phase conjugated output spectrum of SOA

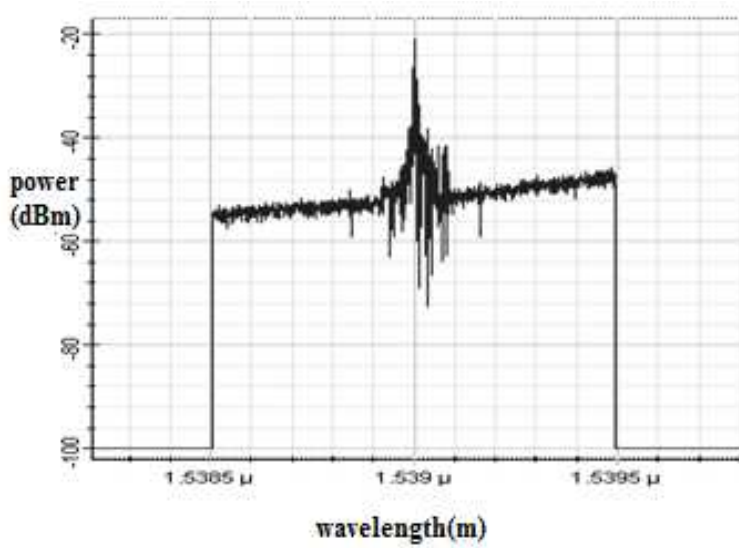


Fig. 5.4 Filtered optical phase conjugated signal of SOA

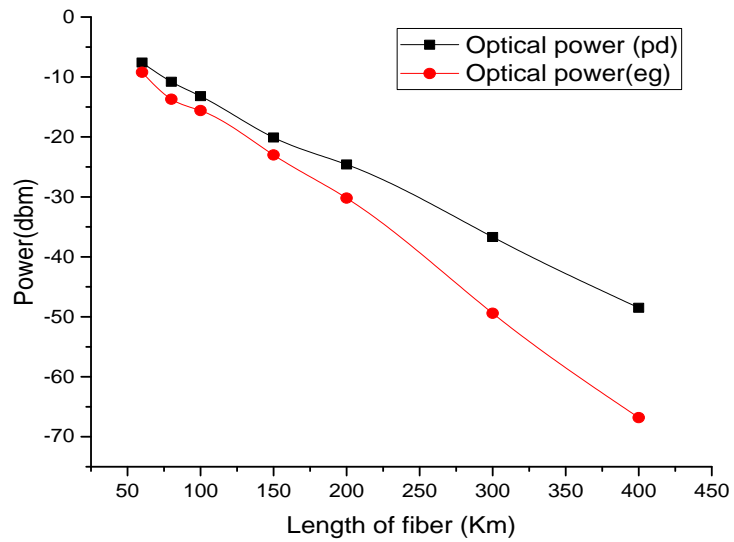


Fig. 5.5 Optical output power of the existing method (pd) and proposed method (eg)

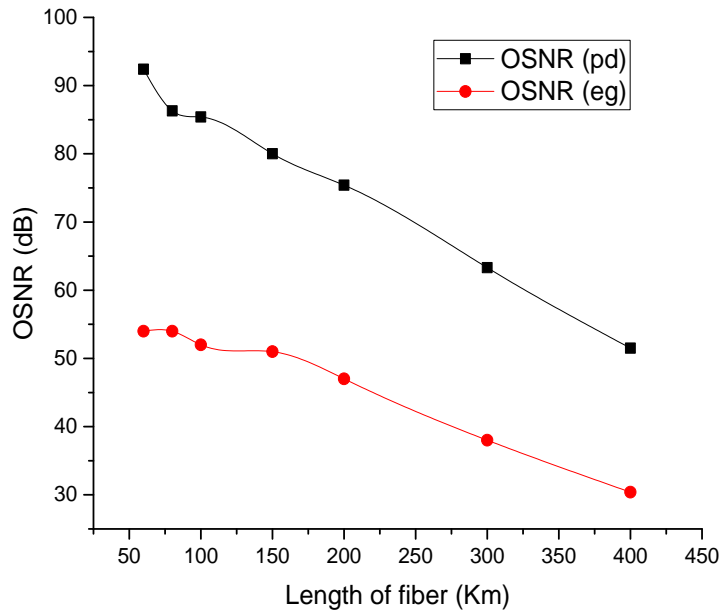


Fig. 5.6 OSNR of the converted signal using proposed method (pd) and existing method (eg)

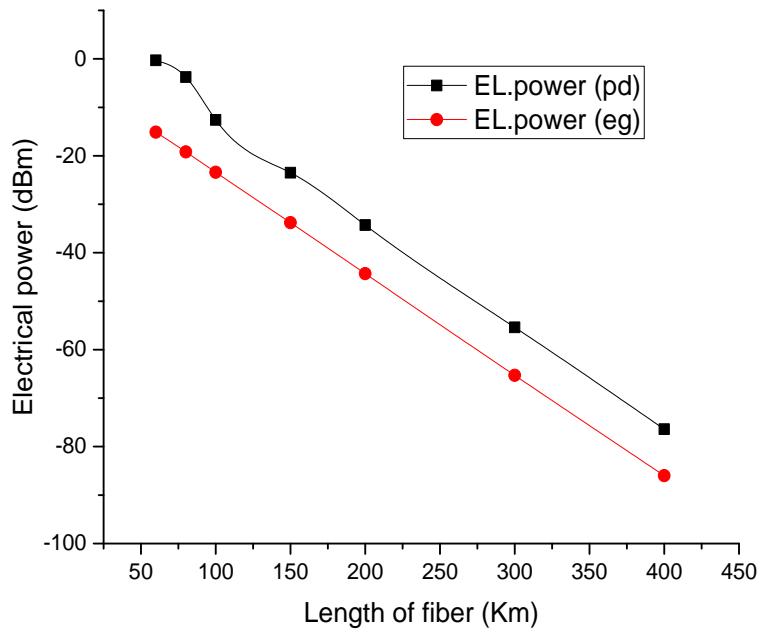


Fig. 5.7 Electrical power output of proposed (pd) and existing method (eg)

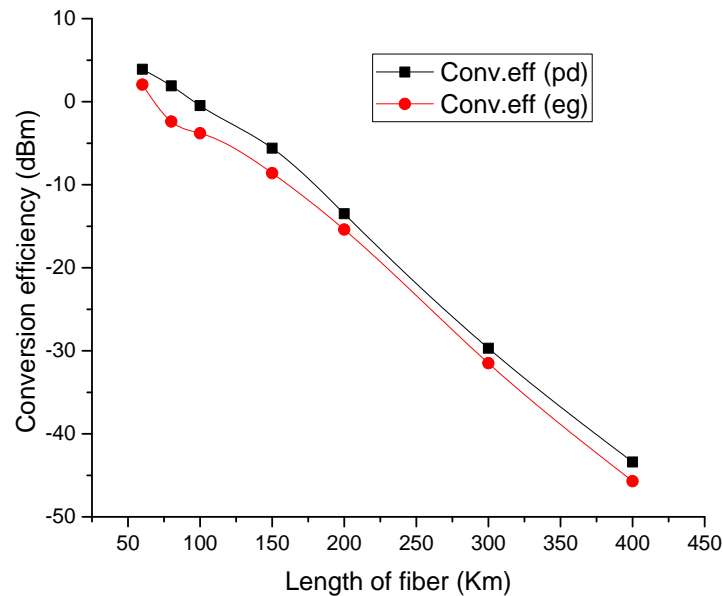


Fig. 5.8 FWM conversion efficiency of the SOA for proposed (pd) and existing method (eg)

5.2.3 Results and Discussion

Fig.5.3 shows the optical phase conjugated output spectrum of the SOA. The phase converted signal is filtered through an FBG and the resultant signal is obtained as in Fig.5.4. Fig.5.5 shows the optical power of both proposed method (pd) and existing method (eg). The graphs show that the proposed method can increase the output power by about 18dB from the existing method. Fig. 5.6 shows the OSNR of the proposed method (pd) and existing method (eg). The graphs show that the proposed method can improve the OSNR by about 38dB from the existing method. Fig. 5.7 shows the electrical power output of the proposed method (pd) and the existing method (eg). Results show that the electrical power of the proposed method is 14dB better than the existing method. Fig. 5.8 shows the FWM conversion efficiency of proposed (pd) and existing (eg) method. The graphs show that efficiency of the proposed method is improved by about 3dB from the existing method.

5.2.4 Conclusion

We have demonstrated a novel chromatic dispersion compensation method using FWM technique of traveling wave SOA. Its performance is compared with the existing method [203] in terms of output optical power, OSNR, conversion efficiency, and output electrical power. The results show that our method can improve the performance of the existing method. It can also transmit at a higher data rate of 80 Gbps to a long transmission distance of 400 km, which is higher than the existing methods. Therefore, this highly efficient configuration can give better results in future optical transmission systems. This configuration has shown good performance over the conventional external modulated system.

5.3 Case 2: Group Velocity Dispersion and Third Order Dispersion in External and Direct Intensity Modulated RoF Link

5.3.1 Overview

There is a considerable growth in the use of analog optical links in the remote areas, RoF, and optical signal processing [206]-[210]. Recent research has focused to enhance the performance of RoF links. The limitations include the undesirable effects of electronic-optical conversion at the transmitter, and optical-electronic conversion at the receiver. In addition, GVD, TOD and nonlinearities in the fiber affects the transmission performance.

MZM is a common modulator used in RoF system, and its intrinsic nonlinearity can introduce nonlinear distortion in the process of modulation, which affects the Spurious Free Dynamic Range (SFDR) of the RoF system. The linearity and dynamic range of the RoF system shall be highest in wireless

applications especially for complex modulation methods. Therefore, alleviating the system's nonlinear distortion and enhancing its dynamic range are important research subjects in this field. Many works have been done to eliminate nonlinear distortions such as Inter Modulation Distortion (IMD), and AM-AM and AM-PM distortions. Few works has been done on OSSB-RoF systems based on MZM and succeeded in eliminating the harmonic components. But the effect of third-order inter modulation distortion (IMD3) has not been analyzed on the system's nonlinearity [211]–[214].

5.3.2 The Optical Link Challenges

The nonlinear modulation process produces harmonics on both sides of the optical carrier. The optically modulated mm wave undergoes different impairments while propagating through the RoF link. The nonlinearity of the electrical-optical modulator, nonlinearities in the optical fiber and weak modulating process results in fragile optical signals [215].

Several Dispersion Managed (DM) techniques are used to compensate the dispersion effects. Three methods are very useful, one using the DCF, optical Fiber Bragg Grating (FBG) and High-Order Mode (HOM) fiber [216]. A higher order adaptive filter based nonlinearity compensation scheme is proposed in [217]. Chirped Fiber Bragg Grating (CFBG) can be effectively used up to ultra high capacity (100 Gbps) long haul transmission systems for dispersion slope compensation. It is shown that the FBG effectively compensates for the dispersion slope while keeping intact in-line filtering [218].

A VCSEL has higher RF to optical power conversion efficiency than an external MZM and a DFB laser diode with the same output optical power [219]–[221]. Also it has less nonlinearity compared to MZM for the same

output power [222]. In practice, higher modulated power can be obtained with MZM for higher input optical power.

Many UWB RoF systems have used SMF which is suited for long-distance access applications. A RoF system using VCSEL direct modulation of impulse radio UWB signals in the 3.1 GHz - 10.6 GHz band has been demonstrated over 100m MMF [223]. The MZM modulator is biased in the linear range (between maximum and minimum) and the modulation signal is superimposed onto the bias voltage. We should sacrifice the extinction ratio for high linearity.

The theoretical modeling and comprehensive software simulations of the performance characteristics of VCSEL and MZM based RoF links are performed over a wide range of data rates and optical powers. Both the GVD and TOD under external modulation and direct modulation are analyzed. The noise performance of the VCSEL is estimated by simulation at data rates ranging from 20 Gbps to 90 Gbps. The obtained results can be used to design and characterize a RoF link using a direct modulation with VCSEL, SMF and a PIN photodiode. We quantify the contribution of the MZM on GVD, TOD and the noise performance of the RoF link by evaluating the Q-factor, received RF signal power and eye diagram. In addition, we consider both a short fiber link (20 km) and a relatively long fiber link (90 km). We have compared the Q-factor, RF power and eye diagrams of both links at a high frequency of 10 GHz.

5.3.3 Theoretical Analysis

Spatial evolution of the pulse envelope in a moving frame at a transmission distance z and a time t is described by the following generalized nonlinear Schrödinger equation [224]

$$\frac{\partial A}{\partial Z} = -\frac{\alpha}{2} A - i \frac{\beta_2}{2} \left(\frac{\partial A}{\partial T} \right)^2 + \frac{i \beta_3}{6} \left(\frac{\partial A}{\partial T} \right)^3 + i |A|^2 A \quad (5.2)$$

where A is slowly varying envelope of the electric field, α is the fiber loss, β_2 and β_3 are GVD and TOD, respectively, and γ is the nonlinear parameter that represents the Kerr non-linearity [225]. $T = t - \frac{Z}{V_g}$ (t is physical time, V_g is group velocity). The parameters β_2 , β_3 and γ are related by commonly used parameters as follows,

$$\beta_2 = \frac{-\lambda^2 L}{2\pi C} \quad (5.3)$$

$$\beta_3 = \left(\frac{\lambda^2}{2\pi C} \right)^2 D'' + \frac{\lambda^2}{2\pi^2 C^2} D \quad (5.4)$$

$$\gamma = \frac{2\pi n_2}{\lambda A_e} \quad (5.5)$$

where λ is the center wavelength of pulse and C is the speed of light in vacuum. A_e and n_2 are the effective beam cross section and the nonlinear refractive index of the DCFs, respectively [226]. The dispersion parameter is,

$$D = \frac{2\pi C}{\lambda^2 \beta_2} \quad (5.6)$$

The phenomenon of dispersion has two contributions, intermodal dispersion and intramodal dispersion. The main advantage of SMF is that intermodal dispersion is absent. However, intramodal dispersion still takes place and pulse broadening does not completely disappear [226]. The group velocity linked with the fundamental mode is frequency dependent because of chromatic dispersion. Each frequency travels at different group velocities and this phenomenon is related to Group Velocity Dispersion (GVD). A specific spectral component travels through a fiber of length L in a time $T=L/v_g$, where v_g is the group velocity and is defined as,

$$V_g = \frac{d(\beta)}{d\omega} \quad (5.7)$$

where β is the propagation constant, $\beta = \frac{n\omega}{c}$. The group index \bar{n}_g is given by,

$$\bar{n}_g = \bar{n} + \omega \left(\frac{dn}{d\omega} \right) \quad (5.8)$$

Group velocity causes pulse broadening because different spectral components of the pulses are distributed during propagation and do not reach simultaneously at the fiber output. GVD and TOD can be expressed by expanding $\beta(\omega)$ in a Taylor series as,

$$\beta(\omega) = \beta_0 + \beta_1(\Delta\omega) + \frac{\beta_2}{2}(\Delta\omega)^2 + \frac{\beta_3}{6}(\Delta\omega)^3 + \dots \quad (5.9)$$

where β_0 and $\beta_1 = \left(\frac{d\beta(\omega)}{d\omega} \right) = \frac{1}{v_g}$. The parameter $\beta_2 = \frac{d^2\beta}{d\omega^2}$ is known as the GVD parameter.

Generally, fiber dispersion is defined by two parameters [226].

$$D = \frac{d}{d\lambda} \left(\frac{1}{v_g} \right) = \frac{-2\beta_2 c}{\lambda^3} \quad (5.10)$$

$$S = \frac{dD}{d\lambda} = \frac{d^2}{d\lambda^2} \left(\frac{1}{v_g} \right) \quad (5.11)$$

$$= \frac{2\beta_2 c^2}{\lambda^3} + \frac{4\beta_3 c}{\lambda^4} \quad (5.12)$$

where D is the dispersion parameter, in units of [ps/(nm.km)] and S is the dispersion slope, measured in [ps/(nm².km)].

For a fiber link containing two different fibers of lengths L_1 and L_2 , the conditions for broadband dispersion compensation are

$$\beta_2 L_1 + \beta_2 L_2 = 0 \quad (5.13)$$

and

$$\beta_3 L_1 + \beta_3 L_2 = 0 \quad (5.14)$$

where β_2 and β_3 are the GVD and TOD parameters of fiber .

5.3.4 Simulation Setup and Results

The Optisystem software is used to simulate the optical communication experiments. The system performance is analyzed through visualizing tools, like optical spectrum analyzer, RF spectrum analyzer and constellation visualizer. They are used to display the spectrum at the output of the system components. Fig. 5.9 shows a 10 GHz, 90Gbps externally modulated RoF transmission system with DEMZM, which is operated at the quadrature operating point. A user defined random sequence with RF analog signal as input is generated to modulate the DEMZM. The intensity modulation results an optical carrier with a Double-Sideband (ODSB) spectrum. The optical spectrum at the output of the MZM is symmetric and is centered at a frequency of 193.1 THz. The optical spectrum is spread over a wide range of frequencies which affects the quality of the signal when it is transmitted through the optical fiber link. The two sidebands produce two beat frequencies at the receiver and they join to form the RF signal. When the ODSB signal has propagated through the optical fiber, GVD and TOD produce pulse broadening and introduce a phase difference between the sidebands and the optical carrier. A SSMF of attenuation 0.2 dB/km and dispersion 16.75 ps/nm/km is used. At the photodetector, the square-law process has generated two components, which are shifted in phase with respect to the carrier. This causes degradation in the output RF power. Fig. 5.10 shows the Q factor and RF signal output of MZM in the presence of TOD for data rates ranging from 20 Gbps to 90 Gbps. Q

factor is 40 dB for 20 Gbps and 8 dB for 90 Gbps. RF signal amplitude is -12 dBm for 20 Gbps and -45 dBm for 90 Gbps. Q-factor and RF power decrease with the increase in data rate. Fig. 5.11 shows the Q factor and RF signal output of MZM in the presence of GVD. Fig. 5.12(a) and Fig.5.12(b) show the eye diagrams obtained at the receiver for transmission distance of L=20 km and L =90 km. Eye diagrams show that as the transmission distance increases, the eye becomes more distorted. Fig. 5.13(a) shows the relation between Q factor and BER.

As the Q factor decreases BER increases. Fig. 5.13(b) shows the relation between eye amplitude and Q factor. Noises decrease with the increase in eye amplitude. Fig. 5.13(c) shows the variation of amplitude of the eye for different data rates (D). Eye amplitude is highest for D= 20Gbps and lowest for D=90Gbps.

Table 5.1 Typical Values of Parameters

Parameters	Value
Optical Fiber	
Length	90 km
Attenuation	0.2dB/Km
Differential group delay	3ps/Km
Effective Area	80 μm^2
Nonlinear index of refraction,(n_2)	2.6*E ⁻²⁰
EDFA	
Noise Figure	4dB
Noise center frequency	193.1THz
Photodetector	
Responsivity	1A/W
Dark current	10nA

Table 5.1 shows the simulation parameters of optical fiber, EDFA and photodetector . Table 5.2 shows the parameters of CW laser, VCSEL and MZM used for the simulation of the system.

Table 5.2 Typical Values of Parameters

Parameters	Value
CW Laser	
Frequency	193.1THz
Noise threshold	-100dB
VCSE Laser	
Center frequency	193.1THz
Bias current	5mA
Maximum input current	40mA
MZM	
Exinction ratio	60dB

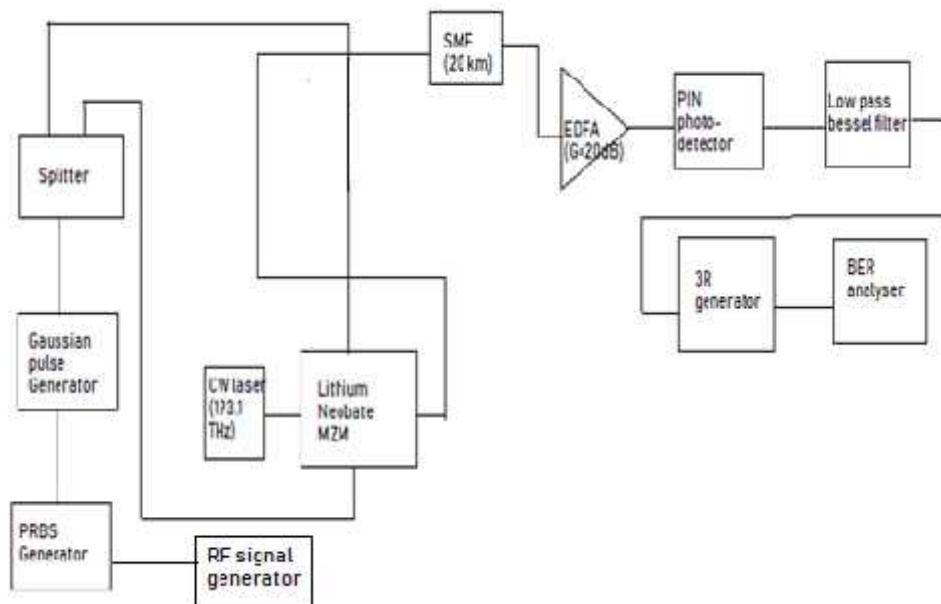


Fig. 5.9 External modulation using dual electrode MZM

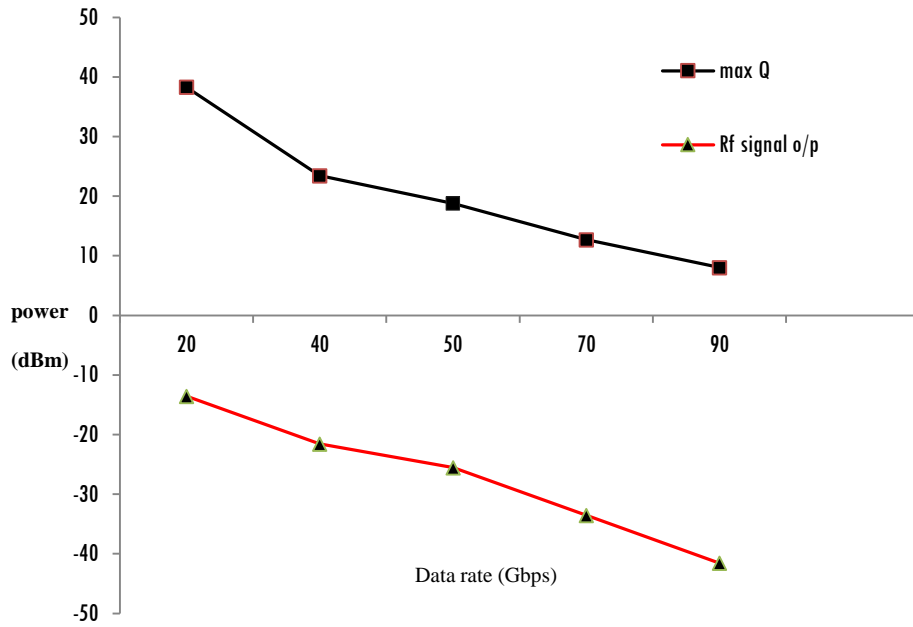


Fig. 5.10 Q factor and RF signal output of MZM in the presence of TOD

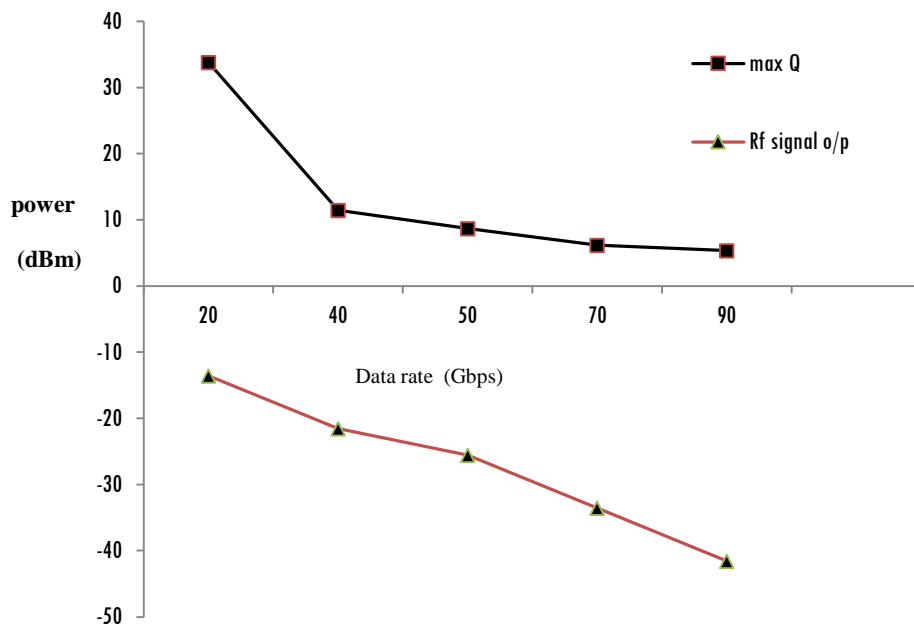


Fig. 5.11 Q factor and RF signal output of MZM in the presence of GVD

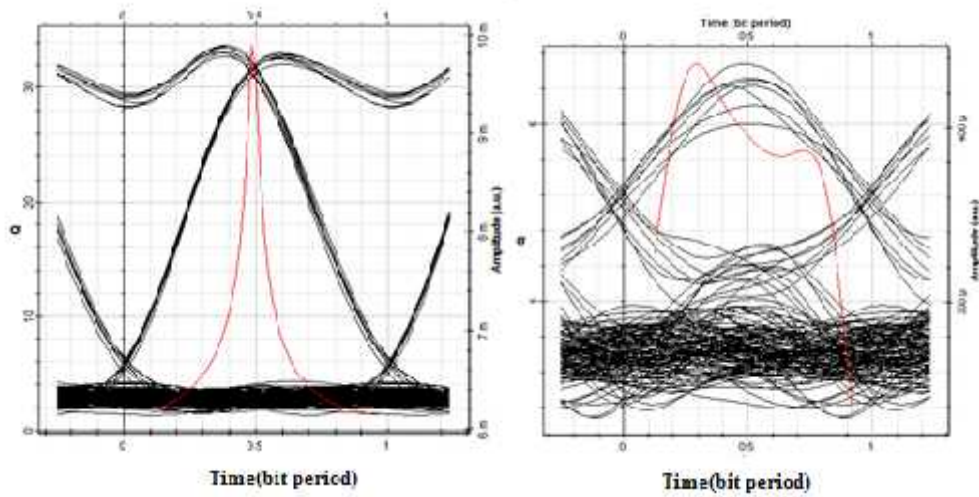


Fig. 5.12 Eye diagram of the electrical signal at the receiver (a) L=20 km, (b) L=90 km

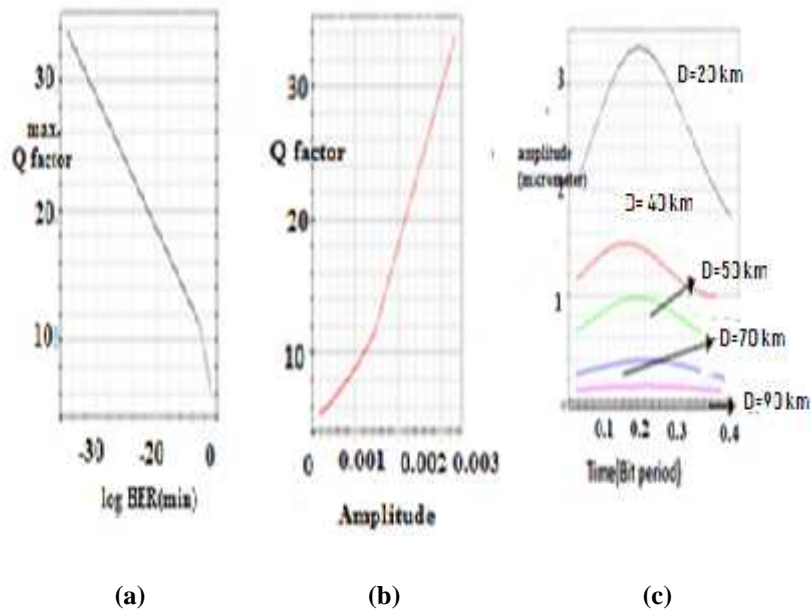


Fig. 5.13(a) Relationship between Q-factor and BER (b) Relationship between Q-factor and eye amplitude (c) Relationship between eye amplitude and time

Fig. 5.14 shows the direct modulation scheme, where a Gaussian pulse is applied directly to the VCSEL to modulate its optical density. VCSEL is operated at a center frequency of 193.1 THz. A SSMF of attenuation 0.2 dB/km and dispersion 16.75 ps/nm/km is used for simulation. A PIN photodetector is used as the optical receiver. All the global parameters used in the direct modulation and external modulation using MZM are same. The parameters of the optical filter following the VCSEL are changed to implement a pass band well-suited with the optical carrier and the upper side band. The optical spectrum of the VCSEL is not entirely symmetric (Fig. 5.15(b)), but the optical spectrum created by the MZM in quadrature operating point is perfectly symmetric (Fig. 5.9). The optical carrier is centered on 193.1 THz, with upper and lower sidebands located at 193.11 THz and 193.09 THz, respectively.

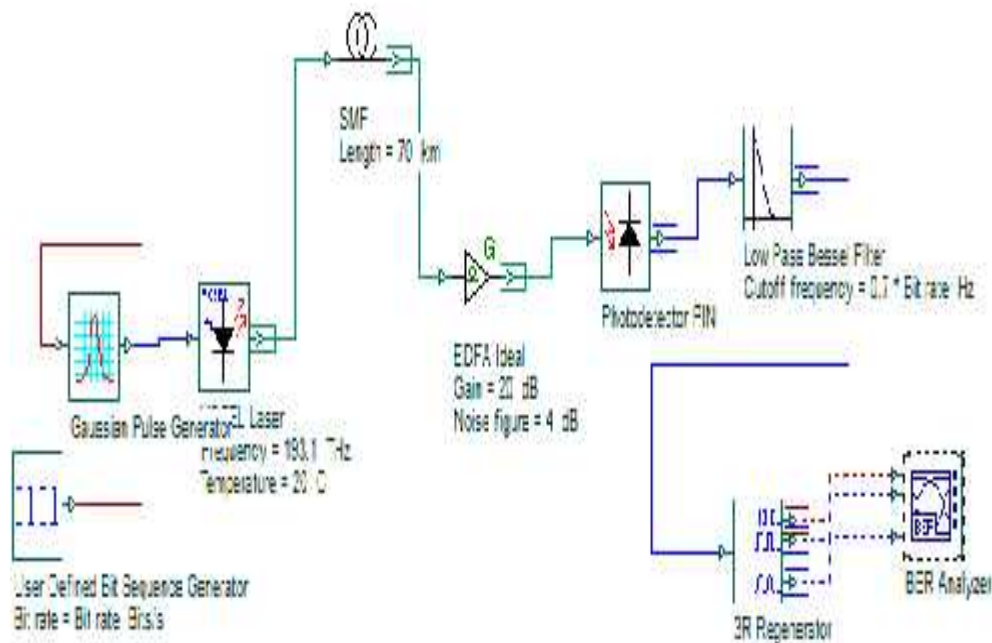


Fig. 5.14 Direct modulations using VCSEL

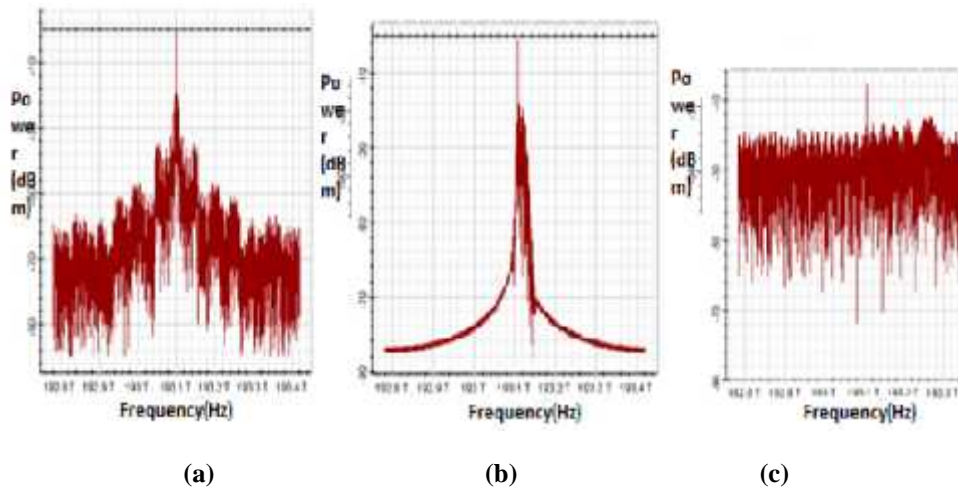


Fig. 5.15 Spectrum of (a) Direct laser (b) VCSEL (c) Saturated VCSEL

As in the new spectrum at the output of the VCSEL (Fig.5.15 (b)), the spectrum symmetry is enhanced but it is not centered at 193.1 THz and it contains adjacent harmonics. The source power of the VCSEL is important, because a high-power input signal causes VCSEL to saturate (Fig. 5.15(c))

Fig. 5.16(a) shows the V-I curve of VCSEL biased at 5mA.

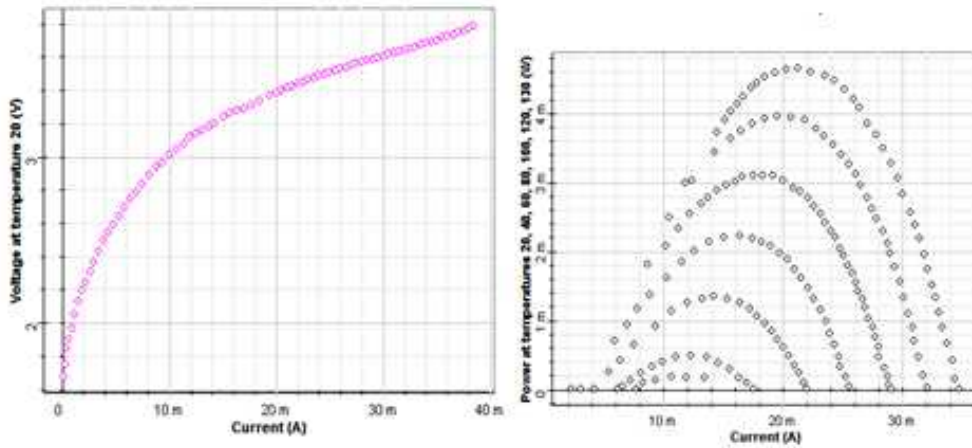


Fig. 5.16 (a) Measured V-I curve (b) Measured L-I curve of VCSEL

Fig. 5.16(b) shows the L-I curve of a VCSEL for different temperature

values at a biasing current of 5 mA. In order to avoid nonlinearity in the gain and saturation at 20°C, the bias current should not go above 5 mA. When the temperature becomes greater than 20°C due to self-heating of the device a nonlinear response is obtained.

5.3.5 Results and Discussion

Fig. 5.10 shows the Q factor and RF signal output of MZM in the presence of TOD for data rates ranging from 20Gbps to 90 Gbps. Qfactor is 40dB for 20Gbps and 8dB for 90Gbps. RF signal amplitude is -12dBm for 20Gbps and -45dBm for 90 Gbps. The Q factor and RF power decrease with the increase in data rate. Fig. 5.11 shows the Q factor and RF signal output of MZM in the presence of GVD. Fig. 5.12(a) and Fig.5.12(b) show the eye diagrams obtained at the receiver for transmission distance of L=20 km and L=90 km. Eye diagrams show that as the transmission distance increases, the eye becomes more distorted. Fig. 5.13(a) shows the relation between Q-factor and BER. As the Q factor decreases BER increases. Fig. 5.13(b) shows the relation between eye amplitude and Q factor. Noises decrease with the increase in eye amplitude. Fig. 5.13(c) shows the variation of amplitude of the eye for different data rates (D). Eye amplitude is highest for D= 20Gbps and lowest for D=90Gbps.

5.3.6 Conclusion

In this chapter, we have presented the effects of GVD and TOD on VCSEL-based direct modulated and MZM-based externally modulated RoF link. The performances are examined in terms of Q factor, eye diagram and BER. This is done at data rates ranging from 20 Gbps to 90 Gbps at different transmission distances. In the simulation, all other nonlinearities are kept at zero except GVD and TOD. From the results, we can see that the VCSEL

transmission can reduce the effect of GVD in terms of Q factor by about 20 dB[223]. In the presence of TOD, Q factor can be increased by about 18 dB. Also RF output power is increased up to 17 dBm approximately. Eye diagrams also show that noise is high in MZM modulation compared to VCSEL modulation. The performance analysis recommends that RoF architecture using VCSEL modulation can support high data rates with less GVD and TOD and is a suitable solution for the future RoF access networks. The results presented here will be useful for designing and implementing high speed long distance optical fiber communication system.

5.4 Case 3: Fiber Dispersion Compensation in Single Side Band optical Communication system using Ideal Fiber Bragg Grating and Chirped Fiber Bragg Grating without DCF

5.4.1 Overview

RoF communication is used in many microwave applications, 4G/5G wireless communications, radar and radio telescopes [227]. Optical fiber has many merits like low loss, high bandwidth, low weight, and immunity to electromagnetic interference over conventional transmission lines [228]. But the performance of the RoF is reduced by the chromatic dispersion (CD) of the optical fiber [227]. Dispersion reduces the information carrying capacity at high transmission speeds and effective bandwidth. It is important to develop an effective dispersion compensation technique in optical communication systems [229]. The optical amplifiers (EDFA, SOA) have reduced the problem of optical fiber losses in the long distance transmission without electronic regenerators. The wavelength is varied the group refractive index and the chromatic dispersion is generated. Chromatic dispersion compensation can be

reduced by Dispersion Compensating Fibers (DCF) and dispersion compensators [230], [231]. A DCF can be used to compensate the dispersion effects of the fiber. But a DCF can increase the optical loss, nonlinear effects and cost of the optical transmission system [232].

CFBG is proposed to reduce the chromatic dispersion instead of DCF. The CFBGs can help in reducing the nonlinear effects and cost. The dispersion compensation using CFBG was proposed by Quette [233] and Williams et.al. [234]. A FBG consists of an optical fiber with a variation in the core refractive index along the propagation direction. Different portions of the grating reflect different wavelengths. The delays that are generated by wavelengths are at different amounts of time. This will produce pulse narrowing and the compensation of the chromatic dispersion of the fiber link. FBGs are widely used in optical communication systems [235] and optical sensors [236].

Automatic dispersion compensation for digital optical communication systems is verified in [237] but this method is not proposed for the RoF system. Tunable dispersion compensation with nonlinearly chirped FBGs for both single and multichannel 40 Gbps transmission system has been studied.

The dispersion of a 10 Gbps system with 1000 km transmission distance is fully automatically equalized [238]. Different methods have been proposed and verified to achieve Single Sideband (SSB) modulation [239]-[249]. The SSB modulation is obtained by filtering one of the sidebands [243]-[245], with the SSB modulators [242]-[244], and amplifying one of the sidebands [245]. SSB modulation is generated using injection locked semiconductor lasers [246]-[247]. The longer wavelength of the modulated sidebands is amplified by the injection-locked laser [246]. The distributed feedback (DFB) laser is used as a wavelength-selective modulator [247].

These methods suffer from a low level of receiver sensitivity due to the difference of the power of the optical carrier and the modulated sideband.

5.4.2 Theoretical analysis

5.4.2.1 Single Sideband Theory

The optical SSB signal can be generated as in Fig.5.17[252].

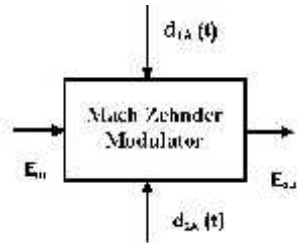


Fig. 5.17 Generation of optical SSB signal

The output electric field of the dual arm MZ modulator as in Fig.5.17 can be represented in a complex exponential form [252] as,

$$E_o = \frac{E_{i1}}{2} \exp\left(j \frac{d_1}{V}\right) + \frac{E_{i2}}{2} \exp\left(j \frac{d_2}{V}\right) \quad (5.15)$$

where V_{π} is the modulator's switching voltage, d_1 and d_2 are the electrical drive signals for each arm of the modulator, and E_{i1} is the amplitude of input electric field. The time dependent drive signals for each arm of the MZ modulator to generate a chirp free optical SSB signal are,

$$d_{1A}(t) = xV_{\pi}(m(t) + \hat{m}(t)) - \frac{V_{\pi}}{4} \quad (5.16)$$

$$d_{2A}(t) = xV_{\pi}(-m(t) + \hat{m}(t)) + \frac{V_{\pi}}{4} \quad (5.17)$$

where 'x' is a modulation parameter, $m(t)$ is an ac coupled version of the original Non Return to Zero (NRZ) binary data, and $\hat{m}(t)$ is the Hilbert transform of the binary data. The DC component of the NRZ data is removed in $m(t)$ since it would affect the modulator bias position.

5.4.2.2 Fiber Bragg Grating (FBG)

The maximum reflectivity of FBG is produced at the wavelength, which satisfies the Bragg condition [250], and is given as,

$$\lambda_B = 2n_e \quad (5.18)$$

Here n_e , Λ , and λ_B represent the effective core refractive index, grating period, and Bragg wavelength, respectively. The forward and backward propagating fields of a uniform Bragg grating are given as [246],

$$\frac{dV}{dz} = i\kappa V(z) + iK U(z) \quad (5.19)$$

$$\frac{dU}{dz} = -i\kappa^* U(z) - iK^* V(z) \quad (5.20)$$

Here, V and U are the transmitted and reflected fields, respectively. κ is the AC coupling coefficient and κ^* is the DC self-coupling coefficient. For a single mode Bragg reflection grating, K is represented as [251],

$$K(z) = K^*(z) = -\sqrt{\kappa \kappa^*} \exp(i\delta z) \quad (5.21)$$

$$\kappa(z) = \frac{\delta}{2} + i\frac{\delta^2}{2\kappa} \quad (5.22)$$

$$= \frac{\delta}{2} \sqrt{\kappa \kappa^*} \quad (5.23)$$

$$= 2 \kappa \left(\frac{1}{2} - \frac{\delta}{\kappa} \right) \quad (5.24)$$

Here ‘ δ ’ is the detuning parameter that is measured by the frequency deviation ratio and the design wavelength. The design wavelength λ_B is the wavelength at which the Bragg condition is obtained. The grating fringes are generated by sinusoidal modulation of the refractive index of the fiber core and given as [252],

$$n_e(z) = \overline{n_e}(z) \left\{ 1 + V \cos \left[\frac{z}{\Lambda} + \phi(z) \right] \right\} \quad (5.25)$$

Here ' $\overline{n_e}$ ' is the average refractive index difference of the grating, V is the fringe visibility of index change; Λ is the grating period and $\phi(z)$ is the grating chirp. The group delay and dispersion are calculated from the phase information is given [238] and is given as,

$$\tau_g = \frac{d}{c} \quad (5.26)$$

$$D = -\frac{2}{c} \frac{d^2 \phi}{d^2 z} \quad (5.27)$$

$$D = \frac{d}{c} = \frac{2}{c} \frac{d}{dz} \left(\frac{d\phi}{dz} \right)^2 \quad (5.28)$$

Here τ_g , D and ϕ are the group delay, dispersion parameter and phase of the power reflectivity spectrum respectively.

5.4.3 Simulation Setup

All the simulations are done in Optisystem 7.0 simulation software. The global parameters used in the system simulation are shown in Table 5.3. Fig. 5.18 shows the block diagram of the system. In the simulation, the transmitter section consists of data source with analog RF signal as source, Gaussian pulse generator, laser source, and MZM. We use a Continuous Wave (CW) laser with a frequency of 193.1THz and a Gaussian pulse generator to operate MZM with an extinction ratio of 30 dB. MZM is operating at quadrature operating point and one of the MZM arm is applied with 90 degree phase shift to obtain SSB modulation. A SMF of length 10 km is used as the transmission medium. The transmission length is varied from 20 km to 80 km. FBG and chirped FBG are used as the dispersion compensators. Their performances are compared with the help of BER analyzers. At the receiver side, the PIN diode is used as a photo detector, which converts the optical signals into electrical, with 1 A/W responsivity and 10 nA of dark current.

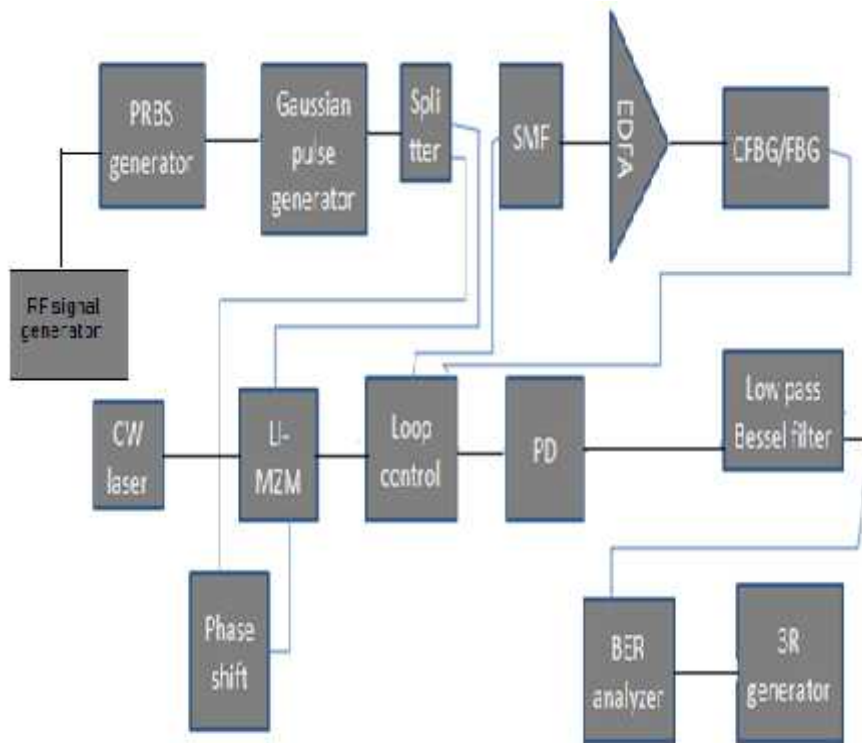


Fig. 5.18 Block diagram of dispersion compensation in SSB optical communication using FBG and chirped FBG

Table 5.3 Simulation Parameters

parameter	Value
CW laser	
Frequency	193.1 THz
Power	0 dBm -8 dBm
MZM	
Extinction Ratio	30 dB
Insertion loss	4 dB
EDFA	
Gain	20 dB
Noise figure	4 dB
Photodetector	
Responsivity	1 A/W
Dark Current	10 nA

5.4.4 Results and Discussion

Figs. 5.19 and 5.20 show the performance of CFBG and FBG for different fiber lengths ranging from 20 km to 80 km. Fig 5.19 and fig.5.20 show that the performance parameters like Q factor, Extinction Ratio (ER). ER is the ratio of energy used to transmit a logic level 1 to the energy used to transmit a logic level 0. Q-factor depicts the quality of a digital signal from an analog point of view; therefore, it is judged as a signal/noise ratio. From Fig. 5.19, ER and RF power are decreased with increased length of fiber. Fig.5.19 shows maximum Q factor is 42 dB, maximum ER is 49 dB and RF power is 7.5 dB. Fig. 5.20 shows that maximum Q factor is 22 dB, ER is 6 dB and RF power is 11 dB. Results show that CFBG can improve the Q performance by about 20 dB, ER by about 42 dB and output RF power by about 3.5 dB in SSB communication system. Table 5.3 shows the global parameters used in the system.

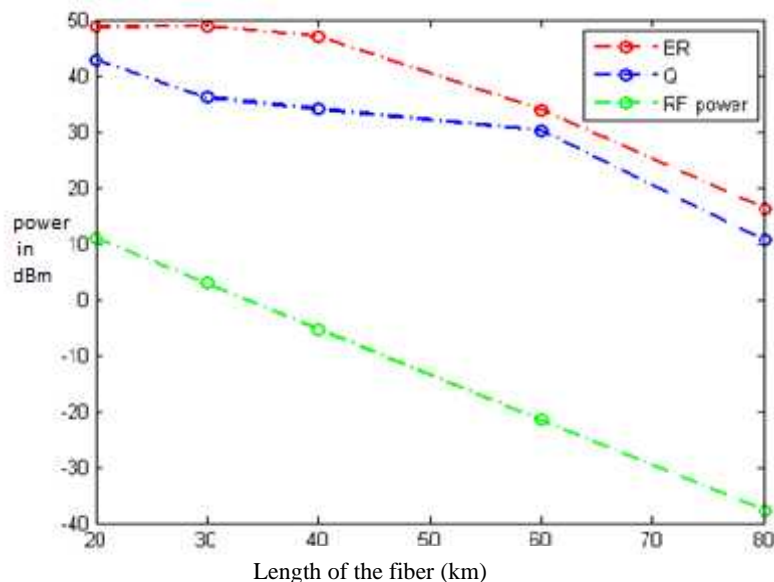


Fig. 5.19 Performance of ER, Q-factor, and RF output power for chirped FBG

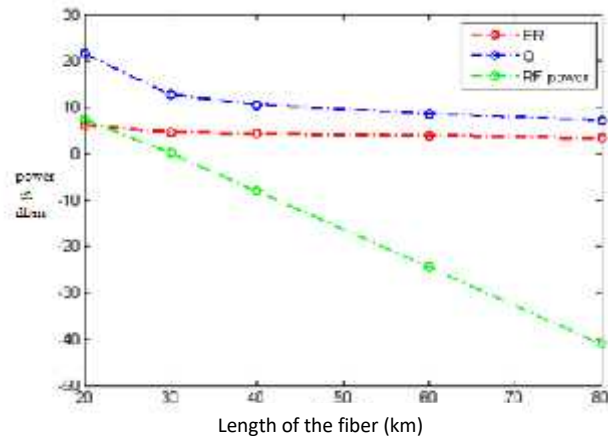


Fig. 5.20 Performance of ER, Q-factor and RF output power for FBG

Fig. 5.21 shows the Q factor, BER and signal power of FBG for input power varies from 0 dBm to 8 dBm. The graph shows that the Q factor is improved from 3dB to 21dB for FBG. The signal power varies from 11 dB to 25 dB for FBG. The BER is increased from -20 dB to -1 dB for input power variation from 0dBm to 8 dBm.

Fig. 5.22 shows the Q factor, BER and signal power of FBG for input power varies from 0 dBm to 8 dBm. The graph shows that the Q factor increases from 16dB to 23 dB for CFBG. The signal power varies from 9 dB to 25 dB. The BER decreases from -32 dB to -35 dB for input power varies from 0 dBm to 8 dBm.

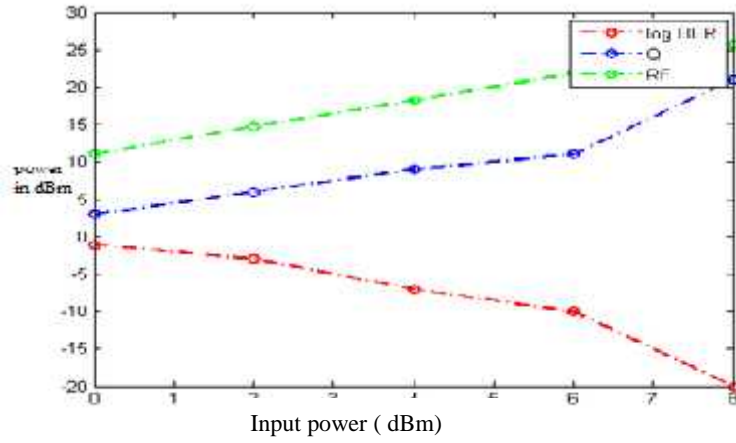


Fig. 5.21 Performance of Q factor ,BER and electrical signal power for FBG

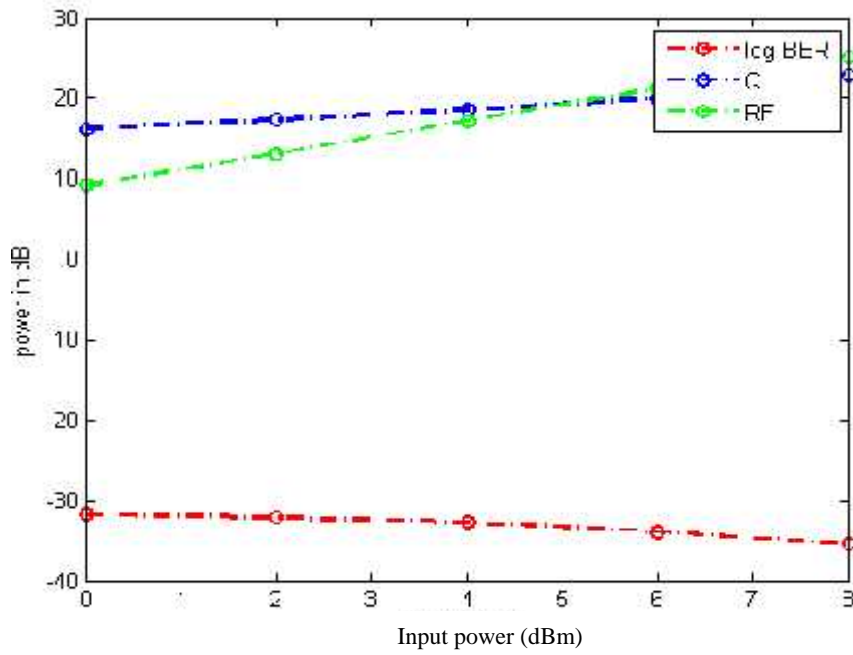


Fig. 5.22 Performance of Q factor, BER and electrical signal power for chirped FBG of fiber length 20 km [input power = 0dBm to 8dBm]

5.4.5 Conclusion

A novel SSB communication system with dispersion compensation using CFBG is proposed here without any DCF. The simulations are conducted for short length and long length fibers from 20 km to 80 km and for different input optical powers ranging from 0 dBm to 6 dBm. Results show that CFBG can improve the Q factor maximum by about 20 dB for various transmission distances. ER is increased by about 21 dB and RF power is by about 3.5 dB. The Q factor is improved by about 3 dB for CFBG with input powers ranging from 0 dBm to 8 dBm. The BER is 15 dB lesser in CFBG than FBG. The performance deviations are high for short distances and low for long distances. These results are helpful for future SSB communication systems.

5.5 Case 4: Mitigation of Chromatic Dispersion using Symmetrical Compensation

5.5.1 Dispersion Compensation Using DCF Technology

DCF has become a more useful method of dispersion compensation. There is positive second-order and third-order dispersion value in SMF (single mode fiber), while the DCF dispersion value is negative. So by placing one DCF with negative dispersion after a SMF with positive dispersion, the net dispersion will become zero. Thus, for DCF compensation,

$$D_S \times L_S = -D_D \times L_D \quad (5.29)$$

Here D and L are the dispersion and length of each fiber segment respectively [253].

Dispersion compensation has a high negative dispersion parameter of -70 ps/nm.km to 90 ps/nm.km and can be used to compensate the positive dispersion of transmitter fiber in C and L bands. According to relative position of DCF and SMF, post-compensation, pre-compensation, mix

compensation is proposed. DCF Pre-compensation scheme achieves dispersion compensation by placing the DCF before a certain conventional single mode fiber. Post compensation scheme achieves dispersion compensation by placing the DCF after a certain conventional SMF. Mix compensation scheme consists of post compensation and pre-compensation i.e. the DCF is once placed before SMF and then placed after SMF. Mix-compensation method largely reduces the non-linear effects as compared to pre-compensation and post-compensation method. Symmetrical/mix compensation has a minimum bit error rate indicating best performance in comparison to pre and post compensation. Advantages of DCF are that they can be easily constructed and are highly reliable. DCF provides continuous compensation over a wide range of optical wavelengths. A DCF module should have low insertion loss, low polarization mode dispersion and low optical nonlinearity. In addition to these characteristics DCF should have large chromatic dispersion coefficient to minimize the size of a DCF module. However, a DCF has a high insertion loss. A 60 km compensator can exhibit 6 dB of loss or more. Because of this, DCF's are usually co-located with EDFA's which also increases the overall cost of the fiber. DCF has a small core size which may make it prone to certain types of nonlinearities and also has high optical nonlinearities. DCF compensation depends on the wavelength and they can perfectly act only in a narrow band of frequency [253] -[255].

5.5.2 System Description and Simulation Details

An optical communication system involving external modulator has been simulated using Optisystem 7 so as to investigate the effect of chromatic dispersion on system performance. Chromatic dispersion is reduced using post-compensation in Fig. 5.23, pre-compensation in Fig. 5.24 and symmetrical

compensation in Fig. 5.25. Here, the system being considered is a RoF optical communication system.

In the pre-compensation method, compensation has been done before SMF and in the post-compensation method, the compensation has been done after SMF. In the symmetrical compensation method, the compensation has been done before and after the SMF. The symmetrical compensation method has the benefits of pre-compensation and post-compensation methods.

The LiNbO₃ MZM is driven by an RF signal of frequency f_{RF} which is equal to 0.1THz. The CW laser source is taken with power of 0 dBm and center emission frequency 193.1THz. The half wave switching voltage V_{π} of LiNbO₃ MZM is 4V. After being modulated at the external modulator, the intensity modulated optical carrier will be transmitted through the optical fiber and detected by the photodetector. We use the parameters in Table 5.4 in mandate to simulate the system.

Table 5.4 Simulation parameters

Parameter	Value
Bit rate	100 Gbps
Frequency of sine generator	0.1THz
Frequency of CW Laser	193.1THz
Power of CW laser	0 dBm
Half wave switching voltage, V_{π} of LiNbO ₃ MZM	4V
Extinction ratio of LiNbO ₃ MZM	20 dB
Insertion loss of LiNbO ₃ MZM	5 dB
Switching RF voltage of LiNbO ₃ MZM	4V
Fiber dispersion	16ps/ns/km
Photodetector responsivity	1A/W

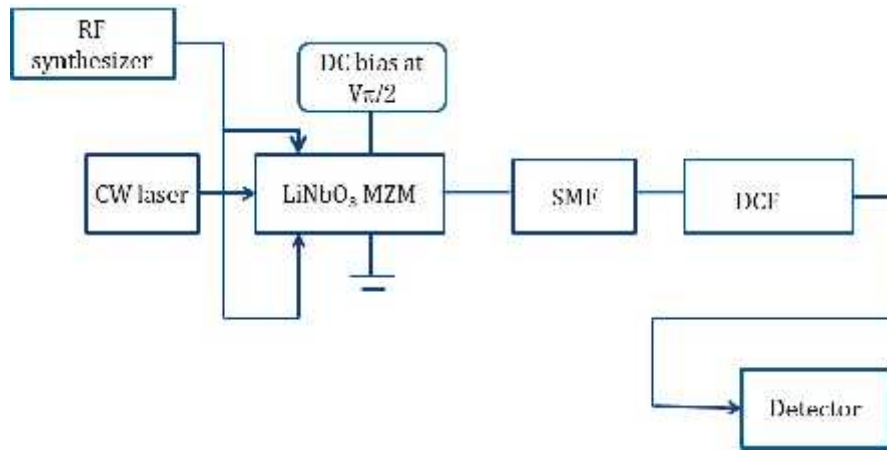


Fig. 5.23 Post compensation using DCF

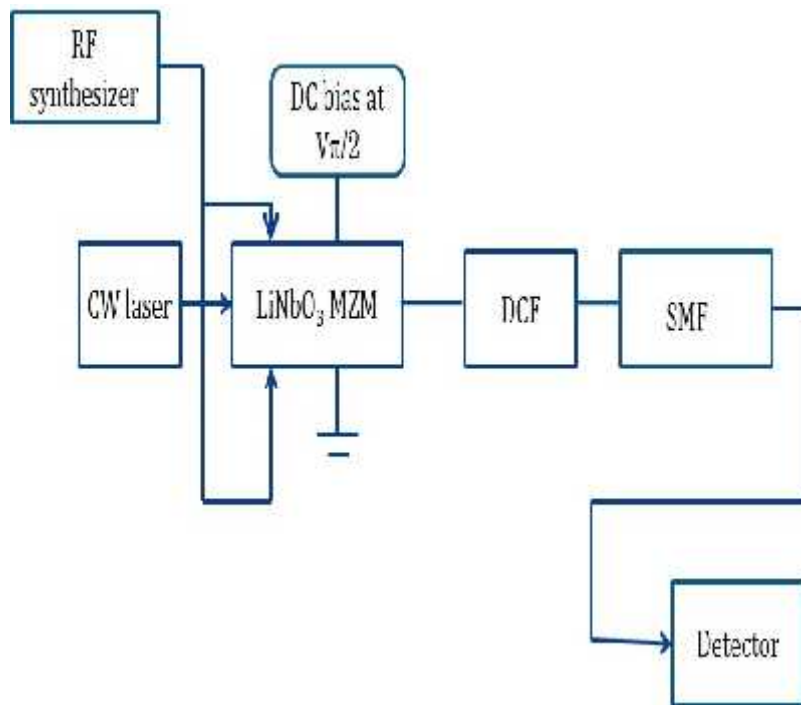


Fig. 5.24 Pre-compensation using DCF

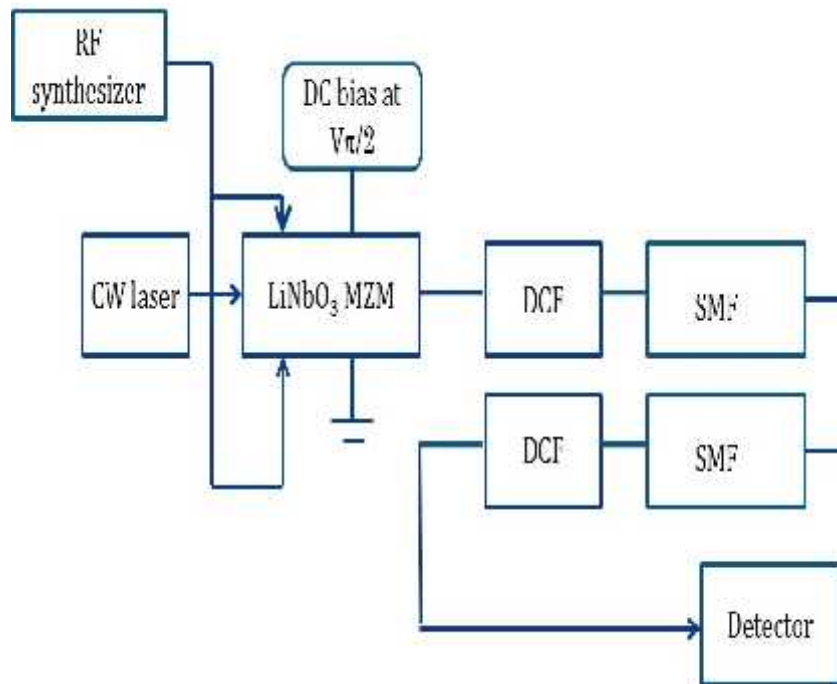


Fig.5.25 Symmetric/mix compensation using DCF

5.5.3 Results and Discussion

In optical communication systems, OSNR alone could not accurately measure the system performance, especially in WDM systems. The eye diagram is a common indicator of performance in digital transmission systems. The eye diagram is an oscilloscope display of a digital signal, sampled to get a good representation of its behavior. For effective communication, eye is closed. As the noise increases, the distortions also increase.

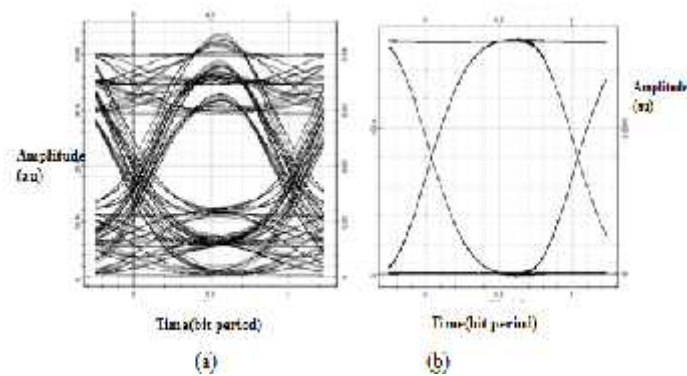


Fig. 5.26 Eye diagram obtained (a) without compensation (b) with pre compensation using DCF

When the intensity modulated optical carrier along with the two sidebands is transmitted through the dispersive fiber, RF power fading occurs. As a result, the eye diagram obtained will be distorted as shown in Fig. 5.26(a).

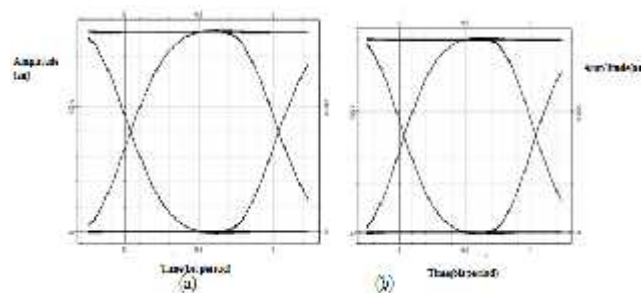


Fig.5.27 Eye diagram obtained (a)with post compensation using DCF (b) with symmetric compensation using DCF

But when dispersion compensation is provided with the DCF, better eye diagram is obtained and it indicates that dispersion has been reduced. The eye diagrams for the three DCF compensation schemes are shown in Figs. 5.26 (b), 5.27 (a) and 5.27 (b).

Fig. 5.28 shows the Q factor comparison of pre-compensated, post compensated and symmetric (mixed) compensated 100 GHz external modulated RoF communication system. Q factor is highest for mixed

compensation. Fig. 5.29 shows the received signal power of symmetrical compensated and uncompensated RoF communication system. The output signal power is high for compensated system. The power varies from -13 dBm to 8 dBm for compensated system. It varies from -26 dBm to -15 dBm for uncompensated system. The difference is high for high input powers. The compensated system provides a power variation of 25 dB from the uncompensated system.

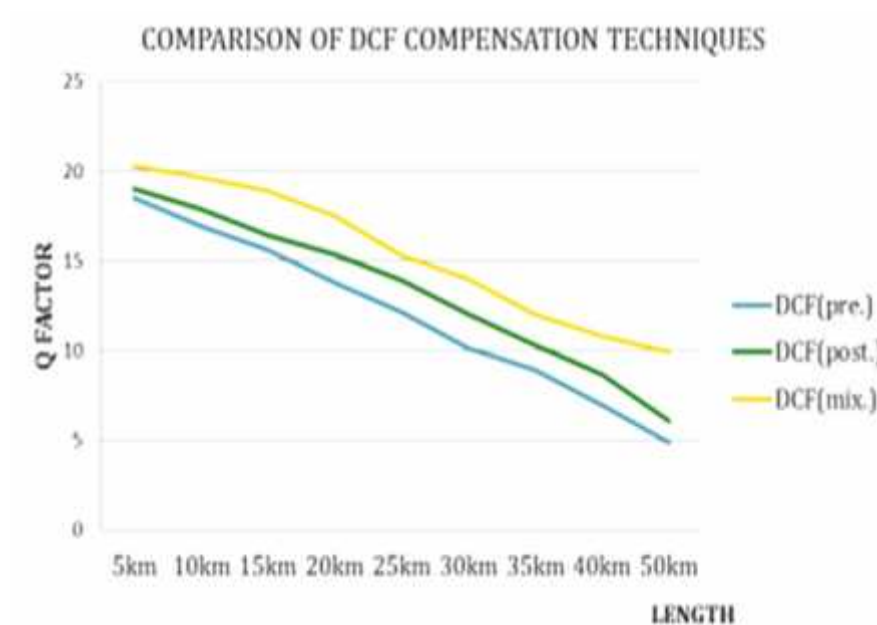


Fig. 5.28 Comparison of DCF compensation techniques

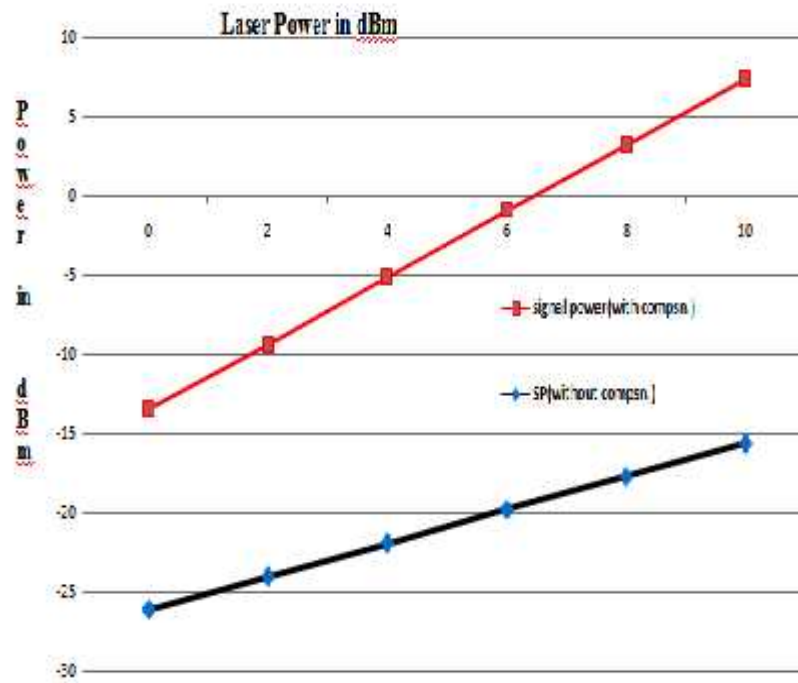


Fig. 5.29 Signal power of the symmetric compensated and uncompensated system

5.5.4 Conclusion

Table 5.5 shows the different performance parameters of existing and proposed methods. Four different methods have been used to reduce the nonlinear distortion in the fiber. The methods are Symmetrical Compensation (SC), dispersion reduction using CFBG, nonlinear distortion reduction using VCSEL, and chromatic dispersion using SOA respectively. Results show that dispersion has been effectively reduced by using SOA. Performance of the different methods are compared in terms of transmission distance, OSNR, received power, and Q factor.

Table 5.5 Result analysis of various existing and proposed methods

Author	Transmission distance (km)	Received power (dBm)	OSNR	Q factor
Meenakshi et.al [248]	100	-10	13	11
Herrera et.al [249]	120	-50		
Ying Wang et.al [250]	120	-29	10	8
Lim A et.al [251]	100	-14	9	7
H K Sung et.al [252]	40	-2	25	28
Christina Lim et.al [253]	100	-28	93	71
Farah Diana et.al [254]	100	-21	22	20
Symmetrical Compensation	40	-17	32	42
	100	-11	31	24
	120	-15	29	14
CFBG	40	-18	49.8	41.7
	100	-10	37.8	11.5
	120	-13.4	33.8	6.4
VCSEL	40	-16.5	38.8	4
	100	-17.8	26.6	3.9
	120	-19.7	22.2	3.7
SOA	100	-9.5	91.8	89
	140	-10.7	89	86
	200	-15	85	82
	400	-18	82	79
	600	-41	59	56

5.5.5 Validation

The symmetrical compensation [Transmission distance- 100 km] method is validated with the method in [248]. The OSNR and Q factor are 30 dB and 22.6 dB respectively for [248]. The OSNR and Q factor have been improved about by 1dB and 1.4 dB respectively for the proposed method as shown in the table 5.6. The performance of CFBG is compared with the results in [250]. The OSNR and Q factor could be improved by about 1.5 dB and 2.5 dB respectively as shown in the table 5.6. The performance of VCSEL is validated with the results in [251]. The OSNR and Q factor are improved by about 0.6 dB and 0.7 dB respectively as shown in the table 5.6. The performance of SOA is compared with the method in [254]. The obtained values for OSNR and Q factor are 55 dB and 54 dB respectively. With the proposed method, the results could be improved about by 4 dB and 2 dB respectively as shown in the table 5.6.

Table 5.6 Validation of results

	Transmission distance	OSNR	Q factor
Proposed method-symmetrical compensation	100 km	31 dB	24 dB
Meenakshi et.al [248]	100 km	20 dB	14 dB
Proposed method-CFBG	120 km	33.8 dB	6.4 dB
Ying Wang et.al [250]	120 km	32.3 dB	3.9 dB
Proposed method-VCSEL	120 km	21.6 dB	3 dB
Lim A et.al [251]	120 km	22.2 dB	3.7 dB
Proposed method- SOA	600 km	59 dB	56 dB
Farah Diana et.al [254]	600 km	55 dB	54 dB

Multiband Access RoF Link Optical Millimeter Wave Dispersion Tolerant Transmission

6.1 Introduction

6.2 Theoretical Analysis

6.3 Simulation Setup and Results

6.4 Conclusion

Abstract

This chapter deals with a multiband RoF communication system with simple decomposition method. Three bands of mm frequencies are generated. The Q factor and eyediagram performance are measured. This method of mm wave generation helps in reducing different nonlinearities in the existing method. This chapter ends up with the conclusion that the proposed system has better performance as compared to the existing system.

6.1 Introduction

Current high definition video services need higher bandwidth for wired and wireless data transmission. The mm wave technology is a dominant method to support multi-gigabit services [255],[256]. It has a wide frequency band to handle high data rate signals. Hybrid Access Networks (HAN) can support different data networks [257]-[260]. They can integrate different RoF and Fiber to the Home (FTTH) technology. They can transmit RF and baseband signals through a single fiber. The multi-band signals generation techniques can improve the efficiency of RoF and HAN configurations [263]-[267]. These configurations can support multi-gigabit services in different wireless and wire-line applications. In [263], multiband signals are generated by connecting a phase modulator and a MZM with an Optical Signal to Noise

Ratio (OSNR) boosting circuit for Fiber to the X (FTTX) and RoF networks. The mm wave band is a significant research topic for high speed wireless data transfer [268]. The RoF technologies can be used for fixed and mobile users with huge capacity, coverage, and mobility [269]-[270]. To get full advantage of integrated optical fiber and wireless system, the RoF technology has been selected as one of the smartest solutions for the wireless network. It can improve the coverage of the mm wave band wireless signals [271]-[272]. The multiband modulation and transmission have been demonstrated [273]-[274]. The Electro-Absorption Modulator (EAM) nonlinearity, chirp, and the crosstalk among three signals reduce the performance in [271]. The scheme proposed in [274] is very expensive and complicated.

An emerging technology is developed with huge communication capacity and low cost [275]. Recently, the generation and transmission of the multiband signals have been demonstrated in [276]-[286]. In [276]-[278], the multiband electrical signals are combined and then converted into an optical signal through a single EAM. In these schemes, the optical modulator must be properly operated at its optimal operation point. Its performance is affected by the distortion produced by the nonlinearity of EAM. The signal performance in these schemes is limited by the EAM nonlinearity, residual chirp, and the crosstalk between multiband signals. A method is proposed with a wavelength division multiplexed-passive optical network and a 60 GHz RoF system using $N \times 1$ single-drive MZMs for an N -channel wavelength-division multiplexed passive optical network is proposed in [279]. In this method, the electrical wired and 10 GHz wireless data are combined in the electrical domain. So the wired and wireless data are independent of each other. They are modulated on the first order sideband and optical carrier.

At the optical network units/base stations, the wired and wireless users can only receive their data and the method can only provide two-band signals. A hybrid mode-locked laser with 5 WDM-PON is presented with RoF channels [280]. This scheme has the same issues in [279]. In [281], an Arrayed Waveguide Grating (AWG) multiplexer is used to enable the integration of dense WDM multiband signals with channel spacing of 12.5 GHz. This method uses three laser sources along with three modulators in the central office and makes the system more expensive. In the work presented in [282], a scheme has been proposed based on a dual-parallel MZM followed by a single-drive MZM to generate the multiband signals through optical carrier suppression and frequency shifting techniques. The multiband signal generation is expensive with a complicated modulator. The spectrum structure of the optical mm wave signal is complex. In the spectrum, each sideband carries the downstream data and the beating tones induce amplitude fading effects.

To improve the dispersion tolerance, a method with multiband generation is proposed in [283]-[284] using two cascade MZMs. The first one is used to generate a DSB optical signal and the second one is operated at the minimum transmission point to generate an optical carrier suppression signal. The scheme has high dispersion tolerance, but an optical filter must be used to convert the DSB optical mm-wave signal to the SSB one after the first MZM. They have proposed a full-duplex RoF system, transmitting downlink wireless 20GHz, 60GHz, mm-wave, and wired baseband data via a single MZM [285]. However, it has the same problems as [282] with complex spectrum. A bidirectional three-band lightwave transport system is proposed [286]. By cascading a Phase Modulator (PM) and a MZM, multiple coherent beams are used to generate downstream Base Band (BB) /microwave (MW) / mm Wave signals. All multiple coherent light waves carry the downstream data which

induces the fading effect due to the fiber dispersion and degrades the generated RF signal performance as they are heterodyne beating at the base station.

Compared with the previous reports [286]–[290], this method is potentially novel with several advantages. One single mm wave oscillator and a nested MZM are required in the CS, which makes the CS cost-efficient. One frequency of the optical signal carries the downstream data, so the effect of the fiber chromatic dispersion can be significantly reduced. Compared with the report [291], this method can reduce the cost of CS in the optical domain since no FBGs and optical filters are used in the circuit. This method has employed a novel baseband decomposition method at the BS. This proposed method is also used at a higher data rate of 80Gbps. It has offered more signal power by about 15dB than the existing method. Q factor is in the range of 14 dB. BER is also low for two bands. Simulation results show that the proposed method can perform better in terms of BER, Q factor, OSNR and data rate.

6.2 Theoretical Analysis

Fig.6.1 presents the architecture of the proposed multiband RoF transmitter using a nested MZM and a laser source. In the CS, the light wave from the Continuous Wave (CW) laser, represented by $E_c(t) = E_c \exp(j\omega t)$, is divided into two beams by the first Y-branch in the nested MZM. Then the two beams are independently injected into two sub-MZMs in the main MZM. The two arms of the upper sub-MZM-1 are operated by the Local Oscillator (LO₁) at $2\omega_{RF}$, as shown in Fig.6.1. The amplitudes of the two driven signals are same and the phase difference between them is $\frac{\pi}{2}$. The relative DC bias voltage between the two arms is set to $\frac{V_\pi}{2}$. Here, V_π is the half-wave of the sub MZM-1, and it has worked on the SSB modulation scheme. The two arms of the lower sub-MZM-2 are biased at the OCS modulation point and it

collaborates in a push pull pattern by another local oscillator (LO₂) as shown in Fig. 6.1. The phase difference between the two driven signals with the same amplitude is π and the relative DC bias voltage of the sub-MZM-2 is V_π . Here, ω_{RF} is the angular frequency of the RF LO₂. In the upper branch, the RF LO₁ is mixed with the QAM signal and can be expressed as,

$$\begin{aligned} D_{RF} - QAM(t) &= V_{RF1}[I(t)\cos 2\omega_{RF}(t) - Q(t)\sin 2\omega_{RF}(t)] \\ &= \sqrt{I^2(t) + Q^2(t)}V_{RF1} \cos [2\omega_{RF}t + \varphi_i(t)] \end{aligned} \quad (6.1)$$

Here, V_{RF1} is the amplitude of the upper driven RF signal, and $I(t)$ and $Q(t)$ are the in-phase and quadrature branches of the downstream QAM signal, respectively. We take the 4-QAM modulation format as an example. So, $\sqrt{I^2(t) + Q^2(t)} = \sqrt{2}$, and $\varphi_i(t) = \arctan(Q(t)/I(t))$. It represents the phase information of the 4-QAM data. The negative first order sideband is suppressed and the second and higher order sidebands are avoided due to their small amplitudes. So the generated SSB optical signal mainly consists of two tones with the frequency spacing of $2\omega_{RF}$: the center carrier at ω_c , and the positive first-order sideband bearing the downstream data at $\omega_c + 2\omega_{RF}$. The SSB optical mm-wave signal can be expressed as,

$$\begin{aligned} E_{SSB}(0, t) &= \frac{\gamma_a}{2} E_c(t) \left[e^{j\frac{\pi}{2}} \sqrt{2} V_{RF1} \cos[2\omega_{RF}t + \varphi_i(t)] + \right. \\ &\quad \left. e^{j\frac{\pi}{2}} \sqrt{2} V_{RF1} \sin[2\omega_{RF}t + \varphi_i(t)] + j\frac{\pi}{2} \right] \end{aligned} \quad (6.2)$$

$$= \frac{\sqrt{2}}{2} \gamma_a E_c e^{j\omega_c t} + m_{ha} E_c \gamma_a [(\omega_c + 2\omega_{RF})t - \varphi_i(t)] \quad (6.3)$$

where γ_a is the sub-MZM-a insertion loss, $m_{ha} = \frac{\pi V_{RF1}}{V_\pi}$ is the modulation index and $J_K(\cdot)$ is the k^{th} order Bessel function of the first kind. In the lower branch, the light wave is modulated by the RF LO₂ at ω_{RF} in push-pull pattern via the sub-MZM-2. The generated OCS optical mm-wave signal mainly

contains the two first-order sidebands at $\omega_c - \omega_{RF}$ and $\omega_c + \omega_{RF}$, respectively, and can be expressed as,

$$E_{OCS}(0,t) = \frac{\gamma_b}{2} E_c(t) \left[e^{\frac{-j\pi v_{RF2}}{v_\pi} \cos(\omega_{RF}t) + j\pi} + e^{\frac{-j\pi v_{RF2}}{v_\pi} \cos \omega_{RF}t} \right] \quad (6.4)$$

$$= \frac{\gamma_b}{2} E_c e^{j\omega_c t} [\exp(j m_{hb} \cos \omega_{RF}t) - \exp(-j m_{hb} \cos \omega_{RF}t)] \quad (6.5)$$

$$= \gamma_b E_c \sum_{k=-\infty}^{\infty} j^k [1 - (-1)^k] J_k m_{hb} e^{j(\omega_c + \omega_{RF})t} \quad (6.6)$$

where γ_b is the sub-MZM-2 insertion loss, and $m_{hb} = \frac{\pi V_{RF2}}{v_\pi}$ is the modulation index. If the modulation index is small, there is $J_1^{(x)} = x$. The residual central carrier at ω_c and the high-order sidebands can be neglected, due to their small optical power compared with the first-order sidebands. Then the generated SSB and OCS optical signals, respectively, from the upper and lower branches are coupled via the second Y-branch in the nested MZM to constitute the optical signal which can be expressed as,

$$E_D(0,t) = \gamma_{bEC} m_{hb} e^{j(\omega_c - \omega_{RF})t} + \frac{\sqrt{2\gamma_a E_c}}{2} e^{j\omega_c t} + \gamma_{bEC} m_{hb} e^{j((\omega_c + \omega_{RF})t + \frac{\pi}{2})} + m_{ha} E_c \gamma_a e^{j((\omega_c + 2\omega_{RF})t - \phi_i)t} \quad (6.7)$$

It can be seen that the four tones keep the frequency spacing of ω_{RF} between the adjacent tones and only the tone at $\omega_c + 2\omega_{RF}$ carries the downstream data, while the other tones are unmodulated. Here, it is worth noting that since the downstream data is modulated in SSB pattern, it only carried by one tone, which significantly reduces the effect of the fiber chromatic dispersion [290].

After being transmitted over the optical fiber with the amplitude attenuation coefficient of α and propagation constant of $\beta(\omega)$ at the angular frequency of ω , the optical signal becomes,

$$E_D(z, t) = e^{-az} \left\{ \left[\gamma_b E_C m_{hb} e^{j[(\omega_c - \omega_{RF})t + \frac{\pi}{2} - \beta[(\omega_c - \omega_{RF})z]}] + \right. \right. \\ \left. \left. \frac{\sqrt{2}}{2} \gamma_a E_C e^{j(\omega_c t - \beta(\omega_c)z)} + \gamma_b E_C m_{hb} e^{j[(\omega_c + \omega_{RF})t + \frac{\pi}{2} - \beta[(\omega_c - \omega_{RF})z]} + \right. \right. \\ \left. \left. \gamma_a E_C m_{ha} e^{j[(\omega_c + 2\omega_{RF})t + \frac{\pi}{2} - \beta[(\omega_c - 2\omega_{RF})z - \phi_1[t - [\omega_c + 2\omega_{RF}]]^{-1} \beta((\omega_c + 2\omega_{RF})z)]]} \right] \right\} \quad (6.8)$$

Fig. 6.5 shows the Base Station (BS) of the multiband access. The four-tone optical signal can be decomposed as three different SSB optical signals, as demonstrated by the optical spectra in Figs. 6.7(a), 6.7(b) and 6.7(c), respectively, at the BS. After a high-speed square-law photodetector, the mm wave signal is generated based on heterodyne beating. In the first case, the RF signal is generated with a frequency of ω_{RF} with the help of product modulator with a local oscillator frequency of ω_{RF} . In the second case the mm wave at $2\omega_{RF}$ is produced by the photodetector and product modulator tuned with a local oscillator frequency of $2\omega_{RF}$. The last case is to generate the mm wave signal at $3\omega_{RF}$. The local oscillator of the product modulator is tuned to $3\omega_{RF}$. An antenna is used to radiate the mm wave signals to the user terminals for wireless transmission in the real system. The wireless end users can receive the wireless signal and recover the downstream baseband data through the coherent demodulation in the electrical domain. So, the proposed scheme generates the multiband mm wave wireless accesses and the most significant advantage of our proposed scheme is that the downstream data is only modulated on one frequency of the optical signal with single sideband modulation technique. The three generated RF signals with different frequencies highly tolerate to the fiber dispersion. In other words, the limit of transmission distance caused by chromatic dispersion can be mitigated theoretically.

6.3 Simulation Setup and Results

The multiband RoF-based link with SSB optical mm-wave signals is shown in Fig.6.1, to prove our proposed scheme for simultaneous multiband generation and transmission. In the CS, the light wave with a frequency at 193.1THz, an output power of 15dBm and a line-width of 10MHz is emitted from the CW laser. Its power is divided into two beams. Then they are applied into the sub-MZM-1 and sub-MZM-2 to generate the SSB and OCS optical mm-wave signals, respectively. In the upper branch of the main MZM a 80 GHz sinusoidal wave is mixed with the downstream baseband 4-QAM signal mapped from the 80 Gbps Pseudo Random Binary Sequence (PRBS) with a word length of $2^7 - 1$ to drive the sub-MZM-1. The half-wave voltage of the MZM-1 is 4V and the relative DC bias tension between the two arms is 2 V. The generated SSB optical mm-wave, as in Fig.6.2 (a), mainly consists of two optical frequencies with the optical Carrier to Sideband Ratio (CSR) of 11 dB with a resolution of 0.01 nm. The negative first order sideband is suppressed with a sideband suppression ratio (SSR) of about 8dB, and the other high-order sidebands are avoided due to their smaller power. The OCS output at the lower MZM-2 is shown in Fig. 6.2 (b).

In Fig.6.2 (a), the central carrier at 193.1THz is an unmodulated optical frequency and the positive first order sideband at 193.18THz is broadened due to the QAM data modulation. The frequency spacing between them is 80GHz. The lower branch of the main MZM is modulated by a 40GHz RF clock with a driving voltage of 1V through the sub-MZM-2 that is biased at the minimum transmission point with a half-wave voltage of 4V and with a relative DC bias tension between the two arms as 4 V. The even-order sidebands and the

central carrier are suppressed completely, and the other high-order sidebands are at least 32 dB smaller than the first order ones as shown in the optical spectrum of Fig. 6.2 (b). From Fig. 6.2 (b), we can also see that the frequency spacing between the two first order sidebands at 193.06THz and 193.14THz is 80 GHz. The SSB optical signal generated from the upper branch is coupled with the OCS optical signal from the lower branch to form the optical signal. An optical band pass filter with a central wavelength of 193.1THz and bandwidth of 100GHz is used to filter out the high-order smaller sidebands and the out-of-band noise. The optical signal mainly contains four tones as shown in the Fig. 6.3. The frequency of 193.18THz carries the downstream data and the other frequencies are unmodulated. The generated multiband is transmitted forward to the Base Station (BS) through a SMF with a chromatic dispersion of 16.75ps/nm/km, a power attenuation of 0.2 dB/km and a dispersion slope of 0.075 ps/nm² / km. Fig. 6.4 shows the OSNR and output optical power of the mm-wave transmission. Fig. 6.5 shows the block diagram of multiband base station.

At the BS, they are directly injected into a photodetector with a responsivity of 1 mA/mW, dark current and thermal noise of the photodetector are 10nA and 1e⁻²² W/Hz, respectively. The electrical signal is applied to a product modulator. For the 80 GHz mm wave generation, the local oscillator is adjusted to 80GHz and the unwanted sidebands are avoided with an electrical band pass RC filter at a cut- off frequency of 80GHz. The 40GHz signal can be generated by a local oscillator with a cut off frequency of 40GHz. The 120GHz signal is generated by a local oscillator. The unwanted sidebands are reduced by using a band pass RC filter with a cut-off frequency of 120 GHz.

Fig. 6.6 shows the difference of optical received signal power of RF waves for 80 Gbps (proposed method) and 10 Gbps (existing method [291]). For both methods, the signal power decreases with increasing transmission distances. The signal power has a maximum shift of 15dB from the existing method. The output signal spectra of three frequency bands are shown as in Fig. 6.7(a), Fig.6.7(b), and Fig.6.7(c) respectively. Fig. 6.8 shows the Q factor and eye diagrams of 40GHz, 80GHz and 120GHz millimeter waves. For 40GHz and 120GHz, the eyes are more closed with minimum noise and high Q factors. But for 80GHz, eye diagram is not closed and Q Factor is below 6dB except for BTB transmission. So the performance of 80GHz is worse than other two bands [292].

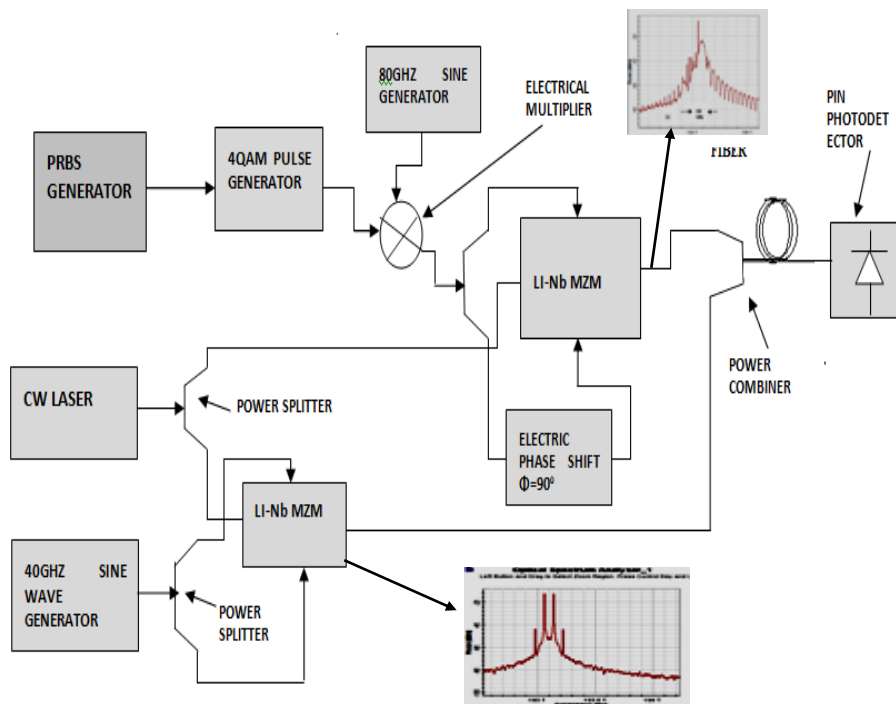


Fig. 6.1Block diagram of multiband transmitter

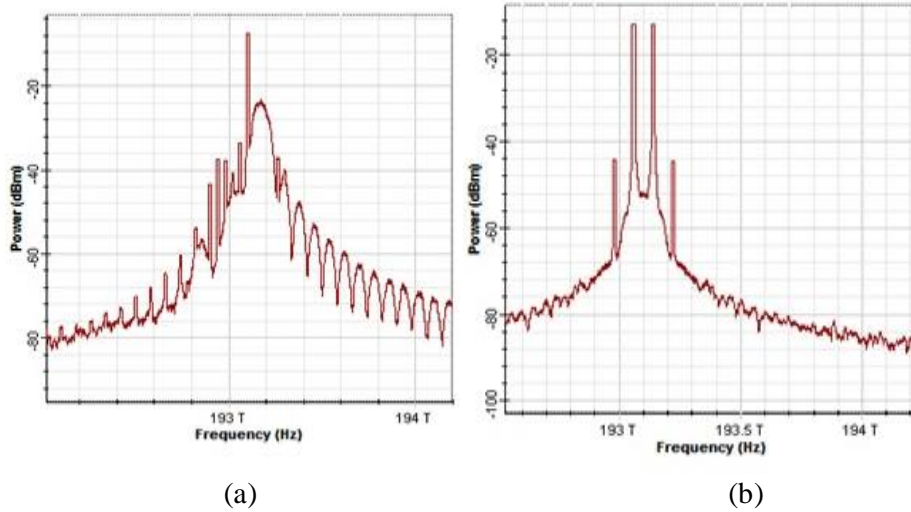


Fig. 6.2 (a) Optical SSB spectrum of the upper MZM, (b) RF-OCS optical spectrum of the lower MZM

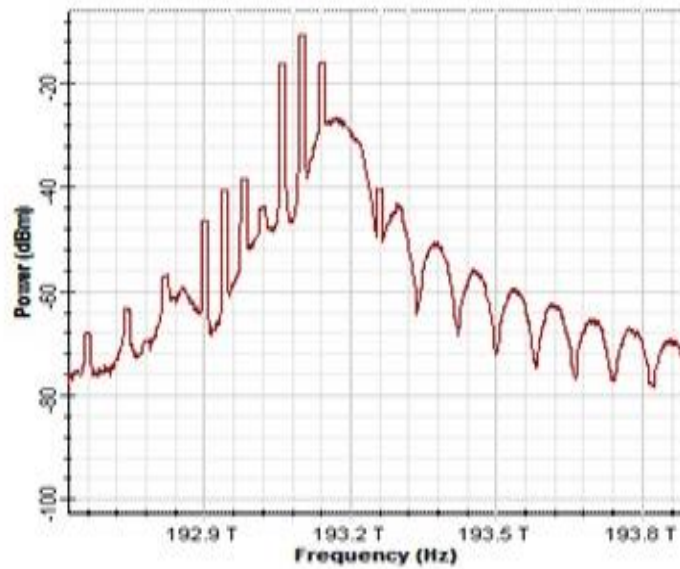


Fig.6.3 Generated optical spectrum of the main MZM

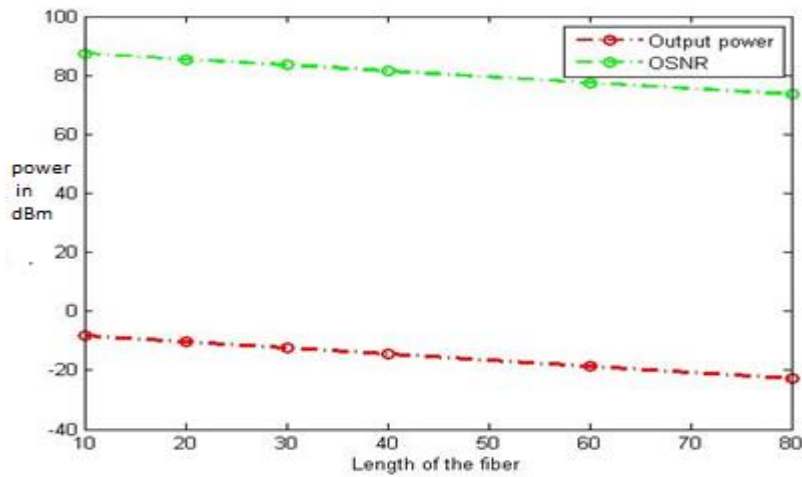


Fig.6.4 Output optical power and OSNR of the generated optical millimeter wave for different length of fiber (km)

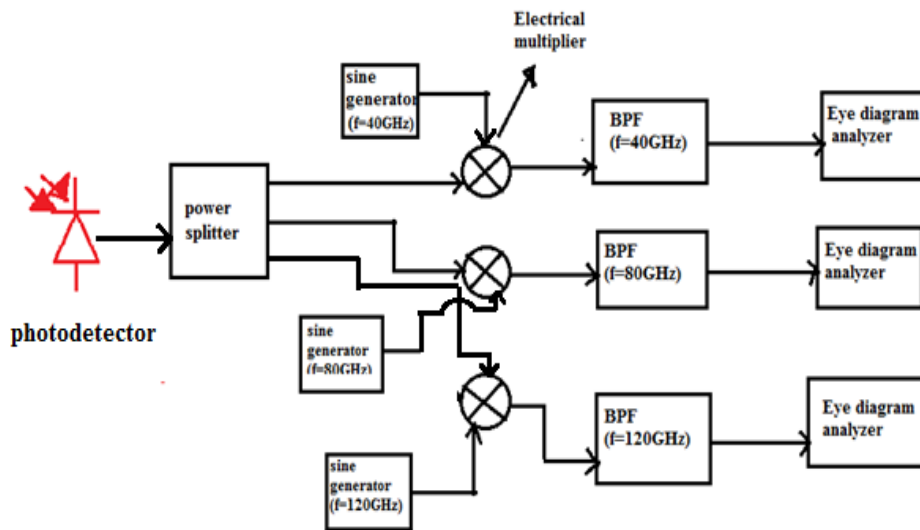


Fig. 6.5 Block diagram of multiband base station

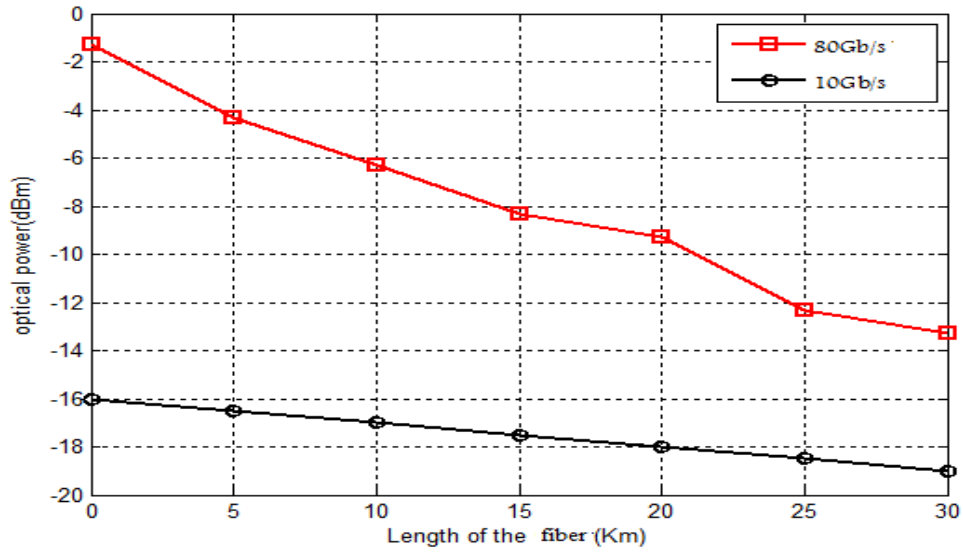


Fig.6.6 Output optical signal power of millimeter wave at data rates of 80 Gbps and 10 Gbps

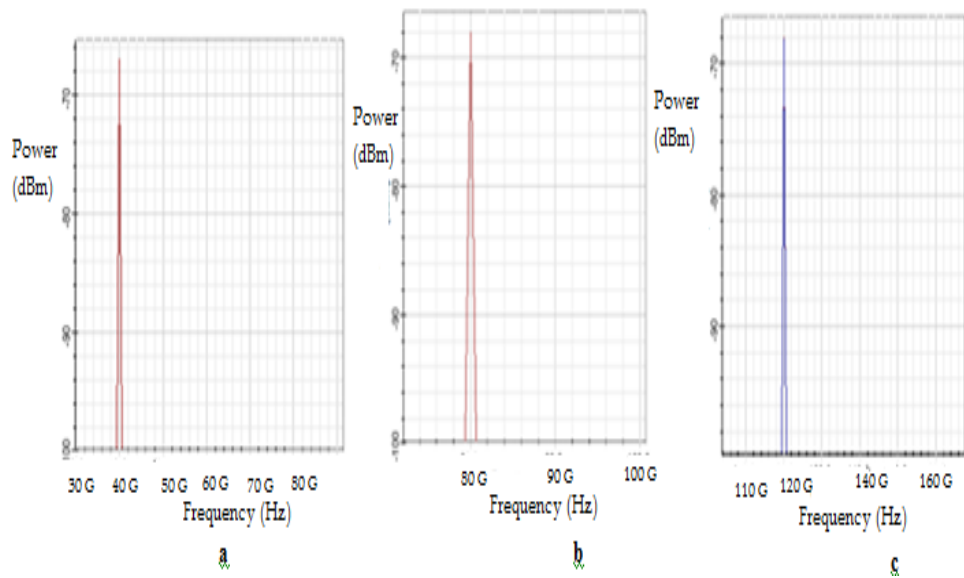


Fig.6.7 Received electrical spectra of millimeter waves at (a) 40 GHz (b) 80GHz (c) 120GHz

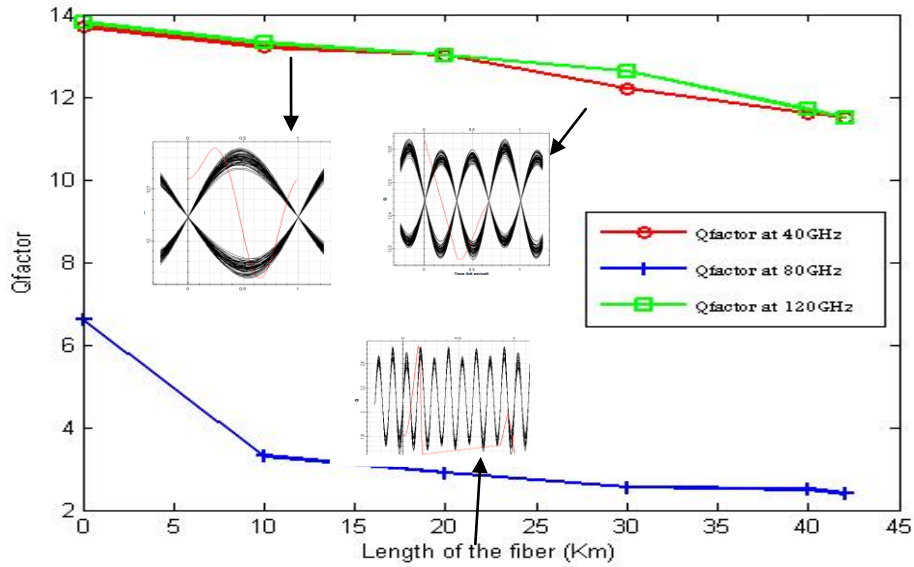


Fig.6.8 Q-factor and eye diagram performance of the received mmwaves for frequencies 40GHz,80GHz and 120GHz

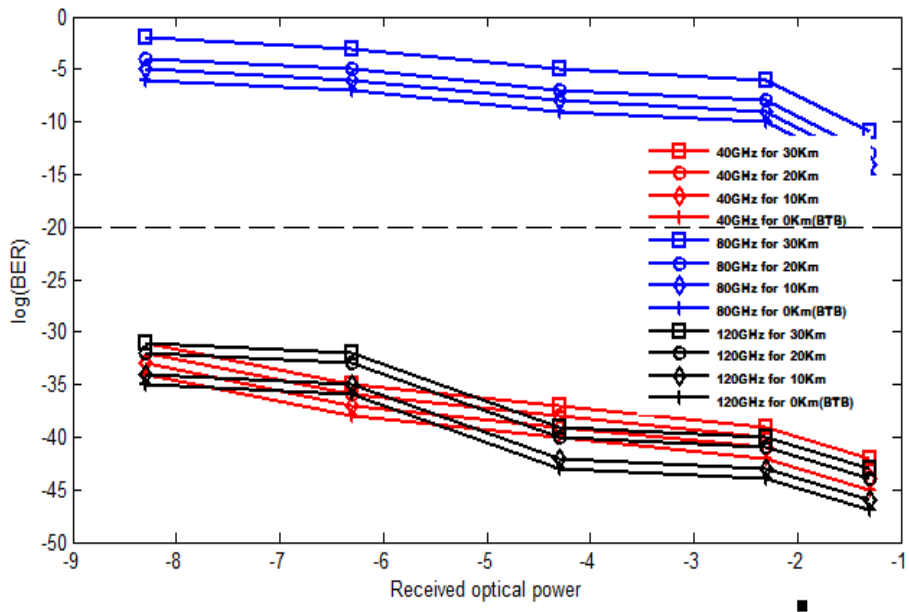


Fig.6.9 BER performances of 40GHz,80GHz and 120GHz millimeter wave signals at B-T-B, 10 km, 20 km and 30 km of transmission distances

Fig. 6.9 shows the graph between the measured BER and received optical power of the 80 Gbps 4QAM signal for the mm-wave signals of 40GHz, 80GHz and 120GHz respectively. Their performances are analyzed for transmission distance of 0 km (B-T-B), 10 km, 20 km and 30 km respectively. The graphs show that the BER gradually decreases with increase in optical powers. It is evident that 80GHz mm wave shows worst performance compared to others. The 120GHz band gives the best performance and the 80GHz band shows the worst performance due to low Q factor as shown in Fig.6.8. As the chromatic dispersion is low, B-T-B transmission shows better performance in three-millimeter bands.

6.4 Conclusion

We have presented a novel low cost RoF link with a SSB optical mm wave signal to carry the 40GHz, 80GHz and 120 GHz mm wave multiband wireless accesses. In the proposed method a simple signal decomposition technique instead of FBGs and optical filters are employed in the existing method. So, the proposed low-cost method can reduce the nonlinearities in the FBGs. The simulation results reveal that our proposed scheme can provide multiband wireless accesses at a data rate of 80Gbps with higher transmission performance in terms of low BER, higher Q factor and higher received optical power. Results show that BER is around 10^{-20} with the higher output optical power of -4 dBm, even while using a SMF of length 30 km. The results show that the proposed method can provide better performance in multiband RoF communication.

6.5 Validation

The performance of the proposed method is validated with the results in [291]. The received optical signal power and OSNR are -4 dBm and 88 dB respectively. The proposed method could be improved the signal power and Q factor about 2 dBm and 1.3 dB respectively as shown in the table 6.1.

Table 6.1 Validation of results

	Received optical power	OSNR
Proposed method	-4 dBm	88 dB
Ruijiao et.al [291]	-6 dBm	86.7 dB

Peer-to-Peer 200 GHz Millimeter Wave Long Haul RoF Networks Through AWGN Wireless channel

- 7.1 Introduction
- 7.2 Generation of Optical Millimeter Wave
- 7.3 Characteristics of Millimeter Wave Signal
- 7.4 Theory and Principle
- 7.5 Simulation Setup
- 7.6 Results and Discussion
- 7.7 Conclusion

Abstract

This chapter discusses about a 200 GHz mm wave signal generation with reduced phase noise and frequency instability. The peer to peer transmission is considered with AWGN channel. Chapter ends with the performance analysis in terms of Q factor and BER.

7.1 Introduction

RoF technique in the multi-gigabit wireless optical networks has emerged as a dominant solution for increasing system capacity, mobility and the cost of networks [293]. The combination of wireless and optical networks can achieve the large bandwidth efficiency of the optical fiber and the benefits of the wireless network. The RoF based optical wireless networks can be used in conferences, shopping malls, airports and Olympics [294]. Multimedia communication must have the Peer-to-Peer (P2P) communication between wireless users in RoF access networks [295]. The signal from the transmitter is sent to its nearest BS which then delivers to the BS close to the destination through the branch network and finally transferred to the destination user. The wireless-optical communication network can reduce the interference and increase the system throughput [296].

The fifth generation (5G) wireless networks have low wireless bandwidth. As the mm wave has huge bandwidth from 30 GHz to 300 GHz, mm wave transmission can be proposed to provide multi-gigabit communication [297],[298]. Current experiments are conducted in the bandwidth of 28 GHz, 38 GHz, 60 GHz and E-band. Complementary Metal-Oxide-Semiconductor (CMOS) RF integrated circuits are used to design electronic components in the mm wave band [299], [300], [301]. Commonly used standards for indoor wireless communication are IEEE 802.11ad [299], ECMA-387 [302], [303] and IEEE 802.15.3c [304]. Due to the differences between mm wave communications and other systems operating in the microwave band there are many challenges in physical (PHY), Medium Access Control (MAC) layers of mm wave transmission.

The mm wave bands can be utilized to provide huge bandwidth and to reduce the frequency jamming problem in the optical–wireless networks [305]. But it is essential to reduce the cost of the BS and complexity of the CS. As mm wave band has high atmospheric attenuation, the area of coverage of the BS is small. At the CS, the optical mm wave signals are produced and processed by cost efficient optical methods. Optical networking technologies are used to increase the transmission distance and to integrate the BS and CS. The BS is designed to support full-duplex operation.

7.2 Generation of Optical Millimeter Wave

Due to distortions in the electronic components, mm wave frequencies suffer from nonlinearity problems to a great extent. It can be avoided by using optical components. Novel methods have been developed for the optical mm wave production, processing and transmission. Three different methods are traditionally used for the generation of mm wave signals. They are Direct

intensity modulation, Remote heterodyning and External intensity modulation. Even though the Direct modulation [305], [306] is the simplest method, it is not suitable for mm wave frequencies. Higher cost of the generation of driving signals and low dispersion tolerance are the disadvantages of external modulation technique at mm wave frequencies. The heterodyning technique is performed by transmitting two or more optical signals concurrently and heterodyned at the receiver. But in this method, the phase noise is reduced by an Electro-optic modulator or a complex optical source [307]. New methods have been attempted for upconversion of radio signals. But they suffer from nonlinear effects in the waveguide, the requirement of high input power and low conversion efficiency [308]. The disadvantage of the method based on cross gain modulation in a Semiconductor Optical Amplifier (SOA) [309], is the requirement of large input power for the SOA. The Cross Phase Modulation (XPM) method using SOA and MZM [310] requires low input power, but the complex structure and the nonlinear crosstalk greatly affect the signal quantity of wireless users.

A mm wave RoF access network [311] with a P2P connection consists of high frequency clock sources and high bandwidth modulators at the BS for signal upconversion. It increases, the architecture complexity and cost on the user side [312]. The frequency conversion for a mm wave system is possible by a self-heterodyne transmission technique [313] without high-bandwidth millimeter-wave oscillator.

Another method has been proposed by beating of two phase-correlated optical carriers in a high-speed photodetector [314]. Different techniques have been proposed, like optical-phase locking [315], external modulation based on MZM [316] and active mode locking [317]. With the method of optical phase locking [318], it is difficult to reduce the phase noise of the mm

wave signal. The frequency quadrupling technique for generating mm wave signal with external modulation and optical carrier suppression has been proposed in recent years [320]. The most common limitation of these schemes is that since the modulation depth is high, the MZM requires additional microwave amplifiers. The active mode locking technique is used to phase lock the laser so that the modulation depth can be lower than that of the external modulation technique and it generates high order optical sidebands. In [321], rational harmonic mode locking technique has been proposed for quadruple-frequency microwave signal generation, but the DC bias and the modulation depth of the MZM must be optimized simultaneously, which makes the system complicated and unstable.

7.3 Characteristics of Millimeter Wave Signals

The characteristics of mm wave signals should be considered in the design of network architectures and protocols. The mm communication suffers from huge propagation loss compared with other communication systems at lower carrier frequencies. The losses due to rain attenuation, atmospheric and molecular absorption of mm wave propagation reduce the range of mm wave communication [322]. For smaller cells in the order of 200 m, the rain attenuation and atmospheric absorption do not create large path loss [323]. Hence, mm wave communication can be mainly used for indoor regions, small cell sizes of the order of 200 m. Major work has been done on mm wave communication at 60 GHz bandwidth [324]. The free space propagation loss increases with the square of the carrier frequency. With a wavelength of about 5 mm, the free space propagation loss at 60 GHz is 28 decibels (dB) more than at 2.4 GHz .

A simple and effective method of optical generation of high frequency 200 GHz mm wave is presented and simulated based on a novel P2P interconnection architecture for mm wave RoF access networks [325]. The signal is upconverted by the beating of the light waves for downlink and P2P transmission at the photodiode. An envelope detector on the user terminal is used to down-convert the mm wave signals and eliminate the frequency instability and poor phase noise characteristics of the two independent signals.

The signal conversion is done without any high frequency clock sources or other high bandwidth devices. Millimeter wave signal at a data rate of 1 Gbps can be transmitted over a SMF for a transmission distance 170 km with low BER.

7.4 Principle

The schematic diagram of the proposed P2P architecture in a 200 GHz mm wave RoF access network is shown in Fig.7.1. Here we consider one of the users who is attached to the base station 1 to be communicating with another user in the BS. The uplink and P2P signals at different mm wave bands are joined at the user terminal 11. The signals are transmitted through the antennas and down-converted at BS 1.

A radio frequency signal is generated from the P2P signal. For the uplink and P2P transmission, the generated signals are modulated by two different wavelengths.

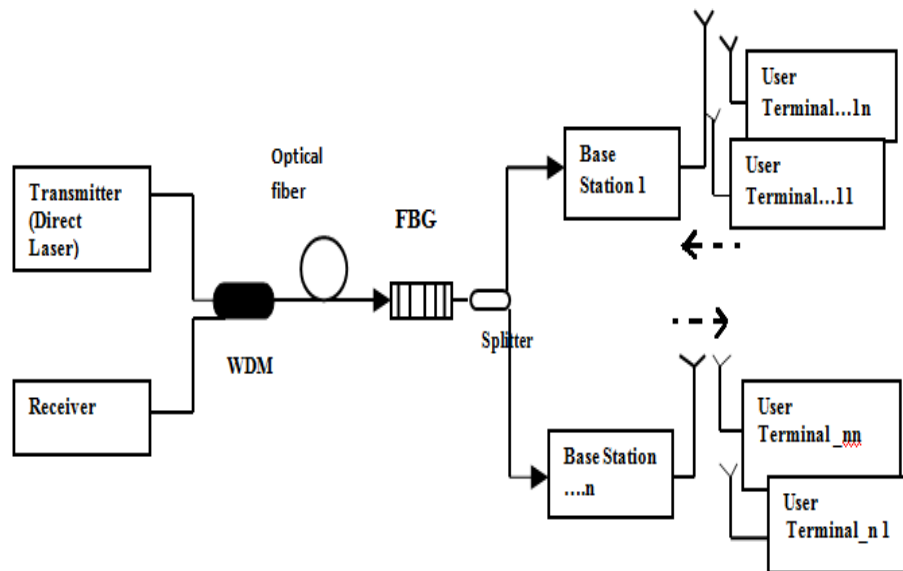


Fig. 7.1 Basic diagram of the proposed P2P interconnected system

The P2P signal from a user terminal is filtered using a Fiber Bragg Grating (FBG) and transmitted through a 1: N WDM multiplexer to all base stations. At the photodetector, the downlink signal and P2P signal with a relative frequency spacing of 200 GHz are generated. An envelope detector is used to down convert the received downlink and P2P signals to their associated radio frequency signals. This can reduce the frequency distortion and poor phase-noise characteristics of the two independent optical signals. Then two RF clock sources with frequencies RF_1 and RF_2 are used to separate the P2P signal from the downlink signal and thus realize the communication between the two wireless users. For downlink and P2P signal up/down-conversion, this scheme is proposed, thus eliminating any high frequency clock sources or other high bandwidth devices. Fig. 7.1 shows the basic

diagram of data up/down conversion [324]. The two optical signals before photodetector, can be represented as:

$$E(t) = Ae^{j\omega_c t} + A_1(t)e^{j(\omega_c + \omega_{RF1})t} + B_1(t)e^{j[\omega_c + \omega_f - \omega_{RF2}]t + \Phi(t)} + Be^{j[(\omega_c + \omega_f)t + \varphi(t)]} \quad (7.1)$$

Here A and B are the amplitude of CW lights from light sources used for downlink and P2P transmission. The terms ω_c, ω_{RF1} , and ω_{RF2} are the angular frequencies of the CW light from downlink light source. The intermediate RF frequencies RF_1 and RF_2 is around 200 GHz, which is the relative frequency between two CW lights. The relative phase difference between the two free-running heterodyned light sources is $\theta(t)$. $A_1(t)$ and $B_1(t)$ are the downlink data and P2P transmitting data, respectively. Single sideband signals can reduce the useless sidebands generated by the two beat frequencies at the photodetector. The generated RF electrical signal in the 200 GHz mm wave band can be expressed as,

$$R(t) = 2\mu_1 AB \cos[\omega_f t + \theta(t)] + 2\mu_1 A_1^{(t)} B \cos[(\omega_f - \omega_{RF1})t + \theta(t)] + 2\mu_1 AB_1(t) \cos[(\omega_f - \omega_{RF2})t + \theta(t)] + 2\mu_1 A_1^{(t)} B_1^{(t)} \cos[(\omega_f - \omega_{RF1} - \omega_{RF2})t + \theta(t)] \quad (7.2)$$

Here μ_1 is the responsive efficiency of the photodetector, $\theta(t)$, which is measured as phase noise, makes the generated millimeter wave signals as very unstable. when the signal is transmitted through the antennas, the undesired sideband is nearly filtered out and signal becomes,

$$R_1^{(t)} = 2\mu_1 AB \cos[\omega_f t + \theta(t)] + 2\mu_1 A_1^{(t)} B \cos[(\omega_f - \omega_{RF1})t + \theta(t)] + 2\mu_1 AB_1^{(t)} \cos[(\omega_f - \omega_{RF2})t + \theta(t)] \quad (7.3)$$

This signals are fed in to an envelope detector which has its output at a low-frequency band as

$$\begin{aligned}
V(t) &= \mu_2 \left| R_1^{(t)} \right|^2 & (7.4) \\
&= 2\mu_1^2 \mu_2 A^2 B^2 + 2\mu_1^2 \mu_2 A_1^2(t) B^2 + 2\mu_1^2 \mu_2 A^2 B_1^2(t) + \\
&\quad 4\mu_1^2 \mu_2 A B A_1^{(t)} B_1^{(t)} \cos(\omega_{RF1} - \omega_{RF2})t + \\
&\quad 4\mu_1^2 \mu_2 A B^2 A_1^{(t)} \cos(\omega_{RF1})t + 4\mu_1^2 \mu_2 B A^2 B_1^{(t)} \cos(\omega_{RF2}) & (7.5)
\end{aligned}$$

μ_2 is the envelope detector's responsive efficiency. Due to the low output bandwidth of the envelope detector, the high frequency ($>RF2$) terms are reduced. As in equation (7.5), the two desired signals at ω_{RF1} and ω_{RF2} do not consist of the phase-noise term $\theta(t)$ and is free of the local carrier frequency ω_F . Therefore, the frequency distortion and poor phase-noise characteristics of the two free-running light sources will not have an effect on the final required signals.

A fixed line of sight wireless channel is considered an AWGN channel [307] with flat fading channel. The AWGN has a constant power spectral density through the channel bandwidth and a Gaussian type amplitude probability density function. This Gaussian noise is combined with the transmitted signal before the receiver as shown in Fig. 7.2. The transmitted signal 's(t)', white Gaussian noise 'n(t)', and received signal

'r (t)' are expressed by the following equation as,

$$r(t) = s(t) + n(t) \quad (6.6)$$

Here 'n(t)' is the sample function of the AWGN process.

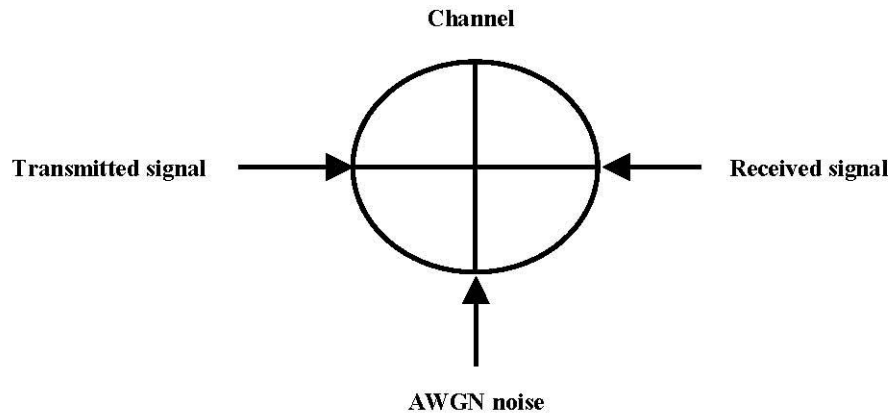


Fig.7.2 Schematic diagram of AWGN channel

The in-phase and quadrature components of the AWGN are considered to be statistically independent, fixed Gaussian noise process with zero mean and two-sided PSD of $N_0/2$ Watts/Hz. Because variance is used to completely characterize the zero-mean Gaussian noise, this model is particularly simple to use in the detection of signals and in the design of optimum receivers [307]. So, it was developed using, “awgn” function which is also available in MATLAB.

7.5 Simulation setup

The block diagram of the proposed scheme is shown in Fig. 7. 3. A 1 Gbps Pseudo-Random Bit Sequence (PRBS) stream is generated using a Pseudo Random Sequence Generator and RZ pulse generator, is modulated on a CW light from a 192.1 THz laser at a radio frequency of 6 GHz for the downlink transmission. The generated RF signal is modulated by a MZM and it is launched into a 25 km SSMF to the Remote access Network (RN). The downlink signal is combined with the coming P2P light from the BS-1 by a WDM multiplexer. The combined signals are transmitted through a long distance SSMF of length 110 km into a PIN photodetector at BS- 2 . The mm wave signals are generated through the beating of two carriers. When the

signal is transmitted over an offline AWGN channel, the received downlink signal at the remote station is down-converted by an envelope detector. The experiments are conducted for different transmission lengths and different input powers. Then they are demodulated and filtered to their associated 6 GHz RF band. The generated electrical spectrum is shown in Fig.7.4.

In the P2P transmission, a continuous wave with 192.3THz is generated at a radio frequency of 10 GHz. Then the generated RF signal is externally modulated by a MZM and combined with the downlink signal by a 2 by 1 WDM multiplexer. Then the P2P signal is amplified by an EDFA of length 5 m. Then it is transmitted through the AWGN channel and demultiplexed by a 1 by 2 WDM multiplexer at the remote station.

It is detected by an envelope detector and the combined millimeter signal at 200 GHz is shown in Fig.7.4. The mm signal is demodulated using an electrical demodulator and a 10 GHz electrical band pass filter at a cutoff frequency of 10 GHz.

Table 7.1 simulation Parameters

Serial No.	Parameters	Value
1	CW laser	
1.1	Wavelength	192.1 THz to 193.1 THz
1.2	Power	-2 dBm to 6 dBm
1.3	Line width	10 MHz
2	MZM extinction ratio	30 dB
3	SMF attenuation	0.2 dB/Km
4	BPF cut off frequencies	6GHz, 10GHz
5	Photodetector	
5.1	Responsivity	1 A/W
5.2	Dark current	10 n/A

Table 7.1 shows the simulation parameters used in the mm wave generated system. A SMF of dispersion 16.75ps/nm/km is used as the optical channel. BER analyzers are used for BER measurement.

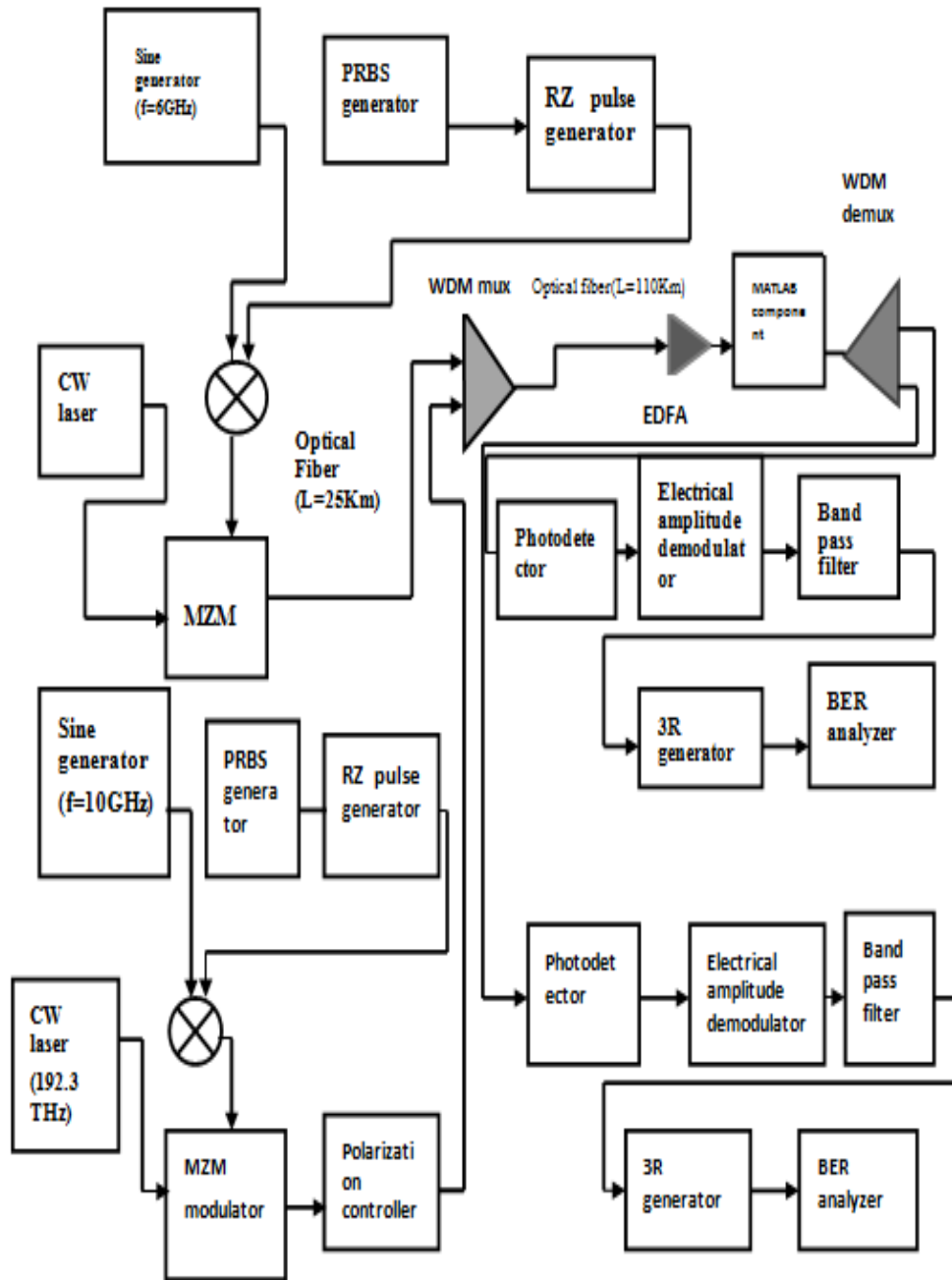


Fig.7.3 Block diagram of 200 GHz peer to peer millimeter wave RoF transmission

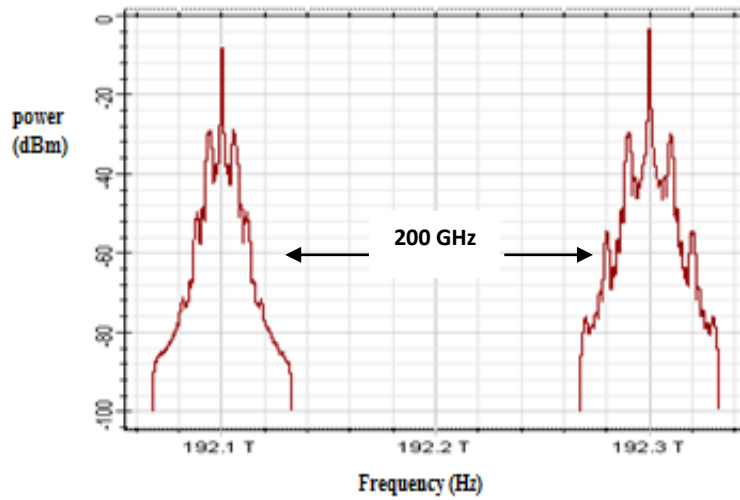


Fig.7.4 200 GHz millimeter wave generated spectrum

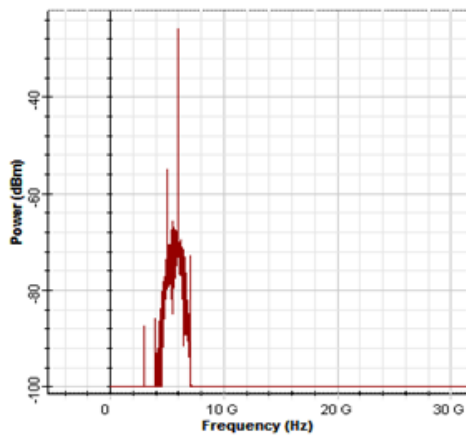


Fig.7.5 6GHz millimeter wave received spectrum

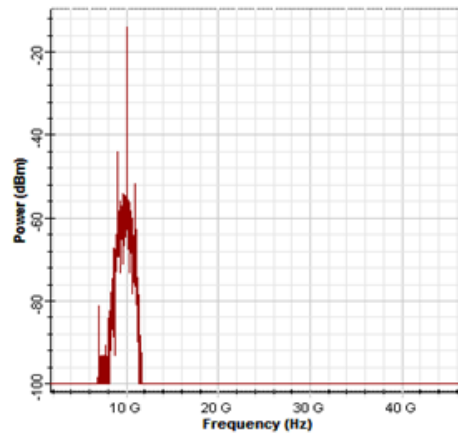


Fig.7.6 10GHz millimeter wave received spectrum

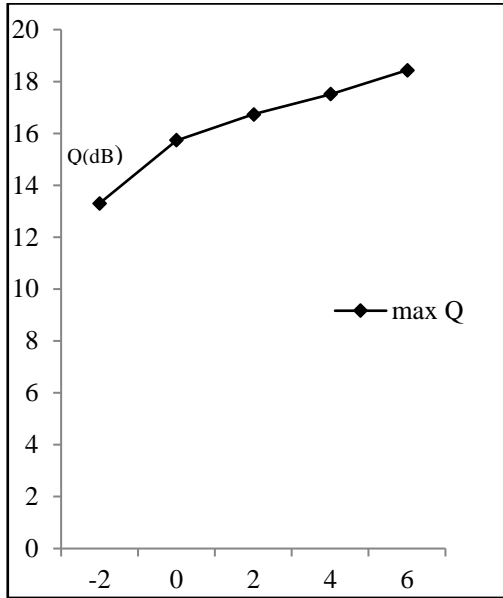


Fig.7.7 Q factor for different input powers

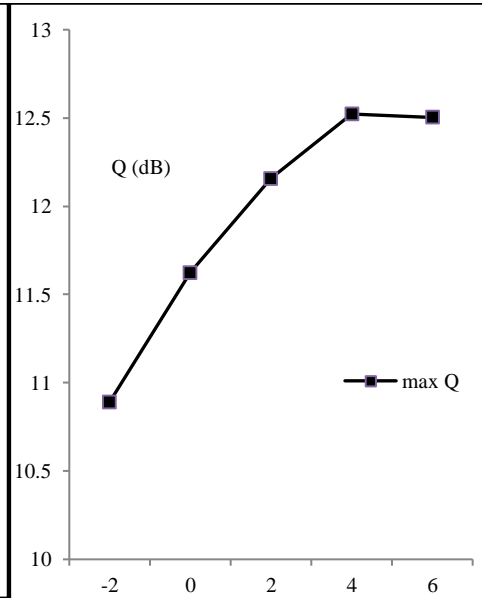


Fig.7.8 Q factor for 10GHz Peer to Peer transmission (6GHz downlink frequency)

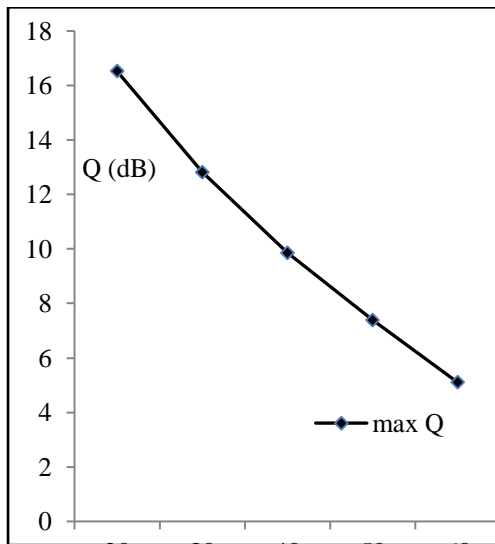


Fig.7.9 Q factor for different transmission distances (6GHz)

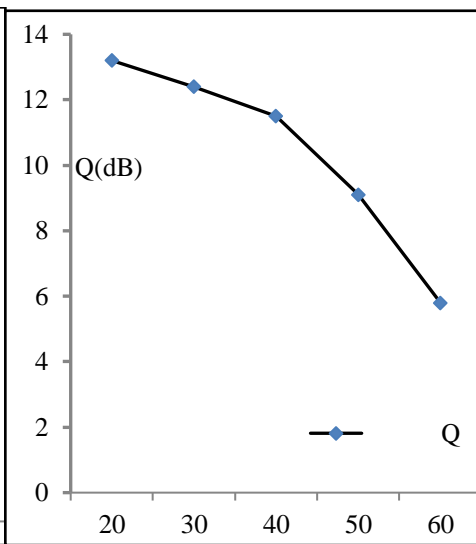


Fig.7.10 Q factor for different transmission distances (10GHz)

7.6 Results and Discussion

The optical spectrum of the combined mm wave signals are shown in Fig. 7.4. It shows that the frequency spacing between the downlink and P2P carriers is around 200 GHz. Fig.7.5 and Fig.7.6 can show the electrical spectrum of the 6 GHz and 10 GHz mm wave signals after down conversion by an envelope detector. The 200 GHz, RF spectrum cannot be shown due to the limited bandwidth of the spectrum analyzer.

Fig.7.7 and Fig.7.8 can show the Q-factor performance of the downlink and P2P signals, in both cases for and after 50 km (downlink) or 110 Km (P2P) SSMF transmission. The optical power is varied from -2 dBm to 6 dBm. As the input power increases, Q factor also increases. Fig.7.9 and Fig.7.10 show the Q factor of downlink and P2P signals for different fiber transmission lengths. The length of the fiber is varied from 20 km to 60 km. The maximum Q factor obtained is about 20 dB for the 6 GHz downlink frequency. When the transmission length is increased, the Q factor is decreased from 20 dB to 8 dB for P2P and downlink. The high Q factor provides a quality P2P millimeter wave signal transmission.

7.7 Conclusion

A 200 GHz mm wave RoF access network using a P2P interconnection architecture is proposed and simulated using OptiSystem software. An AWGN with long haul Single Mode Fiber of 170 km transmission length is used against the wireless channel. Phase noise and frequency instability between the two independent light waves have been reduced by an envelope detector in the user terminal. It can also down convert the two mm wave signals to their associated radio frequencies. The signal up/down conversion is done without any high-frequency clock sources or other high bandwidth devices. Error-free

transmission of the 1 Gbps signals is possible over 170 km fiber (downlink) or 110 km fiber (P2P) plus AWGN wireless link. A maximum Q factor of 20 dB is secured for an input optical power of -2 dBm to 6 dBm with a maximum downlink distance of 170 km. Results show that an effective downlink and P2P transmission with high frequency mm wave is done with high Q factor and low BER in the range of -60 dB.

7.8 Validation

The performance of the proposed method is validated with the results in [324]. The received signal power (Existing method) and Q factor are -21 dB and 16 dB respectively. The proposed method could be improved the received power and Q factor about 5 dB and 4dB respectively as shown in the table 7.2.

Table 7.2 Validation of results

	Received optical power	Q factor
Proposed method	-16 dB	20 dB
J. Liu et.al[324]	-21 dB	16dB

Performance Improvement of RoF Communication System

8.1 Introduction

8.2 Performance Improvement and Cost Reduction Methods in RoF Communication

8.3 Design Issues

8.4 RoF Communication System with Integrated Nonlinearities Reduction Methods

8.5 Result and Discussion

8.5 Conclusion

Abstract

This chapter integrates the different methods proposed for the reduction of nonlinear distortions in the previous chapters. The SNR performance of the existing system and the proposed system is compared. This chapter ends up with the conclusion that the proposed system has better performance as compared to the existing system.

8.1 Introduction

RoF is considered as a key technology for the distribution of future high-capacity wireless signals over a large coverage area. Unfortunately, there are many technical obstacles to overcome, such as nonlinear distortion induced by the transmission response of the optical modulator [326]. The nonlinearities lead to the generation of harmonic and intermodulation distortion, which severely degrade the performance of RoF distribution systems. External modulators, such as LiNbO₃-MZM, and Electro-Absorption Modulator (EAM), have been preferred for broadband RoF systems [327]. EAM has many advantages over MZM, such as low driving voltage, being free from dc drift, low power consumption, small size, broad operational bandwidth, and monolithic integration capability with other semiconductor devices [329].

Both the intensity [329] and the angle [330] of the optical carrier can be modulated using external modulators. External intensity modulation can be implemented using a Mach-Zehnder Modulator (MZM) or an Electro-Absorption Modulator (EAM). External modulation is more expensive than direct modulation due to the need for additional equipment, while the direct modulation of lasers suffers from several drawbacks, thereby giving rise to the cost versus performance tradeoff.

An optical fiber consists of an inner core through which the light propagates and an outer cladding. Optical fibers may operate either in a single-mode or in multi-mode fashion, depending on whether single or multiple propagation modes exist in the fiber. The cross-section of the core in the multi-mode fiber is larger than that of the single mode fiber [331].

All the architectures considered Single-Mode Fiber (SMF), because it provides a larger optical bandwidth and hence it is capable of supporting longer transmission distances without a repeater. However, the cost of multi-mode fiber is lower than that of a single-mode fiber, thereby giving rise to the cost versus performance trade-off. Fiber impairments refer to the fiber characteristics that affect the signal transmitted in the fiber. The signal power decreases as the signal propagates through the optical fiber, which is due to the impurities of the material and owing to Rayleigh scattering [331].

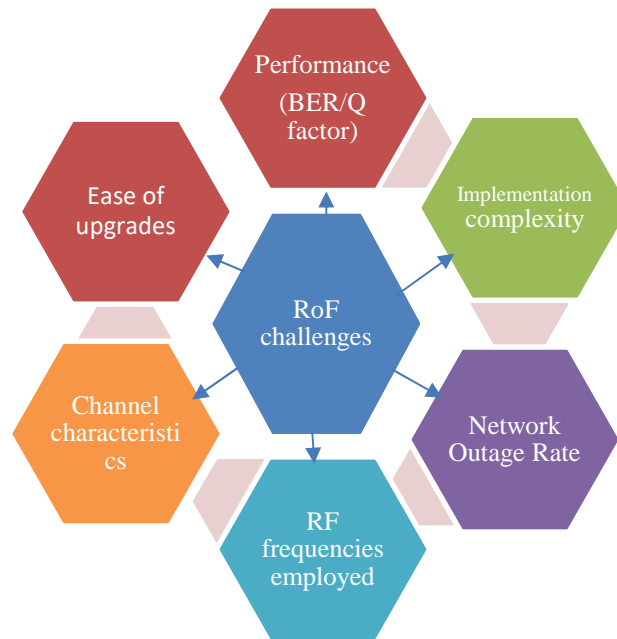


Fig.8.1 RoF Challenges

The deployment of higher RF frequencies causes higher fiber dispersion, which degrades the BER. The BER may be reduced by using dispersion compensation techniques, which cause higher implementational complexity and cost of the system. Otherwise, the BER may be reduced by using lower-order modulation schemes, which could reduce the overall throughput. The overall throughput can be improved by schemes like Dense Wavelength Division Multiplexing (DWDM), but which will increase the implementational complexity and cost[332].

The network outage rate or probability featuring in Fig. 8.1 is defined as the proportion of time for which the network is unable to serve the MSs [330]. A common reason for outage is that the RAP is overloaded by a large number of MSs and hence it is unable to maintain the minimum signal to interference plus noise ratio required for communication with each MS [330]. The outage rate is also increased by shadowing imposed by large obstructing structures. The network outage rate can be reduced by having a larger number of RAPs, which would reduce both shadowing as well as the load (or MSs) per RAP. However, this would increase the system's cost and complexity. Thus, most design questions usually boil down to a cost versus performance tradeoff.

There are several challenges associated with good mm wave RoF communication, like the generation and secure transmission of the wireless signal over the optical channel. When designers have tried to improve the performance, the cost has been increased.

In the previous chapters we have tried to reduce the distortions in the photodetector, wireless channel, optical fiber and receiver. In chapter 3 reduction of nonlinear distortion in the photodetector using SQRT nonlinear equalizer is proposed in optical single sideband and optical double sideband suppressed carrier system and performance shows that SQRT nonlinear equalizer could reduce the nonlinear distortion in the photodetector effectively. In chapter 4, reduction of nonlinear distortion in the wireless channel (AWGN, Rayleigh and Rician) is reduced using Weiner filter. In chapter 5 different nonlinearities in the optical fiber is reduced. Chromatic dispersion in the optical fiber is reduced using SOA. Group velocity and third order distortion in the optical fiber is reduced using VCSEL. Dispersion is compensated using CFBG and ideal FBG. Chromatic dispersion is compensated with symmetrical compensation method. In this chapter we

integrate the different nonlinear distortion reduction methods in the previous chapters to improve the performance of the overall RoF communication system. All reduction methods are integrated to improve the overall performance of the system. The SNR performance of the RoF communication link is compared with the proposed optical source using VCSEL and existing MZM external modulator.

8.2 Performance Improvement and Cost Reduction Methods in RoF Communication

Interleave multiplexing method can be used to improve the spectral efficiency of the conventional WDM, but requires more complicated methods for multiplexing and demultiplexing of the signals [333], [334].

The depth of optical modulation can be increased by suppressing the optical carrier, and there by improve the receiver sensitivity [335]-[338]. The carrier suppression has been done using FBG, bandpass filter, and Fabry Perot filter [339], [340]. MZM can be operated at low bias voltages [341], [342]. Optical injection locking method was proposed for a fiber distance of 65 km [343], [344].

Third order distortion was reduced with optical feed forward linearization [336] and it has been demonstrated that fiber nonlinearities can be reduced and chromatic dispersion compensated [337]. Some cost reduction methods could be used with the existing Fiber To The Home networks [338], [339] and wavelength reuse technique [340], [341].

8.3 Design Issues

Performance and cost are two design constraints in the RoF communication system. Fig. 8.2 shows different parameters that are affected the performance and cost of the RoF communication system. For effective RoF communication, performance and cost are balanced. In this integrated system, both are balanced by using two cost reduction methods and two performance improvement methods. Performance is improved by a single mode fiber and channel with equalizer. The equalizer is used to reduce the nonlinearity in the wireless channel. Cost is reduced by using direct photodetection and direct modulation. As a direct modulator is used at the optical source, expensive optical source and external modulator can be avoided. At the receiver since direct photodetection is used, receiver complexity and cost can be reduced. Thus the cost effective methods and performance improvement methods are integrated.

The performance and cost are very important constraints in the design of a system. Both should be considered and a balanced system can only satisfy these two.

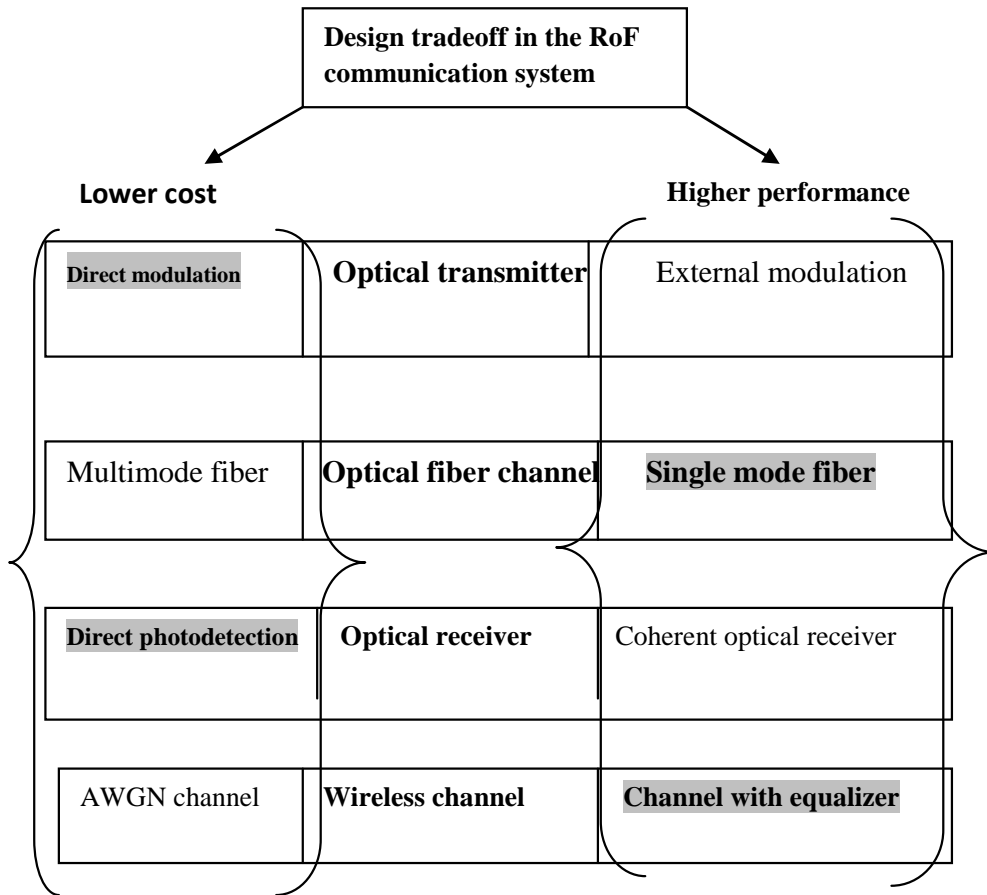


Fig.8.2 Design constraints of RoF communication

8.4 RoF communication System with Nonlinearities Reduction Methods

Our main objective is to improve the overall efficiency of the RoF communication system. So the different nonlinear distortion reduction methods proposed in the previous chapters are integrated and the SNR performance is analyzed. The performance of RoF communication system with MZM external modulator and direct modulation with VCSEL is compared. In the first method MZM is used as the modulator and in the second method direct modulator is used. In the direct modulation method, the VCSEL

laser is used as the optical source which helps in reducing the cost, the GVD and TOD effects of optical fiber as compared to external modulation. The chromatic dispersion of SMF has been reduced using optical phase conjugation with SOA. A Wiener filter is used to reduce the nonlinearities in the AWGN channel. At the receiver, the nonlinearities in the photodetector is reduced by a SQRT nonlinear equalizer. The overall performance is analyzed in terms of SNR performance. Fig.8.3 shows the architecture of the RoF communication system with different nonlinearity reduction techniques.

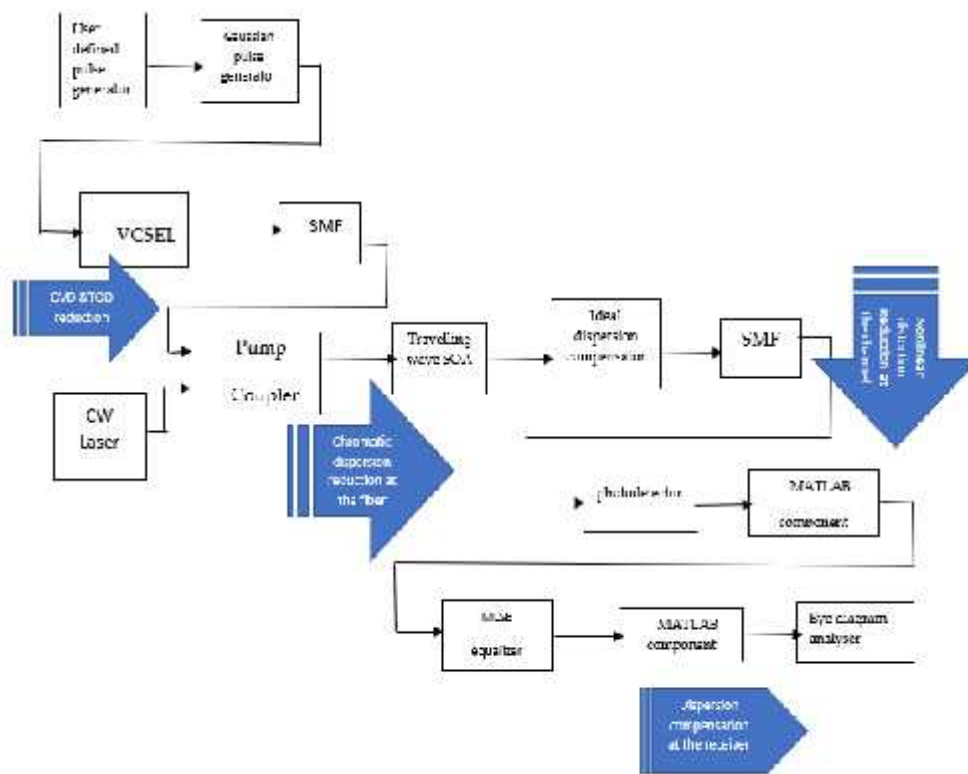


Fig.8.3 Integrated Nonlinearity Reduction Methods in RoF communication system with VCSEL source

8.5 Results and Discussion

Fig.8.4 shows the SNR performance comparison of RoF system with external modulation using MZM and direct modulation using VCSEL. SNR is improved by about 30 dB from the existing system [335].

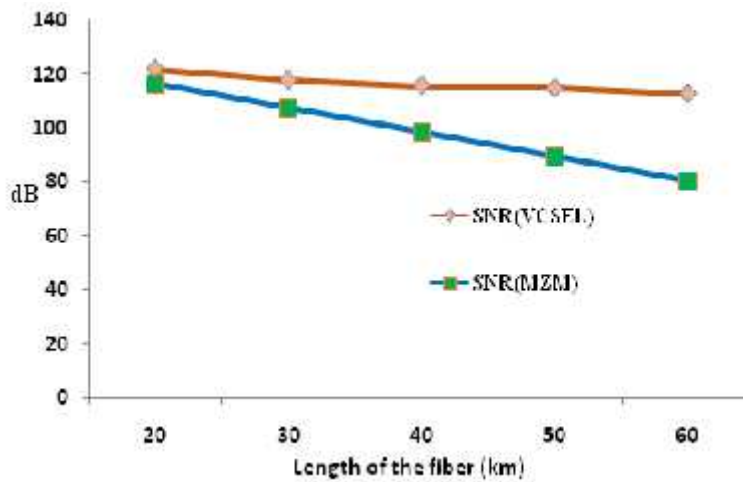


Fig.8.4 Performance comparison of VCSEL and MZM modulated integrated methods

8.6 Conclusion

The design issues show that for an effective RoF communication system, the cost and performance have to be balanced. In the proposed system, distortion and dispersion in the fiber, wireless channel and photodetector are considered. Cost reduction methods and performance improvement methods are integrated. Therefore, this balanced system has provided a good performance. The SNR has improved by about 30 dB from the conventional system.

9.1 Conclusion

The thesis presents methodologies to improve the performance of the RoF communication system through the reduction of nonlinear distortion and dispersion. The RF signals suffer from a number of signal impairments in RoF links such as harmonic distortions and intermodulation distortions. They are due to the nonlinear modulation characteristics of the optical modulators. The square-law characteristic of the photodiode produces nonlinear distortion in the detected signal. The nonlinearities in the wireless channel and receiver have reduced the performance of RoF communication. In addition, the impact of fiber chromatic dispersion on the transported RF signals becomes more pronounced with increasing RF carrier frequency. Different strategies are proposed and demonstrated to measure and overcome these impairments.

In chapter 3, a method has been proposed to reduce the nonlinear distortion in the photodetector using a SQRT nonlinear equalizer. This method has been implemented in an SSB RoF communication system and ODSB-CS communication system. Their performances are evaluated in terms of SNR, the Q factor and BER. Results are compared with and without an equalizer. Also the results are compared to existing and proposed methods. Their performances are compared in terms of transmission distance, received power and SNR. Results show that the proposed method has improved the performance.

The performance of the RoF communication system is affected by the nonlinearities in the wireless channel. In chapter 4, a method is to improve the system performance in the AWGN channel, Rayleigh fading channel, and Rician channel. Their performances are compared with OFDM modulation and DPSK modulation. It is concluded that the proposed method using Weiner filter has improved the SNR performance of the RoF communication system.

The performance of the RoF communication system is deteriorated by the nonlinearities and dispersion in the optical fiber. Chapter 5 proposes different methods for the reduction of nonlinear distortions and chromatic dispersion in the fiber. Four different methods are proposed and their performances have been analyzed in terms of transmission distance, Q factor, OSNR, and received power. The performance of the system with the employment of SOA is found to be better compared with the others. The performances are compared with the existing methods and proposed methods. Chapter 5 concludes with the findings that the proposed methods outperform the existing methods.

Chapter 6 and chapter 7 describe the methods for the reduction of nonlinearities at the receiver. In chapter 6, a novel low cost RoF link with a simple baseband decomposition to carry the 40 GHz, 80 GHz and 120 GHz mm wave multiband wireless accesses is presented. The proposed method uses a simple signal decomposition technique instead of FBGs and optical filters in the existing method. Therefore, the proposed low cost method helps in reducing the nonlinearities that may be introduced when FBGs are used. The simulation results reveal that our proposed scheme has provided multiband wireless accesses at the data rate of 80Gbps with higher transmission performances in terms of low BER, higher Q factor and higher received optical power. The proposed method is compared with the existing method and results show that the proposed method has better performance.

In chapter 7, a 200 GHz, mm wave RoF access network using a P2P interconnection architecture is presented. An envelope detector is used at the receiver to eliminate the frequency instability and phase noise. The proposed method is compared with the existing method and results shows that the proposed method has better performance.

The different methods proposed in the previous chapters for the reduction of nonlinear distortions have been combined and presented in chapter 8. The SNR performance of the existing system and proposed system is compared. Results show that the proposed system has better performance as compared to the existing system. The proposed system considers nonlinearities in different parts of the RoF communication system. The nonlinearities in the fiber, wireless channel and receiver are reduced.

The overall conclusion of the research work is presented with the inference that the proposed method have helped in improving the performance of the existing RoF communication systems. As we are considering different nonlinearities in the RoF communication system, suppression techniques are promising.

9.2 Future Work

This thesis proposes different methods of reduction of nonlinear distortion and dispersion in the fiber. The nonlinearities introduced by the optical source and modulators can be considered in future work. As a scope for future work, methods for the reduction of nonlinearities in the optical source and modulators can be tried out. In addition, if all the electronic processing methods are replaced by optical processing methods, the performance of the system can be far better.

Work can be attempted in certain research areas like, integrating different mm wave techniques with RoF, probability of using multimode fibers instead of single mode fibers in RoF, use of plastic fibers instead of single mode fibers, and use of low cost optical sources.

References

1. V. Sarup, A. Gupta, "A Study of various Trends and Enabling Technologies in Radio over Fiber (RoF) Systems" *Optik - International Journal for Light and Electron Optics* , Vol.126, No. 20, pp.2606-2611, October 2015.
2. Mazin Al Noor, "Green Radio Communication Networks Applying Radio-over-Fiber Technology for Wireless Access", Ph.D Thesis, 2011.
3. Christina Lim, Ampalavanapillai Nirmalathas, Masduzzaman Backul, Prasanna Gamage, Ka Lun Lee, Yizhuo Yang, Dalma Novak and Rod Waterhouse. "Fiber-Wireless Networks and Subsystem Technologies" *Journal of Lightwave Technology*, Vol.28, No.4, pp.390-405, February 2010
4. Navid Ghazisaidi and Martin Maier, "Fiber-Wireless (FiWi) Networks: Comparative Techno Economic Analysis of EPON and WiMAX", *Global Telecommunication Conference*, Vol.1, pp. 1-6, March 2010
5. Anthony Ng'oma, "Radio-over Fiber Technology for Broadband Wireless Communication Systems" Ph.D Thesis, 2005
6. W. Chen, S.Y. Li, P.X. Lu, D.X. Wang, W.Y. Luo, "Dispersion Compensation Optical Fiber Modules For 40 Gbps WDM Communication Systems" *Frontiers of Optoelectronics in China*, Vol. 3, No. 4, 2010, pp. 333-338, January 2010
7. H. B. Kim and A. Wolisz, "Radio over Fiber based Wireless Access Network Architecture for Rural Areas," in *Proc. 14th IST Mobile & Wireless Commun. Summit*, Dresden, Germany, June 2005
8. Koonen, A. M. J., Larrodé, M. G., Ng'oma A., Wang K., Yang, H., Zheng Y., Tangdionga Y., "Perspectives of Radio over Fiber Technologies", *Conference*

- on Optical Fiber communication/National Fiber Optic Engineers Conference (OFC/NFOEC), pp. 1-3, 2008
9. G.J. Simonis, K.G. Purchase, “Optical generation, distribution, and control of microwaves using laser heterodyne”, *IEEE Trans. Microwave Theory Technol.*, Vol.38 , No.5, pp.667–669, May 1990
 10. D. Wake, C.R. Lima, P.A. Davies, “Optical generation of mm-wave signals for fiber-radio systems using a dual-mode DFB semiconductor laser” *IEEE Trans. Microwave Theory Technol.*, Vol.43, No.9 , pp.2270–2276, September 1995
 11. D. Novak, Z. Ahmed, R.B. Waterhouse, R.S. Tucker, “Signal generation using pulsed semiconductor lasers for application in mm-wave wireless links”, *IEEE Trans. Microwave Theory Technol.*, Vol.43, No.9, pp.733–734, September 1995
 12. D. Kim, M. Pelusi, Z. Ahmed, D. Novak, H.F. Liu, Y. Ogawa, “Ultra-stable mm-wave signal generation using hybrid mode-locking of a monolithic DBR laser”, *Electronic Letters.*, Vol. 31, No.15, pp. 733–734, 1995
 13. L.D. Westbrook, D.G. Moodie, “Simultaneous bidirectional analogue fiber optic transmission using an electro-absorption modulator”, *Electron Lett.*, Vol. 47, No.7, pp.1806–1807, 1996
 14. Stohr, K. Kitayama, D. Jager, “Full-duplex fiber-optic RF subcarrier transmission using a dual-function modulator/photodetector”, *IEEE Trans. Microwave Theory Technology*, Vol.47, No.7, pp. 1338–1341, July 1999
 15. T. Kuri, K. Kitayama, Y. Takahashi, “60-GHz-band full-duplex radio-on-fiber system using two-RF-port electro-absorption transceiver”, *IEEE Photonics Technol. Lett.*, Vol. 12, No.4, pp 419–421, April 2000

16. T. Kurniawan, A. Nirmalathas, C. Lim, D. Novak, R. Waterhouse, "Performance analysis of optimized millimeter-wave fiber radio links", *IEEE Trans. Microwave Theory Tech.*, Vol. 54, No. 2, pp. 921–928, 2006
17. Jianxin Ma, J. Yu, Chongxiu Yu, Xiangjun Xin, Huiying Huang, Lan Rao, "Generation and transmission of the double-sideband optical millimeter-wave with signal carried only by optical carrier", *Opt. Commun.*, Vol.281, No.10, pp. 2799-2805, May 2008
18. Tianliang Wang, Minghua Chen, Hongwei Chen, Shizhong Xie, "RoF downlink transmission system using FWM effect of SOA for generating mm-wave", *Opt. Commun.*, Vol.282, No.16, pp. 3360–3363, August 2009
19. Jie Yin, Kun Xu, Da-peng Wang, Jin-tong Lin, "A novel scheme to generate multi-band millimeter wave signals for 40 GHz full duplex radio-over-fiber system", *J. Chin. Uni. Posts and Telecommun.*, Vol.16, No.1, pp. 62–65, September 2009
20. Ying Wang Shen, Rong Pu Tao, A novel technique to generate microwave signal based on multiple-frequency Brillouin fiber-ring laser, in *Proc. of Communications and Photonics Conference and Exhibition*, pp. 1–2, 2009
21. Jian Gong Zhao, Zengji Liu, Xiangling Liu, Tao Shang, Peng Yue, Generation of radio signals using a novel Mach–Zehnder modulator with four arms, *Opt. Commun.*, Vol. 282, No.22, pp. 4353–4357, November 2009
22. P. Perry, L.P. Barry, Optical millimeter-wave generation and transmission system for 1.25 Gbit/s downstream link using a gain switched laser, *Opt. Commun.*, Vol. 282, No.24, pp. 4789–4792, December 2009

23. J. Ma, J. Yu, C. Yu, X. Xin, X. Sang, Q. Zhang, 64 GHz optical millimeter-wave generation by octupling 8 GHz local oscillator via a nested LiNbO₃ modulator, *Opt. Laser Technol.*, Vol.42, No.2, pp. 264–268, March 2010
24. X. Liu, Z. Liu, J. Li, T. Shang, J. Zhao, Generation of optical carrier suppression millimeter-wave signal using one dual-parallel MZM to overcome chromatic dispersion, *Opt. Commun.*, Vol .283, No.16, pp.3129-3135, August ,2010
25. P.-T. Shih, J. Chen, C.T. Lin, W.J. Jiang, H.-S. Huang, P.-C. Peng, S. Chi, Optical millimeter-wave signal generation via frequency 12-Tupling, *J. Light wave Technol.* Vol.28, No.1,pp.71-78, 2010
26. C.Cox,E. Ackerman, R. Helkey and G.E Betts, "Techniques and Performance of intensity modulation direct detection analog optical link", *IEEE transactions on microwave theory and techniques*, Vol.45,No.8,pp.1375-1383, August1997
27. D.Wake,A.Nkansah,N.J.Gomes,G.de,Valicourt,R.Brenot,M.Violas,Z.Liu,F.Fer rera and S. Pato, "A comparison of Radio over fiber link types for the support of wideband Radio channels, *IEEE journal of lightwave technology*, Vol.28, No.16,pp.2416-2422,August 2010
28. K.Nojuchi,O.mitomi and H.Miyazawa, "Millimeter wave Ti:Li NbO₃ optical modulators" ,*IEEE journal of lightwave technology*,Vol.16,No.4, pp.615-619, April 1998
29. G.H Smith, D.Novak and Z.Ahmed, "Overcoming CD effects in fiber wireless systems incorporating external modulators", *IEEE transactions in microwave theory of technique*,Vol.45, No.5, pp.1410-1415, August 199

30. U.Gliese, S.Ngrskov, T.N Nielsen, "Chromatic dispersion in fiber optic microwave and millimeter wave links", Vol.44, No.10, pp.1716-1724, October 1996
31. G. P. Agrawal, "Fiber-Optic Communication Systems", 3rd ed. Hoboken, NJ, USA: Wiley publishers, John & Sons, 2002
32. L. Hanzo, M. El-Hajjar, and O. Alamri, "Near-capacity wireless transceivers and cooperative communications in the MIMO era: Evolution of standards, waveform design, future perspectives" Proceedings of IEEE, Vol. 99, No. 8, pp. 1343–1385, August 2011
33. H. Al-Raweshidy and S. Komaki, "Radio Over Fiber Technologies for Mobile Communication Networks", 1st ed. Norwood, MA, USA: Artech House, 2002.
34. O. Omomukuyo, M. Thakur, and J. Mitchell, "Simple 60-GHz MBOFDM ultrawideband ROF system based on remote heterodyning," IEEE Photon. Technol. Lett., Vol. 25, No. 3, pp. 268–271, February 2013
35. L. Hanzo, Y. Akhtman, L. Wang, and M. Jiang, "MIMO-OFDM for LTE, WiFi and WiMax: Coherent Versus Non-Coherent and Co-Operative Turbo Transceivers", 1st ed. Hoboken, NJ, USA: Wiley, 2011
36. T. Rappaport et al. , "Millimeter wave mobile communications for 5G cellular: It will work!", IEEE Access, vol. 1, pp. 335–349, May 2013.
37. W. Roh et al., "Millimeter-wave beam forming as an enabling technology for 5G cellular communications: Theoretical feasibility and prototype results," IEEE Communication Magazine., Vol. 52, No. 2, pp. 106–113, February 2014
38. X. Fernando and A. Anpalagan, "On the design of optical fiber based wireless access systems," in Proc. IEEE ICC, Vol. 6, pp. 3550–3555, June 2004

39. X. Fernando, "Improved expression for intensity noise in multimedia over fiber networks," in Proc. of 1st Int. Conf. Ind. Inf. Syst., pp. 425–429, August 2006
40. G. Smith and D. Novak, "Broad-band millimeter-wave (38 GHz) fiber wireless transmission system using electrical and optical SSB modulation to overcome dispersion effects," IEEE Photon. Technol. Letters., Vol. 10, No. 1, pp. 141–143, January 1998
41. C. Carlsson, A. Larsson, and A. Alping, "RF transmission over multimode fibers using VCSELs—Comparing standard and high-bandwidth multimode fibers," Journal of Lightwave Technology., Vol. 22, No. 7, pp. 1694–1700, July 2004
42. J. Ma et al., "Fiber dispersion influence on transmission of the optical millimeter-waves generated using LN-MZM intensity modulation," Journal of Light wave Technology, Vol. 25, No. 11, pp. 3244–3256, November 2007
43. J. Corral, J. Marti, and J. Fuster, "General expressions for IM/DD dispersive analog optical links with external modulation or optical up-conversion in a Mach–Zehnder electro-optical modulator," IEEE Trans. Microwave Theory Technology., Vol. 49, No. 10, pp. 1968–1976, October 2001.
44. J. Park, W. Sorin, and K. Lau, "Elimination of the fibre chromatic dispersion penalty on 1550 nm millimetre-wave optical transmission," Electron. Lett., Vol. 33, No. 6, pp. 512–513, March 1997.
45. R. Kashyap, Fiber Bragg Gratings, 1st ed. San Diego, CA, USA: Academic Press, 1999
46. J. Yu et al., "DWDM optical millimeter-wave generation for radio-over-fiber using an optical phase modulator and an optical interleaver," IEEE Photon. Technol. Lett., Vol. 18, No. 13, pp. 1418–1420, July 2006

47. M. Weiss et al., "60-GHz photonic millimeter-wave link for short to medium range wireless transmission up to 12.5 Gb/s," *J. Lightwave. Technology.*, Vol. 26, No. 15, pp. 2424–2429, August 2008
48. K.J. Williams, R.D. Esman, "Optically amplified down-converting link with shot noise-limited performance", *IEEE Photonics Technol. Lett.*, Vol. 8, No.1, pp. 148–150,1996 (two times)
49. C.K. Sun, R.J. Orazi, S.A. Pappert, "Efficient microwave frequency conversion using photonic link signal mixing", *IEEE Photonics Technology. Letters.*, Vol. 8, No.1,pp.154–156,1996
50. R. Helkey, J.C. Twichell, C. Cox, "A down-conversion optical link with RF gain", *IEEE Journal of Light wave Technology*, Vol.15, No.6, pp. 956–961,1997
51. G.H. Smith, D. Novak, "Broadband millimeter-wave fiber-radio network incorporating Remote up/down conversion", in *Proc. of Microwave Symposium Digest*, *IEEE MTT-S*, Vol. 3, pp. 1509–1512,1998
52. K. Kitayama, R.A. Griffin, "Optical down-conversion from millimeter-wave to IF band Over 50 km long optical fiber link using an electro-absorption modulator", *IEEE Photonics Technol. Lett.*, Vol. 11, No.2, pp.287–289, 1999
53. G.J. Simonis, K.G. Purchase, "Optical generation, distribution, and control of Microwaves using laser heterodyne", *IEEE Trans. Microwave Theory Technol.* Vol.38,No.5,pp. 667–669, May 199
54. D. Wake, C.R. Lima, P.A. Davies, "Optical generation of millimeter-wave signals for fiber-radio systems using a dual-mode DFB semiconductor laser", *IEEE Trans. Microwave Theory Technol.*, Vol.43, No.9,pp. 2270–2276, September 1995

55. D. Novak, Z. Ahmed, R.B. Waterhouse, R.S. Tucker, "Signal generation using pulsed semiconductor lasers for application in millimeter-wave wireless links", *IEEE Trans. Microwave Theory Technol.*, Vol.43, No.9, pp. 733–734, September 1995
56. D. Kim, M. Pelusi, Z. Ahmed, D. Novak, H.F. Liu, Y. Ogawa, "Ultra-stable millimeter-wave signal generation using hybrid mode-locking of a monolithic DBR laser", *Electronic Letters*, Vol. 31, No.9, pp. 733–734, 1995
57. L.D. Westbrook, D.G. Moodie, "Simultaneous bidirectional analogue fiber optic transmission using an electro-absorption modulator, *Electron Letters*", Vol.47, No.7, pp. 1806–1807, 1996
58. A. Stohr, K. Kitayama, D. Jager, "Full-duplex fiber-optic RF subcarrier transmission using a dual-function modulator/photodetector", *IEEE Trans. Microwave Theory Technol.*, Vol. 47, No.7, pp. 1338–1341, July 1999
59. T. Kuri, K. Kitayama, Y. Takahashi, "60-GHz-band full-duplex radio-on-fiber system using two-RF-port electro-absorption transceiver", *IEEE Photonics Technol. Lett.*, Vol. 12, No.4, pp. 419–421, April 2000
60. T. Kurniawan, A. Nirmalathas, C. Lim, D. Novak, R. Waterhouse, "Performance analysis of optimized millimeter-wave fiber radio links", *IEEE Trans. Microwave Theory Tech.*, Vol. 54, No.2, pp. 921–928, 2006
61. Jianxin Ma, J. Yu, Chongxiu Yu, Xiangjun Xin, Huiying Huang, Lan Rao, "Generation and transmission of the double-sideband optical millimeter-wave with signal carried only by optical carrier", *Opt. Communication* Vol.281, No. 10, pp. 2799–2805, May 2008

62. Tianliang Wang, Minghua Chen, Hongwei Chen, Shizhong Xie, “RoF downlink transmission system using FWM effect of SOA for generating mm-wave”, *Opt. Commun.*, Vol. 282, No.16, pp. 3360–3363 August 2009
63. Ying Wang Shen, Rong Pu Tao, “A novel technique to generate microwave signal based on multiple-frequency Brillouin fiber-ring laser”, *Communications and Photonics Conference and Exhibition*, ,pp. 1–2, 2009
64. Jie Yin, Kun Xu, Da-peng Wang, Jin-tong Lin, “A novel scheme to generate multiband millimeter wave signals for 40 GHz full duplex radio-over fiber system”, *J. Chin. Uni. Posts and Telecommun.*, Vol.16, No.1, pp. 62–65, September 2009
65. Jian Gong Zhao, Zengji Liu, Xiangling Liu, Tao Shang, Peng Yue, “Generation of radio signals using a novel Mach–Zehnder modulator with four arms”, *Opt. Commun.*, Vol.282, No.22, pp. 4353–4357 November 2009
66. P. Perry, L.P. Barry, “Optical millimeter-wave generation and transmission system for 1.25 Gbit/s downstream link using a gain switched laser”, *Opt. Commun.*, Vol.282, No.24, pp.4789–4792, December 2009
67. J. Ma, J. Yu, C. Yu, X. Xin, X. Sang, Q. Zhang, “64 GHz optical millimeter-wave generation by octupling 8 GHz local oscillator via a nested LiNbO₃ modulator”, *Opt. Laser Technol.*, Vol.42 No.2, pp. 264–268, March 2010
68. X. Liu, Z. Liu, J. Li, T. Shang, J. Zhao, Generation of optical carrier suppression millimeter-wave signal using one dual-parallel MZM to overcome chromatic dispersion, *Opt. Commun.*, Vol. 283, No.16, pp.3129–3135, August 2010

69. H.-C. Chien, Y.-T Hsueh, A. Chowdhury, J. Yu, G. Chang, G.-K. Chang, “Optical millimeter-wave generation and transmission without carrier suppression for single and multi-band wireless over fiber applications”, *Journal of Light wave Technol.*, Vol. 28, No.16, pp. 2230–2237,2010
70. P.-T. Shih, J. Chen, C.T. Lin, W.J. Jiang, H.-S. Huang, P.-C. Peng, S. Chi, “Optical millimeter-wave signal generation via frequency 12-Tupling”, *J. Light wave Technol.* Vol. 28, No.1, pp. 71-78,2010
71. G.J. Meslener, Chromatic dispersion induced distortion of modulated “Monochromatic light employing direct detection”, *IEEE J. Quantum Electron.*, Vol. 20, No.10, pp. 1208–1216,1984
72. H. Schmuck, “Comparison of optical millimeter-wave system concepts with regard to chromatic dispersion”, *Electron. Letters.*, Vol.31, No.21, pp. 1848–1849,1995
73. U. Gliese, S. Ngrskov, T.N. Nielsen, “Chromatic dispersion in fiber-optic Microwave and millimeter-wave links”, *IEEE Trans. Microwave Theory Tech.*, Vol.47, No.10, pp. 1716–1724,1996
74. K.J. Williams, R.D. Esman, “Optically amplified down-converting link with shot noise-limited performance, *IEEE Photonics Technol. Lett.*, Vol. 8, No.1, pp. 148–150,1996
75. C.K. Sun, R.J. Orazi, S.A. Pappert, “Efficient microwave frequency conversion Using photonic link signal mixing”, *IEEE Photonics Technol. Lett.*, Vol.8, No.1, pp. 154–156,1996

76. R. Helkey, J.C. Twichell, C. Cox, "A down-conversion optical link with RF gain", *IEEE Journal of Light wave Technology*, Vol.15, No.6, pp. 956–961, 1997
77. G.H. Smith, D. Novak, "Broadband millimeter-wave fiber-radio network incorporating remote up/down conversion", *Microwave Symposium Digest, IEEE MTT-S*, Vol. 3, pp. 1509–1512, 1998
78. K. Kitayama, R.A. Griffin, "Optical down-conversion from millimeter-wave to IF band over 50-km-long optical fiber link using an electro-absorption modulator", *IEEE Photonics Technol. Lett.*, Vol.11, No.2, pp. 287–289, 1999
79. G.H. Smith, D. Novak, Z. Ahmed, "Optimization of link distance in fiber-radio systems incorporating external modulators", *Proceedings of Australian Conf. on Opt. Fiber Technol.*, Gold Coast, Australia, pp. 141–144, December 1996
80. G.H. Smith, D. Novak, Z. Ahmed, "Overcoming chromatic-dispersion effects in fiber-wireless systems incorporating external modulators" *IEEE Trans. Microwave Theory Tech.*, Vol. 45, No.8, 1408–1415, 1997
81. S. Walklin, J. Conradi, "Effect of Mach–Zehnder modulator DC extinction ratio on residual chirp-induced dispersion in 10-Gb/s binary and AM-PSK duobinary light wave systems", *IEEE Photonics Technol. Lett.*, Vol. 9, No.10, pp. 1400–1402, 1997
82. V. Sharma, A. Singh, A.K. Sharma, "Simulative investigation on the impact of laser-spectral width in single-tone radio-over-fiber transmission system using Optical single side-band technique", *Opt. Lasers Eng. Elsevier*, Vol.47, No.11, pp. 1145–1149, 2009

References

83. R.A. Griffin, P.M. Lane, J.J. O'Reilly, "Dispersion-tolerant subcarrier data modulation of optical millimeter-wave signals", *Electron. Lett.*, Vol. 32, No.24,pp. 2258–2260,1996
84. J.M. Fuster, J. Marti, J.L. Corral, "Chromatic dispersion effects in electro-optical up-converted millimeter wave fiber optic links", *Electron. Lett.*, Vol. 33, No.23,pp.1969–1970,1997
85. Z. Jia, J. Yu, G.-K. Chang, "A full-duplex radio-over-fiber system based on optical Carrier suppression and reuse", *IEEE Journal on Light wave Technol.*, Vol.18, No.16,pp. 1726–1728,2006
86. J. Park, W.V. Sorin, K.Y. Lau, "Elimination of the fiber chromatic dispersion Penalty on 1550 nm millimeter wave optical transmission", *Electron. Lett.*, Vol.33, No.6,pp. 512–513,1997
87. J. Marti, J.M. Fuster, R.I. Laming, "Experimental reduction of chromatic dispersion Effects in lightwave microwave/millimeter-wave transmissions using tapered Linearly chirped fiber gratings", *Electron. Lett.*, Vol.33, No.13,pp. 1170–1171,1997
88. E. Vourch, D. Le Berre, D. Herve, "Lightwave single sideband wavelength self tunable filter using InP: Fe crystal for fiber-wireless systems", *IEEE Photonics Technol. Lett.*, Vol.14, No.2, pp. 194–196,2002
89. J. Capmany, D. Pastor, P. Munoz, S. Sales, B. Ortega, A. Martinez, "WDMSSB Generation and dispersion mitigation in radio over fiber systems with Improved performance using an AWG multiplexer with flat top resonances", *Proc. Microwave Photonics*, pp.39–42,2003

90. F. Ramos, J. Marti, V. Polo, J.M. Fuster, "On the use of fiber-induced self-phase Modulation to reduce chromatic dispersion effects in microwave/millimeter wave Optical systems", *IEEE Photonics Technol. Lett.*, Vol.10, No.10, pp. 1473–1475,1998
91. F. Ramos, J. Marti, V. Polo, "Compensation of chromatic dispersion effects in microwave/millimeter-wave optical systems using four-wave-mixing induced in dispersion-shifted fibers", *IEEE Photonics Technol. Lett.*, Vol.11, No.9,pp. 1171–1173,1999
92. P.C. Won, W. Zhang, J.A.R. Williams, "Self-phase modulation dependent dispersion Mitigation in high power SSB and DSB + dispersion compensated Modulated radio-over-fiber links", *Proc. IEEE MTTS IMS*,pp.1947–1950, 2006
93. J. Marti, F. Ramos, "Compensation for dispersion-induced nonlinear distortion In subcarrier systems using optical-phase conjugation", *Electron. Lett.*, Vol.33, No.9,pp. 792–794,1997
94. R. Hofstetter, H. Schmuck, R. Heidemann, "Dispersion effects in optical millimeter-wave systems using self-heterodyne method for transport and generation", *IEEE Trans. Microwave Theory Technol.*, Vol.43, No.9,pp. 2263–2269,1995
95. R. Braun, G. Grosskopf, D. Rohde, F. Schmidt, "Low-phase-noise millimeter-wave Generation at 64 GHz and data transmission using optical sideband injection locking", *IEEE Photonics Technol. Lett.*, Vol. 10, No.5,pp. 728–730,1998
96. G. Yabre, J. LeBihan, "Reduction of nonlinear distortion in directly modulated Semiconductor lasers by coherent light injection", *IEEE J. Quantum Electron.*, Vol. 33, No.7,pp.1132-1140,1997

97. Kaszubowska, P. Anandarajah, L.P. Barry, "Enhanced performance of an optically fed microwave communication system using a directly modulated laser transmitter using external injection", IEEE/LEOS Annual Meeting, LEOS, Vol.1, p. 314,2001
98. X.J. Meng, D.T.K. Tong, T. Chau, M.C. Wu, "Demonstration of an analog fiber optic link employing a directly modulated semiconductor laser with external light injection", IEEE Photonics Technol. Lett.,Vol. 10, No.11,pp.1620-1622,1998
99. F. Smyth, L.P. Barry, "Overcoming distortion limitations in hybrid radio/photonic systems for the distribution of WCDMA signals", Springer J. Electr. Eng.,Vol.85,No.4, 191-194, 2003
- 100.F. Smyth, A. Kaszubowska, L.P. Barry, "Overcoming laser diode nonlinearity issues in multi-channel radio-over-fiber systems", Opt. Commun., Vol.231,No.1,pp. 217–225,2004
- 101.S.H. Park, Y.W. Choi, "Significant suppression of the third inter-modulation distortion in transmission system with optical feedback forward linearized transmitter", IEEE Photonics Technol. Lett., Vol.17, No.6,pp. 1280–1282,2005
102. V. Sharma, A. Singh, A.K. Sharma, "Simulative investigation of non linear distortion in single and two tone RoF system using direct and external modulation techniques", Optik, Vol. 121, No.17 ,pp. 1545–1549,2010
- 103.Sang Hyun Park, Significant suppression of the third intermodulation distortion in transmission system with optical feedforward linearized transmitter, IEEE photonics technology letters, Vol. 17, No.6, pp. 1280-1282, 2005

-
104. K.J. Williams, R.D. Esman, "Stimulated Brillouin scattering for improvement of microwave fiber-optic link efficiency, *Electron Lett.* Vol.30, No.23, 1965–1966, 1994
105. S. Tonda-Goldstein, D. Dolfi, J.-P. Huignard, G. Charlet, J. Chazelas, "Stimulated Brillouin scattering for microwave signal modulation depth increase in optical links, *Electron Lett.*, Vol.36, No.11, pp. 944-946, 2000
106. M.J. LaGasse, W. Charczenko, M.C. Hamilton, S. Thaniyavarn, "Optical carrier filtering for high dynamic range fiber optic links", *Electron Lett.*, Vol.30, No.25, pp. 2157–2158, 1994
107. R.D. Esman, K.J. Williams, "Wideband efficiency improvement of fiber optic systems by carrier subtraction", *IEEE Photonics Technol. Lett.*, Vol.7, No.2, pp.218-220, 1995
108. M. Attygalle, C. Lim, G.J. Pendock, A. Nirmalathas, G. Edvell, "Transmission improvement in fiber wireless links using fiber Bragg gratings", *IEEE Photonics Technology Letters*, Vol. 17, No.1, pp.190–192, 2005
109. M. Attygalle, C. Lim, A. Nirmalathas, "Extending optical transmission distance in fiber wireless links using passive filtering in conjunction with optimized modulation", *IEEE Journal of Light wave Technology*, Vol. 24, No.4, pp. 1703–1709, 2006
110. C. Lim, M. Attygalle, A. Nirmalathas, D. Novak, R. Waterhouse, "Analysis of optical carrier-to-sideband ratio for improving transmission performance in fiber-radio links", *IEEE Trans. Microwave Theory Tech.*, Vol. 54, No.5, pp. 2181–2187, 2006

111. T. Koonen, A. Ng'oma, M. García-Larrode, F. Huijskens, I. M. Tafur-Monroy, and G.-D. Khoe, "Novel cost-efficient techniques for microwave signal delivery in fiber wireless networks," in Proc. ECOC'04, 2004, Vol. 5, pp. 120–125, Paper Th1.1.1.
112. U. Gliese, S. Norskov, and T. N. Nielsen, "Chromatic dispersion in fiber-optic microwave and millimeter-wave links," IEEE Trans. Microw. Theory Tech., Vol. 44, no. 10, pt. 1, pp. 1716–1724, Oct. 1996
113. D. C. Kilper, R. Bach, D. J. Blumenthal, Optical Performance Monitoring, Journal of Lightwave Technology, Vol. 22, No. 1, pp. 294, 2004
114. D. Stahl, P. J. Winzer, C. R. Doerr, and S. Chandrasekhar, "Extending the chromatic dispersion tolerance by optical equalization at 43 Gb/s," Proc. OFC 2004, Los Angeles, CA, Vol. 2, Paper ThU5.
115. V. Curri, R. Gaudino, A. Napoli, and P. Poggiolini, "Electronic equalization for advanced modulation formats in dispersion-limited systems," IEEE Photon. Technology. Letters., Vol. 16, No. 11, pp. 2556–2558, November 2004
116. J. H. Winters and R. D. Gitlin, "Electrical signal processing techniques in long haul fiber optic systems," IEEE Transaction on Communication., Vol. 38, pp. 1439–1453, Sept. 1990
117. Baljeet Kaur, Ajay K Sharma, Vinod Kapoor, "Performance enhancement with square root module for WDM RoF-EPON link", Optik-International Journal for Light and Electron Optics, Volume 124, Issue 10, May 2012, pp. 967-971.
118. Baljeet Kaur, Ajay K Sharma, Vinod Kapoor, "On WDM RoF-EPON link using OSSB transmission with and without square root module," Optik-

-
- International Journal for Light and Electron Optics, Volume 124, Issue 12, June 2012, pp. 1334-1337
119. Josep Prat, María C. Santos, and Mireia Omella, "Square Root Module to Combat Dispersion-Induced Nonlinear Distortion in Radio-Over-Fiber Systems", IEEE Photonics Technology Letters, Vol. 18, No. 18, September 15, 2006
120. H. Buchali et al., "Reduction of the chromatic dispersion penalty at 10 Gbit/s by integrated electronic equalizers," in Proc. Optical Fiber Communication (OFC 2000), Vol. 3, pp. 268–270
121. Leibrich J. "CF-RZ-DPSK for suppression of XPM on dispersion managed longhaul optical WDM transmission on standard single-mode fiber, IEEE Photon Technology Letter, Vol.14, No.2, pp.155–157, February 2002
122. Serdyuk, V. M., "Dielectric study of bound water in grain at radio and microwave frequencies," Progress In Electromagnetics Research, PIER, Vol.84, pp. 379–406, 2008
123. Lin, C. T., J. Chen, P. C. Peng, C. F. Peng, W. R. Peng, B. S. Chiou, and S. Chi, "Hybrid optical access network integrating fiber-to-the-home and radio-over-fiber systems," IEEE Photon. Technol. Lettters, Vol. 19, No.8, pp.610–612, 2007
124. Oraizi, H. and S. Hosseinzadeh, "A novel marching algorithm for radio wave propagation modeling over rough surfaces," Progress In Electromagnetics Research, PIER 57, pp. 85–100, 2006

References

125. Prat, J., M. C. Santos, and M. Omella, "Square root module to combat dispersion-induced nonlinear distortion in radio-over-fiber systems," *IEEE Photon. Technol. Lett.*, Vol. 18, No.18, pp.1928–1930, 2006
126. Blais, S. R. and J. Yao, "Optical single sideband modulation using an ultranarrow dual-transmission-band fiber bragg grating," *IEEE Photon. Technol. Lett.*, Vol. 18, No.21, pp.2230–2232, December 2006
127. T.L. Koch, and R.C. Alferness, "Dispersion compensation by active predistorted signal synthesis," *J. Lightwave Technol.*, Vol.3, No.4, pp.800–805,1985
128. R.S. Kaler , Ajay K.Sharma, T.S. Kamal, "Comparison of pre-, post- and symmetrical-dispersion compensation schemes for 10 Gb/s NRZ links using standard and dispersion compensated fibers", *Optics Communications* , Vol.209, No.1-3, pp. 107–123, August 2002
129. E. Vourc'h, B. Della, D.L. Berre, D. Herve, "Millimeter-wave power-fading compensation for WDM fiber-radio Transmission using a wavelength-self tunable single-sideband filter", *IEEE Trans. Microwave*, Vol. 50, No.12,pp. 3009– 3015, 2002
130. D. Wake and A. Nkansah and N. J. Gomes, "Radio over Fiber Link Design for Next Generation Wireless Systems," *IEEE Journal of Lightwave Technology*, Vol. 28, No. 16, pp. 2456–2464, August 2010.
131. Lim, A. Nirmalathas, M. Bakaul, P. Gamage, K.L. Lee, Y. Yang, D. Novak, R. "Waterhouse, Fiber-wireless networks and subsystem technologies", *IEEE J. Lightwave Technol.*, Vol.28 , No.4,pp.390-405,2010

132. C.T. Lin, J. Chen, P.C. Peng, C.F. Peng, W.R. Peng, B.S. Chiou, S. Chi, "Hybrid optical access network integrating fiber-to-the-home and radio-over-fiber systems, *IEEE Photo. Tech. Letters.*, Vol.19, No.8, pp. 610–612, 2007
133. H.B. Kim, M. Emmelmann, B. Rathke, A. Wolisz, "A radio over fiber architecture for road vehicle communication systems", *IEEE Vehi. Network Tech. Conference (VTC-2005)*, Vol.5, 2920–2924, 2005
134. J.S. Wu, J. Wu, H.W. Tsao, "A radio-over-fiber network for microcellular system application", *IEEE Trans. Vehicular Tech.*, Vol. 47, No.1, pp.84-94, 1998
135. J. Prat, A. Napoli, J. M. Gené, M. Omella, P. Poggiolini, and V. Curri, "Square root strategy: A novel method to linearise an optical communications system with linear equalizers," in *Proc. ECOC 2005, Glasgow U.K.*, Paper We4.P.106, 2005
136. J. Marti, D. Pastor, M. Tortola, J. Capmany, and A. Montero, "On the use of tapered linearly chirped gratings as dispersion-induced distortion equalizers in SCM systems," *J. Lightwave Technol.*, Vol. 15, No. 2, pp.179–187, February 1997
137. C. Middleton, and R. DdSalvo, "High performance microwave photonic links using double sideband suppressed carrier modulation and balanced coherent heterodyne detection," *proceedings of the 28th IEEE conference on Military Communications*, pp. 124-129, 2009
138. C. T. Lin, J. Chen, S. P. Dai, P. C. Peng, and S. Chi, "Impact of nonlinear transfer function and imperfect splitting ratio of MZM on optical up-conversion employing double sideband with carrier suppression modulation," *Journal of Light wave Technology*, Vol.26, No.15, pp.2449-2459, August 2008

References

139. N. A. Al-Shareefi, S. I. S. Hassan, F. Malek, R. Ngah, S. A. Aljunid, R. A. Fayadh, J. A. Aldhaibani, and H. A. Rahim, "Development of a new approach for high quality quadrupling frequency optical millimeter wave signal generation without optical filter," *Progress In Electromagnetics Research.*, Vol.134, pp.189-208, 2013
140. R. Hui, B. Zhu, R. Huang, C. T. Allen, K. R. Demarest, and D. Richards, "Subcarrier multiplexing for high speed optical transmission," *Journal of Lightwave Technology.*, Vol.20, No.3, pp. 417-427, March 2012
141. Andrew Mercanteuemii ,Shi Pengsi Yao, Thin film lithium niobate electro-optic modulator with terahertz operating bandwidth, *Optics Express* 26(11) May 2018
142. Y.-T. Hsueh, Z. Jia, Hung-Chang Chien, Jianjun Yu, "A Novel Bidirectional 60-GHz Radio-Over-Fiber Scheme With Multiband Signal Generation Using a Single Intensity Modulator", *IEEE Photonics Technol. Lett.*, Vol.21, No.18, pp.1338-1340 2009
143. H. Chi and J. Yao, "Frequency quadrupling and up conversion in a radio over fiber link", *OSA*, *J. Light. Technol.*, Vol.26, No.15, pp.2706-2711, 2008
144. J. Li, T. Ning, L. Pei, and C.H. Qi, "Scheme for a high-capacity 60 GHz radio-over-fiber transmission system", *J. Opt. Communication. Netw.*, Vol.1, No.4, pp. 324-330, 2009
145. Jochen Antes , Florian Boes , Tobias Messinger , Ulrich J. Lewark , Tobias Mahler , Axel Tessmann, Multi-Gigabit Millimeter-Wave Wireless

-
- Communication in Realistic Transmission Environments, IEEE Transactions on Terahertz Science and Technology, Volume: 5 , Issue: 6 , Nov. 2015
146. Yong zhang, Development of Millimeter-Wave Radio-Over-Fiber Technology, Journal of Electronic Science and Technology, Vol. 9, No. 1, March 2011
- 147..David Wake, Anthony Nkansah, Nathan J. Gomes, Christophe Lethien, Cathy Sion, and Jean-Pierre Vilcot, Optically Powered Remote Units for Radio-Over-Fiber Systems, Journal of Lightwave Technology, Vol. 26, No. 15, August 1, 2008
148. Rajbir Singh, Manoj Ahlawat, Deepak Sharma, A Review on Radio over Fiber communication System, International Journal of Enhanced Research in Management & Computer Applications, Vol. 6 Issue 4, April-2017
149. Nathan J. Gomes, Maria Morant, Arokiaswami Alphones, Béatrice Cabon, John E. Mitchell, Christophe Lethien, Mark Csörnyei, Andreas Stöhr, and Stavros Iezekiel, Radio-over-fiber transport for the support of wireless broadband services, Vol. 8, No. 2 / February 2009 / Journal Of Optical Networking
150. Fan-Yi Lin* and Meng-Chiao Tsai, Chaotic communication in radio-over-fiber transmission based on optoelectronic feedback semiconductor lasers, Optics Express, 22 Vol. 15, No. 2, January 2007
151. X.N. Fernando , A Hammerstein-type equalizer for concatenated fiber-wireless uplink, IEEE Transactions on Vehicular Technology , Volume: 54 , Issue: 6 , Nov. 2005

References

152. Lin, C. T., J. Chen, P. C. Peng, C. F. Peng, W. R. Peng, B. S. Chiou, and S. Chi, "Hybrid optical access network integrating fiber-to-the-home and radio-over-fiber systems," *IEEE Photon. Technol. Lett.*, Vol. 19, No.8, pp.610–612, 2007
153. P. Raziq and M. Nakagawa, "Semiconductor laser's nonlinearity compensation for DS-CDMA optical transmission system by post nonlinearity recovery block," *IEICE Transactions on Communications*, vol. E79-B, no. 3, pp. 424-431, Mar. 1996
154. A. Katz, R. Dorval and R. Gray, "Performance of Microwave and Millimeter Wave Power Modules (MPMs) with Linearization," *Proceedings of 2005 IEEE Military Communications Conference*, Atlantic City, Oct. 17-20, 2005.
155. R.S. Kaler , Ajay K.Sharma, T.S. Kamal, "Comparison of pre-, post- and symmetrical-dispersion compensation schemes for 10 Gb/s NRZ links using standard and dispersion compensated fibers", *Optics Communications* , Vol.209, No.1-3, pp. 107–123, August 2002
156. E. Vourc'h, B. Della, D.L. Berre, D. Herve, "Millimeter-wave power-fading compensation for WDM fiber-radio Transmission using a wavelength-self tunable single-sideband filter, *IEEE Trans. Microwave*, Vol. 50, No.12, pp. 3009– 3015, 2002
157. Sharma, G. Singh, "Rectangular microstirp patch antenna design at THz frequency for short distance wireless communication systems", *Springer Link J. Infra. Milli -THz Wave*, Vol.30, No.1, pp. 1-7, 2009)
158. Lim, A. Nirmalathas, M. Bakaul, P. Gamage, K.L. Lee, Y. Yang, D. Novak, R. "Waterhouse, Fiber-wireless networks and subsystem technologies", *IEEE J. Lightwave Technol.*, Vol.28 , No.4, pp.390-405, 2010

159. C.T. Lin, J. Chen, P.C. Peng, C.F. Peng, W.R. Peng, B.S. Chiou, S. Chi, "Hybrid optical access network integrating fiber-to-the-home and radio-over-fiber systems", *IEEE Photo. Tech. Lett.*, Vol.19, No.8, pp. 610–612, 2007
160. H.B. Kim, M. Emmelmann, B. Rathke, A. Wolisz, "A radio over fiber architecture for road vehicle communication systems", *IEEE Vehi. Network Tech. Conference (VTC-2005)*, Vol.5, 2920–2924, 2005
161. J.S. Wu, J. Wu, H.W. Tsao, "A radio-over-fiber network for microcellular system application", *IEEE Trans. Vehicular Tech.*, Vol. 47, No.1, pp.84-94, 1998
162. J. Prat, A. Napoli, J. M. Gené, M. Omella, P. Poggiolini, and V. Curri, "Square root strategy: A novel method to linearise an optical communications system with linear equalizers," in *Proc. ECOC 2005, Glasgow U.K.*, Paper We4.P.106, 2005
163. J. Marti, D. Pastor, M. Tórtola, J. Capmany, and A. Montero, "On the use of tapered linearly chirped gratings as dispersion-induced distortion equalizers in SCM systems," *J. Lightwave Technol.*, Vol. 15, No. 2, pp.179–187, February 1997
164. C. Middleton, and R. DiSalvo, "High performance microwave photonic links using double sideband suppressed carrier modulation and balanced coherent heterodyne detection," *MILCOM*, 2009
165. C. T. Lin, J. Chen, S. P. Dai, P. C. Peng, and S. Chi, "Impact of nonlinear transfer function and imperfect splitting ratio of MZM on optical up-conversion employing double sideband with carrier suppression modulation," *Journal of Lightwave Technology*, Vol.26, No.15, pp.2449-2459, August 2008

References

166. N. A. Al-Shareefi, S. I. S. Hassan, F. Malek, R. Ngah, S. A. Aljunid, R. A. Fayadh, J. A. Aldhaibani, and H. A. Rahim, "Development of a new approach for high quality quadrupling frequency optical millimeter wave signal generation without optical filter," *Progress In Electromagnetics Research.*, Vol.134, pp.189-208, 2013
167. R. Hui, B. Zhu, R. Huang, C. T. Allen, K. R. Demarest, and D. Richards, "Subcarrier multiplexing for high speed optical transmission," *Journal of Lightwave Technology.*, Vol.20, No.3, pp. 417-427, March 2012
168. AHM Razibul Islam, Rishad Ahmed Shafik¹, Md. Shahriar Rahman¹, JuBin Song, "On the Nonlinear Distortion Effects in an OFDM-RoF Link", in *Proceedings of 2nd International Conference on Emerging Technologies*, pp.20-26, November 2006
169. S. L. Jansen, E. Gottwald, DQPSK modulation for robust optical transmission, *Optical Fiber communication/National Fiber Optic Engineers Conference, 2008. OFC/NFOEC 2008*
170. Mohammaed Slim Alouini and Andrea J. Goldsmith "Capacity of Rayleigh fading channels under different Adaptive Transmission and Diversity combining Techniques", *IEEE Transactions on Vehicular Technology*, Vol. 48, No. 4, July 1999
171. A. Sudhir Babu, Dr. K.V Sambasiva Rao, "Evaluation of BER for AWGN, Rayleigh and Rician Fading Channels under Various Modulation Schemes", *International Journal of Computer Applications*, Vol. 26, No.9, July 2011

-
172. Saeed V. Vaseghi *Advanced Digital Signal Processing and Noise Reduction*, Second Edition. Copyright © 2000 John Wiley & Sons Ltd.
173. S. L. Jansen, D. van den Borne, B. Spinnler, S. Calabro, H. Suche, P. M. Krummrich, W. Sohler, G-D. Khoe, and H. Waardt, "Optical phase conjugation for ultra long-haul phase-shift-keyed transmission," *IEEE J. Lightwave Technology*. Vol.-24, No.1, pp.-54-64, 2006
174. Jarajreh, Elias Giacoumidis, Ivan Aldaya, Son Thai Le, Athanasios Tsokanos, Zabih Ghassemlooy, and Nick J. Doran, *Artificial Neural Network Nonlinear Equalizer for Coherent Optical OFDM*, *IEEE Photonics Technology Letters*, 2015
175. Jie Pan and Chi-Hao Cheng, *Nonlinear Electrical Predistortion and Equalization for the Coherent Optical Communication System*, *Journal of Lightwave Technology*, Vol.29, No.18, September 15, 2011
176. W. Shieh, H. Bao, and Y. Tang, *Coherent optical OFDM: theory and design* *Optics Express*, Vol. 16, No. 2, Pp. 841
177. Hwanseok Chung, Sun Hyok Chang, Kwangjoon Kim, *Companding Transform based SPM Compensation in Coherent Optical OFDM Transmission*, *Optics Express* vol.19, No.26, December 2011
178. H. Gnauck and R. M. Jopson, "Dispersion compensation for optical fiber systems, in *Optical Fiber Telecommunications*, . Academic Press, San Diego, 1997

179. T. Ono, Y. Yano, and K. Fukuchi, "Demonstration of high-dispersion tolerance of 20-Gbit/s optical duo binary signal generated by a low-pass filtering method," OFC 1997, paper ThH1.
180. Kim, J. Jeong, J. Lee, H. Lee, H. Kim, S. K. Kim, Y. Kim, S. Hwang, Y. Oh, and C. Shim, "Improvement of dispersion tolerance for electrical-binary-signal-based duo binary transmitters," *Opt. Express*, Vol.13, No.13, pp. 5100-5105, June 2005
181. S. L. Jansen, S. Spalter, G-D. Khoe, Huug de Waardt, H. E. Escobar, L. Marshall, and M. Sher, "16×40 Gbps over 800 km of SSMF using mid-link spectral inversion," *IEEE Photon. Technol. Lett.*, Vol. 16, No.7, pp. 1763-1765, 2004.
182. S. L. Jansen, D. van den Borne, B. Spinnler, S. Calabro, H. Suche, P. M. Krummrich, W. Sohler, G-D. Khoe, and H. Waardt, "Optical phase conjugation for ultra long-haul phase-shift-keyed transmission," *IEEE J. Lightwave Technology*. Vol.-24, No.1, pp.-54-64, 2006
183. L. Spiekman and D. Zimmerman, "Optical amplification for metro: EDFA/EDWA amplifiers & semiconductor technologies," OFC 2003
184. A. Corchia, C. Antonini, A. D'Ottavi, A. Mecozzi, F. Martelli, P. Spano, G. Guekos, and R. Dall'Ara, "Mid-span spectral inversion without frequency shift for fiber dispersion compensation: A system demonstration," *IEEE Photon. Technol. Lett.*, Vol.11, No.2, pp. 275–277, 1999
185. C. Lorattanasane, and K. Kikuchi, "Design theory of long-distance optical phase conjugation," *J. Light wave Technol.*, Vol. 15, No.6, pp-948– 955, 1997

186. Mori K, Morioka T and Saruwatari M, “Wavelength-shift-free spectral inversion with an optical parametric loop mirror”, *Optical letters*, Vol.21, No.2, pp-110-112, January 1996
187. A. Mecozzi, G. Contestabile, F. Martelli, L. Graziani, A. D’Ottavi, P. Spano, R. Dall’Ara, J. Eckner, F. Girardin, and G. Gueskos, “Optical spectral inversion without frequency shift by four-wave mixing using two pumps with orthogonal polarization,” *IEEE Photon. Technol. Lett.*, Vol.10, No. 355–357 , 1998
188. Inoue, K., and Toba, H.: “Wavelength conversion experiment using fiber four-wave mixing”, *IEEE Photon. Technol. Lett.*, Vol. 4, No.-1, pp. 69-72, 1992
189. Tatham, M.C., Sherlock G., and Westbrook, L.D.: “20-nm optical wavelength conversion using non degenerate 4-wave- mixing”, *IEEE Photon. Technol. Lett.*, Vol.5, No.11, pp. 1303–1306,1993
190. Watanabe, S., Naito, T., and Chikama, T. “Compensation of chromatic dispersion in a single-mode fiber by optical-phase conjugation”, *IEEE Photon. Technol. Lett.*, Vol.5, No.1, pp. 92–95,1993
191. Røyset, A., Set, S.Y., Goncharenko, I.A., and Laming, R.I. “Linear and nonlinear dispersion compensation of short pulses using midspan spectral inversion”, *IEEE Photon. Technol. Lett.*, Vol.8, No.3, pp. 449–451 , 1996
192. Set, S.Y., Geiger, H., Laming, R.I., Cole, M.J., and Reekie, L.: “Optimization of DSF- and SOA-based phase conjugators by incorporating noise suppressing Fiber gratings’, *IEEE J. Quantum Electron*, Vol.33, No.10, pp. 1694–1698, 1997
193. Onishi, M., Okuno, T., Kashiwada, T., Ishikawa, S., Akasaka, N., and Nishimura, M.: “Highly nonlinear dispersion shifted fiber and its application

References

- to broadband wavelength converter”, Vol. 2, pp. 115–118 Proc. ECOC’97, Edinburgh, UK, 1997
194. Kelly, A.E., Marcenac, D.D., and Nettet, D., “40 Gbit/s wavelength conversion over 24.6 nm using FWM in a semiconductor optical amplifier with an optimised MQW active region”, *Electron. Lett.*, Vol.33, No.-25, pp. 2123–2124,1997
195. Jopson, R.M., and Tench, R.E., “Polarisation-independent phase conjugation of light wave signals”, *Electron. Lett.*, Vol.29, No.25, pp.2216–2217,1993
196. Inoue, K. “Polarisation independent wavelength conversion using fiber four-wave mixing with two orthogonal pump lights of different frequencies”, *J. Light wave Technol.*, Vol.12, No.-11, pp. 1916–1920,1994
197. Marcenac, D.D., Nettet, D., Kelly, A.E., and Gavrilovic, D. “40 Gbit/s transmission over 103 km of NDSF using polarisation independent mid-span spectral inversion by four-wave mixing in a semiconductor optical amplifier”, *Electron. Lett.*, Vol.34, No.1, pp. 100–101, 1998
198. C.L. Janer and M.J. Connelly, “Optical phase conjugation technique using four-wave mixing in semiconductor optical amplifier, *Electronics letters*, Vol. 47, No. 12, pp.716-717, June 2011
199. D.D. Marcenac, D. Nettet, A.E. Kelly, D. Gavrilovic, “40 Gbps transmission over 103 km of NDSF using polarization independent mid-span spectral inversion by four-wave mixing in a semiconductor optical amplifier”, *Electron.*, Vol.1, pp.100-101,1998

200. S. Singh, R.S. Kaler, “20 Gbps and higher bit rate optical wavelength conversion for RZ-DPSK signal based on four-wave mixing in semiconductor optical amplifier”, *Fiber Integr. Optics*, Vol.26, No.5, pp.295–308,2006
201. S. Singh, R.S. Kaler, “Wide band optical wavelength converter based on four-wave mixing using optimized semiconductor optical amplifier”, *J. Fiber Integr. Optics*, Vol.25, No.3, pp.213-230,2007
202. Ramos, F., and Marti, J. “Compensation for fiber-induced composite second-order distortion in externally modulated light wave AM-SCM systems using optical-phase conjugation”, *J. Lightwave Technol.*, Vol.16, No.8, pp. 1387–1392, 1998
203. J. Herrera, F. Ramos and J. Marti, “ Compensation for dispersion-induced carrier suppression effect in Microwave millimeter-wave optical links using optical phase conjugation in semiconductor optical amplifier”, *IEEE Electronics Letters* ,Vol.42, No.4, pp.238-239, February 2006
204. R.D.O. Ribeiro, M.J. Pontes, M.T.M.R. Giraldi, M.C.R. Carvalho, “Characterization of all-optical wavelength conversion by cross-gain modulation of ASE on a SOA”, in *International Microwave and Optoelectronics Conference Proceedings*, pp. 218–221, 2005,
205. S.L. Lee, P.M. Gong, C.T. Yang, “Performance enhancement on SOA-based four wave-mixing wavelength conversion using an assisted beam”, *IEEE Photon. Technol. Lett.*,Vol.14 , No.12, pp.1713-1715, 2002
206. J. D. McKinney and K. J. Williams, “Sampled analog optical links,” *IEEE Transactions on Microwave Theory Techniques*, Vol. 57, No. 8, pp. 2093–2099, August 2009

207. S.Shimotsu, S.Oikawa,T.Saitou, N.Mitsugi, K.Kubodera, T.Kawanishi, M.Izutsu, “Single side band modulation performance of a LiNbO₃ integrated modulator consisting of four-phase modulator waveguides”, IEEE Photonics Technology Letters, Vol.13, No.4, pp.364-366, April 2001.
208. X.L.Liu,Z.J.Liu,J.D.Li,T.Shang, “Performance improvement of optical single sideband signal using an integrated Mach–Zehnder modulator, Fiber Integrated Optics, Vol.29,bNo.6,pp.453-465, November 2010.
209. J.G. Zhao, Z.J.Liu, X.L.Liu, T.Shang, P.Yue, “Generation of radio signals using a novel Mach–Zehnder modulator with four arms”, Optical Communication, Vol. 282, No. 22, pp.4353–4357, November 2009
210. R. C. Alfernes et.al, “The evolution of configurable wavelength multiplexed optical networks VA historical perspective,” Proc. IEEE, Vol. 100, No. 5, pp. 1023–1034, May 2012
211. B. A. Khawaja and M. J. Cryan, “Characterization of multimode fibers for use in millimeter wave radio-over-fiber systems,” Microwave Optical Technology Letters, Vol. 50, No. 8, pp. 2005–2007, August 2008
212. Chi H. and J. P. Yao. “Waveform Distortions Due to Second- Order Dispersion and Dispersion Mismatches in a Temporal Pulse-Shaping System”, Journal of Light wave Technology, Vol. 25, No.11, pp.3528-3535, November 2007
213. X. N. Fernando and A. B. Sesay, “Adaptive Asymmetric Linearization of Microwave Fiber Optic Links for Wireless Access” IEEE Trans. Vehicular Technology, Vol. 51, No. 6, pp. 1576-1596, November 2002

-
214. E. J. Gualda, L. C. Go´mez-Pavo´ N And J. P. Torres, “Compensation of third-order dispersion in a 100 Gbps single channel system with in-line fibre Bragg gratings”, *Journal of Modern Optics* (Taylor&Fransis), Vol. 52, No. 9, pp.1197–1206, June 2005
215. Ramos, F., Marti, J., and Polo, V. (at.al). “Compensation of chromatic dispersion effects in microwave/millimeter-wave optical systems using four-wave-mixing induced in dispersion shifted fibers”, *IEEE Photonics Technology Letters*, Vol.11,No.9, pp. 1171-1173, September 1999
216. J. Maeda, Y.Fukuchi, “Numerical study of nonlinear pulse transmission in a fiber link with periodical dispersion slope compensation”, *J. LightwaveTechnol.*,Vol.23, No.3, pp.1189–1198,2005
217. S. Wen, “Bi-end dispersion compensation for ultra long optical communication system, *Journal of Light wave Technology*”, Vol.17, No.5, pp. 792–798, 1999
218. M. Seimetz. "High-Order Modulation for Optical Fiber Transmission". Springer Series in Optical Sciences, Vol. 43, 2009
219. Li, Z., Chi, H., Zhang, X., & Yao, J. (et.al). “Pulse Distortions Due to Third-Order Dispersion and Dispersion Mismatches in a Phase-Modulator Based Temporal Pulse Shaping System, *Journal of Lightwave Technology*”, pp. 2865-2872, Vol. 28, No. 19, October 1, 2010
220. Nishimura, M. (et.al), “Optical fibers and fiber dispersion compensators for high-speed optical communication”, *Journal of Optical and Fiber Communications Reports*, Vol.2, No.2, pp.115-139, June 2005

221. J. Azana, N. K. Berger, B. Levit, and B. Fischer, "Reconfigurable generation of high-repetition-rate optical pulse sequences based on time domain phase-only filtering," *Optical Lett.*, Vol. 30, No. 23, pp. 3228–3230, December 2005
222. Gamage P.A, Nirmalathas A, Lim C, Wong, E, Novak D. & Waterhouse R, "Performance comparison of directly modulated VCSEL and DFB lasers in wired and wireless networks", *IEEE Photonics Technology Letters*, Vol. 20, No. 24, pp. 2102–2104, December 2008
223. Rick et.al., "Long-Haul Analog Photonics," *J. Light wave Technol.*, Vol. 29, No.8, pp.1182–1205,2011
224. J. Seeds and K. J. Willims, "Microwave photonics," *J. Light wave Technol.*, Vol. 24, No.12, pp.-4628–4641, 2006
225. M.A.Othman, M.M.Ismail, H.A.Sulaiman, M.H.Misran, M.A.Meor Said, Y.A.Rahim, A.N.Che Pee and M.R.Motsidi, An Analysis of 10 Gbits/sec Optical Transmission System using Fiber Bragg Grating (FBG), *IOSR Journal of Engineering*, Vol. 2, No.7, pp. 55-61, July 2012
226. M. Vengsarkar and W. A. Reed , "Dispersion compensating single-mode fibers: efficient designs for first and second-order compensation," *Opt. Lett.*, Vol.18, No.11, pp.924-926, 1993
227. L.G.Nielsen, S. N. Knudsen , "Dispersion Compensating Fibers", *Optical Fiber Technology*, Vol.6, No.2, pp.164-180, 2000
228. G.P.Agrawal, "Optical Fiber Communications Systems, John Wiley, 1997

-
229. F. Qullette, "Dispersion cancellation using linearly chirped Bragg grating filters in optical waveguides" *Opt. Lett.* Vol.12, No.10, pp- 847-849, October 1987
230. J. A. R. Williams, I. Bennion, K. Sugden, and N. J. Doran, "Fiber dispersion compensation using a chirped in fiber Bragg grating," *Electron. Lett.*, Vol.30, No.12, pp. 985-987, June 1994
231. S. O. Mohammadi, Saeed Mozaffari, and M. Mehdi Shahidi (2011, "Simulation of a transmission system to compensate dispersion in an optical fiber by chirp gratings", *International journal of the Physical Sciences*, Vol.6, No.32, pp.7354-7360, December 2011
232. Scheerer, et al, "Influence of Filter Group Delay Ripples on System Performance", *ECOC*, pp. I-4101, 1999
233. Z. Pan et al., "Tunable chromatic dispersion compensation in 40-Gbps systems using nonlinearly chirped," *J. Light wave Technol.* Vol.20, No.12, pp.2239–2246, 2002
234. M. Tomizawa et al., "Automatic dispersion equalization for installing high-speed optical transmission systems," *J. Light wave Technol.* Vol.16, No.2, pp.184–191, 1998
235. J. Park, W. V. Sorin, and K. Y. Lau, "Elimination of the fibre chromatic dispersion penalty on 1550 nm millimeter-wave optical transmission," *Electron. Lett.*, Vol. 33, No.6, pp. 512–513, 1997
236. J. Yu et al., "A novel scheme to generate single-sideband millimeter wave signals by using low-frequency local oscillator signal," *IEEE Photonic Technol. Lett.*, Vol.20, No.7, pp.478–480, 2008

237. Z. Tang, S. Pan, and J. Yao, "A high resolution optical vector network analyzer based on a wideband and wavelength-tunable optical single sideband modulator," *Opt. Express*, Vol.20, No.6, pp.6555–6560, 2012
238. G. H. Smith, D. Novak, and Z. Ahmed, "Overcoming chromatic dispersion effects in fiber-wireless systems incorporating external modulators," *IEEE Trans. Microwave Theory Tech.*, Vol. 45, No.8 ,pp. 1410– 1415,1997
239. Y. Ogiso et al., "High extinction-ratio integrated Mach–Zehnder modulator with active Y-branch for optical SSB signal generation," *IEEE Photonic Technol. Lett.*, Vol.22, No.12, pp.941–943,2010
240. Z. Li et al., "Optical single-sideband modulation using a fiber-Bragggrating-based optical Hilbert transformer, " *IEEE Photonic Technol. Lett.*, Vol. 23, No.9, pp. 558–560,2011
241. Y. Shen, X. Zhang, and K. Chen, "Optical single sideband modulation of 11-GHz RoF system using stimulated Brillouin scattering," *IEEE Photonic Technol. Lett.*, Vol.17, No.6, pp.-1277–1279,2005
242. H. K. Sung, E. K. Lau, and M. C. Wu, "Optical single sideband modulation using strong optical injection-locked semiconductor lasers," *IEEE Photonic Technol. Lett.*, Vol.19, No.13, pp.-1005–1007,2007
243. Hong et al., "Single-sideband modulation based on an injection locked DFB lasers in radio-over-fiber systems," *IEEE Photonic Technol. Lett.*, Vol.22, No.7, pp. 462–464 ,2010

-
244. J. C. Cartledge and R. G. McKay, "Performance of 10 Gbps lightwave systems using an adjustable chirp optical modulator and linear equalization," *IEEE Photon. Technol. Lett.*, Vol. 4, pp.1394–1397, Dec. 1992.
245. T. Erdogan et.al, "Fibre grating spectra", *Journal of Lightwave Technology*, Vol.15, No.8, pp. 1277-1294,1997
246. Othonos and K. Kalli "Fiber Bragg Gratings: Fundamentals and Applications in Telecommunications and Sensing", Artech House, Inc., 1999.
247. K. O. Hill and G. Meltz, "Fiber Bragg Grating technology fundamentals and overview" *J. Lightwave Technol*, Vol. 15, No.8, pp. 1263-1276, 1997
248. Meenakshi, Jyotsana, Jyoteesh Malhotra, Comparative Analysis of Different Dispersion Compensation Techniques on 40 Gbps DWDM system, *International Journal of Technology Enhancements and Emerging Engineering Research*, Vol 3, Issue 06 34, ISSN 2347-4289
249. J. Herrera, F. Ramos and J. Marti, "Compensation for dispersion-induced carrier suppression effect in Microwave millimetre-wave optical links using optical phase conjugation in semiconductor optical amplifiers", *IEEE Electronics Letters* ,Vol.42,No.4,pp.238-239, February 2006
250. Ying Wang Shen, Rong Pu Tao, A novel technique to generate microwave signal based on multiple-frequency Brillouin fiber-ring laser, in *Proc. of Communications and Photonics Conference and Exhibition*, pp. 1–2, 2009
251. Lim, A. Nirmalathas, M. Bakaul, P. Gamage, K.L. Lee, Y. Yang, D. Novak, R. Waterhouse, Fiber-wireless networks and subsystem technologies, *IEEE J. Lightwave Technol.*, Vol.28 , No.4,pp.390-405,2010

252. H. K. Sung, E. K. Lau, and M. C. Wu, "Optical single sideband modulation using strong optical injection-locked semiconductor lasers," *IEEE Photonic Technol. Lett.*, Vol.19, No.13, pp.-1005–1007, 2007
253. Christina Lim, Ampalavanapillai Nirmalathas, Masduzzaman Backul, Prasanna Gamage, Ka Lun Lee, Yizhuo Yang, Dalma Novak and Rod Waterhouse. "Fiber-Wireless Networks and Subsystem Technologies" *Journal of Lightwave Technology*, Vol.28, No.4, pp.390-405, February 2010
254. Farah Diana Mahad, Abu Sahmah M. Supa et.al, Analyses of semiconductor optical amplifier four wave mixing for future all optical wavelength conversion, *Optik* , Vol.124, No.2013, pp.1-3, 2013
255. J. Yu, M. Huang, Z. Jia, T. Wang and G. Chang, "A Novel Scheme to Generate Single-Sideband Millimeter-Wave Signals by Using Low Frequency Local Oscillator Signal," *IEEE Photonics Technology Letters*, Vol. 20, No. 7, pp. 478-480, April 2008
256. L. Chen, S. Wen, Y. Li, J. He, H. Wen, Y. Shao, Z. Dong and Y. Pi, "Optical Front-Ends to Generate Optical Millimeter-Wave Signal in Radio-Over-Fiber Systems With Different Architectures," *Journal Of Lightwave Technology*, Vol. 25, No. 11, pp. 3381-3387, November 2007
257. S. Fan, H. Chien, Y. Hsueh, A. Chowdhury, J. Yu and G. Chang, "Simultaneous Transmission of Wireless and Wireline Services Using a Single 60-GHz Radio-Over-Fiber Channel by Coherent Subcarrier Modulation," *IEEE, Photonics Technology Letters*, Vol. 21, No. 16, pp. 1127-1129, August 15, 2009.

-
258. C. Lin, P. Shih, J. Chen, P. Peng, S. Dai, W. Jiang, W. Xue and S. Chi, "Cost-Effective Multiservice Hybrid Access Networks With no Optical Filter at Remote Nodes," *IEEE Photonics Technology Letters*, Vol. 20, No. 10, pp. 812-814, May 15, 2008.
259. Z. Jia, J. Yu, G. Ellinas and G. Chang, "Key Enabling Technologies for Optical-Wireless Networks: Optical Millimeter-Wave Generation, Wavelength Reuse, and Architecture," *Journal of Lightwave Technology*, Vol. 25, No. 11, pp. 3452-3471, November 2007
260. C. Lin, J. Chen, P. Peng, C. Peng, W. Peng, B. Chiou and S. Chi, "Hybrid Optical Access Network Integrating Fiber-to-the-Home and Radio-OverFiber Systems," *IEEE Photonics Technology Letters*, Vol. 19, No. 8, pp. 610-612, April 15, 2007
261. V. Urick, F. Bucholtz, P. Devgan, J. McKinney and K. Williams, "Phase Modulation with Interferometric Detection as an Alternative to Intensity Modulation With Direct Detection for Analog-Photonic Links," *IEEE Transactions On Microwave Theory And Techniques*, Vol. 55, No. 9, pp. 1978-1985, September 2007
262. F. Zeng and J. Yao, "Investigation of Phase-Modulator-Based All-Optical Bandpass Microwave Filter," *Journal of Lightwave Technology*, Vol. 23, No. 4, pp. 1721-1728, April 2005
263. C. Y. Li, H. S. Su, C. H. Chang, H. H. Lu, P. Y. Wu, C. Y. Chen and C. L. Ying, "Generation and Transmission of BB/MW/MMW Signals by Cascading PM and MZM," *IEEE, Journal of Lightwave Technology*, Vol. 30, No. 3, pp. 298-303, February 1, 2012

264. H. Chien, Y. Hsueh, A. Chowdhury, J. Yu and G. Chang, "Optical Millimeter-Wave Generation and Transmission Without Carrier Suppression for Single- and Multi-Band Wireless Over Fiber Applications," *IEEE, Journal of Lightwave Technology*, Vol. 28, No. 16, pp. 2230-2237, August 15, 2010.
265. Y. Hsueh, Z. Jia, H. Chien, J. Yu and G. Chang, "A Novel Bidirectional 60-GHz Radio-Over-Fiber Scheme With Multi-band Signal Generation Using a Single Intensity Modulator," *IEEE Photonics Technology Letters*, Vol. 21, No. 18, pp. 1338-1340, September 15, 2009
266. Z. Jia, J. Yu, Y. Hsueh, A. Chowdhury, H. Chien, J. Buck and G. Chang, "Multi-band Signal Generation and Dispersion-Tolerant Transmission Based on Photonic Frequency Tripling Technology for 60-GHz RadioOver-Fiber Systems," *IEEE, Photonics Technology Letters*, Vol. 20, No. 17, pp. 1470-1472, September 1, 2008
267. K. Ikeda, T. Kuri and K. Kitayama, "Simultaneous Three-Band Modulation and Fiber-Optic Transmission of 2.5-Gb/s Baseband, Microwave-, and 60-GHz-Band Signals on a Single Wavelength," *Journal of Lightwave Technology*, Vol. 21, No. 12, pp. 3194-3202, December 2003
268. R. C. Daniels and R. W. Heath, "60 GHz wireless communications: Emerging requirements and design recommendations," *IEEE Veh. Technol. Mag.*, Vol. 2, No. 3, pp. 41–50, September 2007
269. M. J. Koonen and L. M. Garcia, "Radio-over-MMF techniques-part II: Microwave to millimeter-wave systems," *J. Lightw. Technol.*, Vol. 26, No. 15, pp. 2396–2408, August 2008
270. J.J.Vegas Olmos, T. Kuri and K. Kitayama, "Dynamic reconfigurable WDM 60-GHz millimeter-waveband radio-over-fiber access network: Architectural

- considerations and experiment,” *J. Lightw. Technol.*, Vol.25, No. 11, pp. 3374–3380, November 2007
271. Seung-Hun Lee, Hyoung-Jun Kim, and Jong-In Song, Broadband photonic single sideband frequency up-converter based on the cross polarization modulation effect in a semiconductor optical amplifier for radio-over-fiber systems, *Optics Express*, Vol. 22, No.1, pp.183-192, January 2014
272. Chun-Hung Ho, Chun-Ting Lin, Yu-Hsuan Cheng, Hou-Tzu Huang, Chia-Chien Wei, and Sien Chi, High spectral efficient W-band optical/wireless system employing Single-Sideband Single-Carrier Modulation, *Optics Express*, Vol. 22, No. 4, pp.3911-3917, February 2014
273. K. Ikeda, T. Kuri, and K. Kitayama, “Simultaneous three-band modulation and fiber-optic transmission of 2.5-Gb/s baseband, microwave-and 60-GHz-band signals on a single wavelength,” *J. Lightw. Technol.*, Vol. 21, No. 12, pp. 3194–3202, December 2003
274. C. Qingjiang, F. Hongyan, and S. Yikai, “Simultaneous generation and transmission of downstream multiband signals and upstream data in a bidirectional radio-over-fiber system,” *IEEE Photon. Technol. Lett.*, Vol. 20, No. 3, pp. 181–183, February 2008
275. S.Mikroulis, O.Omomukuyo, M.P Thakur, J.E Motchell, Investigation of an SMF-MMF link for a remote heterodyne 60GHz OFDM RoF-based gigabit wireless access topology, *IEEE Journal of Light wave technology*, Vol.32, No.20, pp.3645-3653, May 2014
276. T. Kamisaka, T.Kuri, T.kitayama, Simultaneous modulation and fiber optic transmission of 10Gbps baseband and 60GHz band radio signals on a single

References

- wavelength, IEEE transactions on microwave technology, Vol.49, No.10, pp.2013-2017, October 2001
277. K. Ikeda , T. Kuri , K. Kitayama, Simultaneous three-band modulation and fiber-optic transmission of 2.5-Gb/s baseband, microwave-, and 60-GHz-band signals on a singlewavelength, Journal of Lightwave Technology., Vol.21, No.12, pp.3194-3202, December 2003
278. J.J. Vegas Olmos , Toshiaki Kuri , Ken-ichi Kitayama, Reconfigurable Radio-Over-Fiber Networks: Multiple-Access Functionality Directly Over the Optical Layer, IEEE Transactions on microwave, Vol.58, No.11, pp.3001-3010, October 2010
279. Liang Zhang, Xiaofeng Hu, Pan Cao, Qingjiang Chang, and Yikai Su, Simultaneous generation of independent wired and 60-GHz wireless signals in an integrated WDM-PON-RoF system based on frequency-sextupling and OCS-DPSK modulation, Vol. 20, No. 13, pp.14648-14655, 2012
280. Ivan Aldaya, Gabriel Campuzano, Gerardo castanon, Simultaneous generation of wavelength division multiplexing PON and RoF signals using a hybrid mode-locked laser, Optical Fiber Technology, Vol.23, pp. 53-60, June 2015
281. Masduzzaman Bakaul , Ampalavanapillai Nirmalathas, Christina Lim ; Dalma Novak , Hybrid Multiplexing of Multiband Optical Access Technologies Towards an Integrated DWDM Network, IEEE photonics technology letters, Vol.18, No.21, pp.2311-2313, November 2006
282. Q Chang, H Fu, Y Su -, Simultaneous generation and transmission of downstream multiband signals and upstream data in a bidirectional radio-over-fiber system, IEEE Photonics Technology Letters, Vol.18, No.21, pp.181-183, 2008

-
283. Q Chang, H Fu, Y Su, Simultaneous generation and transmission of downstream multiband signals and upstream data in a bidirectional radio-over-fiber system, *IEEE - Photonics Technology Letters*, vol.20, no.3, pp.181-183, February 2008
284. Zhensheng Jia , Jianjun Yu , Yu-Ting Hsueh , Arshad Chowdhury , Multiband Signal Generation and Dispersion-Tolerant Transmission Based on Photonic Frequency Tripling Technology for 60-GHz Radio-Over-Fiber Systems, *IEEE Photonics technology letters*, Vol.20, No.17, pp.1470-1472, September 2008
285. Yu-Ting Hsueh, Zhensheng Jia, Hung-Chang Chien, Chowdhury, Multiband 60-GHz Wireless Over Fiber Access System With High Dispersion Tolerance Using Frequency Tripling Technique, *IEEE Journal of Lightwave Technology*, Vol.29, No.8, pp.1105-1111, April 2011
286. Hsueh, Y.T, Jia, Z , Chien, H.-C, Yu, J, Chang, G.-K., A novel bidirectional 60-GHz radio-over-fiber scheme with multiband signal generation using a single intensity modulator, *Vol.21, No. 18, 15* , pp. 1338-1340, September 2009
287. Chung-Yi Li , Heng-Sheng Su, Ching-Hung Chang , Hai-Han L, Generation and Transmission of BB/MW/MMW Signals by Cascading PM and MZM, *Vol.30, No.3*, pp.298-303, February 2012
288. H. Kumazaki , Gifu Nat. Y. Yamada; H. Nakamura; S. Inaba , Tunable wavelength filter using a Bragg grating fiber thinned by plasma etching, *IEEE Photonics Technology Let*, Vol.13, No.11, pp.1206-1208, November 2001
289. Z. Li V, K. S. Hsiao ; Z. Chen ; J. Y. Tang , Optically Tunable Fiber Bragg Grating, *IEEE Photonics Technology Let .*, Vol.22, No.15, pp.1123-1125, May 2010

290. S. Choi , T. Eom ; Y. Jung ; B. Lee Broad-band tunable all-fiber bandpass filter based on hollow optical fiber and long-period grating pair, IEEE Photonics Technology Letters , Vol.17, No.1,pp.115-117,January 2005
291. Ruijiao Zhang, Jianxin Ma, Wen Liu, Wei Zhou, Yang Yang, A multi-band access radio-over-fiber link with SSB optical millimeter-wave signals based on optical carrier suppression modulation, Optical Switching and Networking, Vol.18,No.3,pp.235–241,September 2015
292. Zihang Zhu, Shanghong Zhao, Yongjun Li Xiaoping Chen Xuan Li , A novel scheme for high-quality 120 GHz optical millimetre-wave generation without optical filter Optics & Laser Technology, Volume 65, January 2015, Pages 29-35
293. Jia, Z., J. Yu, G. Ellinas, and G.K. Chang, Key enabling technologies for optical-wireless networks: Optical millimeter wave generation, wavelength reuse, and architecture," J. Lightw. Technol.,Vol.25,No.11,pp. 3452-3471, 2007
294. Nirmalathas, A., P. Gamage, C. Lim, D. Novak, and R. Waterhouse, Digitized radio-over-fiber technologies for converged optical wireless access network," J. Lightw. Technol., Vol.28,No.16,pp. 2366-2375,2010
295. Fu, X., C. Cui, and S.-C. Chan, Optically injected semiconductor laser for photonic microwave frequency mixing in radio-over fiber," Journal of Electromagnetic Waves and Applications,Vol.24,No.7, pp.849-860,2010

296. D. Wake, M. Webster, G. Wimpenny, K. Beacham, and L. Crawford, "Radio over fiber for mobile communications," in Proc. Int. Top. Meeting Microw. Photon. , pp. 157–160, October 2004
297. A.Narayanan, S. R., D. Braun, J. Buford, R. S. Fish, A. D. Gelman, Kaplan, R. Khandelwal, E. Shim, and H. Yu, Peer to peer streaming for networked consumer electronics," IEEE Communication Magazine, Vol.45,No.6,pp.124-131,2007
298. Zheng, Z., J. Wang, and J. Wang, A study of network throughput gain in optical-wireless (FiWi) networks subject to peer-to-peer communications," IEEE International Conference on Communications, pp.1-6,2009
299. M. Elkashlan, T. Q. Duong, H. -H. Chen, "Millimeter-wave communications for 5G: fundamentals: Part I [Guest Editorial]," IEEE Communications Magazine, Vol. 52, No. 9, pp. 52–54, 2014
300. M. Elkashlan, T. Q. Duong, H. -H. Chen, "Millimeter-wave communications for 5G Part 2: Applications," IEEE Communications Magazine, Vol. 53, No. 1, pp. 166–167, 2015
301. C. H. Doan, S. Emami, D. A. Sobel, A. M. Niknejad, and R. W. Brodersen,"Design considerations for 60 GHz cmos radios," IEEE Communications Magazine, Vol. 42, No. 12, pp. 132–140, December 2004
302. F. Gutierrez, S. Agarwal, K. Parrish and T. S. Rappaport, "On-chip integrated antenna structures in CMOS for 60 GHz WPAN systems,"IEEE J. Selected Areas in Communications, Vol. 27, No. 8, pp. 1367–1378, October 2009

References

303. T. S. Rappaport, J. N. Murdock, F. Gutierrez, "State of the art in 60-GHz integrated circuits and systems for wireless communications, Proceedings of the IEEE, Vol. 99, No. 8, pp. 1390–1436, August 2011
304. H. Ajourloo, M. T. Manzuri-Shalmani, "Modeling beacon period length of the UWB and 60-GHz mmWave WPANs based on ECMA-368 and ECMA-387 standards," IEEE Transactions on Mobile Computing, Vol. 12, No. 6, pp. 1201–1213, June 2013
305. Bakhtafrooz, A., A. Borji, D. Busuioc, and S. Safavi Naeini, "Novel two-layer millimeter-wave slot array antennas based on substrate integrated waveguides," Progress In Electromagnetics Research, Vol.109, pp.475-491,2010
306. Vegas Olmos, J. J., T. Kuri, T. Sono, K. Tamura, H. Toda, and K.-I. Kitayama, "Wireless and optical-integrated access network peer-to-peer connection capability," IEEE Photon. Technol. Lett., Vol.20, No.13, pp.1127-1129,2008
307. Li, Y., J. Wang, C. Qiao, A. Gumaste, Y. Xu, and Y. Xu, "Integrated fiber-wireless (FiWi) access networks supporting inter-ONU communications," J. Lightw. Technol., Vol.28, No.5, pp.714-724,2010
308. Shen, G.-F., X.-M. Zhang, H. Chi, and X.-F. Jin, "Microwave/millimeter-wave generation using multi-wavelength photonic crystal fiber brillouin laser," Progress in Electromagnetics Research, Vol.80, pp.307–320,2008
309. O'Reilly, J. J., P. M. Lane, R. Heidemann, and R. Hofstetter, "Optical-generation of very narrow line width millimeter-wave signals," Electronics Letters, Vol.28, No.5 1992, pp.2309–2311,1992

-
310. Goldberg, L., H. F. Taylor, J. F. Weller, and D. M. Bloom, "Microwave signal generation with injection locked laser diodes," *Electronics Letters*, Vol.19, No.13, pp.491–493, 1983
311. Fan, Z. and M. Dagenais, "Optical generation of a MHz-linewidth microwave signal using semiconductor lasers and a discriminator aided phase-locked loop," *IEEE Trans. Microw. Theory Tech.*, Vol.45, No.8, pp.1296–1300, 1997
312. Qi, G. H., J. P. Yao, J. Seregelyi, S. Paquet, and C. Belisle, "Generation and distribution of a wide-band continuously tunable millimeter-wave signal with an optical external modulation technique," *Transactions on Microwave Theory and Techniques*, Vol.53, No.10, pp. 3090–3097, 2005
313. Lin, C. T., P. T. Shih, J. Chen, W. J. Jiang, S. P. Dai, P. C. Peng, Y. L. Ho, and S. Chi, "Optical millimeter-wave Up-conversion employing, frequency quadrupling without optical filtering," *Transactions on Microwave Theory and Techniques*, Vol.57, No. 8, pp. 2084–2092, 2009
314. J. G. Proakis, *Digital Communications*, McGraw-Hill Inc., New York, Ny, 1995 (Third Edition).
315. Q. Zhao and J. Li, "Rain attenuation in millimeter wave ranges," in *Proc. IEEE Int. Symp. Antennas, Propag. EM Theory*, pp.1–4, Oct. 2006
316. R. J. Humpleman, P. A. Watson, "Investigation of attenuation by rainfall at 60 GHz," *Proceedings of the Institution of Electrical Engineers*, Vol. 125, No. 2, pp. 85–91, February 1978
317. T. Zwick, T. Beukema, and H. Nam, "Wideband channel sounder with measurements and model for the 60 GHz indoor radio channel," *IEEE Trans. Veh. Technol.*, Vol. 54, No. 4, pp. 1266–1277, July 2005

318. P. Smulders and A. Wagemans, "Wideband indoor radio propagation measurements at 58 GHz," *Electron. Lett.*, Vol. 28, No. 13, pp. 1270–1272, June 1992
319. H. Xu, V. Kukshya, and T. S. Rappaport, "Spatial and temporal characteristics of 60 GHz indoor channel," *IEEE J. Sel. Areas Commun.*, Vol. 20, No. 3, pp. 620–630, April 2002
320. E. Ben-Dor, T. S. Rappaport, Y. Qiao, and S. J. Lauffenburger, "Millimeter wave 60 GHz outdoor and vehicle AOA propagation measurements using a broadband channel sounder," in *Proc. IEEE Global Telecommun. Conf. (Houston, USA)*, pp. 1–6, December 5-9, 2011
321. S. Geng, J. Kivinen, X. Zhao, and P. Vainikainen, "Millimeter-wave propagation channel characterization for short-range wireless communications," *IEEE Trans. Veh. Tech.*, Vol. 58, No. 1, pp. 3–13, January 2009
322. Lin, C. T., P. T. Shih, J. Chen, W. J. Jiang, S. P. Dai, P. C. Peng, Y. L. Ho, and S. Chi, "Optical millimeter-wave Up-conversion employing frequency quadrupling without optical filtering," *Transactions on Microwave Theory and Techniques*, Vol. 57, No. 8, pp. 2084–2092, 2009
323. J. G. Proakis, *Digital Communications*, McGraw-Hill Inc., New York, Ny, 1995 (Third Edition).
324. J. Liu, I. Zhang, S.H. Fan, C. Guo and G.K. Chang, "A Novel Architecture for Peer-to-Peer Interconnect in millimeter-wave Radio-Over fiber Access Networks", *Progress In Electromagnetics Research*, Vol. 126, pp.139–148, 2012

325. C. R. Anderson, T. S. Rappaport, "In-Building Wideband Partition Loss Measurements at 2.5 and 60 GHz," *IEEE Transactions on Wireless Communications*, Vol. 3, No. 3, pp. 922 – 928, May 2004
326. X. Fernando, "Radio over fiber an optical technique for wireless access," *IEEE communications society presentation*, October 2009.
327. G.P. Agrawal, "Fiber-Optic Communication Systems," John Wiley and Sons, Third Edition, 2002.
328. J. Ma, J. Yu, C. Yu, X. Xin, J. Zeng, and L. Chen, "Fiber dispersion influence on transmission of the optical millimeter-waves generated using LN-MZM intensity modulation," *IEEE/OSA Journal of Lightwave Technology*, vol. 25, pp. 3244–3256, November 2007.
329. R. Kalman, J. Fan, and L. Kazovsky, "Dynamic range of coherent analog fiber-optic links," *IEEE Journal of Lightwave Technology*, vol. 12, pp. 1263–1277, July 1994.
330. H.J.R. Dutton, "Understanding Optical Communications," IBM, First Edition, 1998.
331. J.-M. Kelif and M. Coupechoux, "Impact of topology and shadowing on the outage probability of cellular networks," in *IEEE International Conference on Communications (ICC)*, pp. 1–6, June 2009.
332. R. Hui, B. Zhu, R. Huang, C. Allen, K. Demarest, and D. Richards, "Subcarrier multiplexing for high-speed optical transmission," *Journal of Lightwave Technology*, Vol. 20, pp. 417–427, March 2002.

333. H. K. Xijia Gu, Yifeng He and X. Fernando, "Transmission efficiency improvement in microwave fiber-optic link using sub-picometer optic band pass filter," Proceedings of the SPIE Conference Photonic North, Vol. 5971, pp. 597123–1–6, September 2005.
334. M. Farwell, W. Chang, and D. Huber, "Increased linear dynamic range by low biasing the mach-zehnder modulator," IEEE Photonics Technology Letters, Vol. 5, pp. 779–782, July 1993.
335. E. Ackerman, G. Betts, W. Burns, J. Campbell, I. Cox, C.H., N. Duan, J. Prince, M. Regan, and H. Roussel, "Signal-to-noise performance of two analog photonic links using different noise reduction techniques," in IEEE/MTT-S International Microwave Symposium, pp. 51–54, June 2007
336. L. Johansson and A. Seeds, "Generation and transmission of millimeter-wave data-modulated optical signals using an optical injection phase-lock loop," IEEE/OSA Journal of Lightwave Technology, Vol. 21, pp. 511–520, February 2003.
337. L. Chrostowski, X. Zhao, and C. Chang-Hasnain, "Microwave performance of optically injection-locked VCSELs," Microwave Theory and Techniques, IEEE Transactions on, Vol. 54, pp. 788 – 796, feb. 2006.
338. T. Ismail, C.-P. Liu, J. Mitchell, and A. Seeds, "High-dynamic-range wireless-over-fiber link using feed forward linearization," IEEE/OSA Journal of Lightwave Technology, Vol. 25, pp. 3274–3282, November 2007.
339. C.-T. Lin, J. Chen, P.-C. Peng, C.-F. Peng, W.-R. Peng, B.-S. Chiou, and S. Chi, "Hybrid optical access network integrating fiber-to-the-home and radio-

- over-fiber systems,” IEEE Photonics Technology Letters, vol. 19, pp. 610–612, April 2007.
340. R. Llorente, T. Alves, M. Morant, M. Beltran, J. Perez, A. Cartaxo, and J. Marti, “Ultra-wideband radio signals distribution in FTTH networks,” IEEE Photonics Technology Letters, Vol. 20, pp. 945–947, June 2008.
341. M. Huchard, M. Weiss, A. Pizzinat, S. Meyer, P. Guignard, and J. Yu, Z. Jia, 120J. Yu, Z. Jia, T. Wang, and G. Chang, “A novel radio-over-fiber configuration using optical phase modulator to generate an optical mmwave and centralized lightwave for uplink connection,” IEEE Photonics Technology Letters, Vol. 19, pp. 140–142, February 2007.
342. M. F. Huang, J. Yu, Z. Jia, and G. K. Chang, “Simultaneous generation of centralized lightwaves and double/single sideband optical millimeterwave requiring only low-frequency local oscillator signals for radioover-fiber systems,” IEEE/OSA Journal of Lightwave Technology, Vol. 26, pp. 2653–2662, August 2008.
343. Arash Bahrami, Wai Pang Ng, Zabih Ghassemlooy, Sujana Rajbhandari, “Radio over Fibre Transmission Using Optical Millimeter Wave in Nonlinear Fibre Propagation, International Symposium on Communication Systems”, Networks & Digital Signal Processing (CSNDSP 2012)

International Journals

1. **R. S. Asha**, V. K. Jayasree, Mhatli Sofien, Xavier Fernando, Group velocity and third-order dispersion comparison in externally and directly modulated radio over fiber link, Journal of optics, Vol.20, No.28, pp.1-8, June 2019
2. **Asha R.S**, Jayasree V.K, Mhatli Sofien, An 80Gbps Multi-Band Access Radio-Over-fiber Link with Single Side Band Optical Millimeter-Wave Dispersion-Tolerant Transmission without FBG and optical filter, Elsevier Opto-Electronics Review, Vol. 25,pp. 311–317, 2017
3. **Asha R.S**, Jayasree V.K, Sofien Mhatli, Chromatic Dispersion Compensation in 80Gbps ultra high bit rate long-haul transmission with travelling wave Semiconductor Optical Amplifier, Journal of Scientific and Industrial Research (CSIR journal) (accepted)
4. **Asha.R.S**, Jayasree V.K, Simulative Investigation of Coherent Optical OFDM with Nonlinear Distortions in the wireless channel and Receiver, Journal of Optical communication, Degruyter publishers, Vol.38, No.3, pp.243-248, 2016
5. **Asha R.S**, Jayasree V.K, Square Root Nonlinear Equalizer to Combat the Nonlinear Distortion in Single Sideband ROF Communication, Mediterranean journal of Electronics and Communication, Vol. 1, No. 11, pp.831-838, 2015

6. **R.S. Asha** and Jayasree V.K, Simulative Investigation of Coherent Optical OFDM Communication with Gbits/s Data Rates, Bonfring International Journal of Research in Communication Engineering, Vol. 5, No. 3, pp. 22-26, 2015
7. Jayasree Vadakke Kadangote, Neethu Johney, **Asha Radhamany Somasekharan**, Comparison of Different Chromatic Dispersion Compensation Techniques in Radio over Fiber System, American Journal of Optics and Photonics, Vol.3, No.2, pp.24-29,2015
8. **Asha R.S**, Jayasree V.K, An Optical Double Sideband Carrier Suppressed RoF Transmission system with Reduced Photo detector Nonlinearity, International Journal of Computer and Communication System Engineering (IJCCSE), Vol. 2, No.4,pp.614-619,2015
9. **Asha R.S**, Jayasree V.K, Neethu S Johney, Fiber Nonlinearity Compensation for Radio Over Fiber CO-OFDM Systems with Mid Span Spectral Inversion, International Journal of Computer and Communication System Engineering Volume 03, Issue 03 , pp.92-98,2016
10. **Asha R. S**, Jayasree V.K ,Performance Evaluation of SNR in Radio Over Fiber Systems for Different Modulation Schemes in AWGN Channel and Fading Channels, International Conference on Microelectronics, Communication and Renewable Energy (ICMiCR2013)(also Published in IEEE xplore)

11. **Asha R.S**, Jayasree V.K., Sofien Mhatli, Fiber Dispersion Compensation in Single Side Band optical Communication system using Ideal Fiber Bragg Grating and Chirped Fiber Bragg Grating without DCF, Journal of optics, Springer, Volume 47, No.2, pp.-148-153, June 2018 .

International Conferences:

1. **Asha R.S**, Jayasree V.K, A Novel Architecture for Peer-To-Peer Interconnected 200 GHz Millimeter-Wave long hauls Radio-Over Fiber Access Networks through AWGN wireless channel, OSA Conference, Photonics 2016 (IIT Kanpur) and published in Optics infobase
2. **Asha R.S**, Jayasree V.K “Performance Evaluation of SNR in Radio Over Fiber Systems for Different Modulation Schemes in AWGN Channel and Fading Channels”, published in IEEE explore [presented in International Conference on Microelectronics, Communication and Renewable Energy (ICMiCR-2013)]

National Conference

1. **Asha R.S**, Jayasree V.K, Performance comparison of Optical OFDM Radio over Fiber Communication with Coherent Detection, National Conference on Power, Control, Communication and Computing (NPCCC'17)

RESUME

Personal Profile

Name : Asha R.S
Sex : Female
Date of Birth : 23-5-1982
Area of Interest : Radio over Fiber Communication, Optical Communication
Languages Known : English, Hindi, Malayalam, Tamil
Computational skills : Optisystem, MATLAB
Professional Experiences : 4 years of teaching experience
Research Experience : 6 years of research experience in the field of Radio over Fiber Communication , Department of Electronics, Model Engineering College,(Research Center, CUSAT) Thrikkakara

Professional Membership

Associate Member of Institution Engineers (India), Life Time Member- ISTE

Publications

International /National Conferences: 9

Journal Publications: 10

Qualification	Branch /Specialization	Year	University	Percentage/ CGPA
UG	Electronics and Communication Engineering	2006	IEI	GPA 8
PG	Communication Systems	2008	Anna University, Chennai	75%
Ph.D.	Radio over Fiber Communication	From Dec. 2011	CUSAT (Model Engineering College), Ernakulam	GPA 7.3 (Course Work)

Email Address : asharspillai@gmail.com

Permanent Address : Thazhathumanakal (H)
Asamannoor P.O.
Punnayam, Perumbavoor
Ernakulam (Dist.)
PIN: 683549

Phone No (Mob) : 7306377811